NAVAL POSTGRADUATE SCHOOL

MONTEREY, CALIFORNIA

THESIS

BEHAVIOR OF FLOTSAM IN THE CALIFORNIA CURRENT SYSTEM UTILIZING SURFACE DRIFT OF RAFOS FLOATS

by

Dallas Cody Gates

September 2012

Thesis Co-Advisors: Curtis Collins
Tetyana Margolina

Approved for public release; distribution is unlimited

THIS PAGE INTENTIONALLY LEFT BLANK

REPORT DOCUMENTATION PAGE		Form Approved OMB No. 0704-0188

1. AGENCY USE ONLY *(Leave blank)*	2. REPORT DATE September 2012	3. REPORT TYPE AND DATES COVERED Master's Thesis

4. TITLE AND SUBTITLE Behavior of Flotsam in the California Current System Utilizing Surface Drift of RAFOS Floats	5. FUNDING NUMBERS
6. AUTHOR(S) Dallas Cody Gates	
7. PERFORMING ORGANIZATION NAME(S) AND ADDRESS(ES) Naval Postgraduate School Monterey, CA 93943-5000	8. PERFORMING ORGANIZATION REPORT NUMBER
9. SPONSORING /MONITORING AGENCY NAME(S) AND ADDRESS(ES) N/A	10. SPONSORING/MONITORING AGENCY REPORT NUMBER

11. SUPPLEMENTARY NOTES The views expressed in this thesis are those of the author and do not reflect the official policy or position of the Department of Defense or the U.S. Government. IRB Protocol number _____N/A_____.

12a. DISTRIBUTION / AVAILABILITY STATEMENT Approved for public release; distribution is unlimited	12b. DISTRIBUTION CODE A

13. ABSTRACT (maximum 200 words)

The patterns of surface drift of eighty-nine undrogued RAFOS floats in the California Current System have been studied. The floats were launched in the California Undercurrent during 1992–2010 and were tracked by the ARGOS system when they surfaced at the end of their subsurface mission. The surface drift of these floats was typically equatorward in the California Current. However, some floats moved poleward into the Subpolar Gyre, and others drifted westward into the North Equatorial Current. The duration of surface trajectories varied from as short as 11 days to as long as 280 days.

Observations of surface currents typically use drifters which are coupled to the surface layer by drogues which are located at 15 m depth. While drogued observations are useful for studies of circulation of the upper layer of the ocean, a more typical operational problem involves trying to find flotsam that has fallen off the deck of a ship or to predict the path of a floating mine. To better understand the behavior of these surface drifting objects, observations of the surface drift of RAFOS floats in the California Current system were used to compare their motion to wind induced drift and evaluate the drift prediction by three ocean models, Ocean Surface Current Simulator (OSCURS), Global Navy Coastal Model (gNCOM) and Hybrid Coordinate Ocean Model (HYCOM).

The results indicate that summer and fall months provided the best correlation between float drift speed and wind speed. Evaluation of the drift prediction by three ocean models was conducted by comparing observed drifter trajectories with model simulated trajectories at 7-day timescales. The model-simulated trajectories were initially collocated with RAFOS positions and restarted every 15 days. These results showed that OSCURS was able to give better short-term prediction of surface drift than gNCOM and HYCOM when OSCURS model parameters were chosen as to minimize separation between modeled and observed trajectories.

14. SUBJECT TERMS Global Naval Coastal Ocean Model , gNCOM, Hybrid Coordinate Ocean Model, HYCOM, flotsam, Ocean Surface Current Simulator, OSCURS, RAFOS floats, California Current System, California Current	15. NUMBER OF PAGES 191
	16. PRICE CODE

17. SECURITY CLASSIFICATION OF REPORT	18. SECURITY CLASSIFICATION OF THIS PAGE	19. SECURITY CLASSIFICATION OF ABSTRACT	20. LIMITATION OF ABSTRACT
Unclassified	Unclassified	Unclassified	UU

NSN 7540-01-280-5500 Standard Form 298 (Rev. 2-89)
Prescribed by ANSI Std. 239-18

THIS PAGE INTENTIONALLY LEFT BLANK

Approved for public release; distribution is unlimited

BEHAVIOR OF FLOTSAM IN THE CALIFORNIA CURRENT SYSTEM UTILIZING SURFACE DRIFT OF RAFOS FLOATS

Dallas Cody Gates
Lieutenant, United States Navy
B.S., Jacksonville University, 2006

Submitted in partial fulfillment of the
requirements for the degree of

MASTER OF SCIENCE IN PHYSICAL OCEANOGRAPHY

from the

NAVAL POSTGRADUATE SCHOOL
September 2012

Author: Dallas Cody Gates

Approved by: Curtis Collins
Thesis Co-Advisor

Tetyana Margolina
Thesis Co-Advisor

Mary Batteen
Chair, Department of Oceanography

THIS PAGE INTENTIONALLY LEFT BLANK

ABSTRACT

The patterns of surface drift of eighty-nine undrogued RAFOS floats in the California Current System have been studied. The floats were launched in the California Undercurrent during 1992–2010 and were tracked by the ARGOS system when they surfaced at the end of their subsurface mission. The surface drift of these floats was typically equatorward in the California Current. However, some floats moved poleward into the Subpolar Gyre, and others drifted westward into the North Equatorial Current. The duration of surface trajectories varied from as short as 11 days to as long as 280 days.

Observations of surface currents typically use drifters which are coupled to the surface layer by drogues which are located at 15 m depth. While drogued observations are useful for studies of circulation of the upper layer of the ocean, a more typical operational problem involves trying to find flotsam that has fallen off the deck of a ship or to predict the path of a floating mine. To better understand the behavior of these surface drifting objects, observations of the surface drift of RAFOS floats in the California Current system were used to compare their motion to wind induced drift and evaluate the drift prediction by three ocean models, Ocean Surface Current Simulator (OSCURS), Global Navy Coastal Model (gNCOM) and Hybrid Coordinate Ocean Model (HYCOM).

The results indicate that summer and fall months provided the best correlation between float drift speed and wind speed. Evaluation of the drift prediction by three ocean models was conducted by comparing observed drifter trajectories with model simulated trajectories at 7-day timescales. The model-simulated trajectories were initially collocated with RAFOS positions and restarted every 15 days. These results showed that OSCURS was able to give better short-term prediction of surface drift than gNCOM and HYCOM when OSCURS model parameters were chosen as to minimize separation between modeled and observed trajectories.

THIS PAGE INTENTIONALLY LEFT BLANK

TABLE OF CONTENTS

THIS PAGE INTENTIONALLY LEFT BLANK

LIST OF FIGURES

THIS PAGE INTENTIONALLY LEFT BLANK

LIST OF TABLES

THIS PAGE INTENTIONALLY LEFT BLANK

LIST OF ACRONYMS AND ABBREVIATIONS

AFSC	Alaska Fisheries Science Center
CC	California Current
CCS	California Current System
COAPS	Center for Ocean-Atmospheric Prediction Studies
CODE	Coastal Ocean Dynamics Experiment
FNMOC	Fleet Numerical Meteorology and Oceanography Center
GDP	Global Drifter Program
gNCOM	Global Naval Coastal Ocean Model
GSF	Geostrophic Current Factor
HYCOM	Hybrid Coordinate Ocean Model
LHS	Latin Hypercube Sampling
MC	Monte Carlo
MIB	Message in Bottles
MICOM	Miami Isopycnic Coordinate Model
NOGAPS	Navy Operational Global Atmospheric Prediction System
NRL	Naval Research Laboratory
OSCURS	Ocean Surface Current Simulator
POM	Princeton Ocean Model
REFM	Resource Ecology and Fisheries Management
REMSS	Remote Sensing Systems
SVP	Surface Velocity Program
WAD	Wind Angle Deviation
WCSC	Wind Current Speed Coefficient

THIS PAGE INTENTIONALLY LEFT BLANK

ACKNOWLEDGMENTS

This thesis would not have been possible without the help from my two thesis advisors, Professor Curtis Collins and Tetyana Margolina. Thanks to Professor Collins for his patience and his many references to bath tub toys and hockey gloves. Thanks to Tetyana who guided me through all the MATLAB programs and helped me compare Apples to Oranges. Thank you Tarry Rago for his dedication and his superb technical support with RAFOS data. Special thanks to my wife, Mindy Gates, and my daughter, Hailee Gates, for continuing to support me through my military career. Without their support, I would not be where I am today.

OSCURS model was created and implemented by Dr. James Ingraham and Dr. Robert K. Miyahara of Alaska Fisheries Services. A special thanks to Lynn de Witt of Southwest Fisheries Science Center for providing outstanding support and assisting me with OSCURS. Thanks to Patrick Hogan who made it possible to obtain gNCOM and HYCOM model outputs. gNCOM version 2.6 was formulated by Charlie N. Barron, Lucy F. Smedstad, Tamara L. Townsend, Timothy L. Campbell, Paul J. Martin, Pamela G. Posey, and Robert C. Rhodes of NRL and model output was made available to us by Ms. Lucy F. Smedstad of NRL Stennis Space Center. HYCOM experiment 90.8 was formulated by NRL and model output made available to us by Mr. Ole Martin Smedstad of NRL Stennis Space Center.

THIS PAGE INTENTIONALLY LEFT BLANK

I. INTRODUCTION

The study of ocean currents is ongoing. In early years, the study was conducted with the use of drifting flotsam such as Messages in Bottles (MIB) or anything that would float. Today, with the arrival of satellite tracked drifters, global satellite communication systems, and global positioning, the world's ocean surface currents are able to be measured more frequently with higher accuracy. The Global Drifter Program (GDP) is part of the Global Surface Drifting Buoy Array that maintains a global 5x5 degree array of 1250 Argos-tracked surface drifting buoys and provides data for scientific use (NOAA 2012). Maximenko et al. (2012) utilized data of 10,561 Lagrangian drifters (drogued and undrogued) from GDP to measure surface currents and to study the dynamics of marine debris. Data collected from these Lagrangian drifters are also used to develop numerical models in an attempt to better understand the ocean current patterns (Maximenko et al. 2012). These ocean models can in turn be used in an effort to track flotsam or debris on the ocean surface.

Flotsam is floating debris (Merriam-Webster, X ed., s.v. "flotsam"). Flotsam can include debris that has fallen off of container ships, lost fishing equipment, drifting mines deployed in the surface currents by terrorist or a sailor lost off the side of a Navy ship. Flotsam often ends its ocean transit in the middle of ocean gyres such as the "Great Pacific Garbage Patch" (Howell et al. 2012) or possibly washed ashore (Maximenko et al. 2012). Flotsam drifts in the surface currents of the world's oceans. These surface currents are immensely complex throughout the oceans, changing with time and position. Currently, flotsam from the March 2011 Tohoku Japan earthquake and tsunami is floating in the Pacific Ocean, posing threats to navigation (Showstack 2011).

The surface drift of RAFOS floats in the California Current System (CCS) is described here. The data record extended from 1992 to 2010. The California Current (CC) is the eastern boundary current of the anticyclonic Subtropical North Pacific gyre. The CC is a broad and weak current near the coast; the southeastward flow averages

speeds of 0.41 m s^{-1} (Lynn and Simpson 1987). Off the California coast, daily average surface speeds of 0.5 m s^{-1} have been observed utilizing surface drifters (Lynn and Simpson 1987).

The objective of this paper is to understand the surface drift of floats by studying their movement. Charts of float movement will be used to determine geographical and seasonal patterns of movement. Motion of floats will then be compared to the output of three ocean models including Ocean Surface Current Simulator (OSCURS), Global Naval Coastal Ocean Model (gNCOM), and HYbrid Coordinate Ocean Model (HYCOM). By comparing float observed drift to ocean models, we will determine the character of differences between model predictions and the observed float drift. Throughout paper, the term float will be used when referring to the RAFOS float.

The thesis is organized in five chapters. Data are described in Chapter II including float description, processing of trajectories, wind data, and model output. Chapter III is a case study comparing OSCURS model trajectories with float n113. Chapter IV discusses Results and Discussion followed by Summary and Conclusion in Chapter V. There are two appendices: Appendix A covers individual float trajectories and Appendix B contains long-term drift comparisons of float, OSCURS, gNCOM, and HYCOM trajectories.

II. DATA

The thesis analyzes surface drift of RAFOS floats and compares it to wind-induced drift and trajectories simulated using three ocean models. Chapter II describes materials used in these goals, including the NPS dataset of float surface trajectories, wind data, and the ocean models configuration and outputs. In subsection A the general description of floats and the NPS dataset of float surface trajectories is given along with the analysis of the float data spatial and temporal coverage, float behavior at sea surface as flotsam, and a preliminary description of observed patterns of float surface drift. Details on processing of float data are given in Subsection B. Subsection C describes the wind analysis dataset used to model wind drift of float trajectories.

A. RAFOS FLOATS

1. RAFOS Float Description and Use as a Surface Drifter

The RAFOS float (see Figure 1) (Rossby et al. 1986) is a subsurface acoustically tracked non-drogued Lagrangian drifter. The float is constructed from a 0.08 m by 1.52 m glass tube, which houses the electronics required for operation.

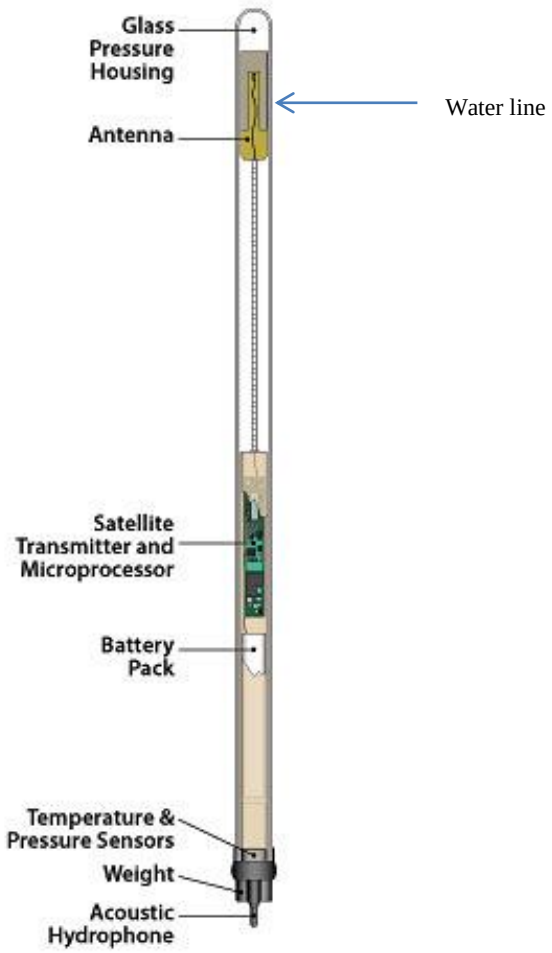

Figure 1. RAFOS Float (Woods Hole Oceanographic Institution 2012). Blue arrow illustrates approximate water level when floating on the ocean surface. Float is constructed from a 0.08 m by 1.52 m glass tube.

Two types of drifters are currently used by oceanographers to measure surface currents. The Surface Velocity Program (SVP) drifter is most widely used (Lumpkin and Pazos 2006). The evolution and construction of the SVP drifter is described by Lumpkin and Pazos (2006). SVP drifters have their drogue at 15 m nominal depth to measure mixed layer currents in the upper ocean. Another commonly used drifter is the Coastal Ocean Dynamics Experiment (CODE) drifter. The CODE drifter is for coastal and marginal sea application and is designed to measure the top meter of the water column (Poulain et al. 2009). Further description of the CODE drifter is given in Davis (1985).

A goal in designing drifters that measure surface currents is to minimize the impact of wind slippage. In the early 1800's, when scientists began using drift bottles, they would weight them down so that they were almost submerged in order to reduce the effect of the wind force on drifting objects (Lumpkin and Pazos 2007). Wind effects on SVP drifters and CODE drifters have been minimized but the effect of wind can still impact the drifters. As a result the drifters might not be a direct representation of the surface currents (Poulain et al. 2009).

In order for a drifter to have as low wind slippage as possible, it should have a high drag area ratio. The drag area ratio is defined as the ratio of the drogue drag area to the area of all other components of a drifter. Niiler and Paduan (1995) showed that a drag area ratio of 40 resulted in a 0.7 cm/s (or 7%) downwind slippage per 10 cm/s wind speed, and was an optimal compromise between low wind slippage and a not too complicated drifter design. When floats are floating on the ocean surface, they have about 0.127 m of freeboard and the rest of the float is submerged (this water level is shown in Figure 1). The freeboard can be used to calculate the drag area ratio of the RAFOS float which is 11.

The ratio of forces, F_w/F_a on the cross section of the float is estimated using the following:

$$\frac{F_w = \frac{1}{2} * \rho_w * Cd * L_w * W * V_w^2}{F_a = \frac{1}{2} * \rho_a * Cd * L_a * W * V_a^2} \qquad (1)$$

where the drag coefficient, *Cd*, is 1.17 for a cylinder, density of air , ρ_a, 1 kg/m^3, density of water. ρ_w, 1000 kg/m^3, width, W, of RAFOS float of 0.086 m, length of RAFOS float exposed to wind forcing, L_a, 0.127 m, length of submerged RAFOS float, L_w, is 1.393 m, velocity of current (V_w) and velocity of wind (V_a). Substituting these values into (1),

$$\frac{\frac{1}{2} * 1000 \frac{\text{kg}}{\text{m}^3} * 1.17 * 1.393\text{m} * 0.086\text{m} * V_w^2}{\frac{1}{2} * 1 \frac{\text{kg}}{\text{m}^3} * 1.17 * 0.127\text{m} * 0.086\text{m} * V_a^2} = \frac{43.53}{6.35}$$

Using a nominal current velocity of 0.25 m/s and wind speed of 10 m/s results in an F_w/F_a ratio of 6.86, e.g., the effect of the current was about seven times greater than that of the wind. As a result, the calculations described below did not include windage or the effects of wind forcing on the floats.

Similar to the SVP and CODE drifters, the position of the drifter was determined from the Doppler shift of its transmission. The positioning algorithm used to determine the position is explained by Argos (2011) and Lumpkin and Pazos (2007). As the satellite passes over the drifter, it begins receiving messages. To calculate the drifter's position four or more messages are required, any less and the position cannot be calculated (Argos 2011).

The error of the position of a drifter is important when using drifter data for analysis. When Argos provided a poor fix, the uncertainty of the position of the drifter increased. A greater distance of uncertainty results in uncorrelated environmental conditions. Figure 2 shows the error of uncertainty of float n113. Accuracy of estimates of the speed and direction of water movement from these floats was contingent upon the accuracy in determining the location of a drifter. Location accuracy of Argos ranged from being better than 250 m (class 3) to being worse than 1500 m (class 0) (Argos 2012). Figure 2 shows the trajectory of float n113 with uncertainty of the position shown as grey circles. Radii of the circles were calculated based on known location classes, none of which was worse than 2, i.e., the location error did not exceed 1500 m.

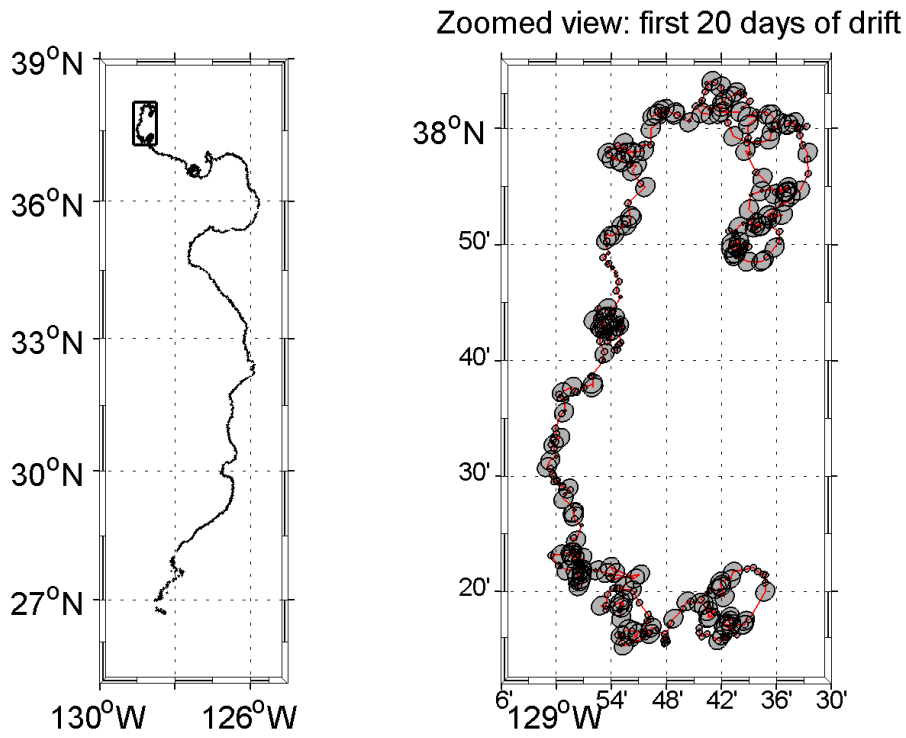

Figure 2. Argos positioning errors of RAFOS float n113. (left) 185-day trajectory. (right) First 20-days of drift. Radius of each circle is equal to the error of the float position provided by Argos.

2. Naval Postgraduate School RAFOS Dataset

Data consist of surface drift of 89 floats in the California Current System. Appendix A contains charts of individual float surface trajectories, and a short description of the float drift where necessary. The floats were launched in the California Undercurrent during 1992–2007 and were tracked by the Argos system during data transmission after the floats surfaced. The data base totaled 10,431 days of surface drift and the duration of the observed surface trajectories varied from as short as 11 days, float n055, to a maximum of 280 days, floats n069 and n105. The lengths of time floats spent on the surface depend on multiple factors. Floats that typically had short subsurface missions experienced short surface trajectories. For any given rate of subsurface data collection, the longer the subsurface mission the longer the surface drift, due to the larger amount of data that must be transmitted to Argos. The first fix of a surfaced float was September 11, 1992, and the final fix for the last float was April 10, 2010.

Figure 3 shows the temporal distribution of the float data. Yearly distribution of float surface drift data was uneven with zero data available in 2009. The data cover all four seasons nearly evenly (Figure 3, lower left). Regional currents delineated by float drift included eastward flow in the North Pacific Drift Current, westward in the North Equatorial Current, and poleward flow along the coast in the Davidson Current/Alaska Current. Trajectories are shown in Figure 4 and encompassed the area of 15°N to 60°N and 115°W to 150°W.

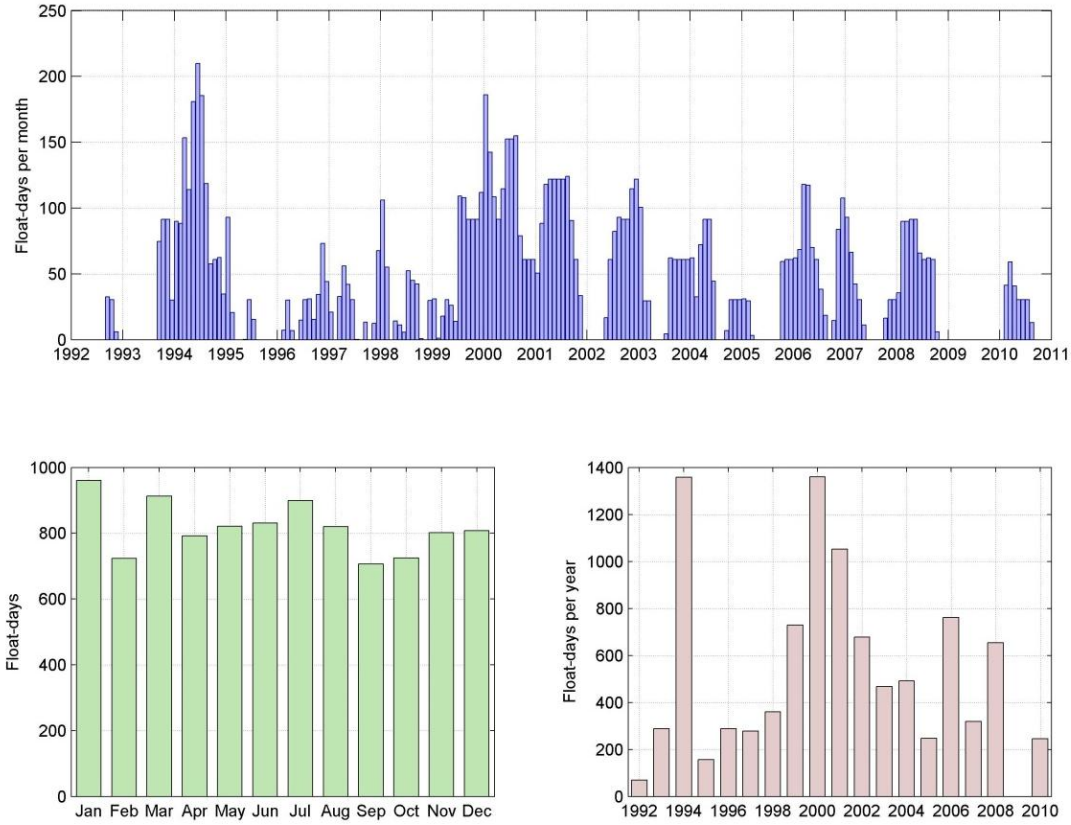

Figure 3. Temporal distribution of RAFOS surface trajectories: distribution of float-days per month by year (upper panel); distribution of float-days by month (lower left panel); distribution of float-days per year by year (lower right panel)

3. Drifter Trajectories

The observed path of a float is called a trajectory. A chart of all the trajectories is referred to as a ‘spaghetti’ diagram and is shown in Figure 4. The trajectories are color

coded based on the season: time periods of December to February, March to May, June to August, and September to November are shown in blue, black, magenta and red, respectively.

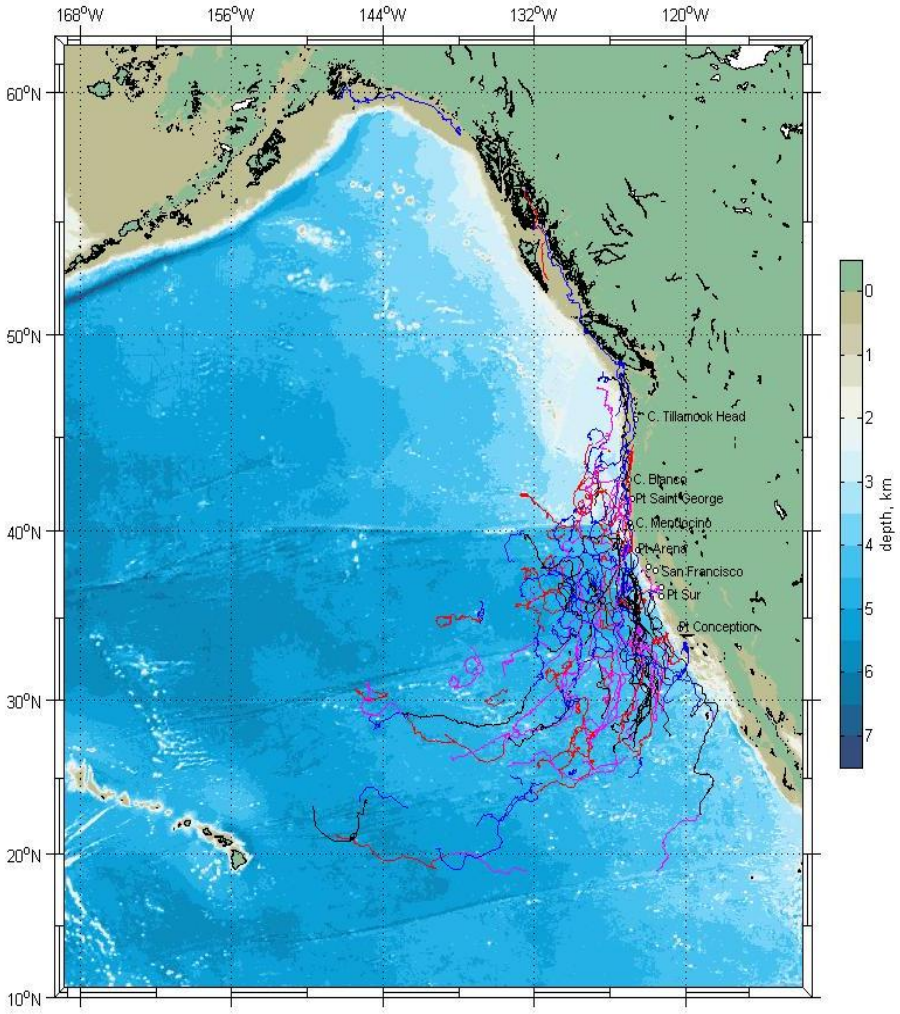

Figure 4. Spaghetti diagram of surface drift of RAFOS floats in the Northeast Pacific Ocean separated by seasons: winter (blue), spring (black), summer (magenta), fall (red). Note the coastal northward drift of floats n039, n048, n102, n108 and n115 to the north of 50°N.

Spatial coverage of float surface data is shown in Figure 5 as number of float days per 2° x 2° bin. The float data are unevenly distributed in space with an area of elevated coverage density located approximately between Pt. Conception and C. Mendocino and elongated perpendicular to the coast in the southwest direction as far as 136°W. Two

main factors contributed to such irregular spatial coverage: the pattern of float launch and surfacing and surface flow pattern in the California Current System.

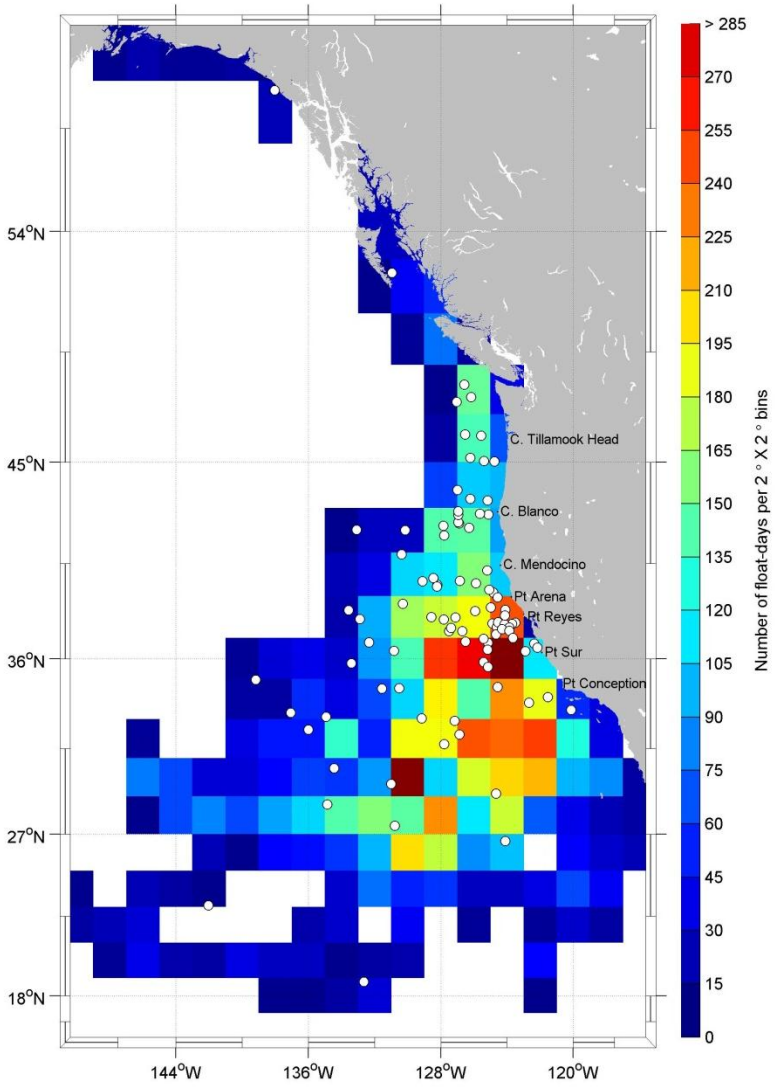

Figure 5. Density of RAFOS float days in 2° x 2° bins. Small white circles denote locations of float surfacing.

Floats were typically deployed in the California Undercurrent at locations over the continental slope at the start of their subsurface mission (Margolina et al. 2006). As a result, the seeding of the CCS was not uniform. Only length of the float subsurface mission (if successful and did not end prematurely) was known beforehand but the location where the float would surface and begin transmitting to Argos (shown as small white circles in Figure 5) was not. There were bins which had a higher number of float

days than others. The 2° x 2° bin at 36°N, 124°W was biased to a large number of float days due to the numerous number of floats that surfaced in the region. Floats that surfaced in this region typically had southward trajectories. A second 2° x 2° bin at 30°N, 130°W with a high number of float days was biased because as floats began to travel westward their velocity would decrease, resulting in the float remaining in the area for a longer period. Float n106 (see Appendix A, Figure A83) contributed to the high number of float days in this region as it surfaced at 27.45°N, 130.78°W and moved in a cyclonic/anticyclonic pattern for 206 days before ending transmissions to Argos at 26.08°N, 130.24°W.

B. PROCESSING OF SURFACE RAFOS TRAJECTORIES

Original files of float surface drift contain longitudes and latitudes of float positions at uneven time intervals ranging from several minutes to hours. As float transmissions were being received by Argos, there were occasions when a float position could not be determined. For example, as mentioned above, four messages must be transmitted from the float to the satellite in order for location to be determined (Argos 2012). Float positions were recorded from seven to 11 times per day. The float positions were smoothed with cubic splines in order to filter out noise and unresolved scales, and then interpolated to a 6-hour time step. Westward and northward components of float velocities were then determined.

There were some circumstances where the floats experienced data gaps. For example float n098 surfaced June 24, 2006 and was tracked until September 24, 2006 when it experienced a gap of two days before obtaining another successful fix on September 27, 2006 (see Appendix A, Figure A79). For float trajectories with gaps, each section was treated as a separate trajectory except in Appendix B where long-term drift was considered. This procedure was applied to floats n067, n068, n072, n080, n081, n082, and n098.

C. WIND DATA

Wind data used in this study was Cross-Calibrated Multi-Platform Ocean Surface Wind Vector L3.0 First-Look Analysis (Atlas et al. 2011). The data contained a value

added 6-hourly gridded analysis of ocean surface winds and combined cross-calibrated satellite winds obtained from Remote Sensing Systems (REMSS) with high-resolution (0.25 degree) gridded analysis. Wind observations and analysis fields were referenced to a height of 10 meters.

The magnitude of surface current drift was calculated from wind data using Equation (2) (Witting 1909).

$$C = k\sqrt{W} \qquad (2)$$

C is the speed or magnitude of the surface current (cm/s) as a result of wind; k is the coefficient of proportionality, which is 4.8 when it includes both the speed of the mixed layer and mass transport by waves at the surface; and W is the wind speed (m/s). Equation (2) is used by the OSCURS model and was used in this study to be consistent with model comparisons. The magnitude of float drift was calculated utilizing u and v components of the vector velocity of float drift.

D. MODELS

There are numerous numerical ocean models today that simulate circulation. These models produce fields of temperature, salinity, currents, sea surface height, etc. It is critical that the modeled fields be assessed against observations. Ocean models can help to interpret observations and identify physical processes. Float trajectories will be used to compare the modeled output of three ocean models (OSCURS, gNCOM, and HYCOM) to observed surface drift.

1. OSCURS

In the late 1970s, the Alaska Fisheries Science Center's (AFSC) Resource Ecology and Fisheries Management (REFM) Division initiated the development of a numerical ocean model, utilizing atmospheric sea level pressure, to investigate how ocean currents might impact fish populations in the North Pacific Ocean and Bering Sea from 1901 to present (Ingraham 1997). This effort led to the development of the OSCURS numerical model (Ingraham 1997).

OSCURS is currently used as a research tool that assists oceanographers and fisheries scientists to analyze daily ocean currents. Currents can be analyzed anywhere in a 90 km ocean-wide grid from Baja California to China and from 10°N to the Bering Strait (Ingraham 1997). OSCURS is available online for public use. OSCURS is user friendly and requires the user to select the start position, latitude and longitude, and dates for start and finish of a desired trajectory. OSCURS then uses historical 6-hour Fleet Numerical Meteorology and Oceanography Center (FNMOC) sea level pressure data as inputs for the model. In addition to sea level pressure inputs, the user can vary three optional parameters to influence the modeled surface current, Wind Current Speed Coefficient (WCSC), Wind Angle Deviation (WAD), and Geostrophic Current Factor (GSF).

The first of the three optional parameters, WCSC, determines how much an object floating on the surface is affected by the surface wind. The optional parameters for WCSC vary from one to two with increments as small as 0.1 [1: 0.1: 2]. Examples of WCSC are 1.0 for water, 1.2 for athletic shoes, 1.4 for hockey gloves, 1.6 for plastic bathtub toys, and 2.0 for large bottles. The value 1.2 corresponds to a floating object traveling 20% faster than the surface current. The second optional parameter, WAD, is used to adjust the angle an object travels in relation to the wind. Ekman theory predicts that objects floating on the ocean surface flow at an angle of 45° to the right of the wind direction. This angle can be adjusted by using a value for WAD between -5 and 5 at 0.1 increments [-5: 0.1: 5]. The third and final parameter, GSF, is used to take into account geostrophic current. The default is set to one and the value can be adjusted from zero, which eliminates geostrophic effects, to five using increments of 0.1 [0: 0.1: 5]. The geostrophic current used by OSCURS was determined from long-term mean/dynamic height (0/3,000) (Ingraham and Miyahara 1989). The parameter can be used to amplify the effect of the geostrophic current or be set to zero to eliminate it and look at pure wind drift. Further details of the physical basis of OSCURS is given by Ingraham and Miyahara (1988).

OSCURS output used below consisted of modeled trajectories with one day time step. More details are given in Chapters III and IV.

2. GNCOM

The Global Navy Coastal Ocean Model (gNCOM) is a 1/8 degree global ocean model that provides nowcasting and forecasting of global ocean environmental conditions (Barron et al. 2006) that utilize 3-hourly atmospheric forcing from the Navy Operational Global Atmospheric Prediction System (NOGAPS) (Smedstad et al. 2010). The purpose of gNCOM, in addition to providing nowcasting and forecasting, includes supporting nested ocean models and to couple with atmospheric models in order to better represent air-sea interactions. gNCOM preserves reasonably high vertical resolution while the horizontal resolution is limited to 1/8° to fit within the limits of its operational computational sources (Barron et al. 2007). The foundation and physics of gNCOM in this study is described in detail by Barron et al. (2006).

gNCOM is primarily based on two previous ocean models: the Princeton Ocean Model (POM) (Blumberg and Mellow 1987) and the Sigma/Z-level Model (Marten et al. 1998). gNCOM is a free-surface ocean model that is based on the baroclinic, hydrostatic, and Boussinesq primitive equations that allow its vertical coordinate to consist of σ coordinates for the upper layers and z-levels below a user-specified depth (Barron et al. 2006, Barron et al. 2007). Surface boundary conditions are surface wind stress, surface heat flux, and effective surface salt flux (Barron et al. 2006). gNCOM extends over coastal regions, continental shelves, and the Arctic, providing global coverage with minimum depth of five meters (Barron et al. 2007). gNCOM modeled output has 19 σ-layers from the surface to 137 m and 21 z-levels from 137 m to 5500 m totaling 40 vertical material layers. gNCOM output used in this study includes surface velocity fields in the Northeast Pacific ocean provided by Naval Research Laboratory (Barron et al. 2006). Only surface circulation fields at 3-hour time resolution for the period from January 1, 2006 to December 31, 2010 were used in the present study.

3. HYCOM

The Hybrid Coordinate Ocean Model (HYCOM), introduced in the late 1990s by Rainer Bleck, is a 1/12° global ocean model with 32 hybrid vertical coordinates (Metzger et al. 2009). It is a hydrostatic model developed from the Miami Isopycnic Coordinate

Model (MICOM) (Yao and Johns 2010). HYCOM is isopycnal in the open stratified ocean but switches to a terrain-following coordinate in shallow coastal regions and then transfers to z-level coordinates in the mixed layer and/or un-stratified seas (Xie and Zhu 2010). NOGAPS, wind speed, wind stress, precipitation, and heat flux (Center for Ocean-Atmospheric Prediction Studies 2012) provides surface forcing to HYCOM. HYCOM produces 5-day hindcast and a 5-day forecast and data is generally available for public use within 2 days at the Center for Ocean-Atmospheric Prediction Studies (COAPS), Florida State University (Potemra 2012). Further description of HYCOM science and physics is provided by Bleck (2002).

Surface velocity fields for this study were provided by the Naval Research Laboratory from HYCOM experiment 90.8 (Center for Ocean-Atmospheric Prediction Studies 2012). During the experiment HYCOM was configured for global ocean with HYCOM 2.2 as the dynamic model and computations were carried out on a Mercator grid between 78°S and 47°N where a bipolar patch is used for areas north of 47°N (Center for Ocean-Atmospheric Prediction Studies 2012). For the present study, daily snapshots of surface velocities were available for the period between January 7, 2010 and December 31, 2010. To generate trajectories, the original grid was used as described in the section four below.

4. Surface Trajectories from Ocean Models

Various techniques can be used to evaluate the performance of models using drifters. In this study, surface float drift will be compared with OSCURS, gNCOM, and HYCOM modeled Lagrangian trajectories. The performance metric will be the time-varying separation of each modeled trajectory from the observed float trajectory.

Obtaining a trajectory from OSCURS is complicated by the need to assign values to three parameters so a detailed example is given in the next chapter. To compare gNCOM and HYCOM modeled trajectories with observed float trajectories, the simulated gNCOM and HYCOM trajectories were started collocated in space and time with the observed float trajectories for 15 day segments. At the end of each segment, the modeled trajectories were reset to the position of the observed drifter. Each segment

along the trajectory can be considered statistically independent. A custom MATLAB function implementing a fourth order Runge-Kutta scheme was used for forward time stepping. The chosen algorithm has been checked to provide a robust solution within the specified 15 day interval. Model surface velocity fields from Global NCOM included 2006 to 2010 and encompassed floats n098, n102, n104, n105, n106 n107, n108, n109, n110, n111, n112, n113, n114, and n115. Surface velocity fields from HYCOM included model output from 2010, which included floats n113 and n115.

III. CASE STUDY: COMPARISON OF OSCURS MODEL TRAJECTORIES WITH FLOAT N113

Ingraham and Miyahara (1989) described how to best reproduce observed surface currents with OSCURS. They took three surface drifters drogued to 20 m and linearly varied the geostrophic and wind component while varying the deflection angle in an attempt to determine the values that provided the best fit between drifter and model trajectories. Results established a 1.2 multiplication factor for computation of the current speed and an average angle of deflection of 26 degrees (clockwise) as the best choices to minimize differences between model and observations within the Gulf of Alaska. Weber's function was part of the OSCURS model at that time and was used to determine angle of deflection but was not available for use in this study. Instead, available OSCURS parameters were used and chosen as described below.

A. FLOAT N113

To compare float drift to OSCURS, a similar approach to Ingraham and Miyahara (1989) was followed. The trajectory for float n113 was chosen because it was a long trajectory, occurred late in the observing period and could be compared with all models, and experienced differing motion regimes, including steady southward drift and mesoscale features. Float n113 surfaced at 38.003°N 128.55°W on February 8, 2010, and was tracked by Argos for 185 days. The long-term drift of n113 was predominately southward in character, reflecting the surface flow of the California Current (Figure 6). Float tracking ceased on August 12, 2010, when float n113 was at 26.68°N, 128.23°W.

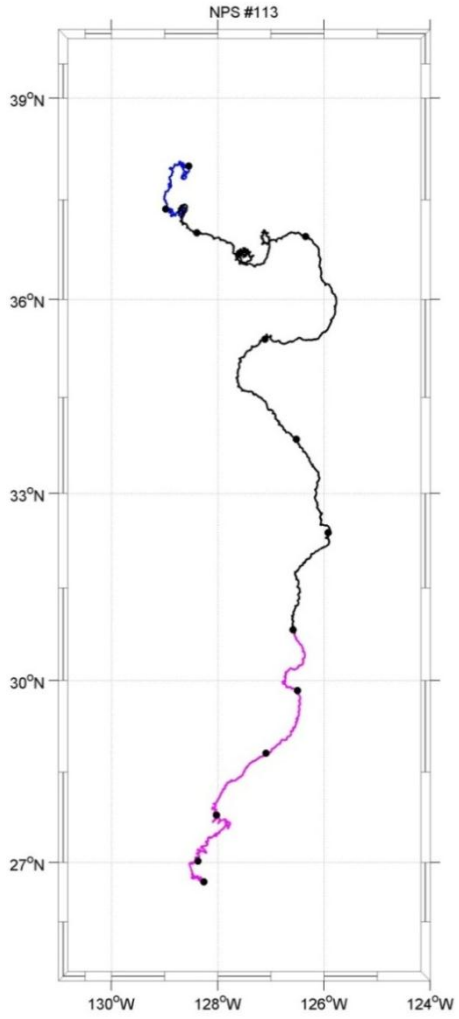

Figure 6. Surface trajectory of RAFOS float n113. The float surfaced February 8, 2010 at 38.003°N 128.55°W and transmitted to ARGOS until its battery failed on August 12, 2010 at 26.68°N 128.23°W. Dots along trajectory are 15 days apart. Colors represent different seasons: blue (winter), black (spring), magenta (summer).

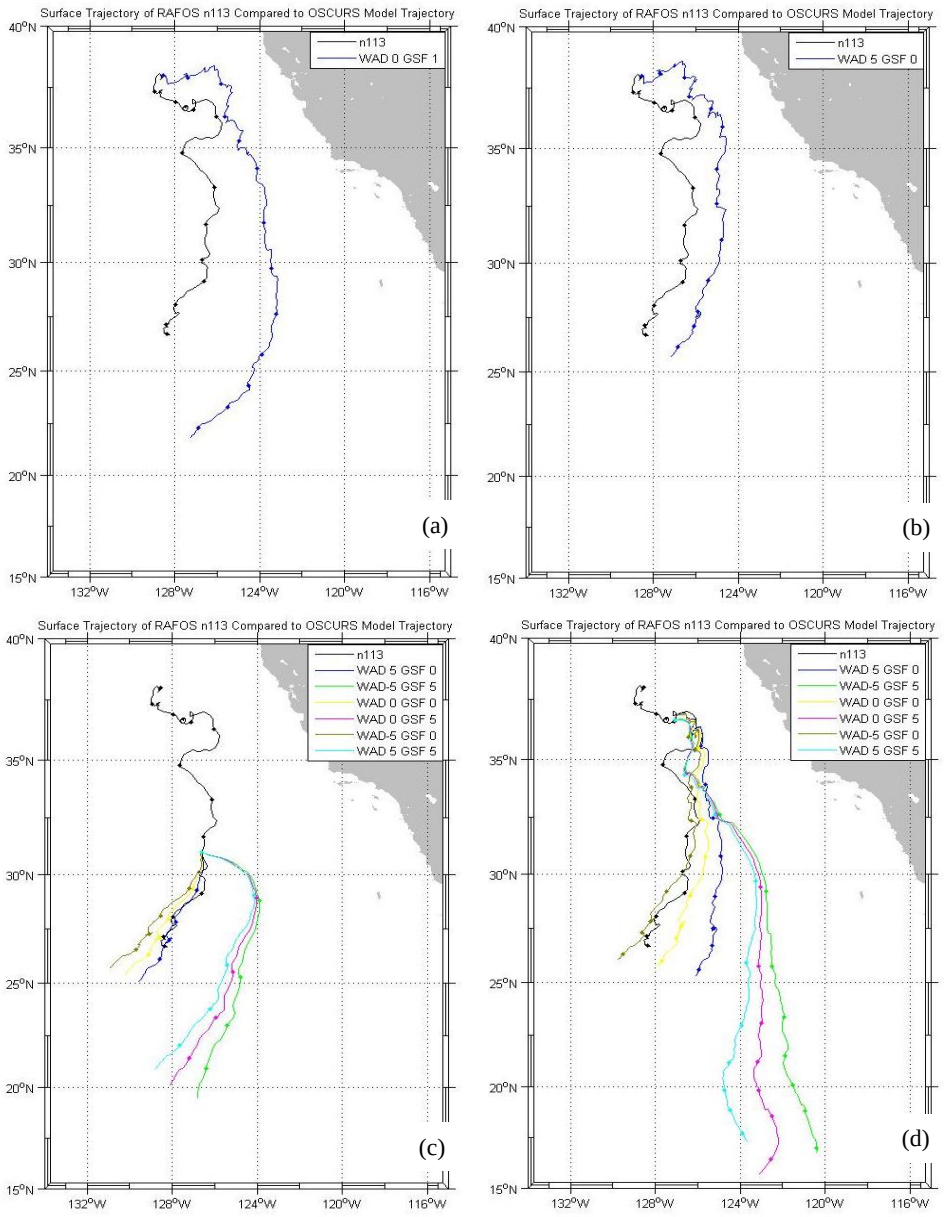

Figure 7. Comparison of the observed trajectory for RAFOS n113 and trajectories modeled by OSCURS with different model parameters (Wind Angle Deflection (WAD) and Geostrophic Current Factor (GSF)) and initial positions: (a) default OSCURS parameters WAD=0.0, GSF=1.0, and initial position collocated with RAFOS surfacing location; (b) WAD=5.0, GSF=0.0, initial position collocated with RAFOS surfacing location; (c) WAD and GSF varied as shown in the legend, trajectory was initialized on May 31, 2010 at position 31.00°N 126.60°W; (d) WAD and GSF varied as shown in the legend and Table 1, trajectory was initialized on March 27, 2010 at 36.67°N 127.07°W. The WCSC was set to 1.0 in all the model runs. Dots are plotted every 15 days along both observed and modeled trajectory.

The time and position of n113 surface location served as input to OSCURS. Parameters for WCSC were set to 1.0 for water, WAD to 0.0, and GSF to 1.0. The resulting trajectory is shown in Figure 7a with float n113. The two trajectories, although somewhat similar, differed so that after 185 days the OSCURS simulated position was 21.84°N 127.26°W while the observed n113 ended at 26.68°N 128.23°W, a distance of 550 km.

B. A FIRST ATTEMPT TO SEE THE EFFECTS OF WIND ANGLE DEFLECTION AND GEOSTROPHIC CURRENT FACTORS

In an attempt to obtain the best fit modeled trajectory to the observed float trajectory the optional parameters, WAD and GSF, were varied in a manner similar to Ingraham and Miyahara (1989). A WCSC value of 1.0, water, was selected since the drag ratio was 11 indicating the float was mostly affected by currents. In order to determine best values for the remaining two optional parameters, WAD and GSF, the parameters were set to zero and maximum and minimum values and run multiple times as listed in Table 1.

Run	WAD	GSF
1	0	0
2	0	5
3	-5	0
4	-5	5
5	5	0
6	5	5

Table 1. Variation of OSCURS parameters during a sequence of six model runs. Wind Angle Deviation (WAD) and Geostrophic Current Factor (GSF) used to compare OSCURS and observed RAFOS trajectories. The Wind Current Speed Coefficient was held constant at 1.0.

The least difference in final position and best correlation with observed trajectory n113 was for WAD set to five and GSF set to zero (Figure 7b) where final separation was 151.9 km.

To better understand how the errors accumulated with time and positions, further examination was undertaken. Since the effect of errors increased with the distance between trajectories, the positions were reset to coincide every fifteen days from the beginning to the end of the trajectory on August 12, 2010. The model was run multiple times, varying WAD and GSF per Table 1. It was observed that the northern portions of the model trajectory tended to follow the observed trajectory when geostrophic currents prevailed and southern parts of the model trajectory were best when wind currents had the largest influence. Subsequently, the trajectories were separated into two parts and the geostrophic components vs. the wind components examined.

For the first three months float trajectory n113 appeared to be affected primarily by geostrophic currents. Trajectory n113 was plotted against OSCURS model trajectories (Figure 7d). OSCURS model was started March 27, 2010 at the point where geostrophic motion appeared to dominate, located at 36.67N° 127.07°W. The WAD and GSF values given in Table 1 were used to compare the n113 trajectory with OSCURS model trajectory (Figure 7d). Markers were placed (Figure 7d) at 15 day intervals in order to compare the OSCURS trajectory to the n113 trajectory.

Analyzing Figure 7d, the first 30 days of the modeled and observed trajectories had similar flow when GSF was set to 5 and WAD set to zero. This means that n113 was predominantly driven by geostrophic currents during this time frame. After 30 days n113 was influenced to a greater extent by wind-driven currents. Note that Figure 7c showed that there was a transition zone from where geostrophy dominated to where the wind-driven currents dominated. The transition zone was better illustrated by running OSCURS model starting May 31, 2010, located at 31.00°N 126.60°W, again varying the optional parameters in accordance with Table 1, and thence comparing to float n113 as seen in Figure 7c. Unlike Figure 7d, the modeled trajectory in Figure 7c followed n113 with optional parameter GSF set to zero. From May 31, 2010 to August 12, 2010, float n113 was mainly influenced by wind induced currents. During this time period, when geostrophy was set to zero, the OSCURS model trajectory tended to follow the observed trajectory of float n113 as opposed to runs where geostrophy was set to five.

C. EXAMINING SPATIAL AND TEMPORAL VARIABILITY OF WIND ANGLE DEFLECTION AND GEOSTROPHIC CURRENT FACTORS

Next, float surface trajectories were divided into 15 day segments. To compare OSCURS modeled trajectories with observed float trajectories the simulated OSCURS trajectories were started at the corresponding float location for each of the 15 day segments. As a first step, OSCURS was run for several selected trajectories while varying the optional parameters, WAD and GSF, following Monte Carlo design (Stein 1987) which defined a domain of all possible inputs and their combinations as follows: WAD was varied linearly from -5 to 5 at 0.1 increments ([-5 : 0.1 : 5]) and GSF was varied linearly from 0 to 5 at 0.1 increments ([0 : 0.1 : 5]). At the same time, OSCURS parameters were also varied following Latin Hypercube Sampling (LHS) design (Stein 1987) to generate a homogeneous random distribution of optional OSCURS parameter values. WAD was varied with Latin Hypercube design from -5 to 5 at 0.1 increments ([-5 : 0.1 : 5]) and GSF was varied with Latin Hypercube design from 0 to 5 at 0.1 increments ([0 : 0.1 : 5]). Examples of Monte Carlo and Latin Hypercube are shown in Figure 9 and Figure 10, respectively.

LHS design provided more homogeneous coverage than random sampling of the same sampling size while requiring fewer samples than the Monte Carlo method. For example, to vary two parameters between N values each, Monte Carlo techniques require N*N samples, while LHS will only need 2*N samples.

To analyze the separation between observed float trajectory and OSCURS modeled trajectories, a threshold of 25 km was selected. The time (days) for each 15 day segment was determined when the separation between modeled and observed trajectories crossed the chosen threshold for the first time. This metric is hereafter called “threshold time” and is measured in days and quantified model prediction skill. A separation threshold plot of the modeled OSCURS output vs. float n113 for each 15 day segment is shown in Figure 8.

To make sure that no details of model output will be lost when applying LHS sampling design instead of Monte Carlo simulations, results given by different sampling designs were compared for 15-day segments of float n113 trajectory using the 25 km

threshold (Figure 8). Each dot corresponded to a single model run with initial time and latitude shown at left and right ordinates, respectively. Model parameters are shown along the abscissa. The latitude was chosen as a marker of float location because this particular float experienced steady southward flow. The dots are color-coded based on the time in days when the separation between observed and modeled trajectories exceeded 25 km for the first time.

As can be seen from Figure 8, the modeled segment initiated on May 10, 2010, yielded the longest prediction of 12 days before separation exceeded the 25 km threshold (Figure 8). Next, the specific latitude where the longest prediction occurred was selected and analyzed to determine which values of WAD and GSF provided these results. Figure 9 is a 2-D slice of Figure 8, which corresponded to the trajectory segment initially collocated in both time and space with the observed trajectory at 33.20N 127.38W. The plot demonstrates how the threshold time changed when OSCURS parameters varied utilizing Monte Carlo methods and shows that with a low GSF, the observed and modeled trajectory separation remained less than 25 km for 12 days.

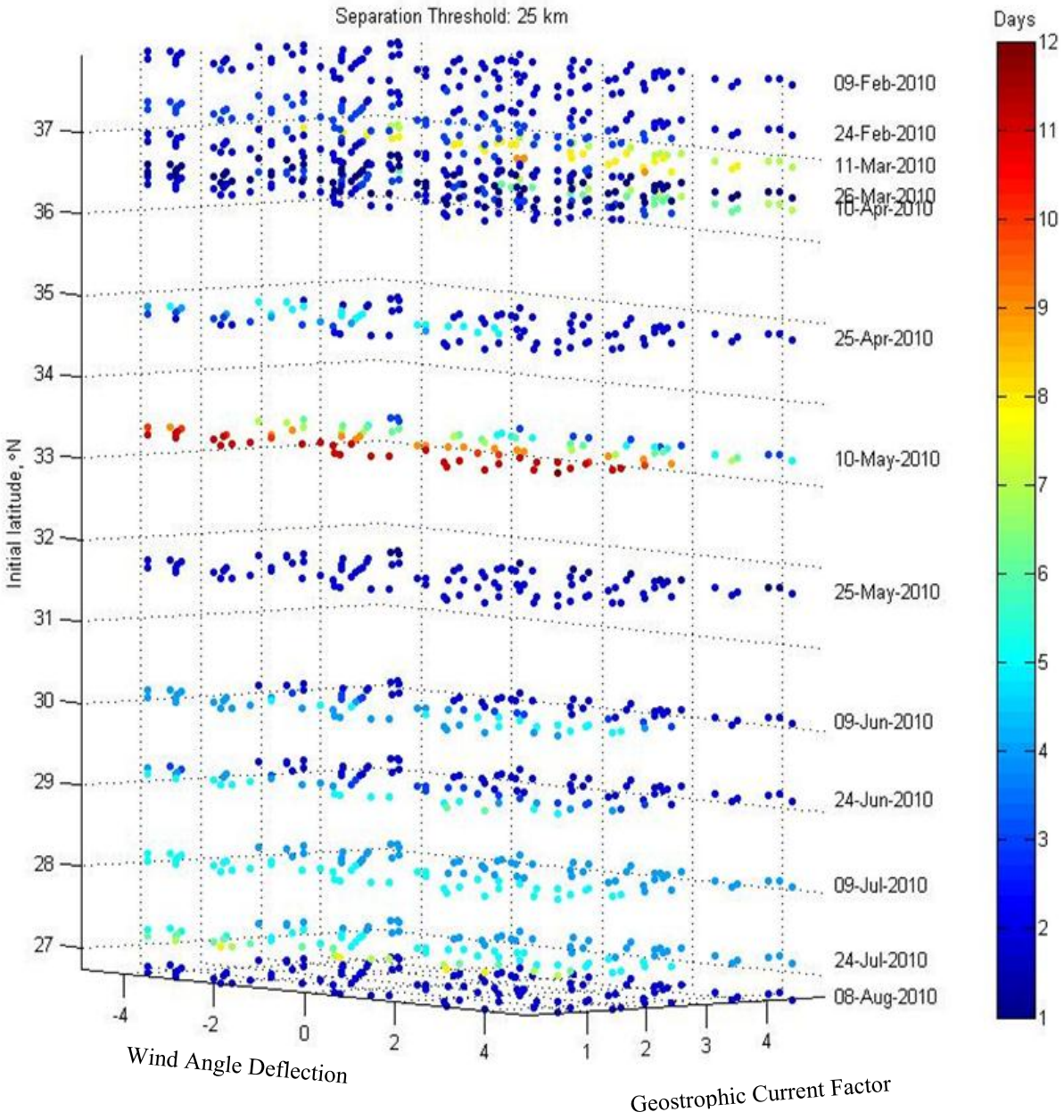

Figure 8. Separation plot of OSCURS modeled output vs. float n113 for the 25 km threshold and 15 day segment. Model parameters were varied by Latin Hypercube sampling. Each color dot corresponds to a single model run with initial time and latitude shown at left and right ordinate, respectively. Model parameters are shown along the abscissa. The dots are color-coded based on the time in days when the separation between observed and modeled trajectories exceeds 25 km for the first time.

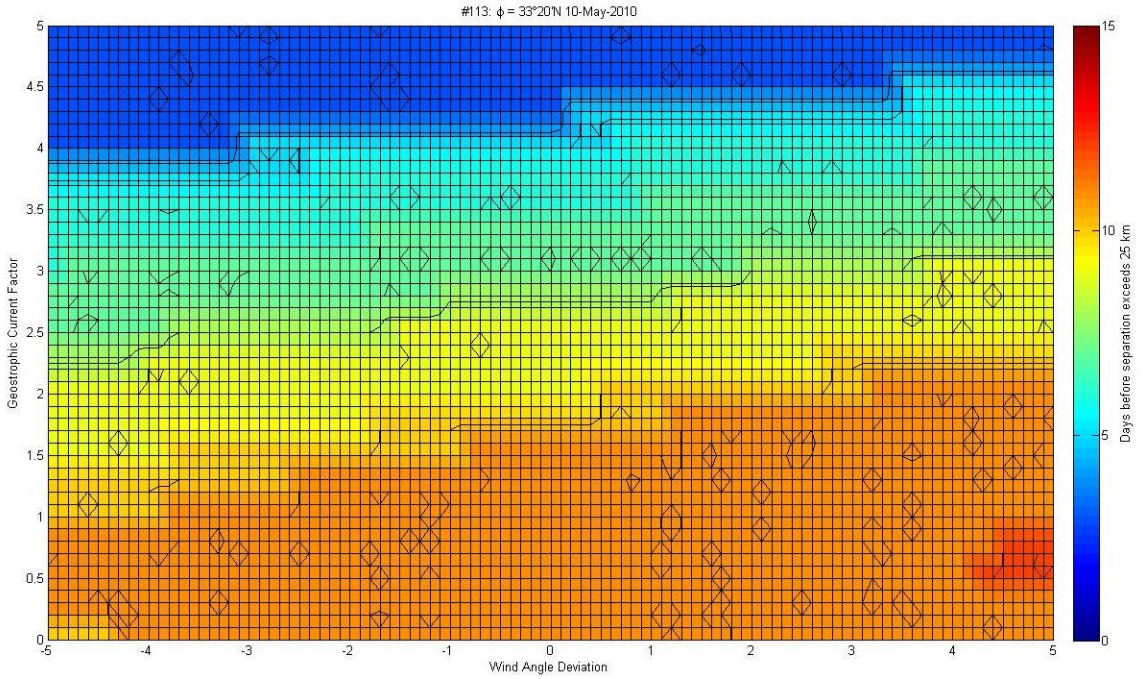

Figure 9. Separation of RAFOS float n113 from OSCURS modeled trajectories using Monte Carlo methods to choose Geostrophic (ordinate) and Wind Angle Deviation (abscissa) parameters. The color bar to the right shows the 25-km threshold time, i.e., the length of time (days) for the separation between model and observed trajectories to exceed 25 km.

Figure 10 shows results of comparing float n113 with OSCURS modeled trajectories utilizing LHS design. Results are shown at the same initial time and position in both Figure 9 and 10 with Figure 9 using the Monte Carlo method and Figure 10 using the LHS method. The LHS method provided results similar to that of the Monte Carlo method. Therefore, for OSCURS trajectories, the LHS design was used. It allowed a significant reduction of time required for computer simulations while preserving the same resolution and results of the Monte Carlo method.

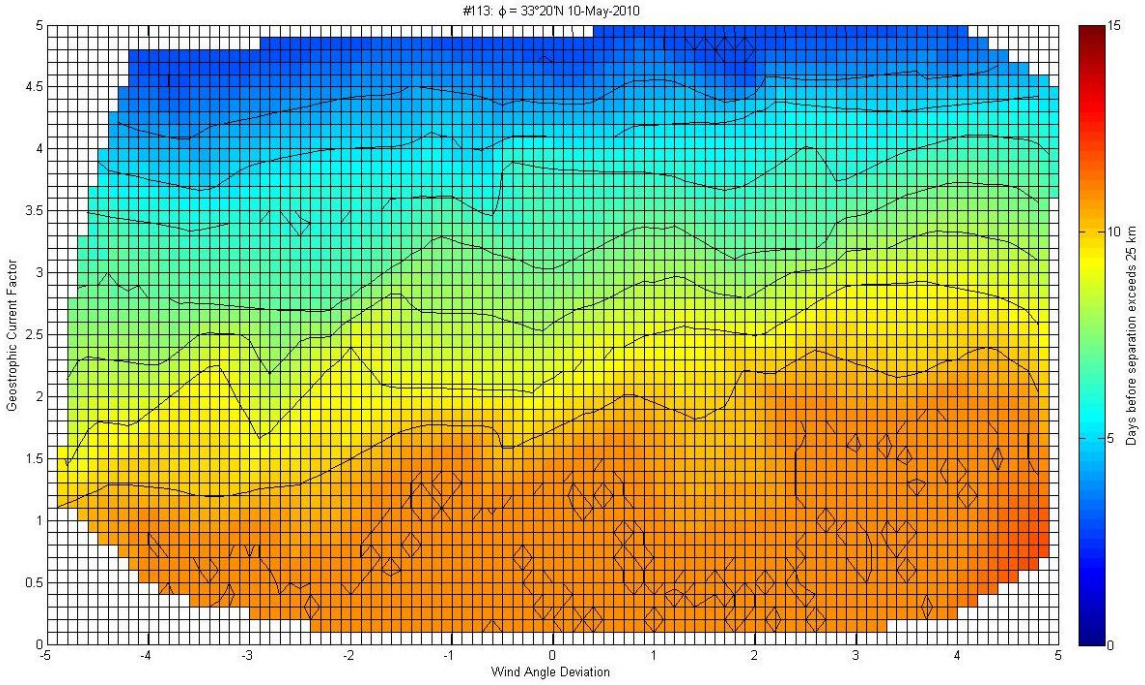

Figure 10. Separation of RAFOS float n113 from OSCURS modeled trajectories using Latin Hypercube methods to choose Geostrophic (ordinate) and Wind Angle Deviation (abscissa) parameters. The color bar to the right shows the length of time (days) for the model and observed trajectories to separate 25 km.

IV. RESULTS AND DISCUSSION

This chapter begins with a description of the observed float trajectories. The float speeds are first compared to those calculated from a simple wind drift model. Next, trajectories are divided into 15-day segments and compared with those produced by three models, OSCURS, gNCOM, and HYCOM. The metric used here for trajectory comparison was the separation of the observed and modeled float as a function of time. Finally, long-term drift comparisons between floats and models are described.

A. FLOAT SURFACE DRIFT PATTERNS AND THEIR SPATIAL-TEMPORAL VARIABILITY

Trajectories of individual floats are included in Appendix A. Figure 4 (Chapter II, above) is a spaghetti diagram which shows all the trajectories on a single chart. Figure 4 is confusing if one attempts to follow a single trajectory but it is meant to give an overview of where the data were collected and how the floats dispersed over the Northeastern Pacific Ocean. Fifty-six percent of surface floats drifted southward. Eleven floats that surfaced south of 37°N (n029, n062, n063, n065, n066, n069, n073, n074, n075, n081, and n113) generally moved southward to 30-32°N where they changed course to southwestward and were tracked as far west as 145°W (n073).

During spring and summer, 12 floats experienced an "S" shaped meandering pattern off either Pt. Sur or Pt. Conception, as they moved southward between 30-38°N and 123–125° (Figure 11); the meandering ceased near 30°N and the floats would then travel westward (n006, n009, n011, n014, n016, n021, n022, n030, n074, n081, and n113). Float n003 also meandered near this location in early fall, 1993. Float n016 had two meanders separated by a three day period, meandering once off of Pt. Sur and then again off Pt. Conception. The period (days) and amplitude (km) of the meander and date the meander occurred are listed in Table 2. The period ranged from 3 to 13 days and the amplitude from 33 to 84 km. Given that these occurred in the summer season, these characteristics are most likely associated with ocean eddies or current meanders as synoptic scale wind variability is typically absent during this period. Note that similar

behavior was observed by Swenson and Niiler (1996) from 1988 to 1989 using Lagrangian mixed layer drifters deployed in late spring. The black dot (Figure 11) approximates the location of meanders noted in Swenson & Niiler (1996). Swenson and Niiler (1996) attributed the observed pattern to a seasonally recurring cyclonic-anticyclonic eddy pair to the north of 34.5°N.

Float #	Period (days)	Amplitudes (km)	Dates
n003	6.49	81.07	September 22 - October 9, 1993
n006	8.91	48.71	April 17 - May 7, 1994
n009	3.54	45.23	May 5 - May 15, 1994
n011	12.92	83.51	March 7 - April 1, 1994
n014	5.98	55.00	April 28 - May 13, 1994
n016	13.16	57.21	March 4 - April 1, 1997
n016	5.18	51.60	April 3 - April 15, 1997
n021	9.15	78.18	July 3 - July 21, 1994
n022	9.51	40.28	June 26 - July 18, 1994
n030	12.48	75.31	June 27 - July 16, 1994
n074	8.22	33.71	April 13 - April 28, 2001
n081	6.70	60.44	June 10 - July 1, 2002
n113	10.23	81.76	April 10 - April 28, 2010

Table 2. Observed meandering behavior listed by float number. The period (days) and amplitudes (km) and dates for each meander are listed.

Observed drift from all floats during March-July totaled 4373 float-days and included 62 different floats. Observed drift during spring-summer for the area 30-40ºN, 120–128ºW was equal to 1713 float-days and 38 floats, respectively. Meandering behavior occurred during 236 float-days (5%) by 12 floats in spring-summer.

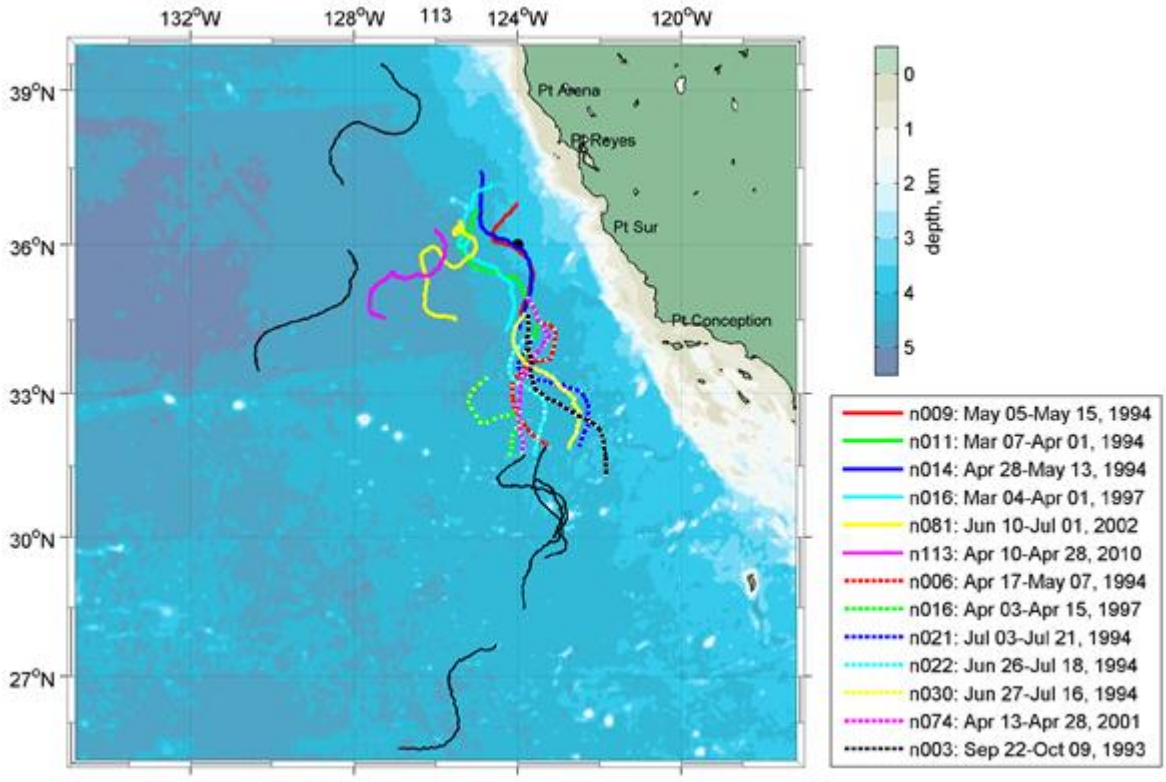

Figure 11. Observed meandering behavior. Black dot at 36°N, 124°W denotes location of meanders noted in Swenson and Niiler (1996). Two groups of meandering ("S" shaped) patterns are shown. One off Pt. Sur and the other off Pt. Conception. The Pt. Sur group is shown by solid colored lines and the Pt. Conception group is shown by dotted colored lines. Floats are indicated in the legend. The color bar to the right indicates water depth. Solid black lines refer to floats n011, n030, n042, n074, n083 that had meanders south of 31.5°N and west of 128°W.

During fall and winter months a seasonal change in direction of float drift from south to north occurred in waters over the slope and shelf along the west coast of the United States. This poleward flowing current extends approximately 150 km from the coast and is called the Davidson Current (Lynn and Simpson 1987). Note that farther north, along the coasts of Canada and Alaska, the flow is poleward year round in the Alaska Current which serves as the Eastern boundary current of the North Pacific Subpolar Gyre. Floats that experienced poleward trajectories surfaced in either fall or winter as far south as 39°N and traveled as far north as 60°N. NPS float 019 (see Appendix A, Figure A19), November 12, 1994 to December 22, 1995, had a southward

flow for about eight days then rotated in an anticyclonic motion, turned northward and traveled poleward along the coast (not shown).

Mean velocities and variance ellipses were calculated using float surface drift for all seasons using 2° x 2° bins (Figure 12). The mean velocities (Figure 12) show the well-documented south, southwest, and westward circulation of the California Current, and the beginnings of the North Equatorial Current---a pattern expected at the Eastern Boundary of the Pacific Subtropical Gyre. For the area 27°N-39°N, 127°W-136°W, typical mean velocities were 5-10 cm/s. Mean velocities along the inshore edge of the California Current and to the west south of 27°N were somewhat larger, 15 cm/s. North of Cape Mendocino, mean velocities were directed northward, 5-10 cm/s, as noted above.

Patterns of flow variability are shown by ellipsis axes in Figure 12 and were normalized so that semi-major axes were the same length for all ellipses. Narrow ellipses were anisotropic which means that the variability of flow was predominately along the semi-major axis; these were typically seen adjacent to the coast where flow variability was constrained by bathymetry. Offshore, circular shapes generally occurred which indicated isotropic conditions, e.g., the currents varied equally in all directions. Greatest variability was seen to the west of Cape Mendocino and to the north of Cape Mendocino where semi-major axes were greater than 5 cm/s. South of Pt. Reyes, semi-major axes were typically 2-4 cm/s.

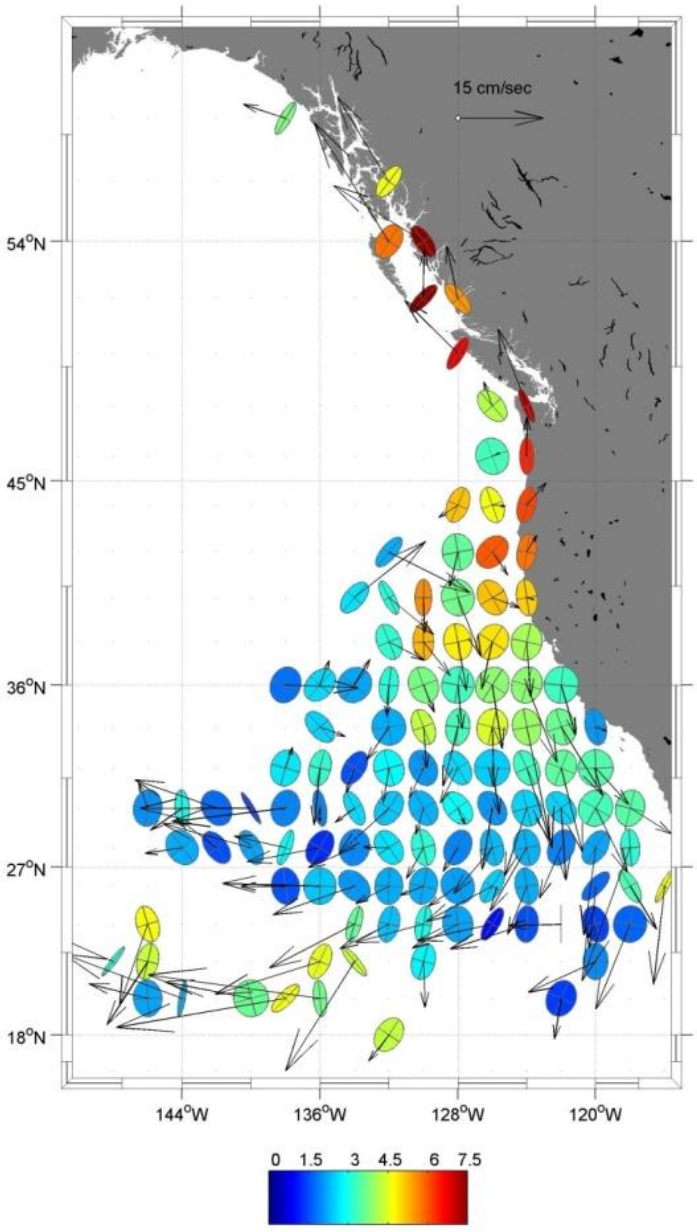

Figure 12. Mean velocities and ellipses for RAFOS float surface drift. Data were sorted into 2° x 2° bins and mean and standard deviation calculated for those bins that had more than 10 observations. Mean velocities are shown as arrows and their scale is given in the upper right corner of the figure. Ellipses are all shown with the same major axis length. The velocity of the semi-major axis of each ellipse is shown by the color bar and has units of cm/s. Minor axis are scaled by the same factor as the major axis so that the shape of the ellipse is correct.

For higher resolution of flow patterns, Figure 13 shows mean float velocities in 1° x 1° bins in the area given by 28–40°N and 120-130°W. The broad southward flow that was seen in Figure 13 is also seen in Figure 12. The ellipses were more elongated, anisotropic, south of 36°N and east of 126°W. Note that the floats did not drift into the region 29–32°N and 127-128°W for the ten days required for mean and ellipse determination. The mean velocity arrows show the currents following a south southwestward pattern and then turning westward in the southern part of the region. For the higher resolution flow patterns, the typical mean velocities were again between 5–10 cm/s with a maximum mean velocity of 30 cm/s at 34–35°N and 123-124°W. Mean velocities were about 5–10 cm/s between 35–38°N, increased to ~15 cm/s at 32–35°N, and then slowed 5–10 cm/s south of 32°N.

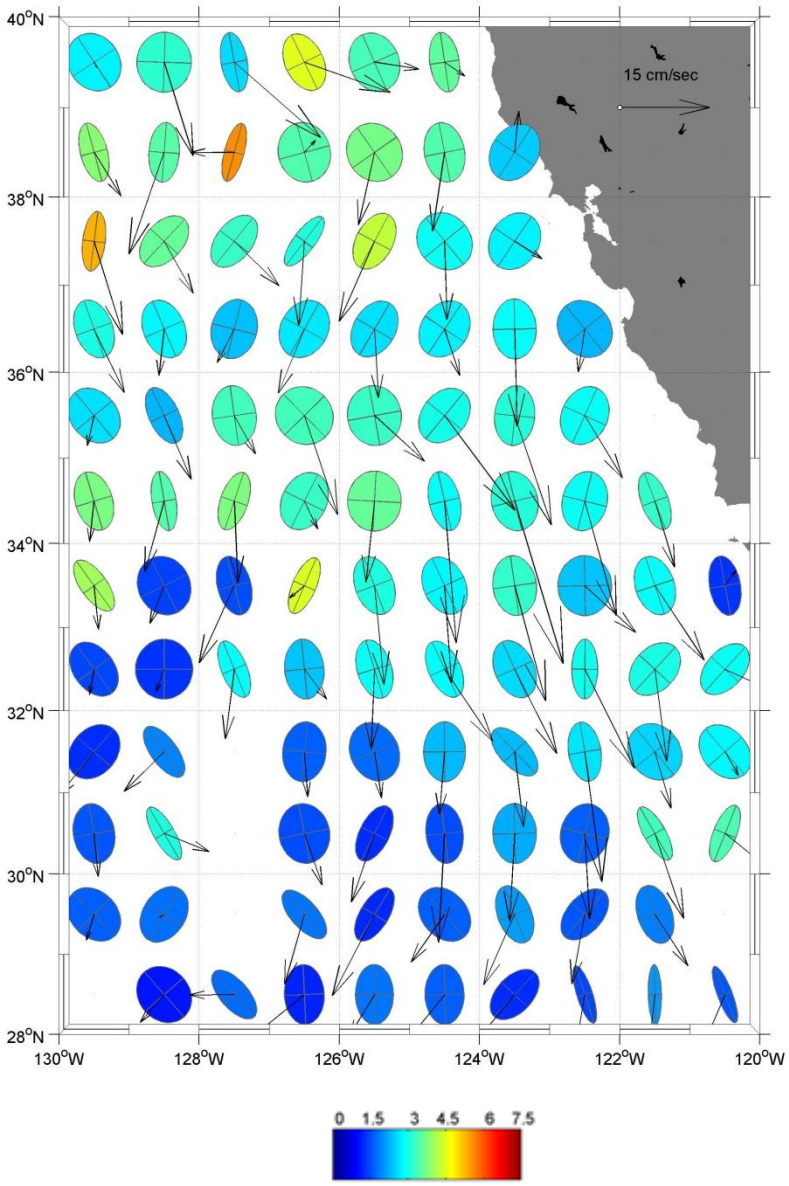

Figure 13. Mean velocities and ellipses for RAFOS float surface drift. Data were sorted into 1° x 1° bins in the area given by 28-40°N and 120–130°W and mean and standard deviation calculated for those bins that had more than 10 observations. Mean velocities are shown as arrows and their scale is given in the upper right corner of the figure. Ellipses are all shown with the same major axis length. The semi major axis length is shown by the color bar and has units of cm/s. Minor axis are scaled by the same factor as the major axis so that the shape of the ellipse is correct.

B. SURFACE FLOAT DRIFT/WIND CORRELATION

There is good enough agreement between wind speed and wind drift current that mariners estimate the magnitude of the wind drift current as 2% of the wind speed when determining a course to make good (Bowditch, 2002). Here a slightly more complicated relationship between wind speed and wind drift current derived by Witting (1909) was used as described above. The speed of the predicted wind drift current was compared to the speed of surface drifter. Analysis was conducted in two geographical areas. The first area, which will be referred to as A1, encompassed all floats within 25-40°N 115–140°W. A second area, A2, encompassed a rectangle with vertices at 35°N 129°W, 35°N 123°W, 27°N 123°W and 27°N 129°W. A2 was selected because the preliminary analysis of float n113 (see Chapter III) demonstrated the float drift in area A2 had strong correlation to wind drift obtained from the OSCURS model. Linear regression analysis (see, for example, Wackerly et al. 2007) was used to determine the percentage of the RAFOS surface drift variability that could be explained by wind drift. Data were sorted into 2.5° x 2.5° bins. Only bins containing at least 25 samples (2-day average) were used (Figure 14).

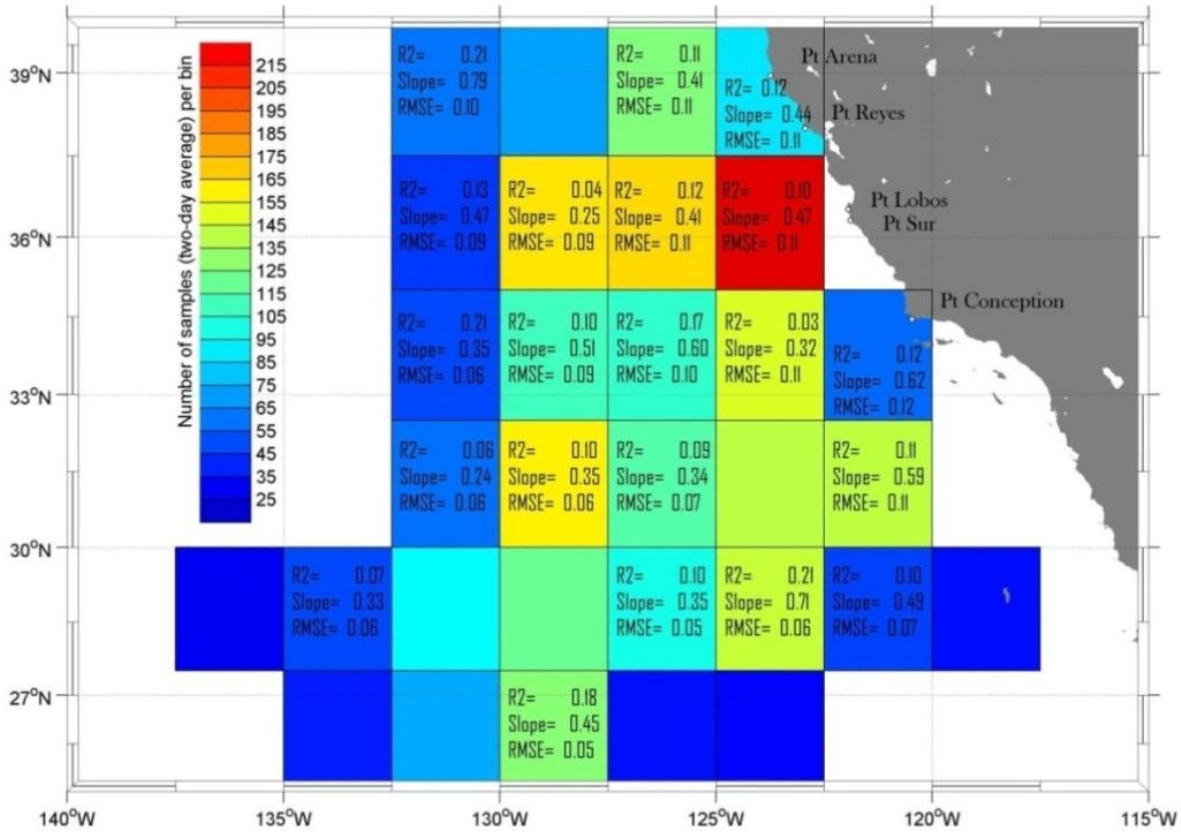

Figure 14. Linear regression diagnosis of surface RAFOS drift speed and wind speed for 2.5° x 2.5° bins. Color shows number of float-days per bin. The coefficient of determination is R^2, Slope is the rate of change of drifter movement compared to the change of wind drift, and RMSE is the root mean square error. Only bins with at least 25 samples (2-day average) were used.

Linear regression coefficients of wind-induced currents and float surface drift were estimated for twenty one 2.5° x 2.5° bins in region A1 as shown in Figure 14. Slope of the regression line for the chosen wind drift model was estimated as 0.36±0.23 (0.50±0.17 and 0.39±0.09% for fall/winter and spring, respectively). 13±6% of float surface drift variability (14±7% and 11±6% for fall/winter and spring, respectively) could be explained by wind-induced drift. For bins where the slope of the linear regression was significantly different from zero (as confirmed by t-test at 95% confidence level), the following numbers are shown (Figure 14): R^2 statistic (coefficient of determination), slope of regression line, and root-mean square error.

Surface float speed and the speed of surface wind drift current were then compared in region A2. Time averaging for one to five days was calculated and four day time averaging produced the best regression results for the data set. Using four day time averages for all data in region A2 showed that 12.9% of the speed of float drift could be explained by wind. Region A2 was then analyzed by restricting the data to different seasons; December-February (winter), March-May (spring), June-August (summer), and September-November (fall) results were 18.0%, 33.7%, 45.4%, and 47.5%, respectively. As an example, results for August-September are shown in Figure 15 when 46% of RAFOS drift could be explained (Slope=1.2 and R^2=0.46). Results indicated that in late summer and early fall correlation was greatest between float speeds and wind speeds.

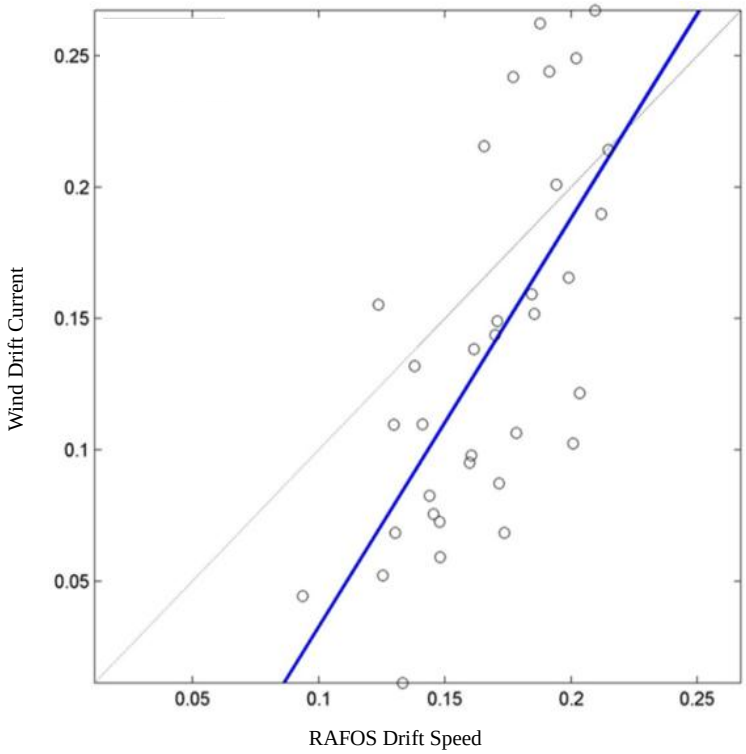

Figure 15. Linear regression analysis of the speed of RAFOS drift and the speed of wind induced current in area 35°N 129°W, 35°N 125°W, 27°N 129°W and 27°N 125°W with four day time averaging for August to September. Small white circles denote data, dark blue line is linear regression

C. COMPARISON OF FIFTEEN DAY MODEL AND FLOAT TRAJECTORIES

Observed float drift was next compared to surface drift from three different ocean models. As metrics of model performance, a time-varying separation (in kilometers) between modeled and observed trajectories for 15 day model runs was used. Quantities derived from this relationship were mean slope of the separation curve from day 1 to 15, i.e., separation growth rate, and the separation after 7-days. These estimates were obtained by averaging of ensembles of 15-day segments for regions and time periods as noted. Three regions will be used for comparison. Region A1, which covered all floats in the data set, is delineated by the area 15-62°N 110-156°W. Region A2, discussed above, encompassed 35°N 129°W, 35°N 123°W, 27°N 123°W, and 27°N 129°W. A3 covered the same latitude and longitude as region A1 but was limited to the following floats n098, n102, n104, n105, n106 n107, n108, n109, n110, n111, n112, n113, n114, and n115 and gNCOM model output from 2006–2010.

1. OSCURS (1992–2010)

The separation between OSCURS and floats were averaged over all 15 day segments in a given month for geostrophic current factor (GSF) and wind angle deflection (WAD). The GSF was varied from 0 to 5 and WAD from -5 to 5. Results are shown in Figure 16. A low GSF (abscissa) provided the lowest separation average per day (ordinate): in August ~ 7 km per day and February ~ 11 km per day. Colors denote the varying WAD parameters for OSCURS and are shown in the legend. Note that during the summer months a higher WAD provided a lower separation rate as compared to winter months where a low WAD provided lower separation rate. April showed a slight decrease in average separation growth rate (slope) with an increase of GSF initially and then the slope began to increase after a GSF of 0.5.

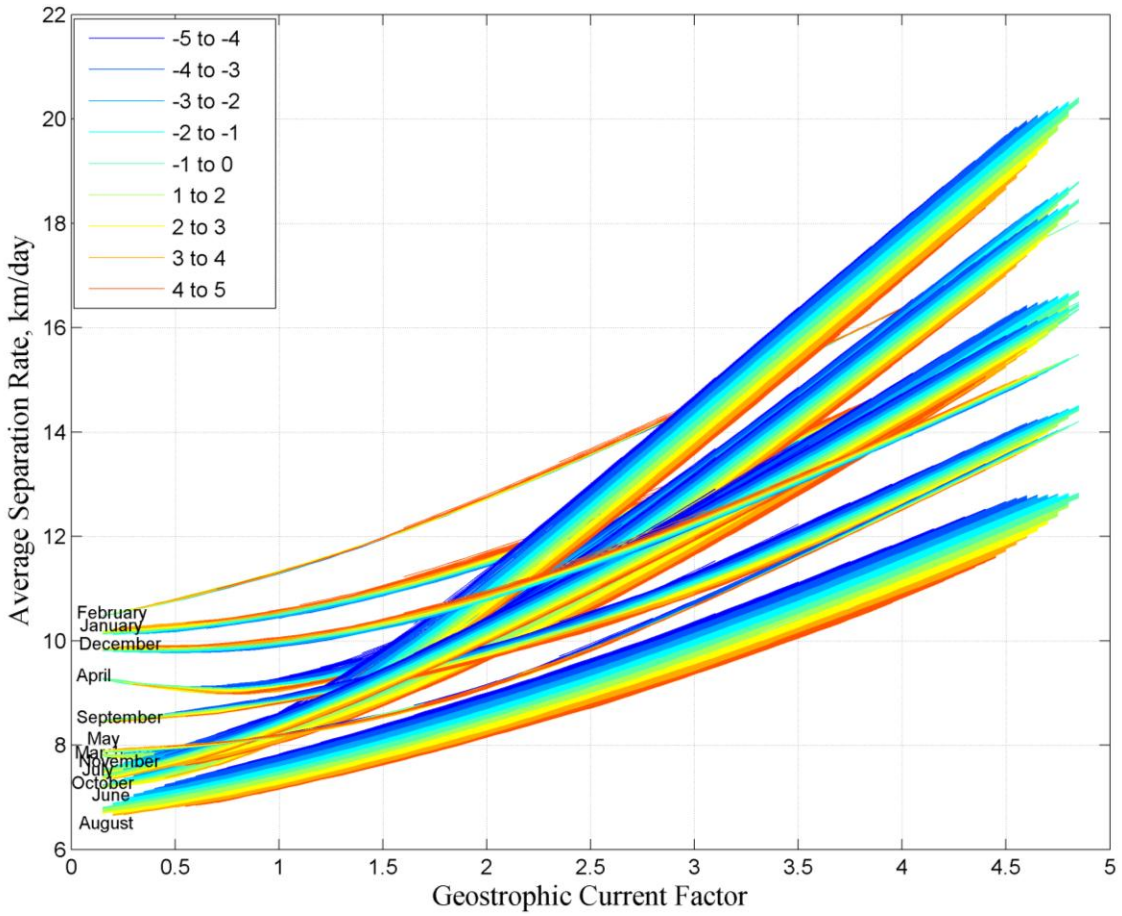

Figure 16. Separation growth rate between OSCURS model and RAFOS trajectories by month. Model trajectories were calculated for Geostrophic Current Factor ranging from 0.1 to 5 as shown along the abscissa and wind angle deflection in the legend.

A Geostrophic Current Factor of 0.5 was found to provide the lowest mean separation rate per day for all months when comparing OSCURS modeled trajectories to float trajectories. Hereafter, the GSF factor of 0.5 was held fixed while examining which WAD factor provided best results in different seasons and regions. Figure 17 shows the separation between OSCURS modeled and float trajectories for the region A1. The grey lines are the separation in km of each 15 day segment while the black error bars are the standard deviation of the mean separation calculated daily. Note that some gray lines are outside the standard deviation at high separation. These outlier gray lines represented 15-day segments where initial separation was high with a large separation rate per day.

These gray lines fell outside two standard deviations from the mean. Results suggest that for mean values the computed OSCURS trajectories were not sensitive to choice of WAD.

Results of separation analysis are also provided in Table 3 for seven days. Within region A1, the mean 7-day separation between observed and OSCURS simulated trajectories was 58.8 km with a standard deviation of 34.2 km and slope of 8.5 km per day. In the same region, with WAD parameter held fixed at -5, the mean 7-day separation decreased to its minimum value for this area and time period, 55.3 km.

Next, monthly variability was examined (Table 3, rows 2 through 13). In general, separation distances were greatest in winter and lowest in summer and fall. For example, Table 3 shows largest (smallest) mean 7-day separation occurred in February (October), 76.0 km (49.1 km), with standard deviation of 37.9 km (31.2 km) and slope of 10.7 km/day (7.7 km/day). Table 3 also gives the WAD associated with the best (lowest) separation and slope. WAD for the monthly results and was typically 4 or 5 except in January, February, March and August when they were about -5. Note that the best WAD for both February and August were either -4 or -5. Results of separation analysis are also provided in Table 3 for seven day timescale.

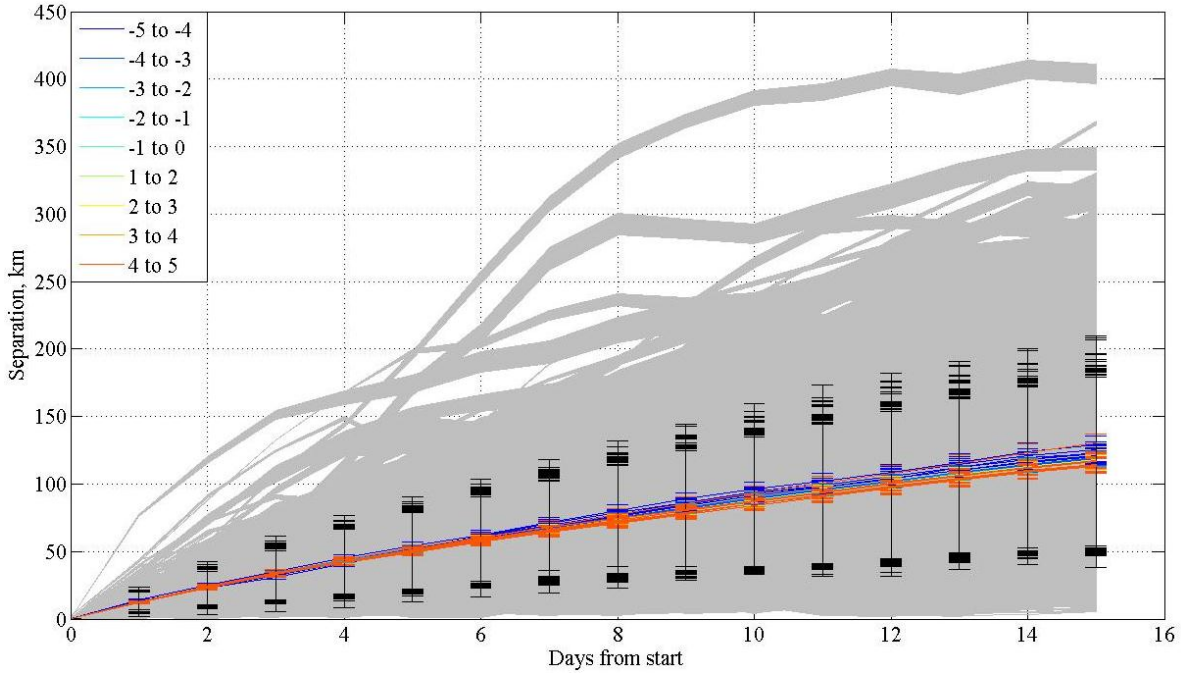

Figure 17. Separation growth rate between OSCURS model and RAFOS float trajectories for all floats. Model trajectories were calculated for wind angle deflection ranging from -5 to 5. Gray lines show separation distance for each 15 day segment. Color lines show mean separation and standard errors at 95% confidence interval for varying wind angle deflection parameters as shown in the legend. Black error bars show standard deviations.

Next, area A2 was selected to compare separation of float trajectories and OSCURS model trajectories. The mean 7-day separation of yearly averaged data decreased to 50.8 km with standard deviation of 28.1 km and slope of 7.3 km per day (Table 3, row 14). The best 7-day separation was obtained in region A2 by fixing the WAD parameter at -5; 7-day separation decreased to 37.6 km with a slope to 6.0 km per day.

Seasonal variability of separation and slope for A2 was analyzed by seasons (Table 3, rows 15–18); December-February (winter), March-May (spring), June-August (summer), and September-November (fall). Worst results were obtained for winter: separation of 64.3 km with a standard deviation of 28.3 km and slope of 8.2 km per day.

Spring yields results similar to the annual mean. Best results were for fall when mean separation was 41.3 km, slope was 6.2 km per day and standard deviation of 27.3 km.

			Slope					Separation				
Region	Start Mon	End Mon	Mean	STD	STD Err	Lowest	Best WAD		STD	STD Err	Least	Best WAD
A1	1	12	8.5	4.6	0.4	8.2	4	58.8	34.2	2.8	55.3	-5
A1	1	1	10.2	5.0	1.3	3.1	-5	69.9	35.1	9.4	34.0	-5
A1	2	2	10.7	4.8	1.4	9.0	-4	76.0	37.9	11.2	33.1	-5
A1	3	3	7.8	5.1	1.4	4.6	5	61.6	37.8	10.2	32.4	-5
A1	4	4	9.1	4.6	1.4	5.7	5	67.1	34.3	10.2	54.9	5
A1	5	5	8.0	3.9	1.1	5.5	5	53.4	27.8	7.9	21.4	5
A1	6	6	7.4	3.7	1.0	6.9	4	50.0	29.9	7.8	38.2	5
A1	7	7	7.7	4.2	1.1	6.3	5	55.5	33.7	8.6	40.3	5
A1	8	8	7.1	3.4	1.0	2.3	-5	49.6	28.8	8.6	26.5	-5
A1	9	9	8.3	4.5	1.4	7.9	4	59.7	33.0	10.2	54.8	5
A1	10	10	7.7	3.8	1.1	5.0	5	49.1	31.2	9.0	28.6	5
A1	11	11	8.0	4.2	1.2	7.7	5	52.4	27.1	7.5	49.4	-4
A1	12	12	10.1	5.9	1.5	3.7	-5	61.2	41.0	10.6	36.6	-5
A2	1	12	7.3	3.5	0.7	6.0	-5	50.8	28.1	5.2	37.6	-5
A2	12	2	8.2	4.9	2.7	9.0	-4	64.3	28.3	16.0	64.0	-5
A2	3	5	7.6	3.2	1.2	6.0	-5	51.2	26.0	10.2	37.5	-5
A2	6	8	7.5	3.1	0.9	6.4	-5	52.9	28.6	8.3	42.3	-5
A2	9	11	6.2	3.7	1.4	6.1	-4	41.3	27.3	10.1	34.2	-4

Table 3. Differences between OSCURS model and RAFOS float trajectories after seven days. OSCURS model data were generated for wind angle deflections (WAD, a parameter used by OSCURS model) ranging from -5 to 5. Data are tabulated for two data sets: A1 includes all data and A2 encompasses the area between 27°N-35°N and 123°W-129°W. Slope is the slope of separation vs. time curve at seven day in km per day.

2. gNCOM (2006 – 2010)

The separation between gNCOM and floats were averaged among all 15 day segments for the period 2006-2010. Hence separation included 15-day segments from 14 floats; n098, n102, n104, n105, n106, n107, n108, n109, n110, n111, n112, n113, n114, n115. Results are shown in Figure 18. As noted for the OSCURS comparison, there are grey lines that are outside of two standard deviations (Figure 17), these were

"rogue" separation curves that were more than two standard deviations from the mean. Each of the rogue gray lines represented 15-day segments where initial separation was high with a large slope (separation growth rate).

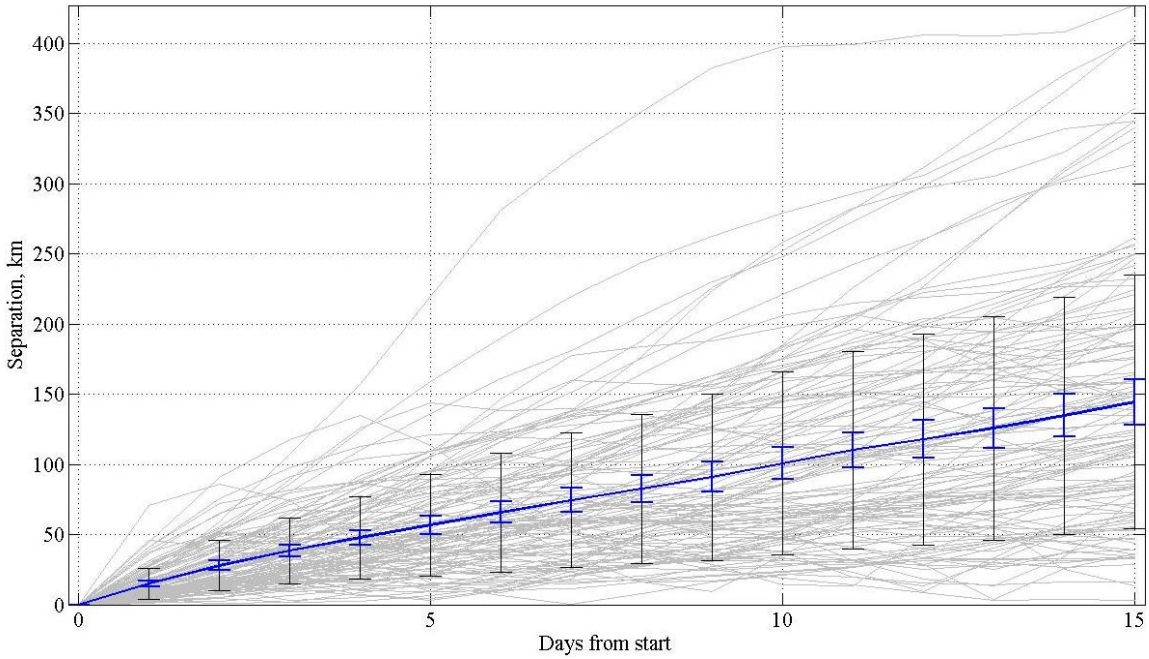

Figure 18. Separation growth rate between gNCOM model and RAFOS float for all floats. Gray lines show separation distance for each 15 day segment. Blue lines show standard error at 95% confidence interval. Gray error bars show standard deviations.

Comparison of 7-day separation of observed trajectories and simulated trajectories is given in Table 4. The annual statistics included all available segments from gNCOM floats. The 7-day separation was 65.8 km with a standard deviation of 42.4 km. Next gNCOM trajectories were compared to float trajectories for each individual month. October revealed the lowest 7-day separation of 45.0 km with a standard deviation of 12.4 km and December revealed the largest 7-day separation with gNCOM floats of 80.6 km with a 90.9 km standard deviation. A2 was then analyzed for all 12 months resulting in a 7-day separation of 62.8 km with a 24.8 km standard deviation. Seasonal variability for A2 was analyzed by season. Largest 7-day separation of 71.3 km with a standard deviation of 26.4 km occurred in winter. Summer revealed the lowest 7-day

separation of 58.3 km with 7.1 km standard deviation. This seasonal variability for model-float separation was similar to those observed for OSCURS.

Region	Start Mon	End Mon	Slope		Separation		
			Mean	STD	7 Day	STD	STD Error
A3	1	12	10.0	6.0	65.8	42.4	7.6
A3	1	1	12.0	4.1	73.6	25.8	15.3
A3	2	2	11.2	5.6	80.4	40.9	18.9
A3	3	3	9.9	5.9	65.0	38.9	18.0
A3	4	4	9.0	6.2	57.4	33.6	19.0
A3	5	5	10.5	7.7	66.2	40.7	25.2
A3	6	6	9.5	3.9	63.6	27.7	17.1
A3	7	7	9.4	7.5	55.7	50.5	31.3
A3	8	8	8.2	4.3	47.7	35.6	28.5
A3	9	9	9.4	6.9	60.7	50.6	57.2
A3	10	10	8.3	1.1	45.0	12.4	14.0
A3	11	11	8.8	5.1	60.8	38.1	23.6
A3	12	12	10.4	10.6	80.6	90.9	63.0
A2	1	12	10.3	4.2	62.8	24.8	10.6
A2	12	2	14.1	1.1	71.3	26.4	21.1
A2	3	5	9.3	3.5	59.9	28.4	16.8
A2	6	8	7.3	5.6	58.3	7.1	7.0

Table 4. Differences between gNCOM model and RAFOS float trajectories after seven days. Data are tabulated for two data sets: A2 encompasses the area between 27°N-35°N and 123°W-129°W. A3, covers all RAFOS floats n098, n102, n104, n105, n106, n107, n108, n109, n110, n111, n112, n113, n114, n115 and area 15-62°N 110-156°W. Slope is the slope of separation vs. time curve at seven day in km per day.

3. HYCOM (2010)

The same approach used for comparison of OSCURS and gNCOM model outputs and float observed trajectories was conducted with HYCOM. Unlike OSCURS and

gNCOM where multiple floats were available in the date range, only two floats (n113 and n115) were available for HYCOM. Float n113 (Figure 6) trajectory was within area A2. Float n115 (Figure 6) occurred during winter and spring months and encompassed poleward flow along the coast north of 45°N. Mean 7-day separation comparison included the combination of n113 and n115 but floats were also compared separately. For these HYCOM comparisons, there were fewer data and both standard deviation and confidence intervals were larger than those for previous comparisons.

The separations between HYCOM and float were averaged among all 15 day segments and are displayed in Figure 19. Again, just as described for OSCURS and gNCOM, there were 15-day segments that lay outside the standard deviation. These segments were distinguished by a large high separation rate in km per day between the observed and simulated segments.

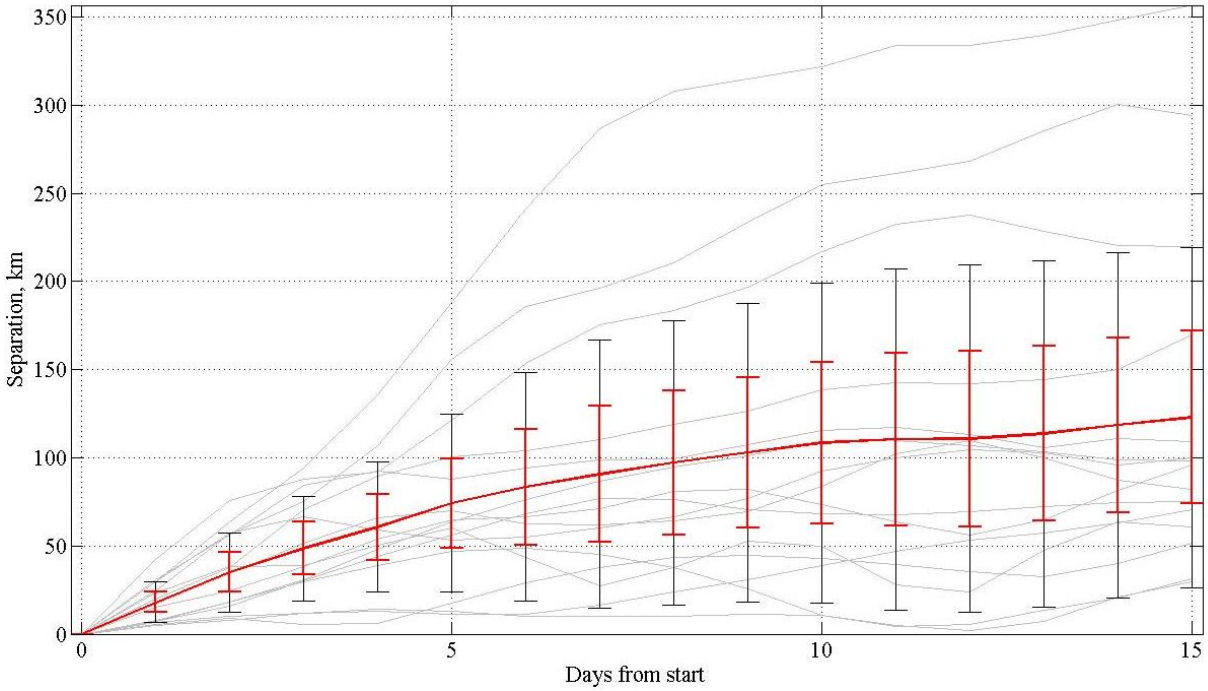

Figure 19. Separation growth rate between HYCOM model and RAFOS float for floats n113 and n113. Gray lines show separation distance for each 15 day segment. Red lines show mean separation at 95% confidence interval. Gray error bars show standard deviations.

Float observed trajectory and HYCOM simulated trajectory results are given in Table 5. Comparison of observed float and HYCOM simulated trajectories for n113 and n115 revealed a 7-day separation of 83.4 km with a 64.9 km standard deviation and slope of 9.9 km per day (Table 5). Observed float n113 segments and the HYCOM simulated segments resulted in a 67.6 km 7-day separation with a 52.7 km standard deviation and slope of 8 km per day while observed float n115 segments and HYCOM simulated segments comparison resulted in a 146.4 km separation at 7-days with an 82.3 km standard deviation and slope of 14.4 km per day. The large separation for n115 can be attributed to the coastal flows which were not captured by HYCOM.

	Slope		Separation		
Floats	Slope	Slope STD	7 Day Sep	STD	STD error
113 & 115	9.9	8.1	83.4	64.9	32.8
113	8.0	6.7	67.6	52.7	29.8
115	14.4	10.3	146.4	82.3	93.2

Table 5. Differences between OSCURS model and HYCOM float trajectories after seven days. Data are tabulated for three data sets: RAFOS floats n113 and n113, RAFOS float n113, and RAFOS float n115. Slope is the slope of separation vs. time curve at seven days in km per day.

4. Model Comparison

The comparison of gNCOM and OSCURS mean 7-day separation between observed and simulated trajectories for region A2 and A3 is shown in Table 6. Analysis of all 15 day segments from A3 shows that difference between gNCOM and OSCURS 7-day separation is low with a 7-day separation of 66.9 km for OSCURS and 65.8 km for gNCOM, and the standard deviation between the two was 38.7 km for OSCURS and 42.4 km for gNCOM.

Next, OSCURS and gNCOM were compared for area A2 (Table 6). This comparison showed that the 7-day separation between observed and simulated trajectories for OSCURS (gNCOM) decreased to 51.2 km (62.8 km) with standard

deviation of 31.7 km (24.8 km). Region A2 was then analyzed by restricting the data to different seasons; December-February (winter), March-May (spring), June-August (summer), and September-November (fall). The 7-day separation with 64.5 km (71.3 km) was greatest in winter with OSCURS (gNCOM) having a standard deviation of 39.7 km (26.4) km for gNCOM. Summer revealed the smallest 7-day separation with OSCURS (gNCOM) having a 7-day separation of 48.9 km (58.3 km) and standard deviation of 13.0 km (7.1 km).

				Slope					Separation				
Model	Region	Start Mon	End Mon	Mean	STD	STD Error	Lowest	Best WAD		STD	STD Error	Least	Best WAD
OSCURS	A3	1	12	9.8	5.2	0.9	8.9	-5.0	66.9	38.7	6.6	61.6	-5.0
gNCOM	A3	1	12	10.0	6.0				65.8	42.4	7.6		
OSCURS	A2	1	12	7.6	3.3	1.6	6.0	-5.0	51.2	31.7	16.1	37.6	-5.0
gNCOM	A2	1	12	10.3	4.2				62.8	24.8	10.6		
OSCURS	A2	12	2	9.5	3.2	2.8	9.0	-4.0	64.5	39.7	38.9	61.0	3.0
gNCOM	A2	12	2	14.1	1.1				71.3	26.4	21.1		
OSCURS	A2	3	5	8.1	4.1	3.0	6.0	-5.0	51.9	37.6	27.4	37.5	-5.0
gNCOM	A2	3	5	9.3	3.5				59.9	28.4	16.8		
OSCURS	A2	6	8	7.1	1.5	1.5	6.4	-5.0	48.9	13.0	12.8	37.4	-5.0
gNCOM	A2	6	8	7.3	5.6				58.3	7.1	7.0		

Table 6. Comparison between OSCURS model and gNCOM model after seven days. Data are tabulated for two data sets covering RAFOS floats n098, n102, n104, n105, n106, n107, n108, n109, n110, n111, n112, n113, n114, n115: A2 encompasses the area between 27°N-35°N and 123°W-129°W. A3 encompasses the area 15-62°N 110-156°W. Slope is the slope of separation vs. time curve at seven days in km per day.

For floats n113 and n115 the comparison of gNCOM, OSCURS, and HYCOM 7-day separation are shown in is shown in Table 7. The comparison covers January 1, 2010 to December 31, 2010 and included15–day segments from only two floats, n113 and n115. The comparison of 7-day mean separation for floats n113 and n115 for OSCURS, gNCOM, and HYCOM show a mean 7-day separation of 67.8 km, 74.5 km, 83.4 km with

standard deviation of 48.2 km, 35.8 km, 64.9 km, respectively. As mentioned above, gNCOM and HYCOM are global models and float n115 trajectory was poleward coastal flow.

Next, model comparison was done for on float n113 in area A2. The comparison of 7-day separation for floats n113 for OSCURS, gNCOM, and HYCOM show a mean 7-day separation of 51.0 km, 62.9 km, 67.6 km with standard deviation of 24.4 km, 24.8 km, 52.7 km, respectively.

		Slope		Separation				
Model	Floats	Mean	STD		STD	STD Error	Least	Best WAD
OSCURS	113 & 115	9.2	6.2	67.8	48.2	24.4	50.7	5.0
gNCOM	113 & 115	9.7	5.1	74.5	35.8	18.1		
HYCOM	113 & 115	9.9	8.1	83.4	64.9	32.8		
OSCURS	113	7.3	3.7	51.0	24.4	13.8	37.6	-5.0
gNCOM	113	10.2	4.2	62.9	24.8	10.6		
HYCOM	113	8.0	6.7	67.6	52.7	29.8		

Table 7. Comparison between OSCURS, gNCOM, and HYCOM model after seven days. Data are tabulated for two data sets: combination of RAFOS floats n113 and n115 and RAFOS float n113. Slope is the slope of separation vs. time curve at seven day in km per day.

The ability to tune OSCURS resulted in OSCURS having lower separation between float observed trajectories and OSCURS modeled trajectories. gNCOM and HYCOM were configured for the open ocean and gNCOM and HYCOM model output comparison to float trajectories along the coast does not fully represent gNCOM and HYCOM model performance.

D. ANALYSIS OF LONG-TERM DRIFT OF RAFOS AND MODEL OUTPUT

With 15-day trajectories, model or observational errors or smaller scale features that were not modeled, could be overlooked. What would actually happen to longer term model trajectories if the separation was not reset to zero? To address this issue, comparisons of long term drift between observed floats drift and simulated model drift for OSCURS, gNCOM, and HYCOM were made (Appendix B). For these comparisons,

the trajectories were not reset every 15 days but allowed to continue until the float could no longer be tracked. Floats n098, n102, n104, n105, n106, n107, n108, n109, n110, n111, n112, n113, n114, n115 trajectories were used. For these comparisons, OSCURS trajectories were simulated with WAD=0, GSF=1, and WCSC=1.

Floats n105 (Figure B5), n107 (Figure B7), n109 (Figure B9), n110 (Figure B10), n111 (Figure B11), and n112 (Figure B12) observed trajectories and simulated trajectories for gNCOM/OSCURS and float n113 (Figure B13) observed and simulated trajectories for gNCOM/OSCURS/HYCOM (n113) experienced the same long-term flow patterns. Each of these comparisons was for floats that were at least 50 km from the coast and moved either westward (n111, n112) or southward (n105, n107, n109, n110, and n113). Float n104 observed trajectory and OSCURS simulated model trajectory (Figure B6) experienced the same long-term southward flow but the gNCOM n104 southward trajectory stayed offshore along the meridian of the first position (126°W) and then turned westward at 130°W.

Comparisons of model output and observed long-term drift for floats that drifted into waters close to the coast indicated poorer agreement. Examples include northward flow for floats n102 (Figure B2) where the model trajectories ended about 5° south of the float, n108 (Figure B8) where the model trajectories ended about 6° south of the float, and n115 (Figure B15) where model trajectories also ended about 6° south of the float. An example of southward flow, float n114 (Figure B14) moved into the Southern California bight while the model trajectories were southward with the OSCURS trajectory ending much farther south, 25°N, than either the gNCOM trajectory, 31°N, or the float, 34°N. These differences were due to horizontal shear in the coastal zone which was not well captured in the models.

Long term drift comparison between observed float trajectories and simulated trajectories was dependent on multiple factors. One factor contributing to errors between observed and simulated long term drift is the accuracy of the initial starting position between float and modeled trajectory. As stated in Chapter II, the accuracy of float position was obtained from Argos and can be in error by as much as 1.5 km. While these errors were small compared to the best model resolution (HYCOM, ~9 km), they could

grow rapidly in the simulated trajectories and the distance between the float and model float would increase. Prediction of long term drift was also limited by dynamical processes that are unresolved in time or space by numerical ocean models, such as inertial oscillations and turbulence in the surface velocity fields. Float n113, in the area of 33-36°N experienced an "S" shaped meander that was not resolved in the model simulated trajectories from OSCURS, gNCOM, or HYCOM (see Appendix B, Figure B13). Note that assimilation of drifter data into ocean models can yield eddies or turbulence that would not be otherwise resolved by model output.

THIS PAGE INTENTIONALLY LEFT BLANK

V. SUMMARY AND CONCLUSIONS

This study described the surface drift of undrogued floats on the ocean surface in the Northeastern Pacific Ocean during 1992 to 2010 and compared the movement of the floats to wind drift and surface currents derived from three models of the ocean surface current, a NOAA Ocean Surface Current Simulator (OSCURS) which is readily accessible and user friendly, and two advanced Navy global models, the Global Naval Coastal Ocean Model (gNCOM), and a more recent global model, the HYbrid Coordinate Ocean Model (HYCOM). The goal of the study was to understand the movement of flotsam and the limits of our ability to predict its movement.

The observed drift pattern of surface floats showed the surface drift of the California Current System similar to the mean patterns depicted on pilot charts or in text books (Sverdrup et al., 1942). The mean velocities, typically 5–10 cm/s, showed the southward and southwestward progression of the California Current flow along the coast of California as well as the beginnings of westward flow in the North Equatorial Current. Mean velocities along the inshore edge of the California Current and to the west south of 27°N were somewhat larger, 15 cm/s. North of Cape Mendocino, mean velocities next to the coast were directed northward, 5-10 cm/s, indicating the presence of the Davidson Current or, off the coasts of Canada and Alaska, the Alaska Current. A pattern of "S" shaped meanders was seen off the California Coast between Point Sur and Point Conception in summer; the period of the meander ranged from 3 to 13 days and the amplitude from 33 to 84 km.

Patterns of the variability of the offshore flow about the mean were generally isotropic, e.g., the currents varied equally in all directions about the mean. Next to the coast, flow was constrained by bathymetry so flow variability was primarily alongshore. Greatest variability was observed to the west of Cape Mendocino and to the north of Cape Mendocino where semi-major axes were greater than 5 cm/s. South of Pt. Reyes, semi-major axes were typically 2–4 cm/s.

The speed of the wind induced current, *C*, was determined from wind speed, *W*, as $C = kW^{½}$, where k = 4.8 (Witting, 1909). Linear regression analysis was used with four day averages to examine the relationship between C and the speed of float drift. Highest correlation occurred during the summer and fall months. By limiting the area analyzed and restricting the time of year to summer months, 47.5% of float variability could be explained by wind forcing and the regression relationship indicated that for each cm/s of wind drift, the floats drifted at a rate of 1.2 cm/s. Using all data, only 13 ± 6% of float variability was explained and each cm/s of wind drift resulted in an increase of 0.5 cm/s of float drift.

Drifter trajectories simulated by three ocean models, OSCURS, gNCOM, and HYCOM were compared with observed RAFOS trajectories to determine how well models predicted the movement of RAFOS floats or flotsam on the ocean surface. For this comparison, float trajectories were broken into 15-day segments with corresponding model trajectories started at the observed float position at the start of each 15-day segment. A limitation of this comparison was that only OSCURS was available for the entire data set; comparisons for gNCOM were possible only for the period 2006-2010 and HYCOM for 2010. Following Ingraham and Miyahara (1989), OSCURS model variables were selected by case study using float n113. It was found by selecting a low Geostrophic Current Factor (GSF) parameter, 0.5, and varying the Wind Angle Deflection (WAD) parameter, OSCURS was able to model short term trajectories with a lower mean separation than gNCOM and HYCOM. No specific WAD parameter produced the best results from OSCURS for the entire data set. When restricting the data to 35°N 129°W, 35°N 123°W, 27°N 123°W and 27°N 129°W, a WAD of -5 or -4 produced the lowest separation. For example, a minimum (maximum) separation was observed in fall (winter) with a 7-day separation of 41.3 km (64.3) and WAD parameter of -4 (-5).

The mean separation between float drift and model drift was calculated for each day and is shown in Figure 20. Results show lowest 7-day separation of 62 km, 72 km, and 85 km for OSCURS, gNCOM, and HYCOM, respectively. OSCURS gave best results due to the ability to choose a WAD that gave the smallest separation. Note too

that for time greater than eleven days, HYCOM separations were less than gNCOM and approached OSCURS mean separation (114 km) at 15-days.

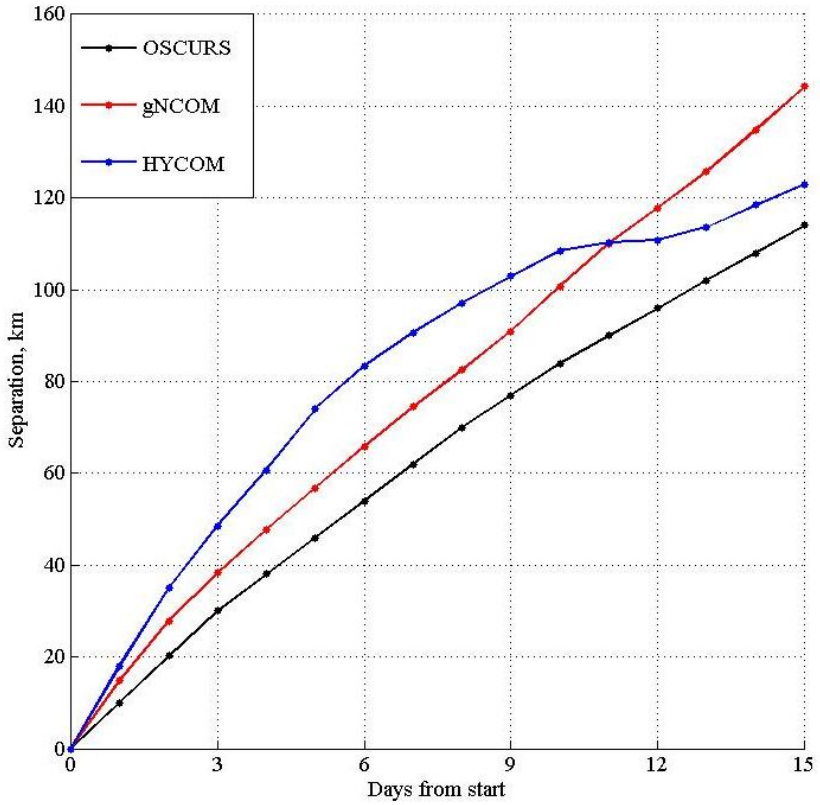

Figure 20. Mean 7-day separation of OSCURS, gNCOM, and HYCOM. OSCURS is black, gNCOM is red, and HYCOM is blue.

Another comparison between models is given for float n113, the only example of a long-term float that was not imbedded in a coastal flow for which trajectories could be produced from all three floats. Breaking the data into 15-day segments and computing mean separation yielded 7-day separation between float n113 and OSCURS of 51 km followed by gNCOM, 62.9 km, and HYCOM 67.6 km. Although HYCOM had the highest 7-day separation, HYCOM's long-term drift trajectory followed the observed trajectory best of the three models (Figure 21). At the end of the 185-day trajectory, the HYCOM modeled float was 168.1 km from float 113 compared to 1073 km (525 km) for gNCOM (OSCURS). But note that HYCOM failed to produce the shoreward

anticyclonic meander of float n113 that occurred near the beginning of the trajectory. Comparison of all three models with nearshore drift (Figure B15) indicate that additional work needs to be done to model flow nearshore; examples of observations that would improve model trajectories in nearshore regions include available CODAR observations as well as possible future coastal satellite altimeters.

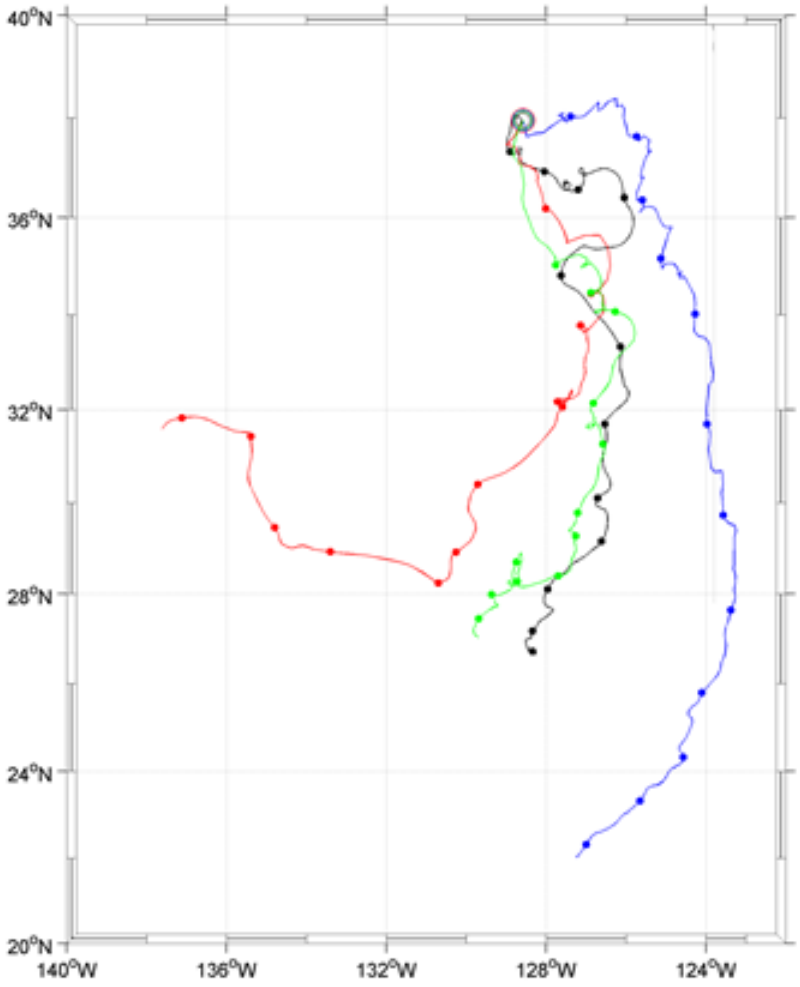

Figure 21. Trajectories for float n113. Black is the observed trajectory, green is the HYCOM trajectory, red is the gNCOM trajectory and blue is OSCURS trajectory. Dots are placed every 15 days along each trajectory. The starting point of the trajectory is circled.

For a seaman trying to locate flotsam, the guidance from this thesis is models will be of limited assistance. Depending on sea conditions and flotsam characteristics, a vessel would need to be within about 1 km to be able to visually sight the flotsam. The average separation rates obtained above for model trajectories yielded initial separation rates of 10-20 km/day (Figure 20). For an object falling overboard, once sight of an object is lost, the best course of action would be to retrace the ship's track using GPS, perhaps using wind drift currents or pilot charts to estimate flotsam movement.

THIS PAGE INTENTIONALLY LEFT BLANK

APPENDIX A

Appendix A contains a short description and chart of each RAFOS float surface trajectory. The description includes the float number, the start and end date of the trajectory, and a brief explanation that is meant to resolve ambiguity of the charted trajectory. The data extracted from ARGOS (not the smoothed, interpolated data used above) were used to create each trajectory. Dots along a trajectory are 15 days apart. The color of the trajectory changes with season: winter (December, January, and February) is blue, spring (March, April, and May) is black, summer (June, July, and August) is magenta, and fall (September, October, and November) is red.

The ARGOS observations of float position are available at http://www.oc.nps.navy.mil/npsRAFOS.

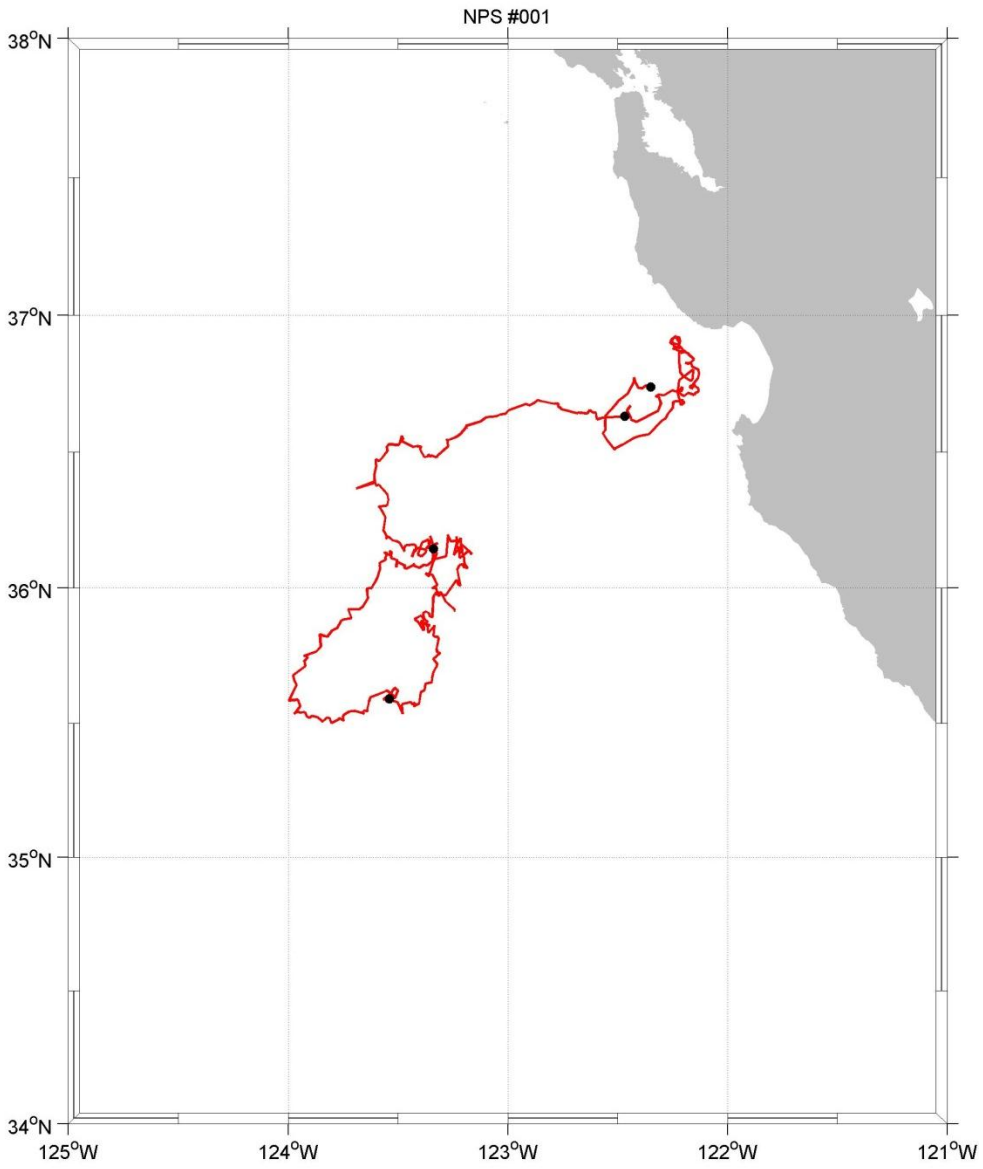

Figure A1. Surface trajectory for RAFOS float n001 from September 11, 1992, to November 5, 1992. Black dots are placed every 15 days along the trajectory. The red trajectory indicates the observations were made in the fall.

Float n001 surfaced west of Monterey Bay at 122.35°W and initially moved cyclonically toward the coast for 7 days, reaching the most northward extent of its trajectory on Sept. 17 near the northern edge of Monterey Bay. It thence retraced its path and moved westward until turning southward near 123.6°W. 30 days after surfacing, it began to loop cyclonically, reaching its most westward excursion on October 17. On November 2 at 36.2°N, it commenced a smaller cyclonic loop. N001 ended at 35.9°, 123.25°W.

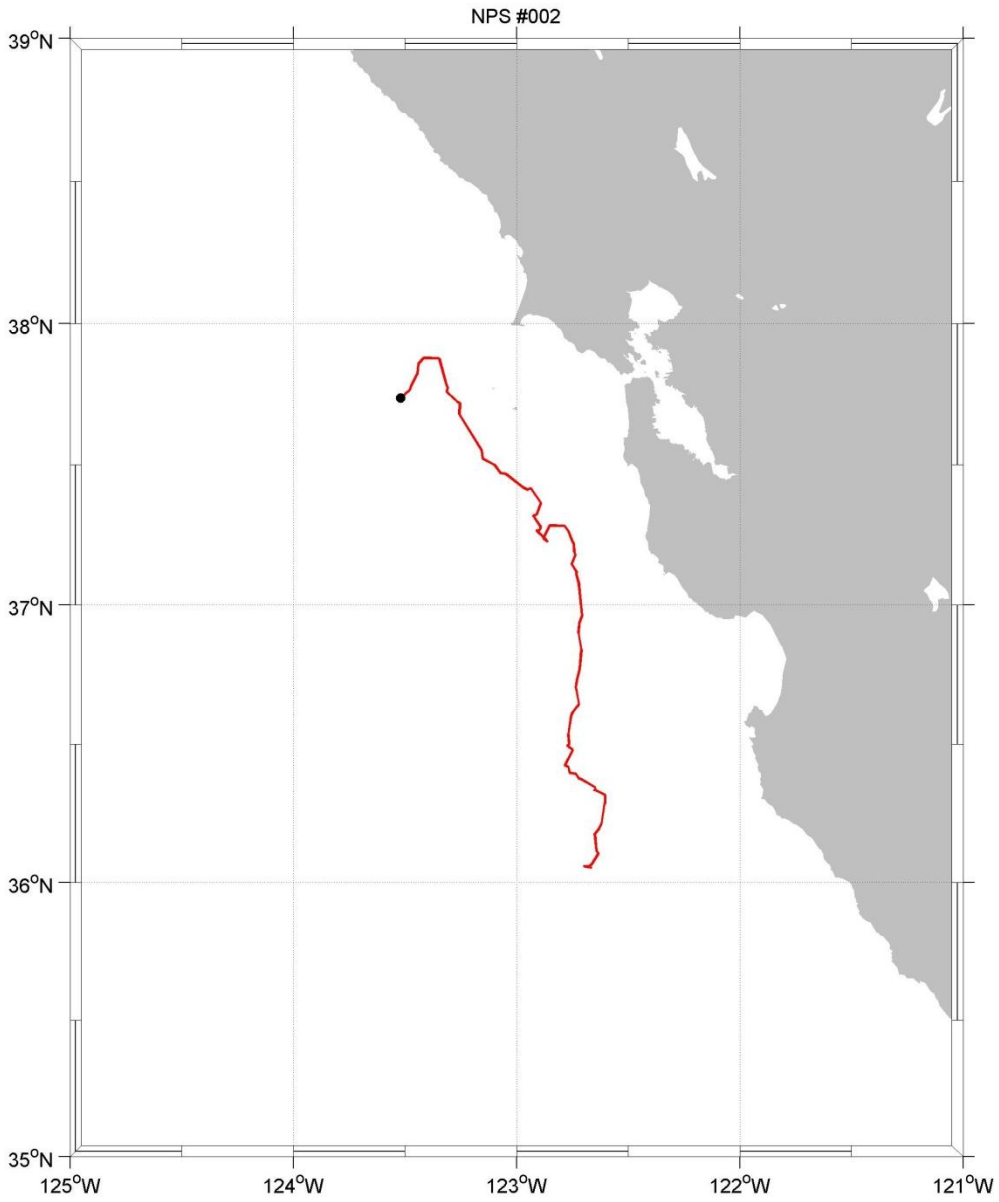

Figure A2. RAFOS float obtained its first fix 37.74°N 123.52°W September 11, 1992, and was tracked until September 24, 1992. The float traveled northeast for 1 day, southeast for 5 days, and southwards for 5 days, then followed a curve from southeast to southwards in 2 days. The long term drift for this float is southward. The red trajectory denotes fall observations.

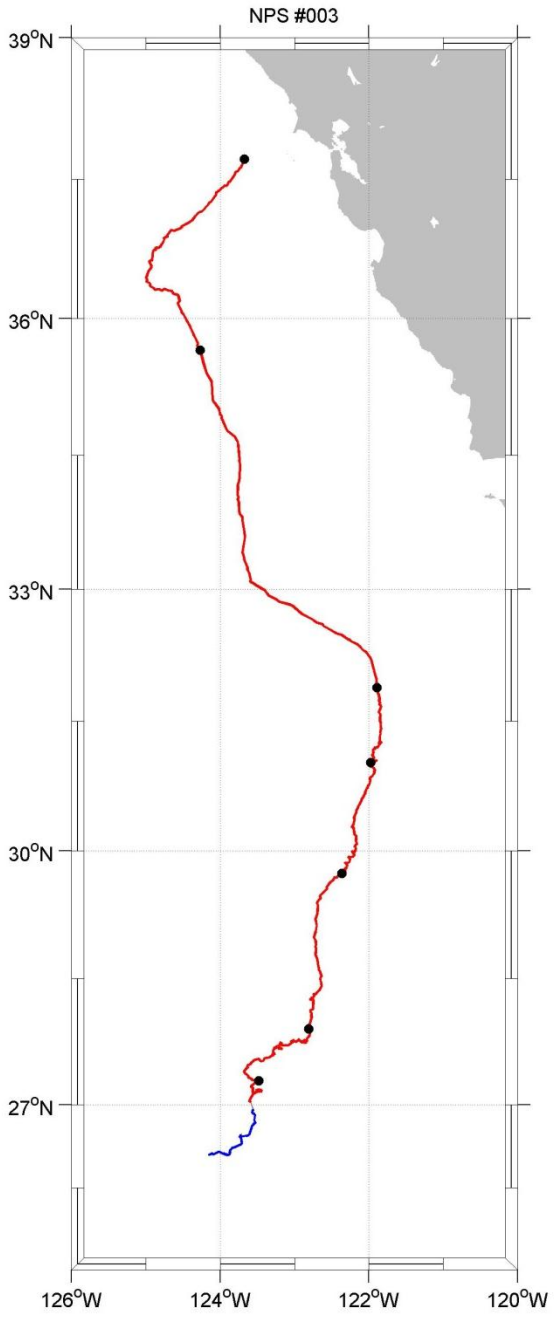

Figure A3. RAFOS float n003 obtained its first fix (37.72°N 123.68°W) September 5, 1993, and was tracked until December 9, 1993. The float generally meandered southward in the California current system. Dots along the trajectory are 15 days apart. A small data gap during the last 15 days is less than two days. Colors represent different seasons in the trajectory: fall (red) and winter (blue).

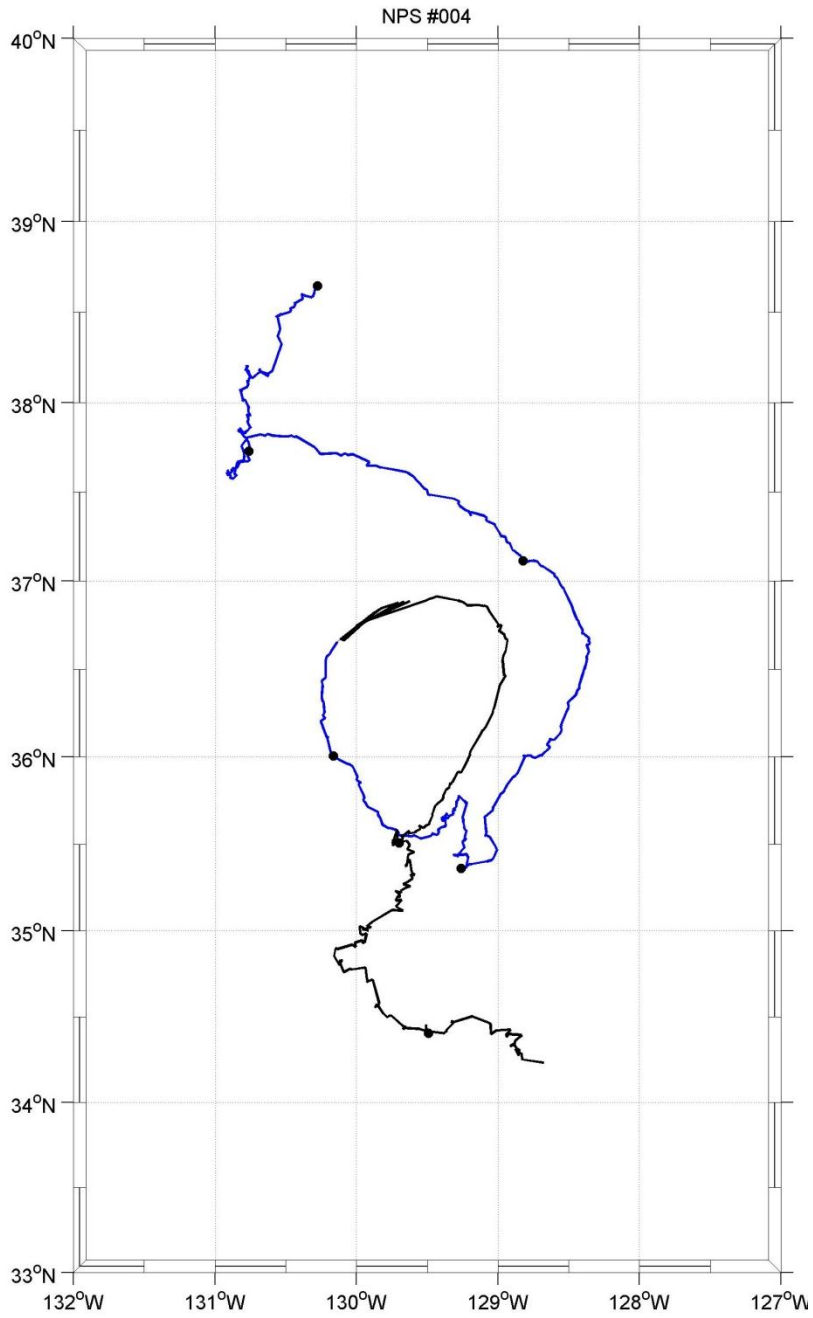

Figure A4. RAFOS float n004 obtained its first fix (38.65°N 130.28°W) January 1, 1994, and was tracked until April 2, 1994. The float traveled southward for 20 days before turning to travel northeast for 5 days. The float then followed an anticyclonic path southward for 20 days. Increased anticyclonic curvature then produced a closed loop in the trajectory over the next 30 days. Finally, the float moved south-southwest (ten days) then south-southeast (10 days). Dots along the trajectory are 15 days apart. Colors represent different seasons in the trajectory: winter (blue), and spring (black).

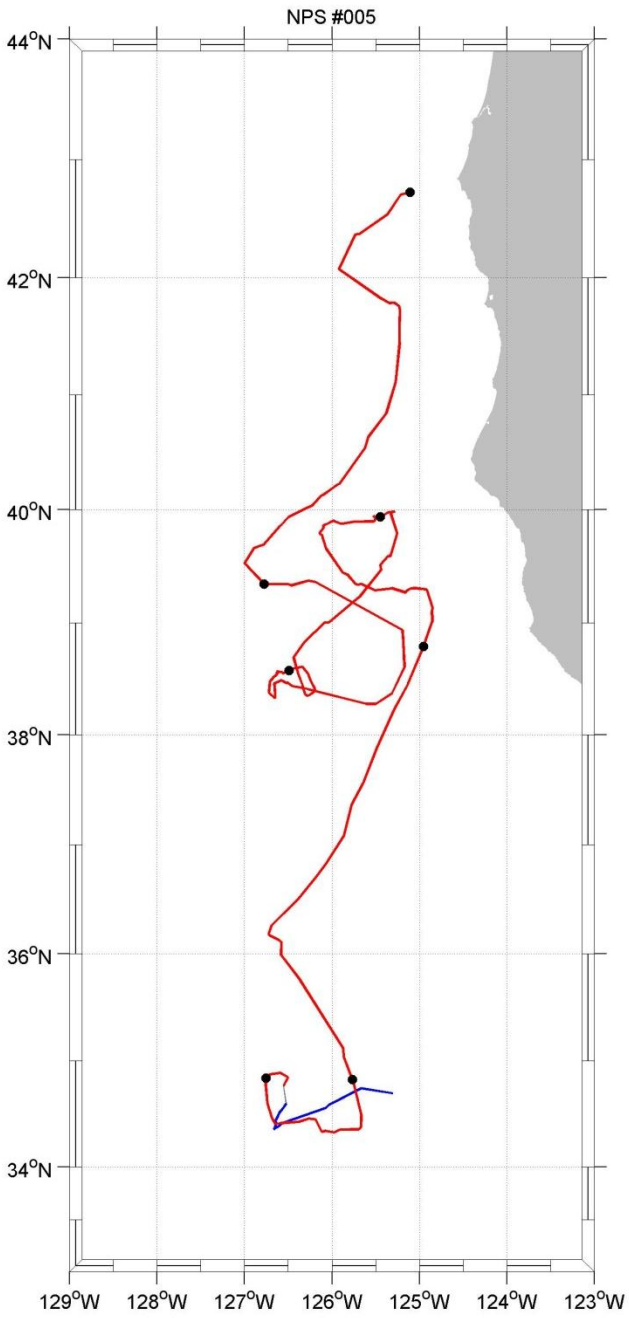

Figure A5. RAFOS float n005 obtained its first fix (42.73°N 125.11°W) September 5, 1993, and was tracked until December 10, 1993. Float n005 meandered southward for approximately 15 days, then executed a north/south figure-8 (anticyclonic, then cyclonic) before continuing generally southward for about 75 days. Dots along the trajectory are 15 days apart. The ~~S~~small data gap during the final 15 days is smaller than 2 days. Colors represent different seasons in the trajectory: fall (red) and winter (blue).

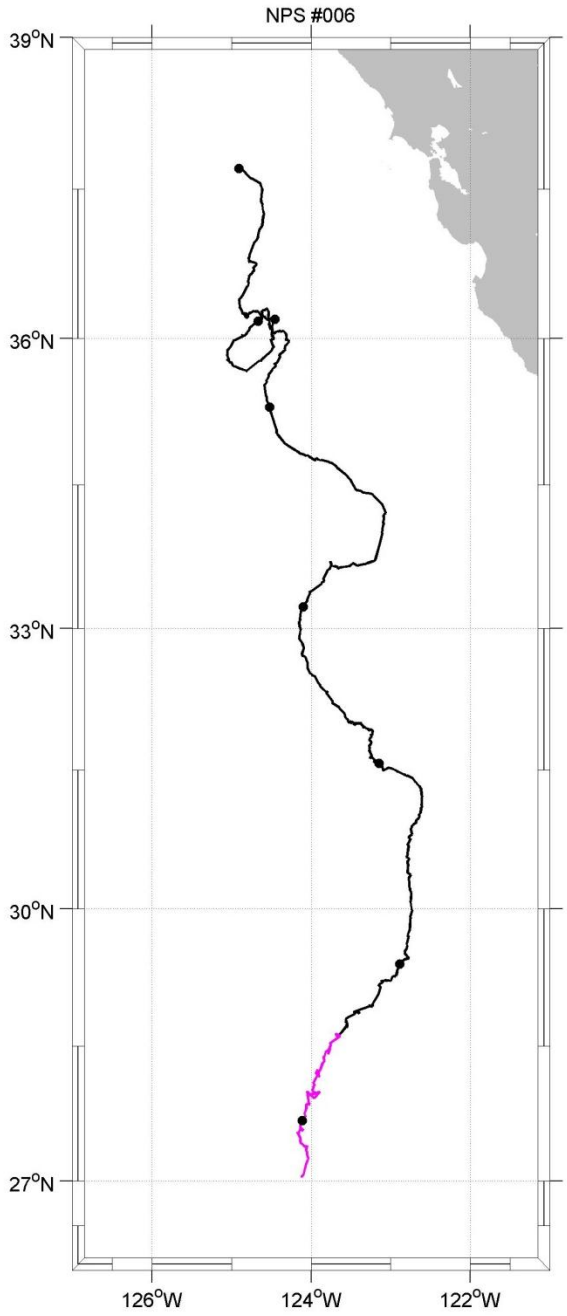

Figure A6. RAFOS float n006 obtained its first fix (37.71°N 124.90°W) March 10, 1994, and was tracked until June 15, 1994. The float generally traveled southward, except for a period of about 30 days (after day 15) when it displayed eddy motion (including a cyclonic loop). Dots along the trajectory are 15 days apart. Colors represent different seasons in the trajectory: spring (black), and summer (magenta).

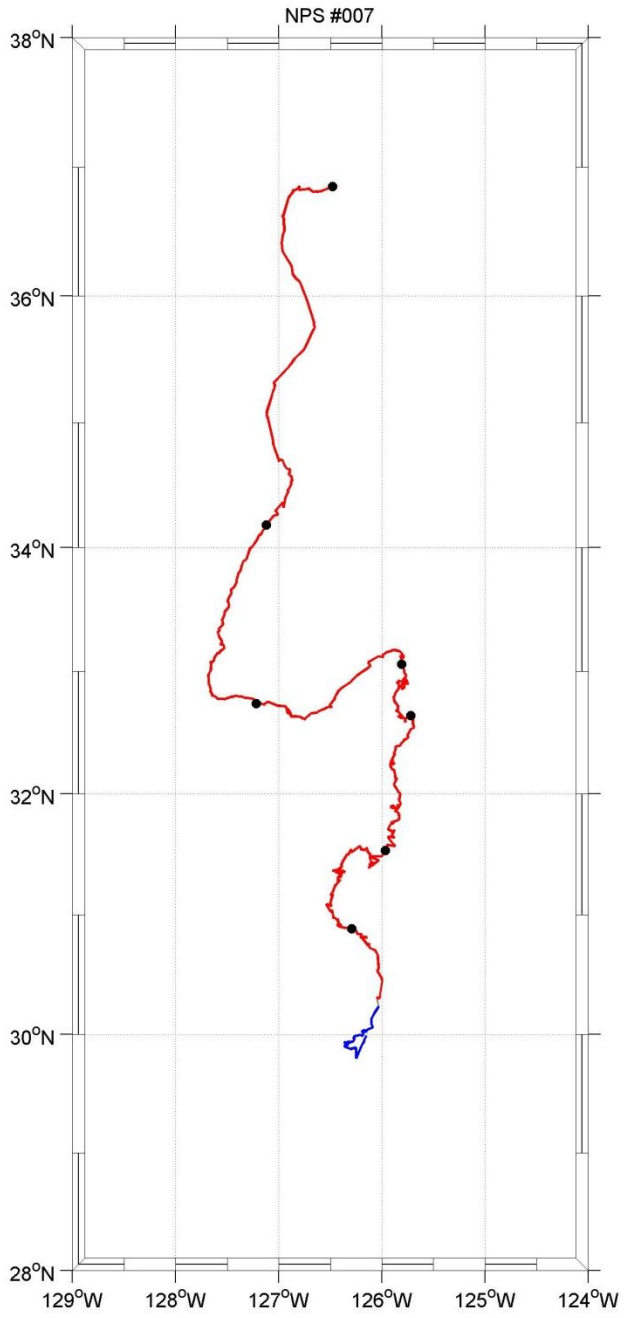

Figure A7. RAFOS float n007 obtained its first fix (36.85°N 126.48°W) September 5, 1993, and was tracked until December 9, 1993. The float generally drifted southward, except for a 15-day eastward turn after day 30. Dots along the trajectory are 15 days apart. Colors represent different seasons in the trajectory: fall (red) and winter (blue).

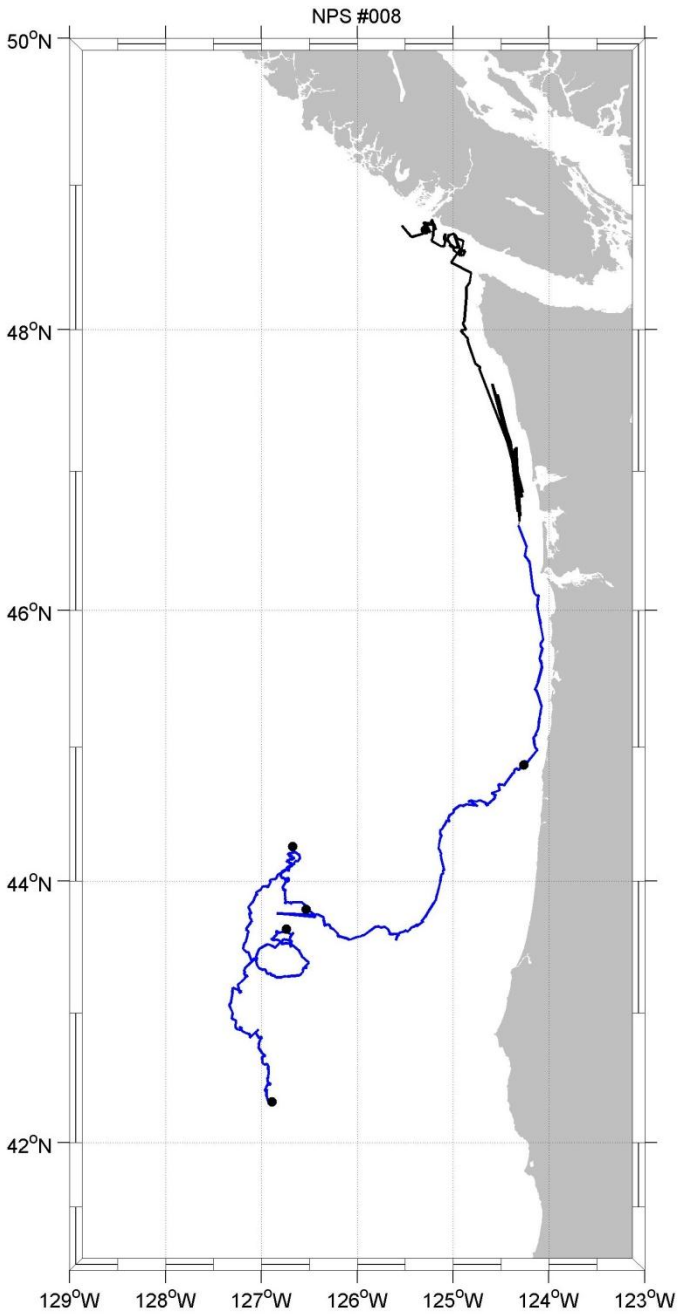

Figure A8. RAFOS float n008 obtained its first fix (42.32°N 126.89°W) December 30, 1993, and was tracked until March 12, 1994. The float traveled northward for 10 days, whereafter it exhibited eddy motion (including an anticyclonic loop) for 25 days. The float then traveled east toward, thence along, the coast for 15 and 15 days, respectively. Finally, the float meandered approximately 10 days just off the coast of Vancouver Island. Dots along the trajectory are 15 days apart. Colors represent different seasons in the trajectory: winter (blue) and spring.

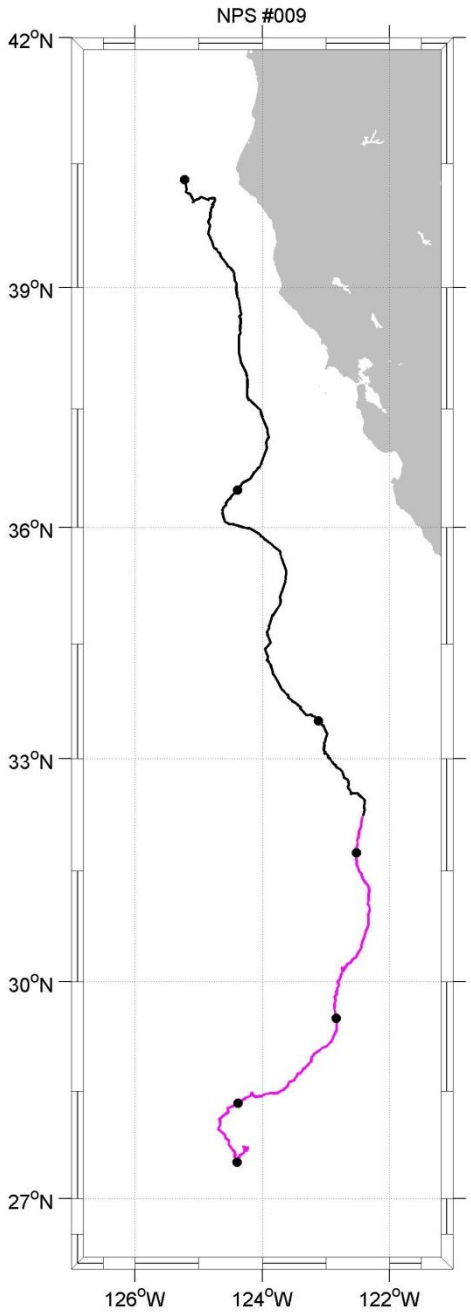

Figure A9. RAFOS float n009 obtained its first fix (40.31°N 125.22°W) April 23, 1994, and was tracked until July 23, 1994. The float generally drifted southward in the California current system. Dots along the trajectory are 15 days apart. Colors represent different seasons in the trajectory: spring (black) and summer (magenta).

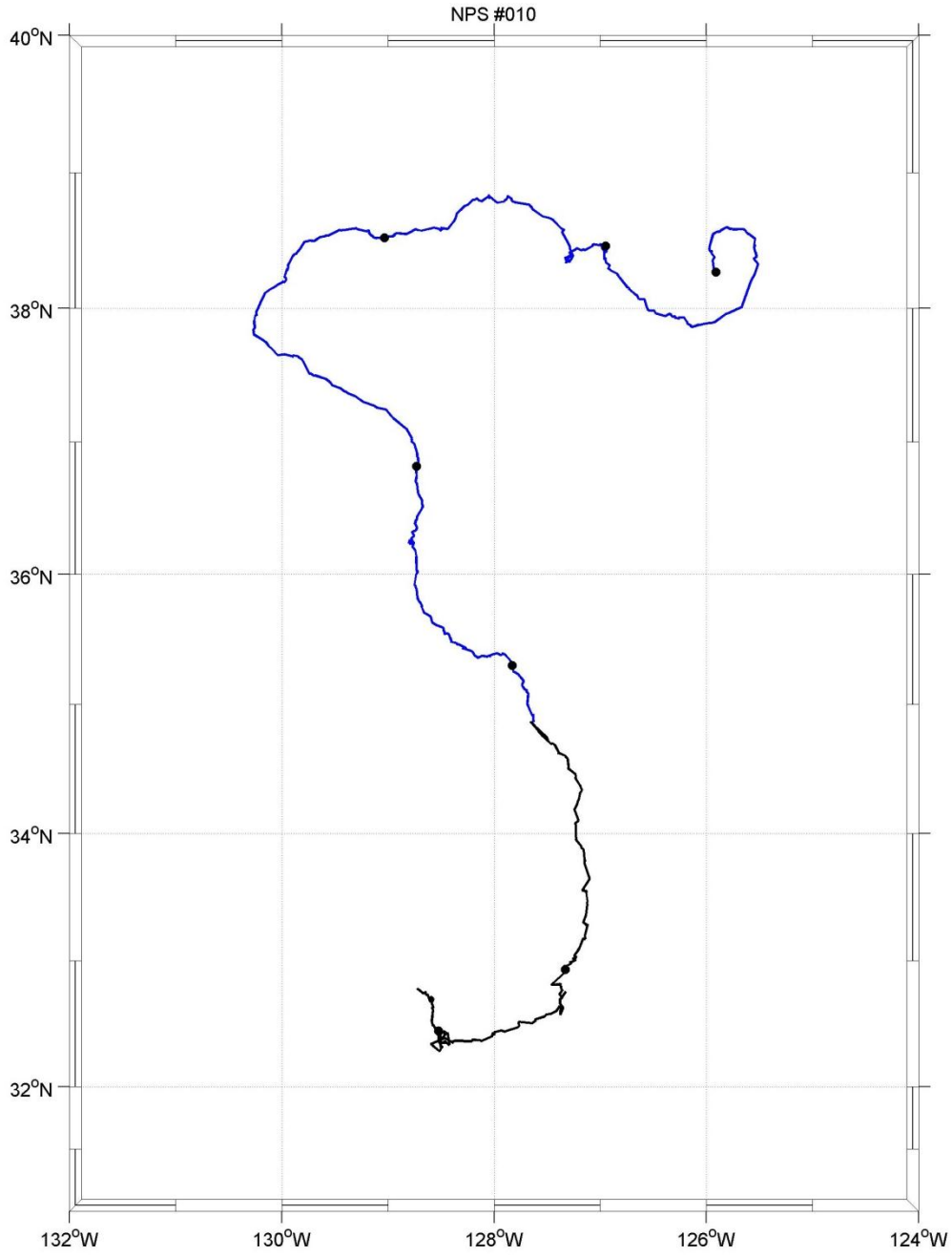

Figure A10. RAFOS float n010 obtained its first fix (38.27°N 125.91°W) January 1, 1994, and was tracked until March 31, 1994. The float made one nearly complete anticyclonic loop before traveling west for 25 days to approximately 130°W. The float then turned south-southeast for 40 days, ending with a brief (~10 days) westward then northward track. Dots along the trajectory are 15 days apart. Colors represent different seasons in the trajectory: winter (blue) and spring (black).

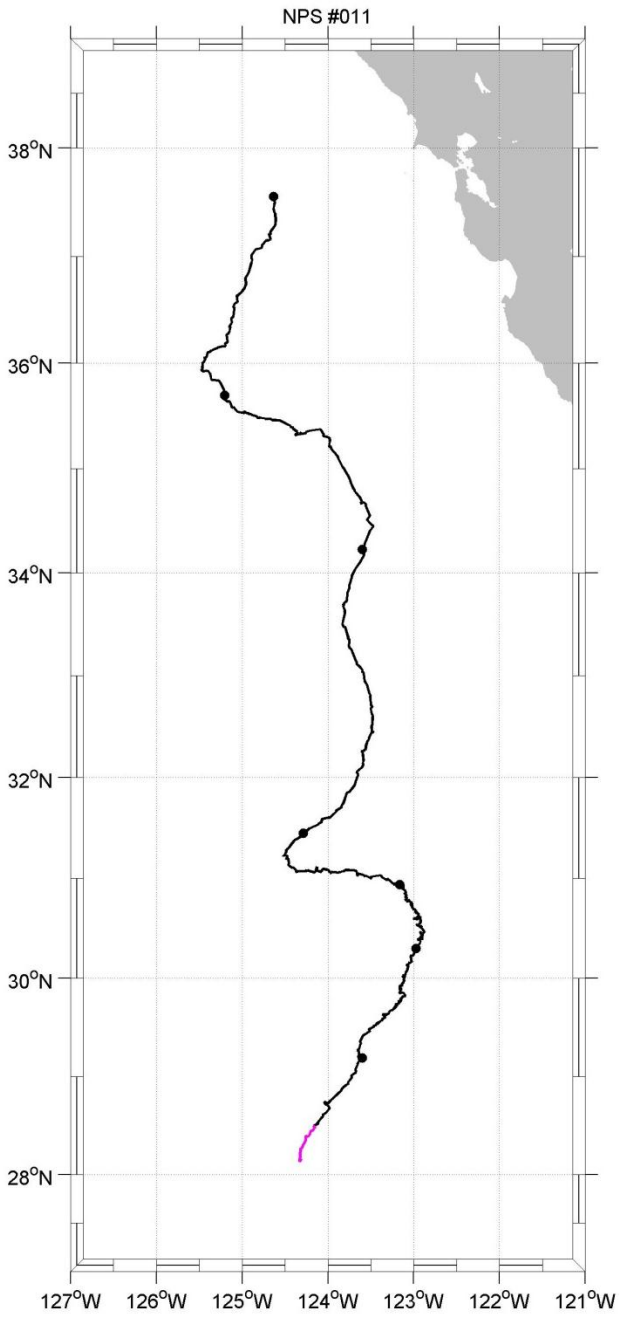

Figure A11. RAFOS float n011 obtained its first fix (37.56°N 124.63°W) March 2, 1994, and was tracked until June 4, 1994. The float generally traveled Dots along the trajectory are 15 days apart. Colors represent different seasons in the trajectory: spring (black) and summer (magenta).

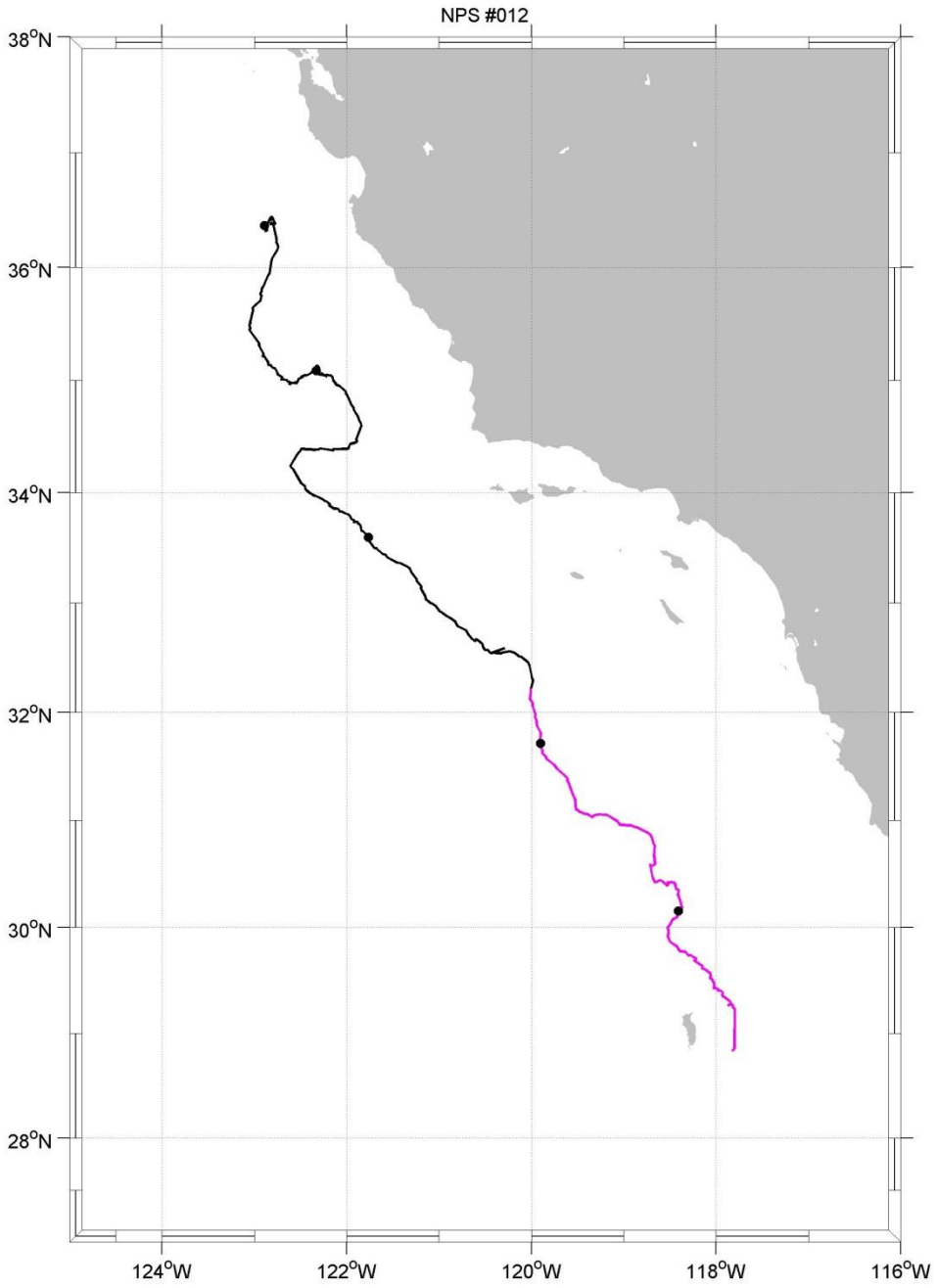

Figure A12. RAFOS float n012 obtained its first fix (36.37°N 122.89°W) April 23, 1994, and was tracked until July 2, 1994. The float drifted south-southeast for the duration it was tracked. Dots along the trajectory are 15 days apart. Colors represent different seasons in the trajectory: -spring (black) and summer (magenta).

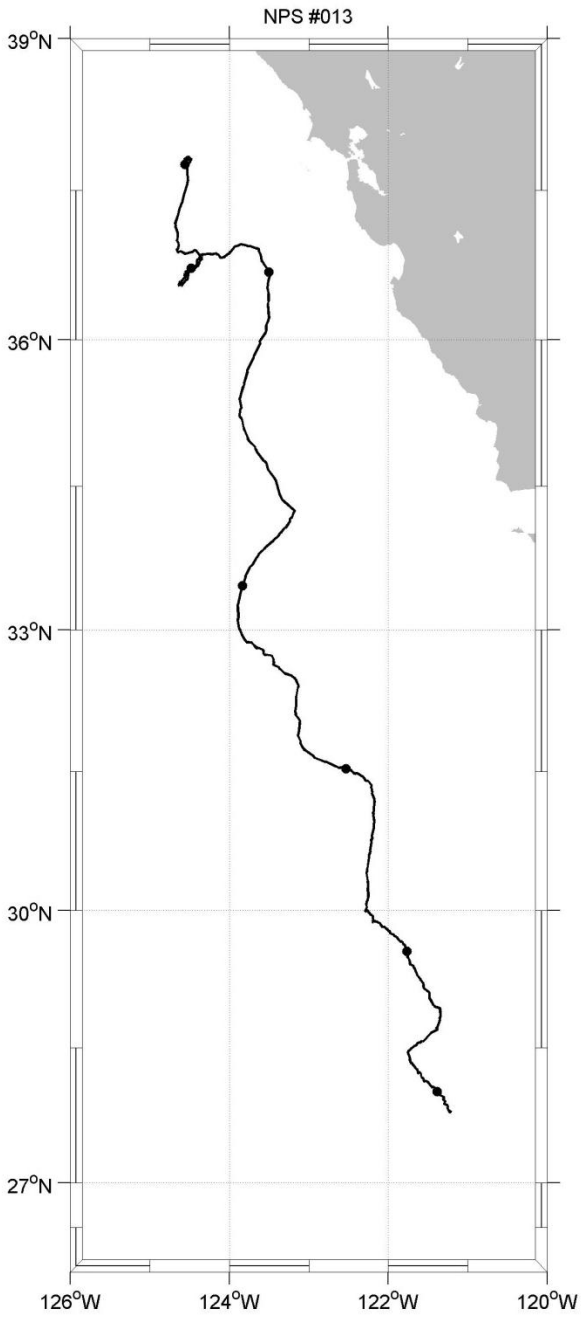

Figure A13. RAFOS float n013 obtained its first fix (37.76°N 124.56°W) March 2, 1994, and was tracked until May 28, 1994. The float generally traveled south-southeast, except that it meandered in eddy motion for over 15 days at about [36.5°N, 124.5°W] Dots along the trajectory are 15 days apart. The black trajectory denotes spring observations.

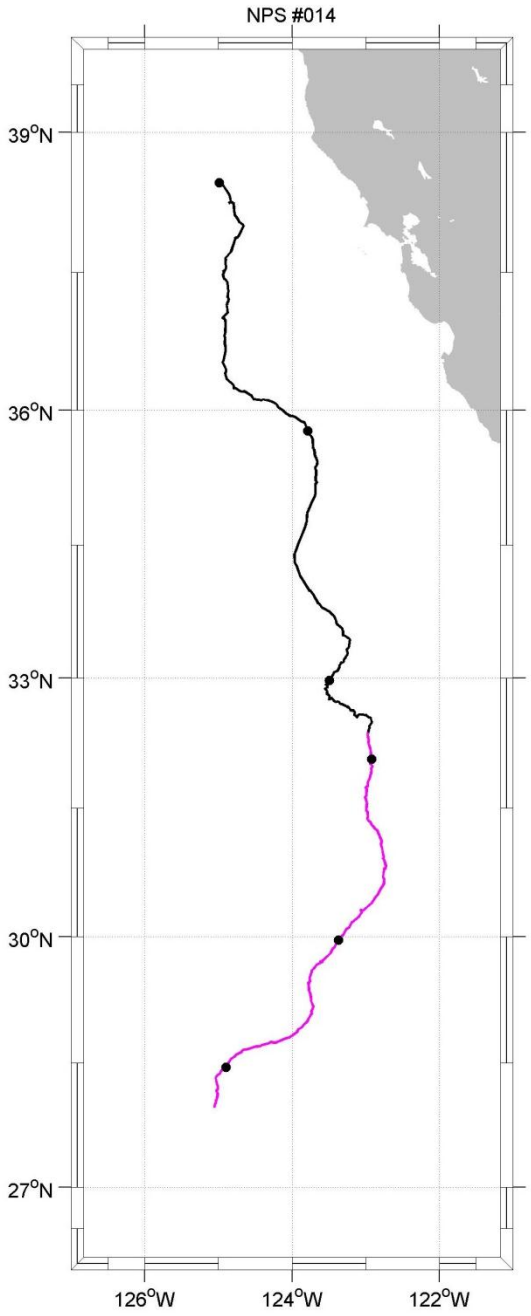

Figure A14. RAFOS float n014 obtained its first fix (38.46°N 124.99°W) April 23, 1994, and was tracked until July 7, 1997. The float generally traveled southward in the California current. Dots along the trajectory are 15 days apart. Colors represent different seasons in the trajectory: spring (black) and summer (magenta).

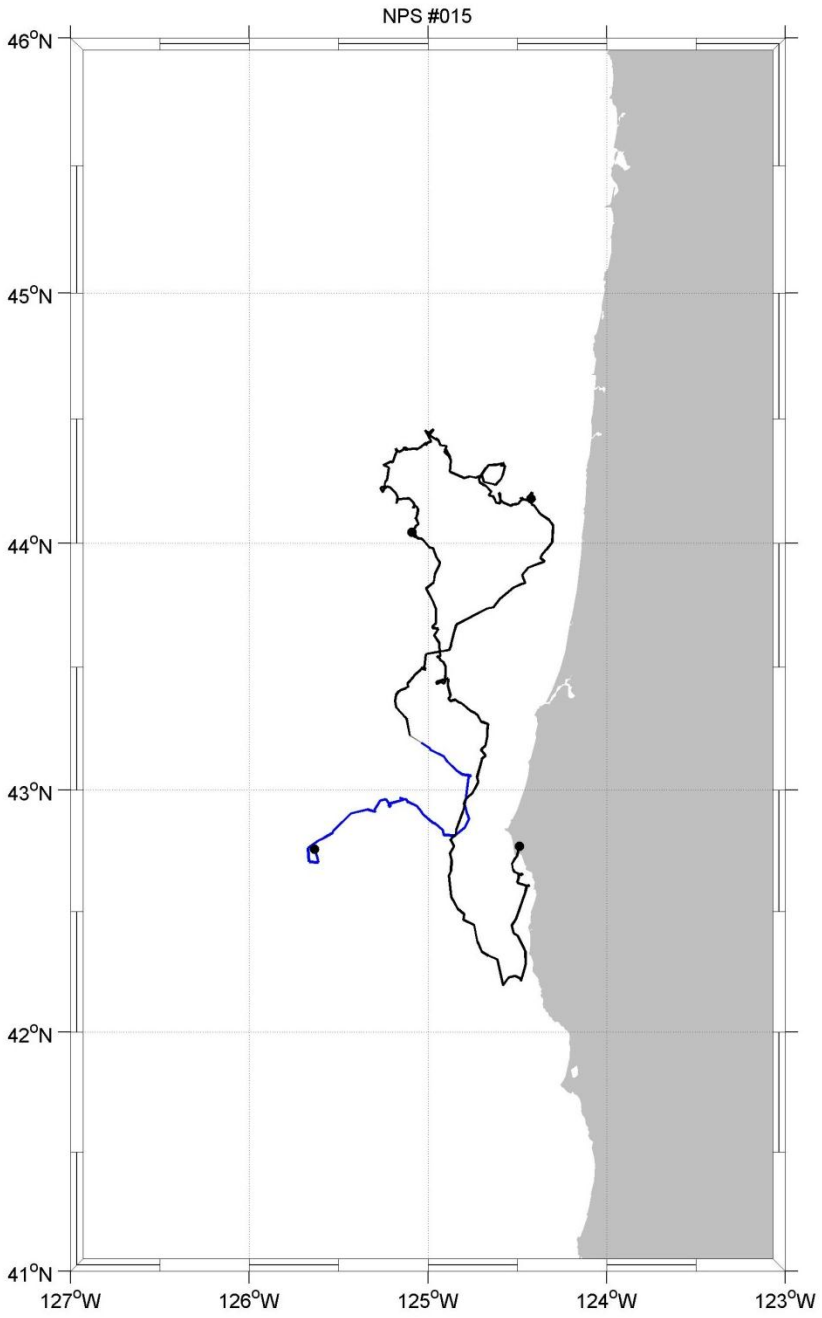

Figure A15. RAFOS float n015 obtained its first fix (42.76°N 125.64°W) February 22, 1996, and was tracked until April 6, 1996. The float initially traveled east for 10 days, then turned northward for 15 days to about 44°N. It then turned eastward for 10 days to about 125.25°W, thence southward for about 12 days to about 42.25°N, where it was recovered off Cape Blanco in 8 to 10 fathoms of water by a crab fisherman on April 3, 1996. He brought the float north to shore 3 days later. Dots along the trajectory are 15 days apart. Colors represent different seasons in the trajectory: winter (blue) and spring (black).

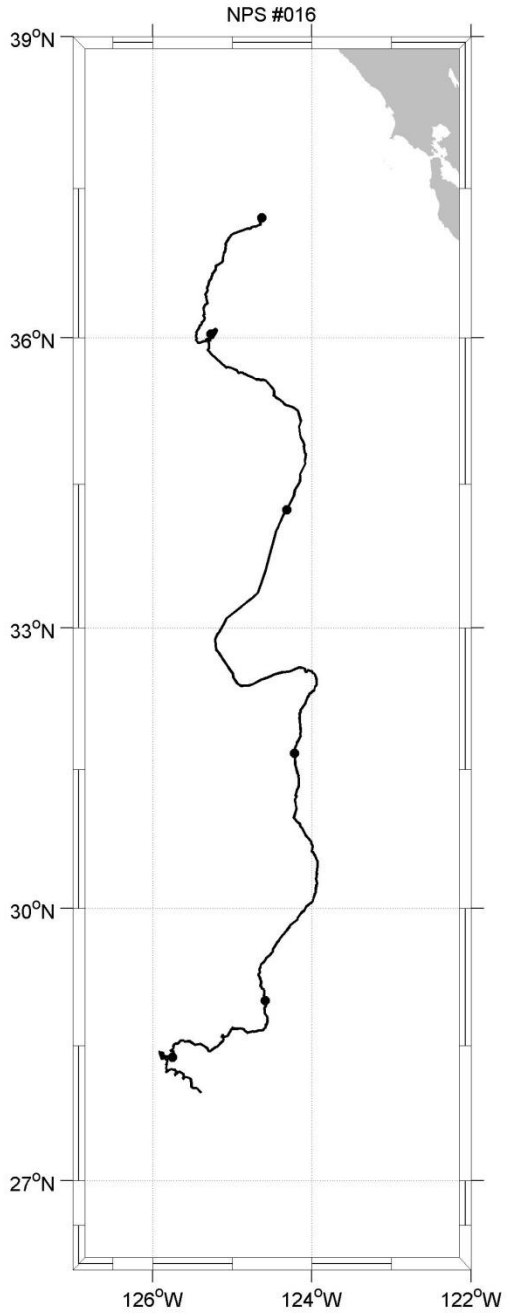

Figure A16. RAFOS float n016 obtained its first fix (37.21°N 124.63°W) March 4, 1997, and was tracked until May 23, 1997. The float generally traveled southward, except that it made an anticyclonic meander at about 36°N. Dots along the trajectory are 15 days apart. The black trajectory denotes spring observations.

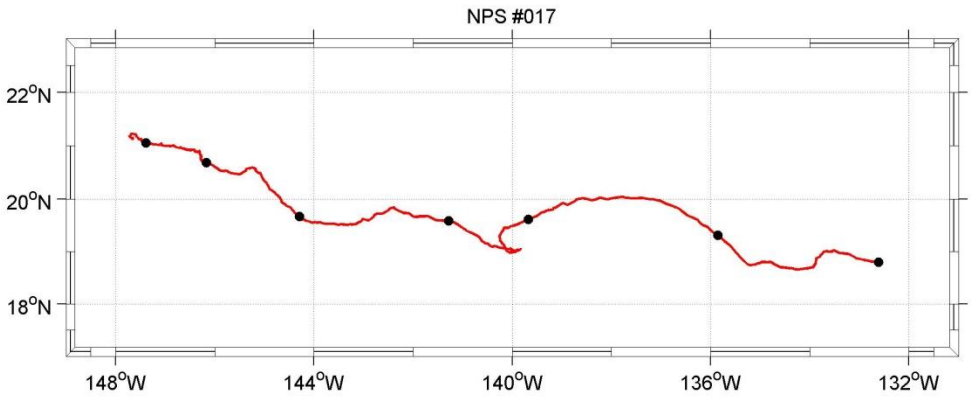

Figure A17. RAFOS float n017 obtained its first fix (18.78°N 132.63°W) September 3, 1994, and was tracked until December 1, 1994. The float generally traveled westward, except that it made a small cyclonic meander at about 140°W. Dots along the trajectory are 15 days apart. The red trajectory denotes fall observations.

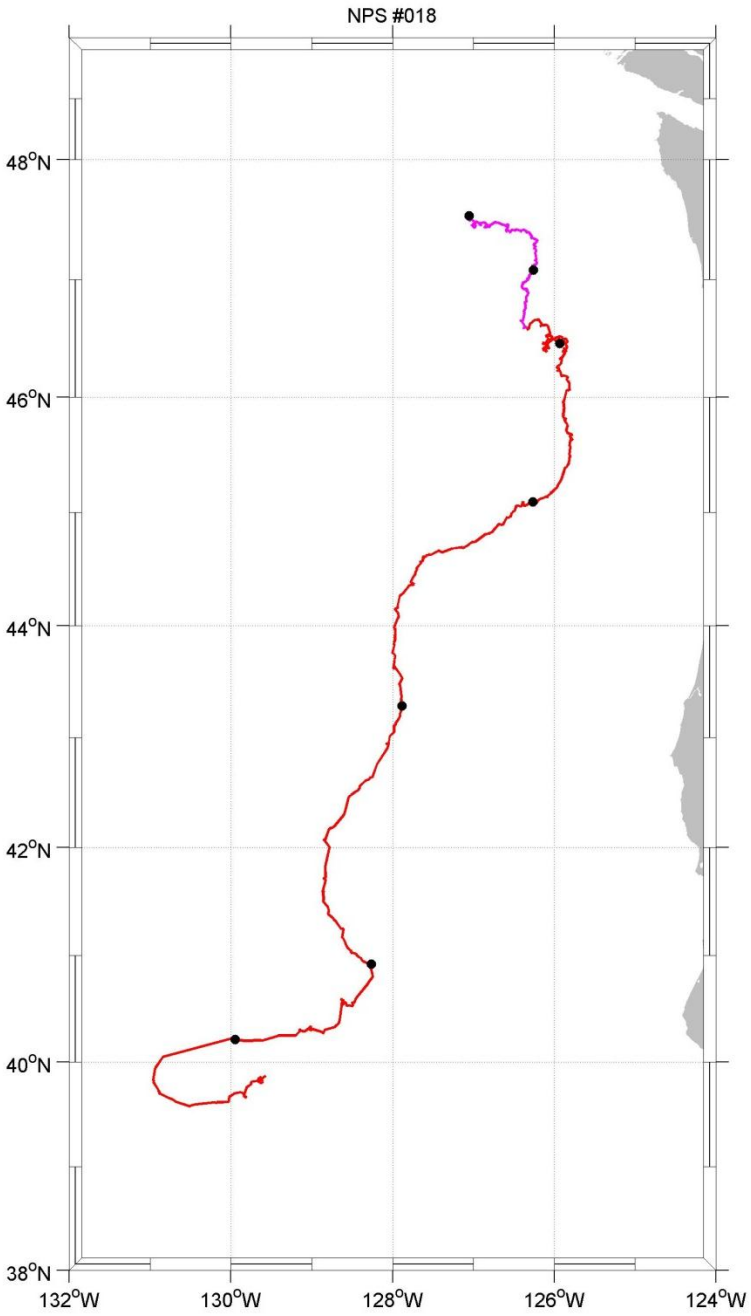

Figure A18. RAFOS float n018 obtained its first fix (47.53°N 127.06°W) August 12, 1994, and was tracked until November 13, 1994. The float initially traveled eastward for 15 days before turning south-southwestward to about 41°N. The float then moved westward along the Mendocino Escarpment for 10 days, before crossing, and then moving eastward for about 13 days south of, the Escarpment. Dots along the trajectory are 15 days apart. Colors represent different seasons in the trajectory: summer (magenta) and fall (red).

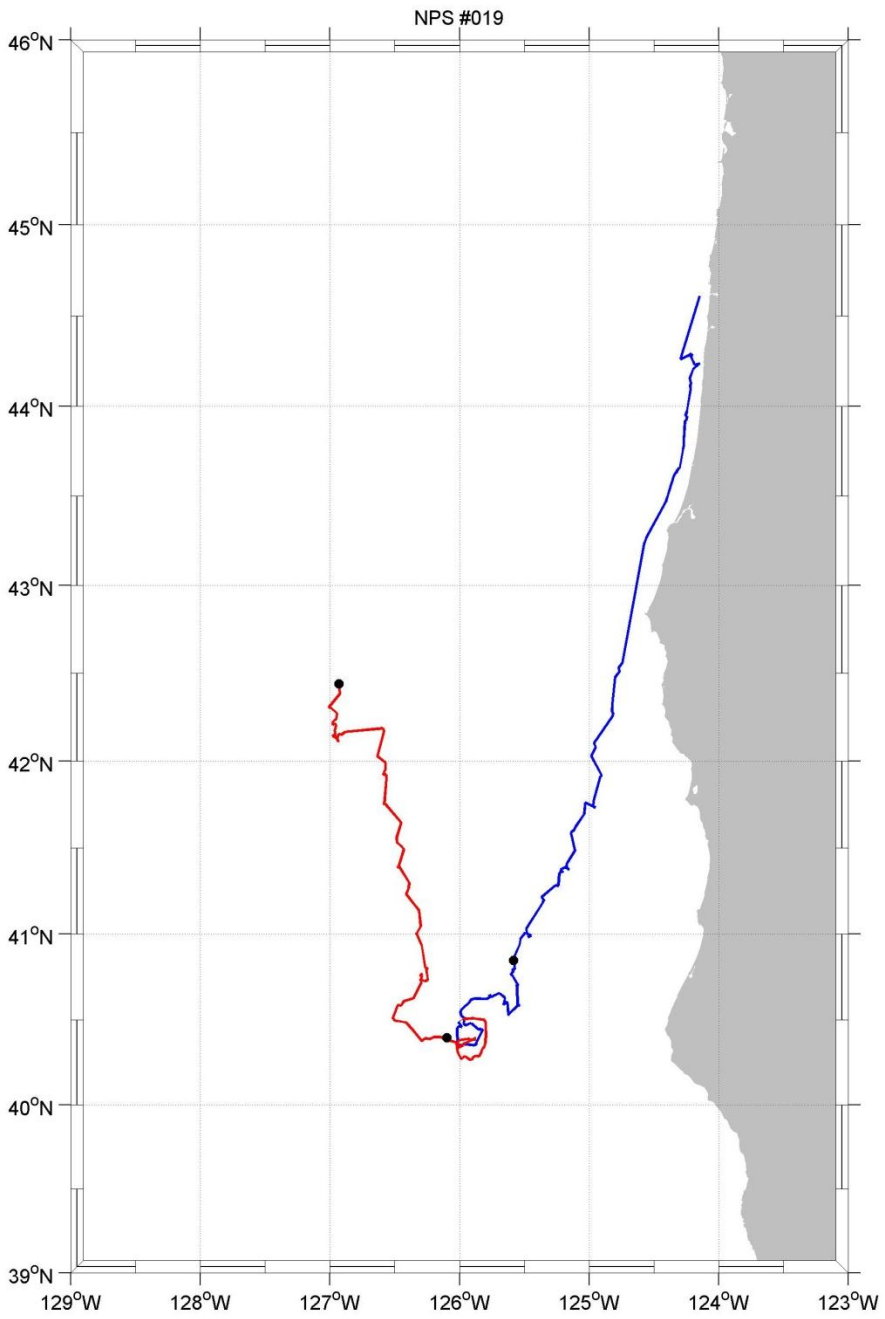

Figure A19. RAFOS float n019 obtained its first fix (42.44°N 126.96°W) November 12, 1994, and was tracked until December 22, 1994. The float initially traveled south for about 23 days to the Mendocino Ridge, where it was caught by a cyclonic eddy for about 15 days. After escaping the eddy, for the next 30 days the float traveled poleward along the coast to shallow water off Cape Blanco and thence to Hecata Head, where it was recovered from a kelp bed by a fishing vessel. Dots along the trajectory are 15 days apart. Colors represent different seasons in the trajectory: fall (red) and winter (blue).

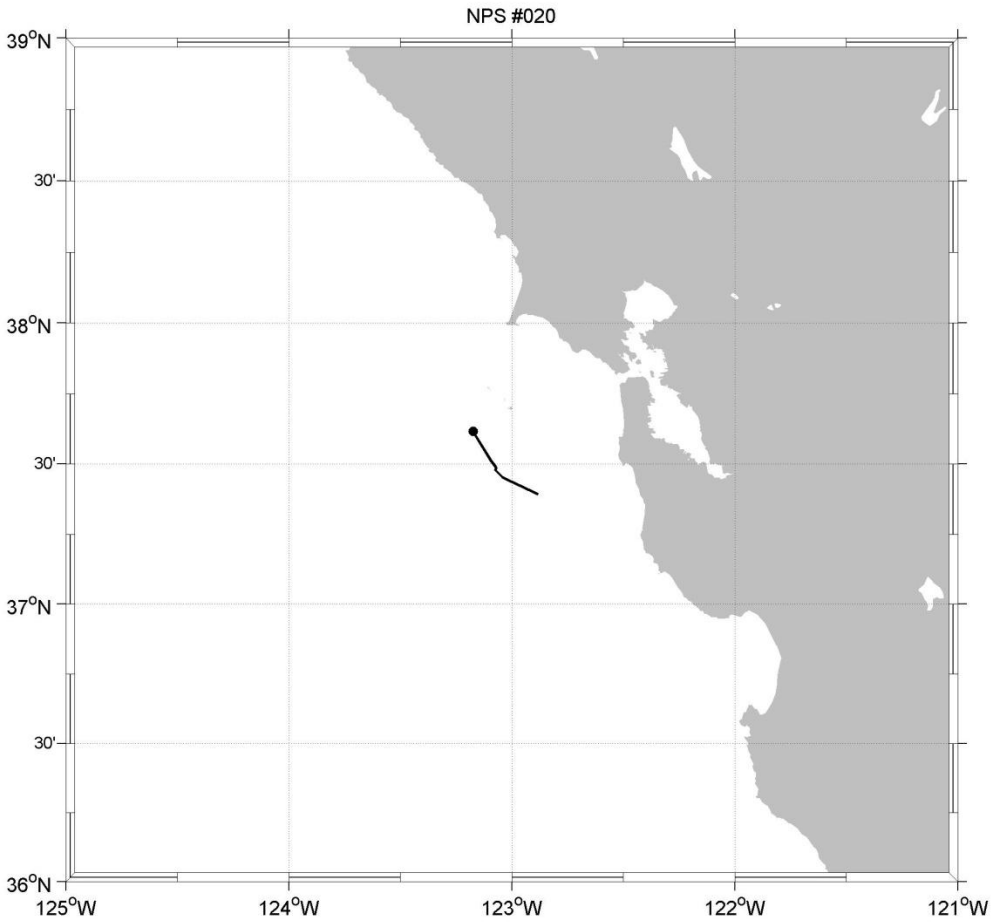

Figure A20. RAFOS float n020 obtained its first fix (37.61°N, 123.17°W) April 30, 1994, and was tracked only two days until May 1, 1994. Float n020's southeasterly trajectory was not used in this study. The black trajectory denotes spring observations.

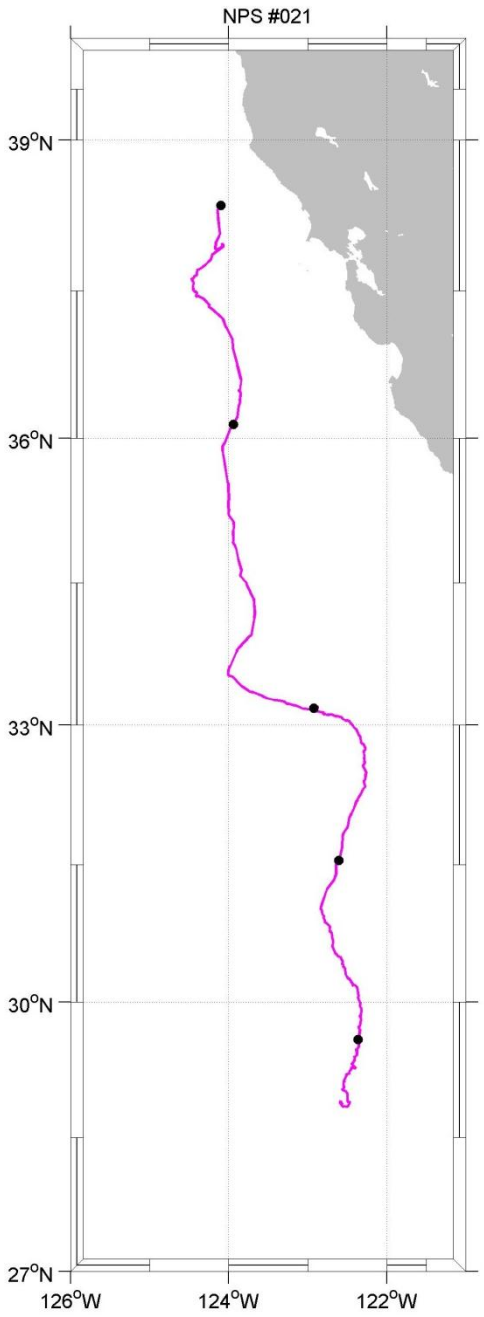

Figure A21. RAFOS float n021 obtained its first fix (38.35°N 124.10°W) June 10, 1994, and was tracked until August 15, 1994. The float traveled southward for the duration of its track. Dots along the trajectory are 15 days apart. The magenta trajectory denotes summer observations.

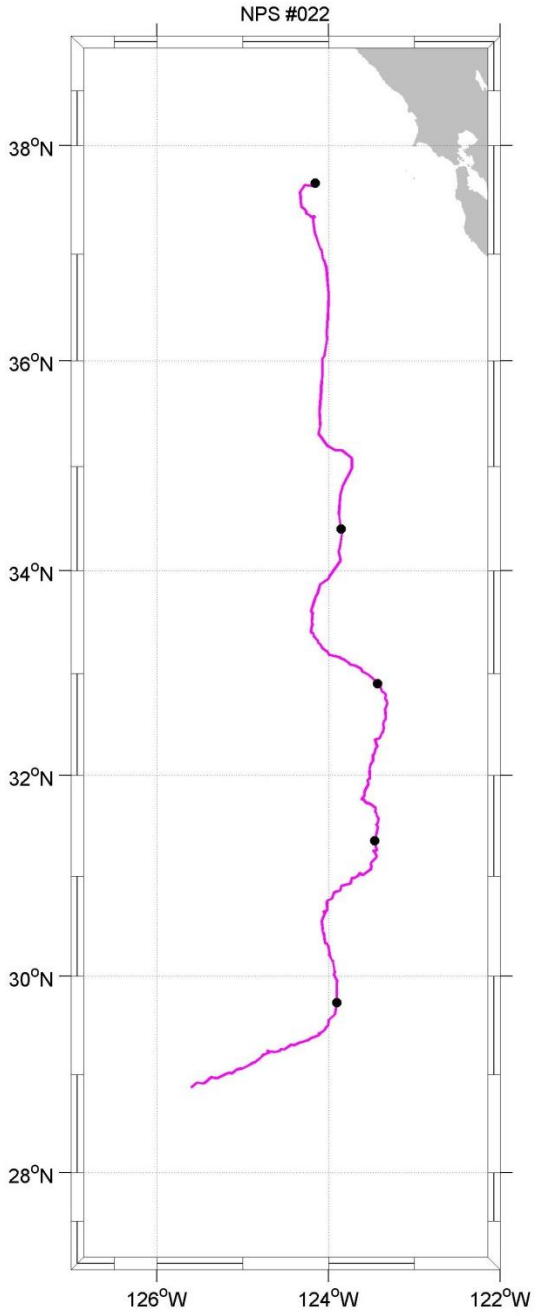

Figure A22. RAFOS float n022 obtained its first fix (37.66°N 124.15°W) June 10, 1994, and was tracked until August 19, 1994. The float traveled south for about 60 days, then turned westward at about 29.5°N for 10 days. Dots along the trajectory are 15 days apart. The magenta trajectory denotes summer observations.

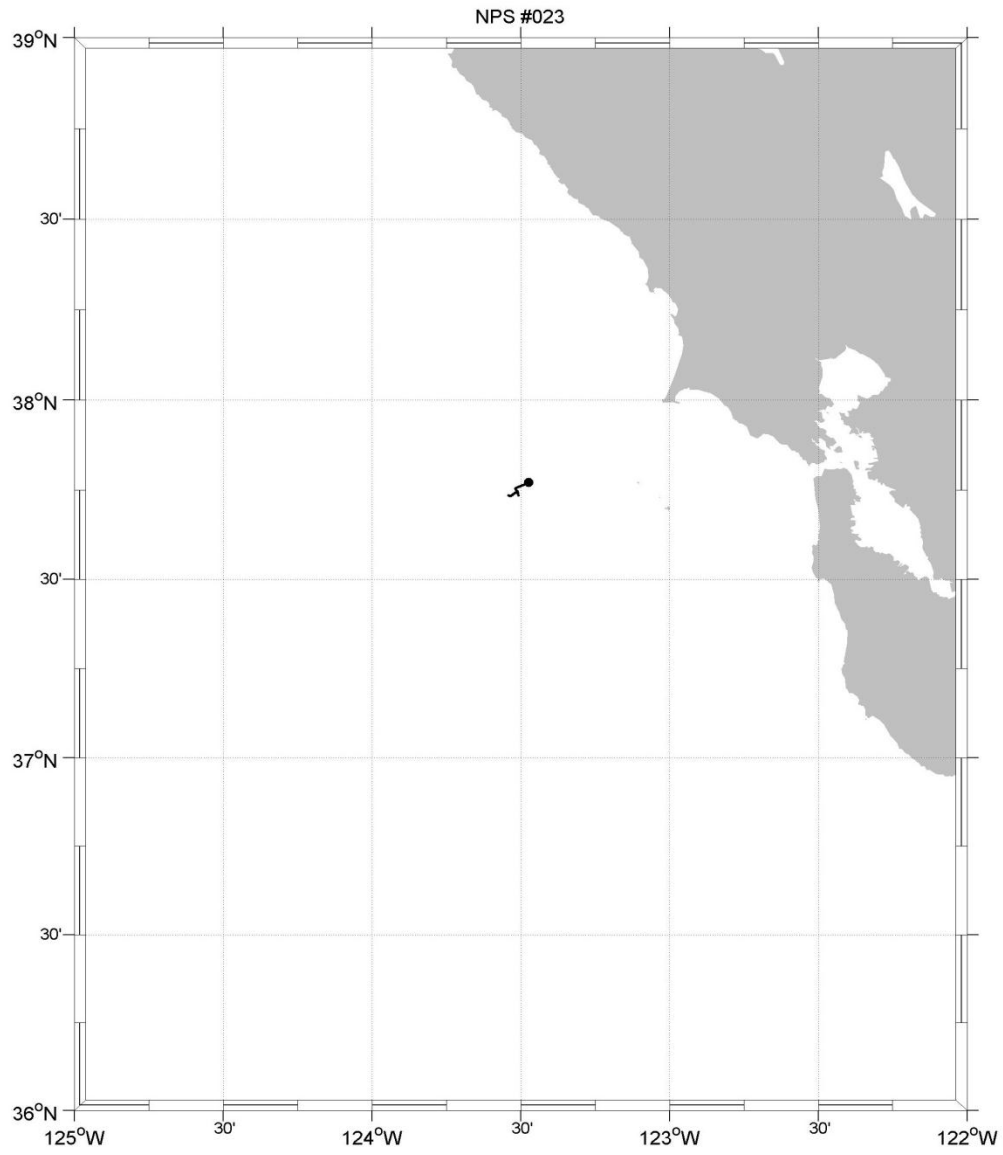

Figure A23. RAFOS float n023 obtained its first fix (37.77°N, 123.47°W) April 30, 1994, and was tracked only three days until May 2, 1994. Float n023's west-southwesterly trajectory was not used in this study. The black trajectory denotes spring observations.

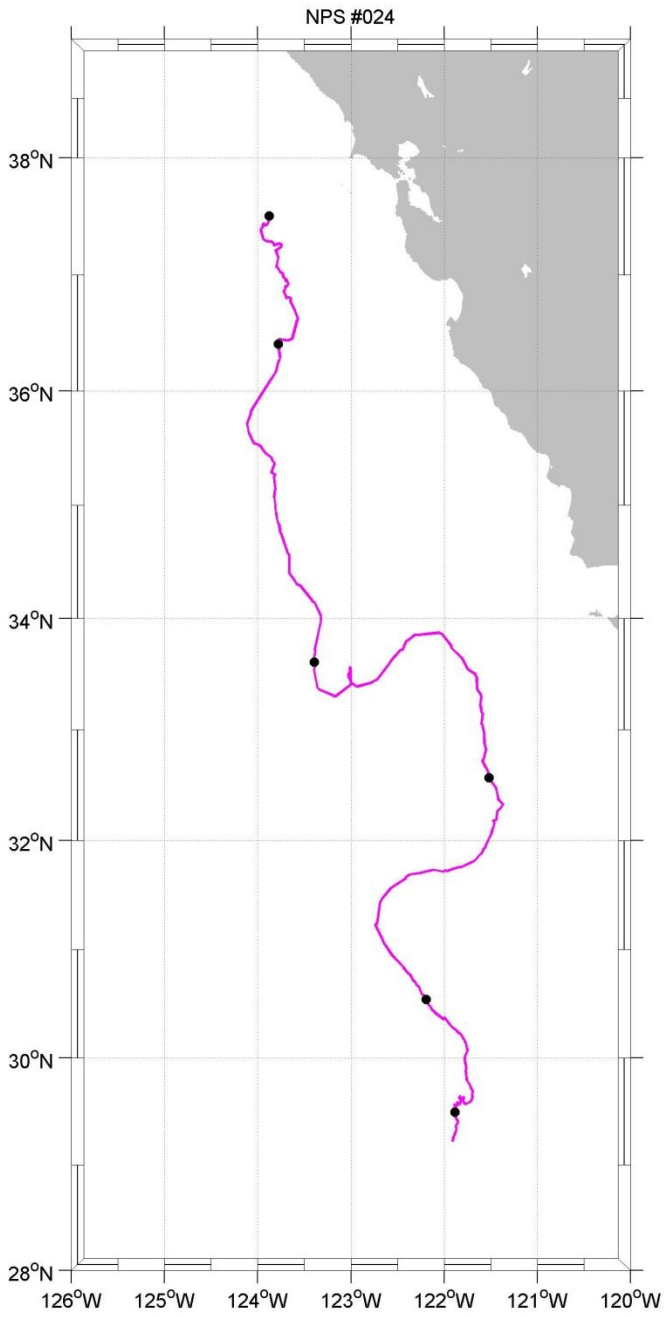

Figure A24. RAFOS float n024 obtained its first fix (37.51°N 123.88°W) June 9, 1994, and was tracked until August 22, 1994. The float essentially traveled southward, except that it effectively jumped to the east between about 33.5°N and 31.5°NThere was also an elongated 2-day cyclonic loop at about 123°W near the start of the float's eastward jump. Dots along the trajectory are 15 days apart. The magenta trajectory denotes summer observations.

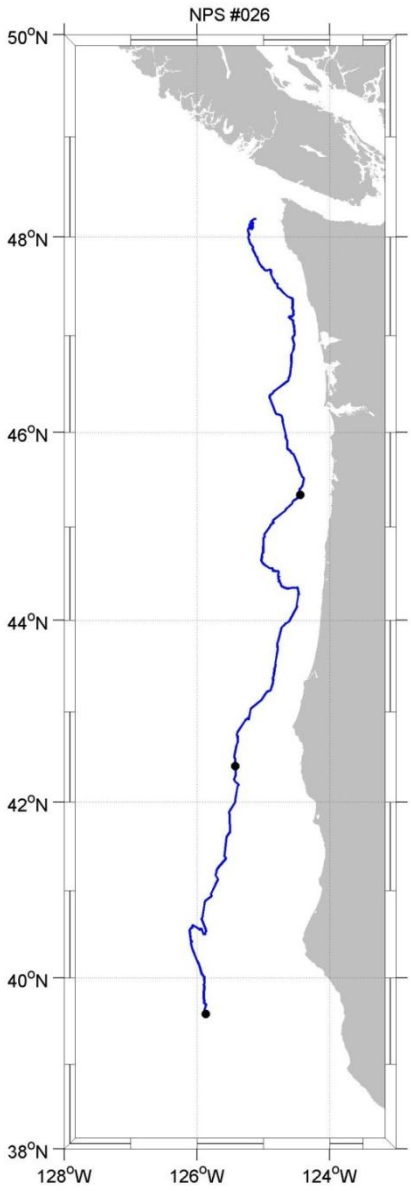

Figure A25. RAFOS float n026 obtained its first fix (39.59°N 125.87°W) December 30, 1994, and was tracked until February 8, 1995. The float tracked generally northward, arriving near the coast at Cape Blanco (~43°N) and effectively following the coastline thereafter to Cape Flattery (~48°N). Dots along the trajectory are 15 days apart. The blue trajectory denotes winter observations.

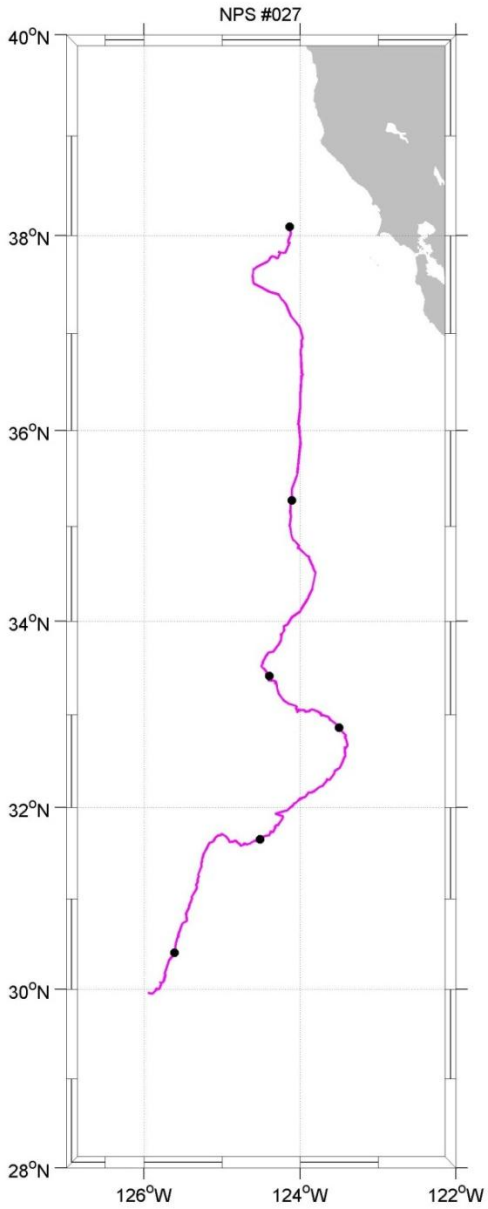

Figure A26. RAFOS float n027 obtained its first fix (38.10°N 124.13°W) June 10, 1994, and was tracked until August 24, 1994. The float drifted south-southwestward. Dots along the trajectory are 15 days apart. The magenta trajectory denotes summer observations.

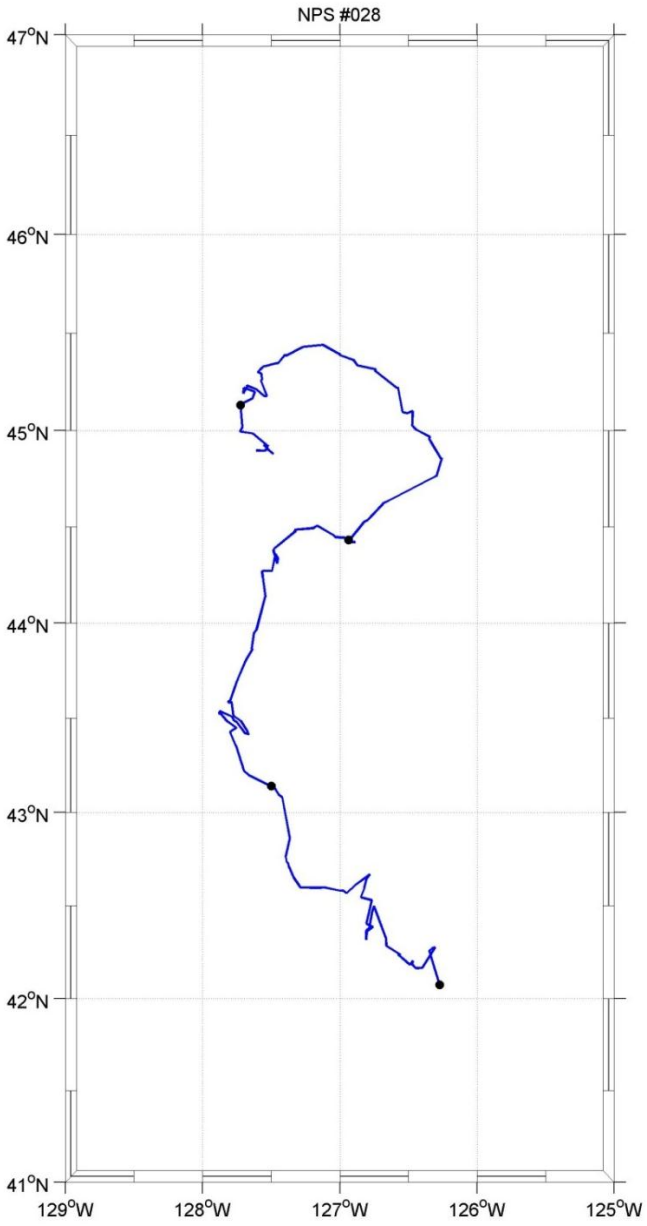

Figure A27. RAFOS float n028 obtained its first fix (42.07°N 126.27°W) December 20, 1994, and was tracked until February 3, 1995. The float followed a meandering anticyclonic track northward to about 44.5°N, where it then executed a nearly-complete cyclonic loop. Dots along the trajectory are 15 days apart. The blue trajectory denotes winter observations.

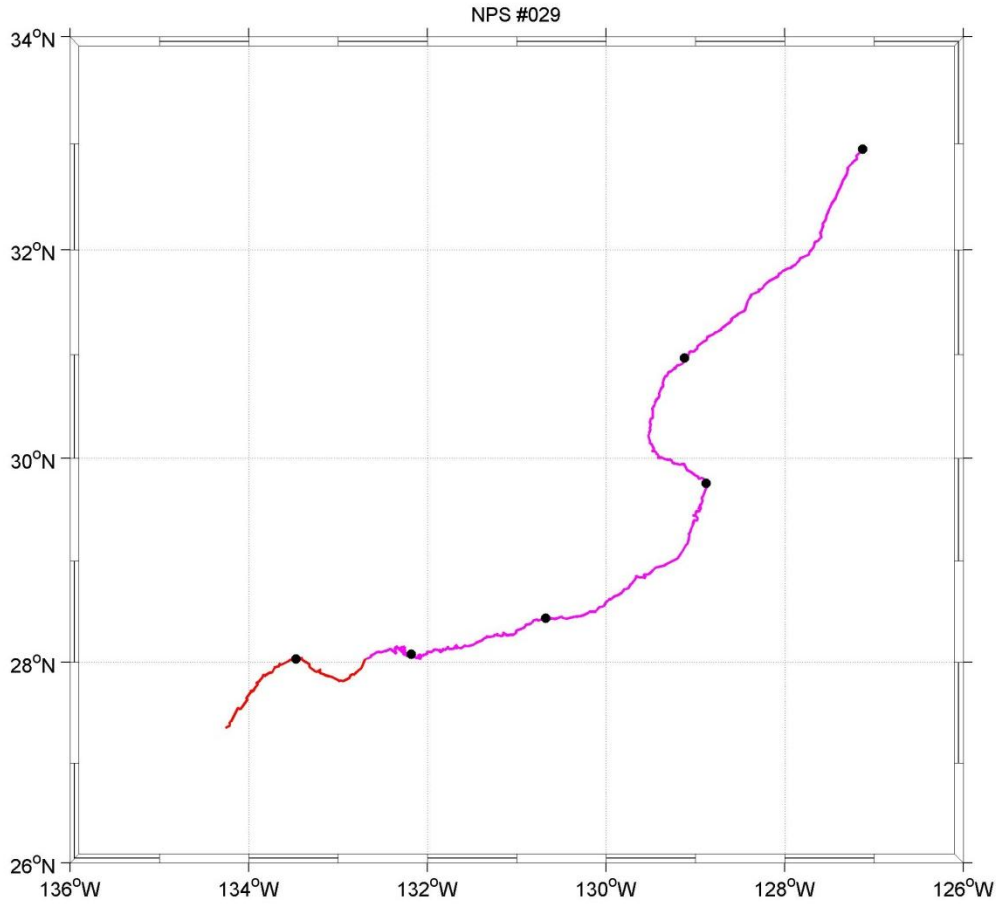

Figure A28. RAFOS float n029 obtained its first fix (32.95°N 127.12°W) June 29, 1996, and was tracked until September 15, 1996. The float followed a southwestward path. Dots along the trajectory are 15 days apart. Colors represent different seasons in the trajectory: summer (magenta) and fall (red).

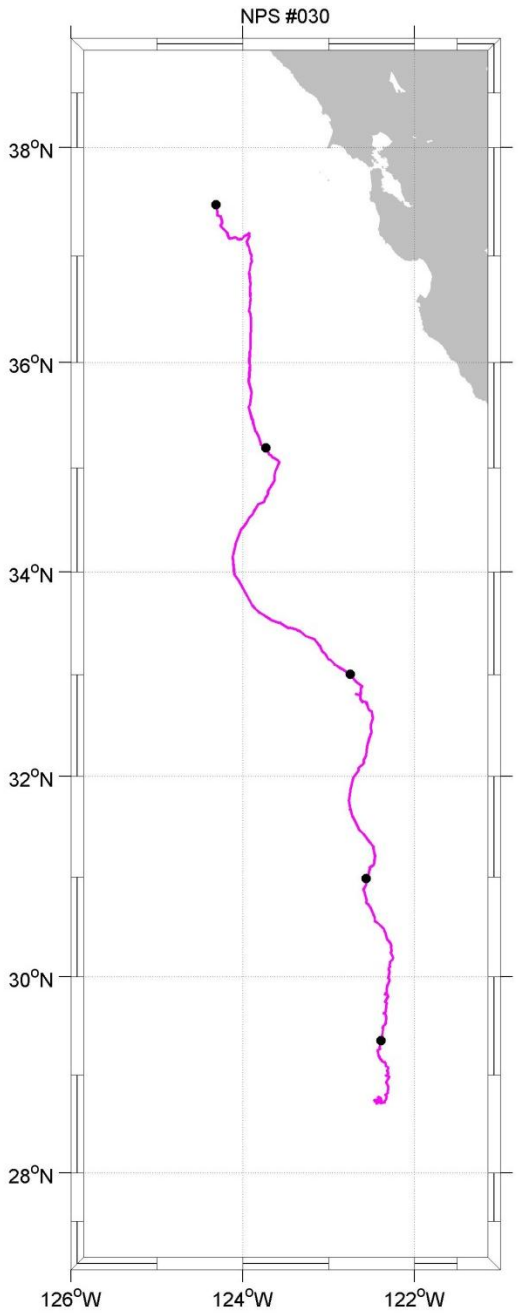

Figure A29. RAFOS float n030 obtained its first fix (37.47°N 124.31°W) June 10, 1994, and was tracked until August 16, 1994. The float essentially drifted southward, except for a southeastward period between approximately 34°N and 33°N. Dots along the trajectory are 15 days apart. The magenta trajectory denotes summer observations.

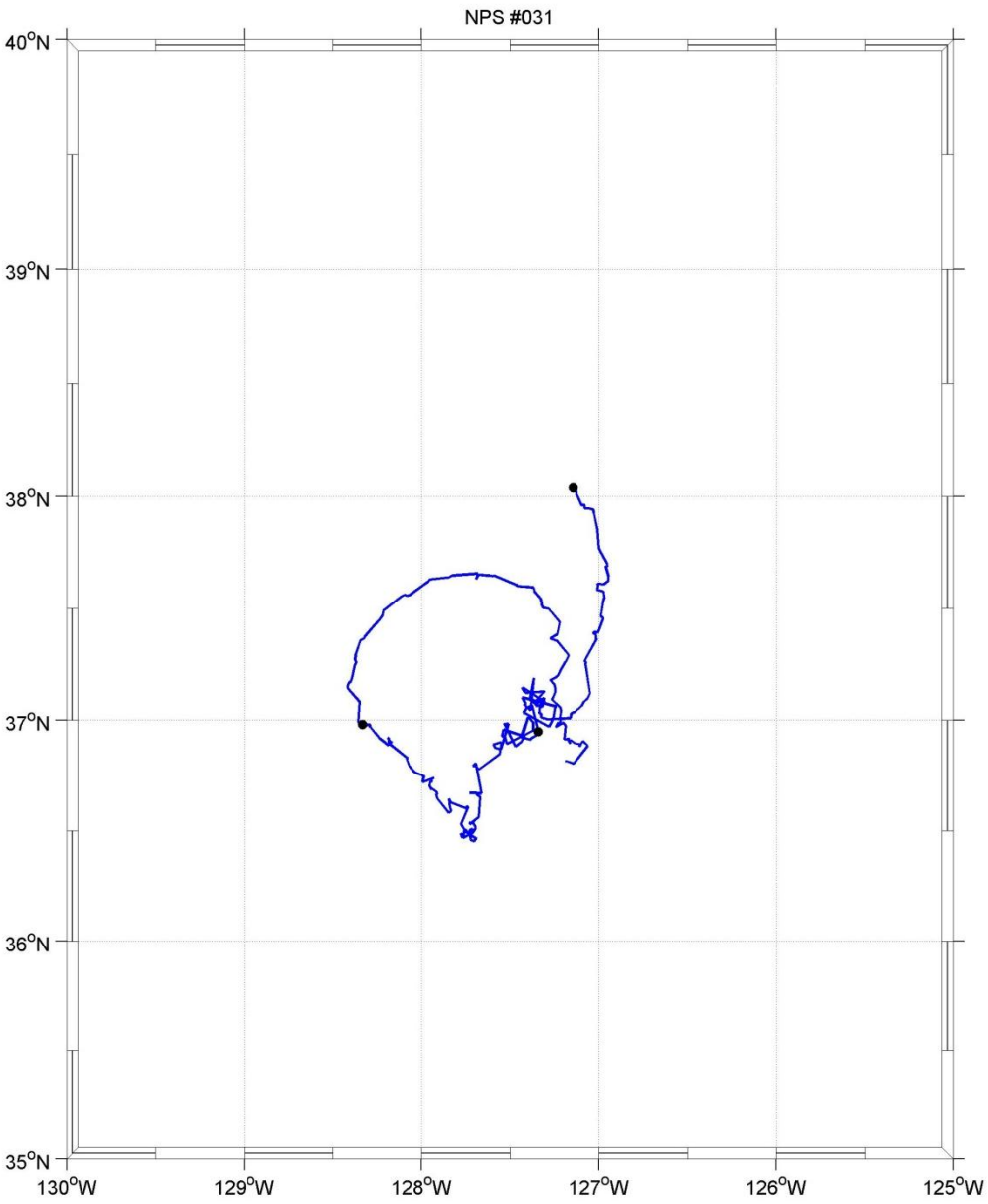

Figure A30. RAFOS float n031 obtained its first fix (38.04°N 127.14°W) December 30, 1994, and was tracked until February 7, 1995. The float initially executed a series of small southwestward-translating anticyclonic loops embedded within a larger southward-translating anticyclonic loop. After the smaller loops subsided (about 127.5°W), the larger single loop was smoothly completed. Dots along the trajectory are 15 days apart. The blue trajectory denotes winter observations.

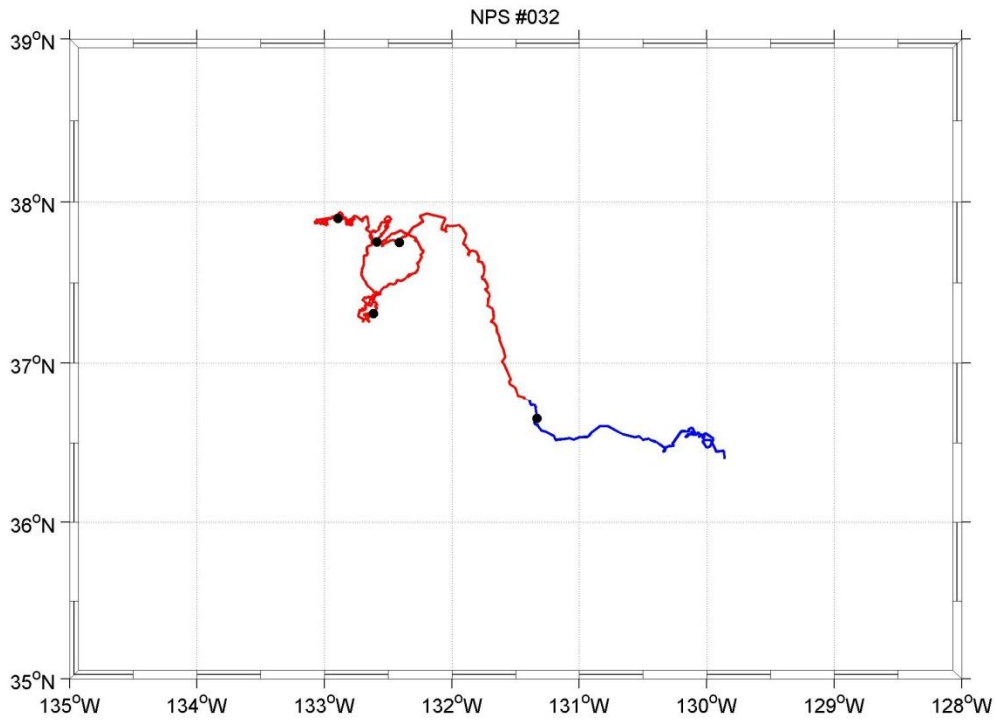

Figure A31. RAFOS float n032 obtained its first fix (37.90°N 132.89°W) October 6, 1996, and was tracked until December 13, 1996. The float seemed to be caught in a rapidly translating (compared to its rotational speed) anticyclone that produced small anticyclonic loops and epicycloids along its entire trajectory. Initially the float tracked westward, before reversing eastward. A misshapen figure-8 was generated at about 132.5oW, followed by southerly motion to about 36.5oN, whereafter the float turned eastward during December. Dots along the trajectory are 15 days apart. Colors represent different seasons in the trajectory: fall (red) and winter (blue).

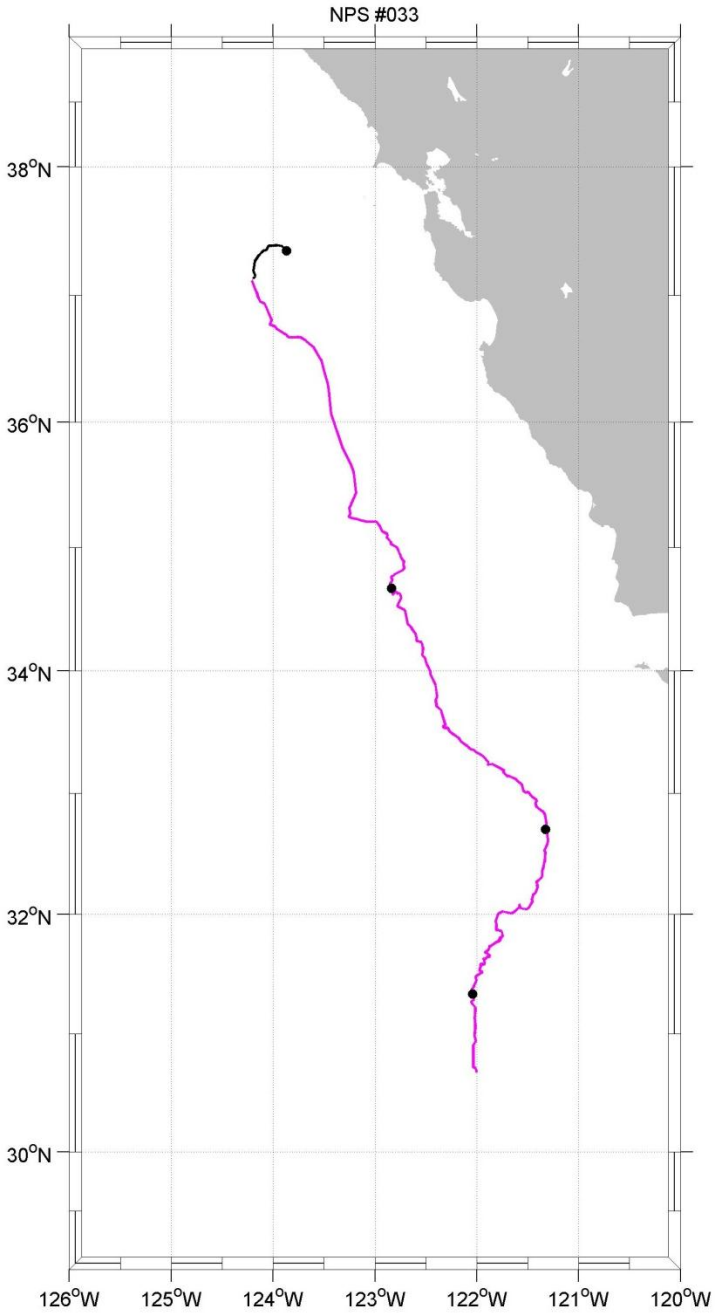

Figure A32. RAFOS float n033 obtained its first fix (37.35°N 123.87°W) May 30, 1995, and was tracked until July 15, 1995. In general, the float tracked south-southeastward. Dots along the trajectory are 15 days apart. Colors represent different seasons in the trajectory: spring(black) and summer (magenta).

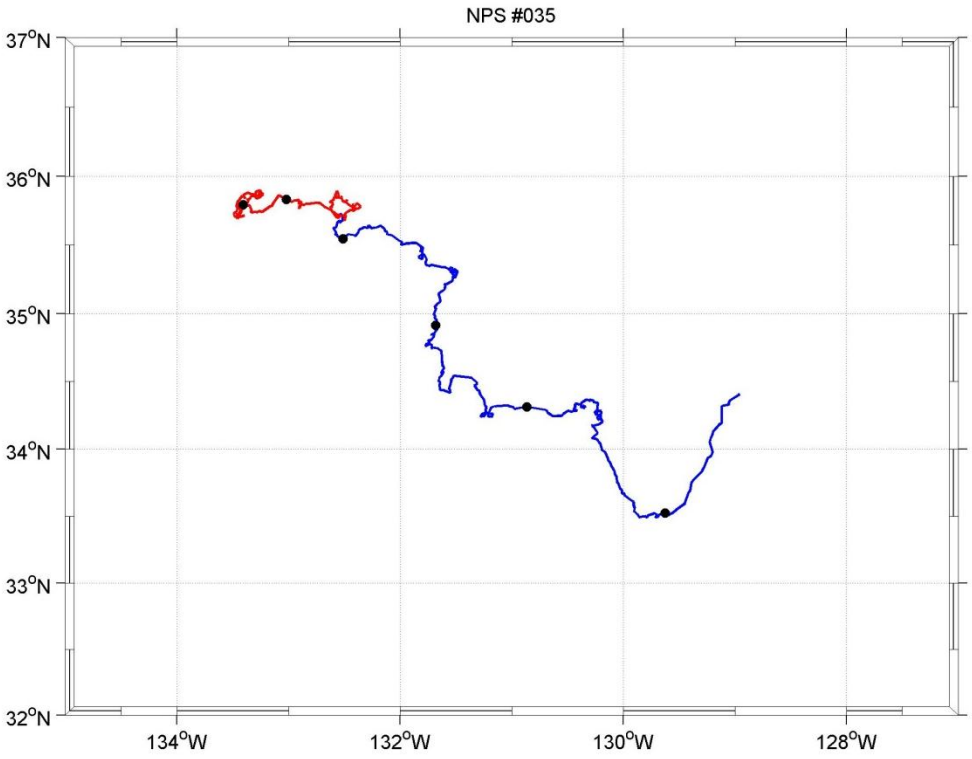

Figure A33. RAFOS float n035 obtained its first fix (35.79°N 133.41°W) November 5, 1996, and was tracked until January 20, 1997. Initially the float meandered southwest, then northeast and back to the southwest, before tracking eastward to about 132.5°W, where a cyclonic loop was executed. The float next tracked generally southeastward to about [33.5°N, 129.75°W], before heading northeastward to about [34.5°N, 129°W]. Dots along the trajectory are 15 days apart. Colors represent different seasons in the trajectory: fall (red) and winter (blue).

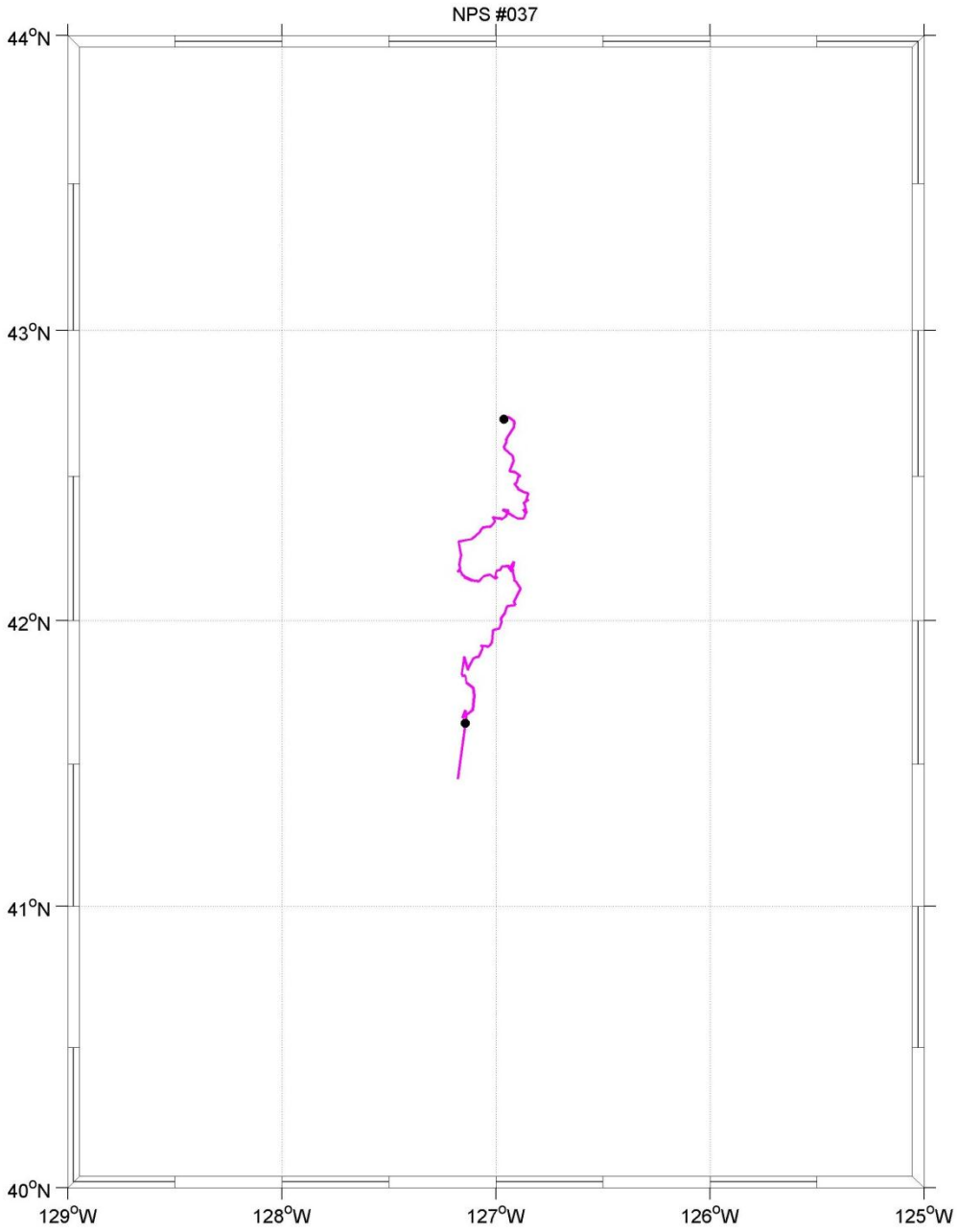

Figure A34. RAFOS float n037 obtained its first fix (42.70°N 126.96°W) June 10, 1996, and was tracked until 1996. The track was generally southward. Dots along the trajectory are 15 days apart. The magenta trajectory denotes summer observations.

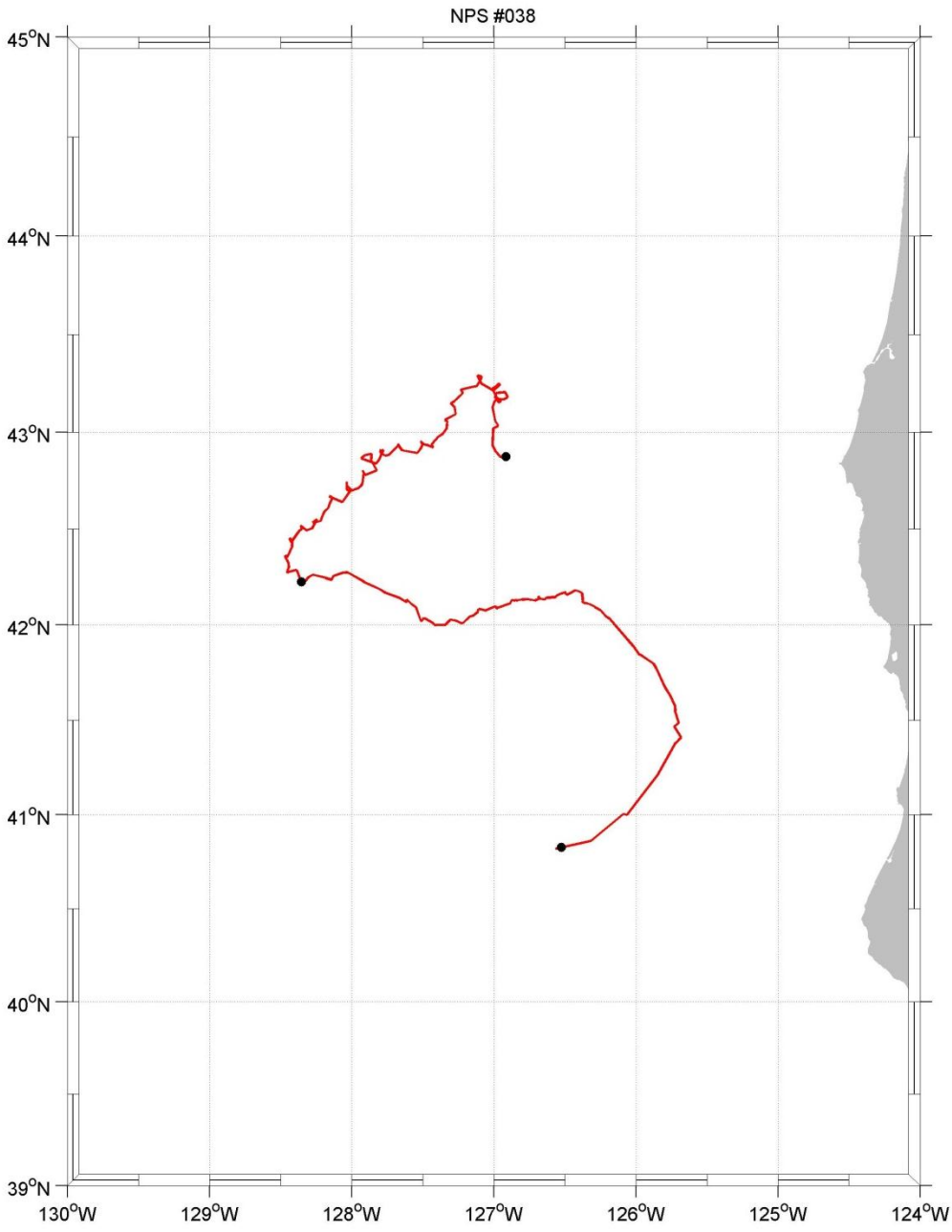

Figure A35. RAFOS float n038 obtained its first fix (42.87°N 126.91°W) October 20, 1996 and was tracked until November 17, 1996. Initially, the float seemed to be caught in a rapidly translating (compared to its rotational speed) anticyclone that produced small anticyclonic loops and epicycloids along its generally southwestward trajectory to about 128.5°W. Thereafter, the float escaped the anticyclone, moving eastward to about 126.5°W. Finally, the float followed an anticyclonic curve southward to about 41°N, where the float was recovered by a fisherman. Dots along the trajectory are 15 days apart. The red trajectory denotes fall observations.

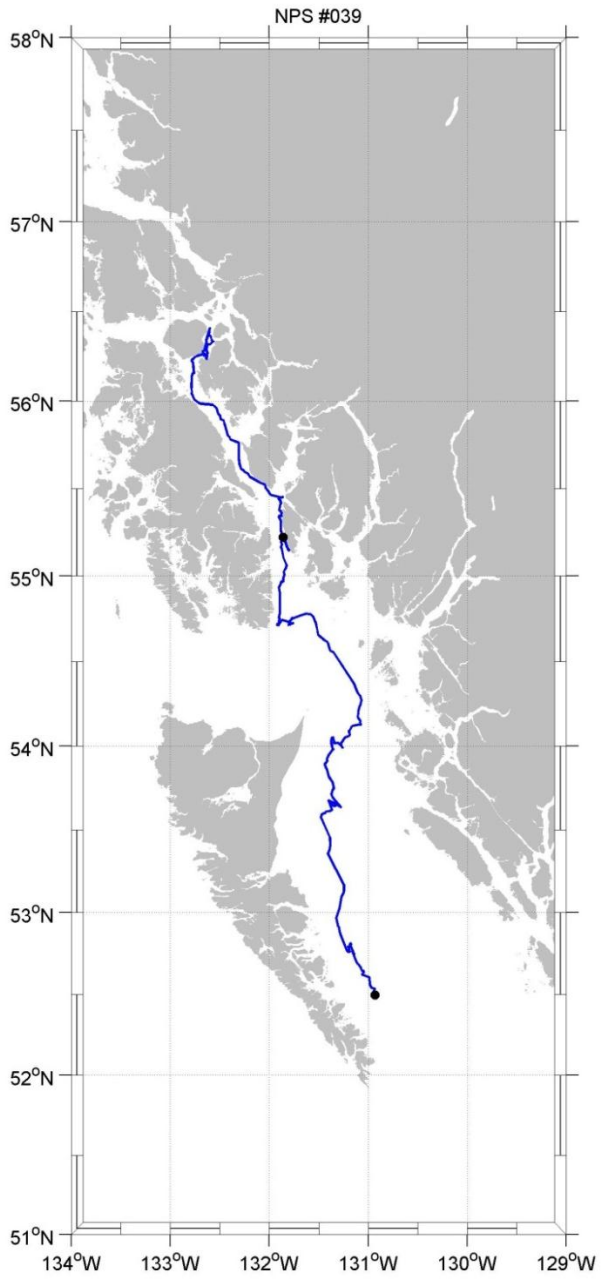

Figure A36. RAFOS float n039 obtained its first fix (52.50°N 130.93°W) December 10, 1997, and was tracked until January 2, 1998. The float worked its way northward among the Queen Charlotte Islands of Canada and into the fjords and inlets of Alaska and Canada. Dots along the trajectory are 15 days apart. The blue trajectory denotes winter observations.

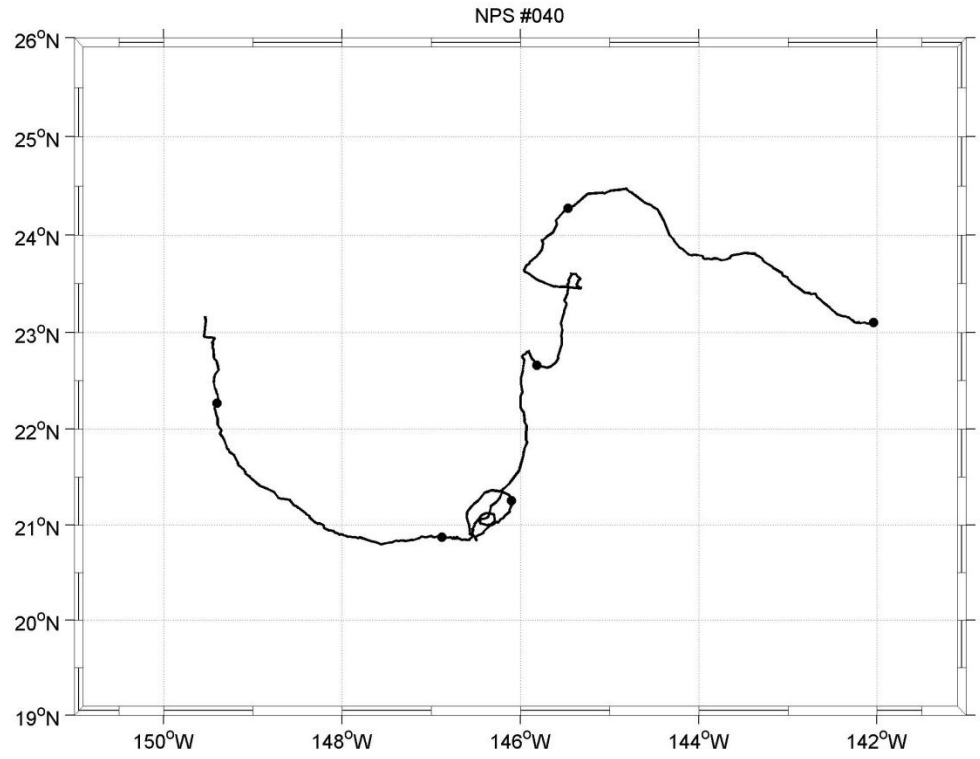

Figure A37. RAFOS float n040 obtained its first fix (21.31°N 142.01°W) March 12, 1999, and was tracked until May 26, 1999. The float generally tracked westward, with some northward/southward excursions. During April at about 146.25°W, the float made 2 complete cyclonic rotations. Dots along the trajectory are 15 days apart. The black trajectory denotes spring observations.

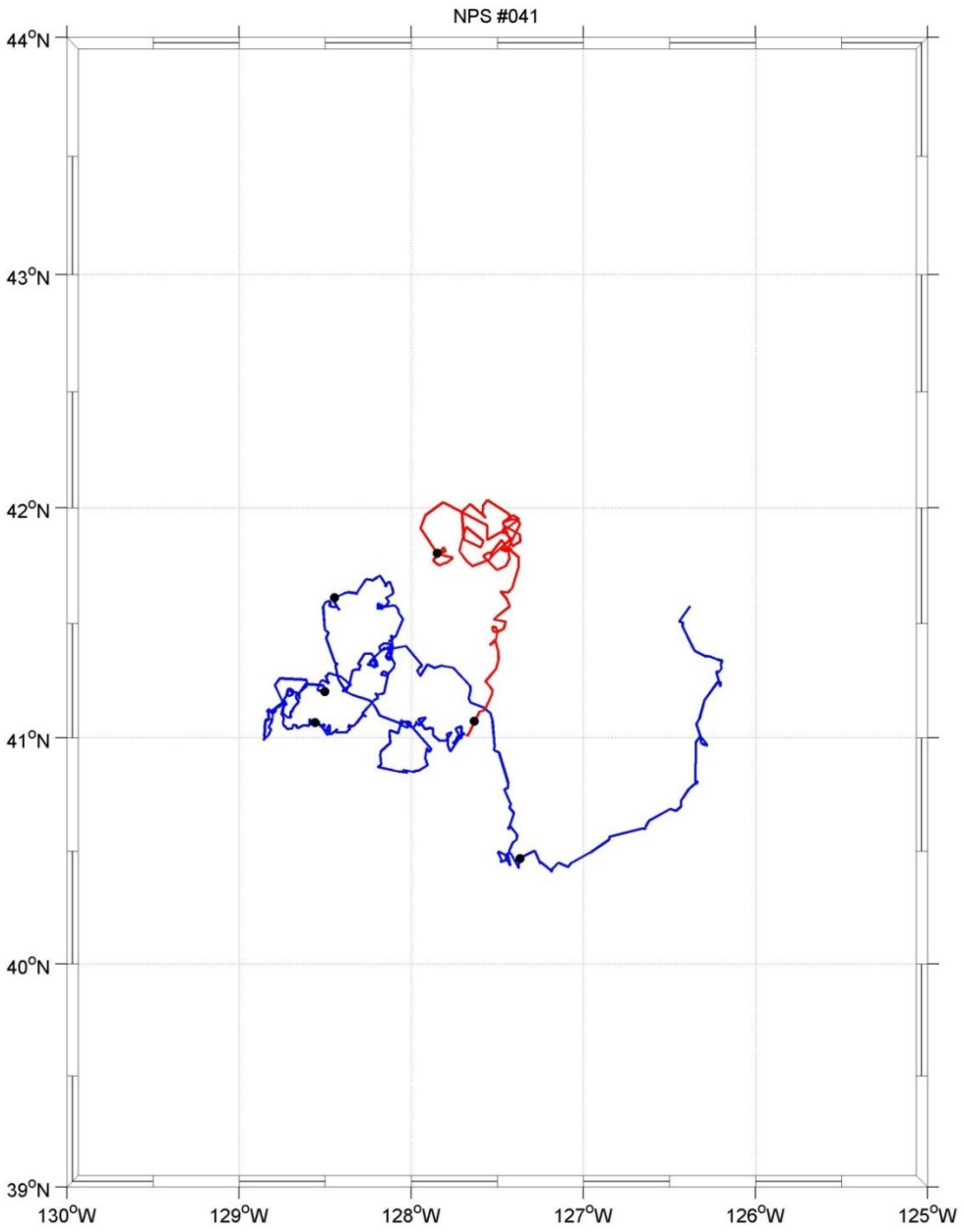

Figure A38. RAFOS float n041 obtained its first fix (41.81°N 127.85°W) November 17, 1997, and was tracked until February 5, 1998. The float appeared to be caught in an eddy, executing a series of anticyclonic loops and epicycloids, initially at a stationary location (about [41.75°N, 127.5°W]), then moving southward to about 41°N, then westward to about 129°W, and finally eastward to about 128°W. Thereafter, the float appeared to escape the eddy, moving southward to about 40.5°N, thence northeastward to about [41.5°N, 126.5°W]. Dots along the trajectory are 15 days apart. Colors represent different seasons in the trajectory: fall (red) and winter (blue).

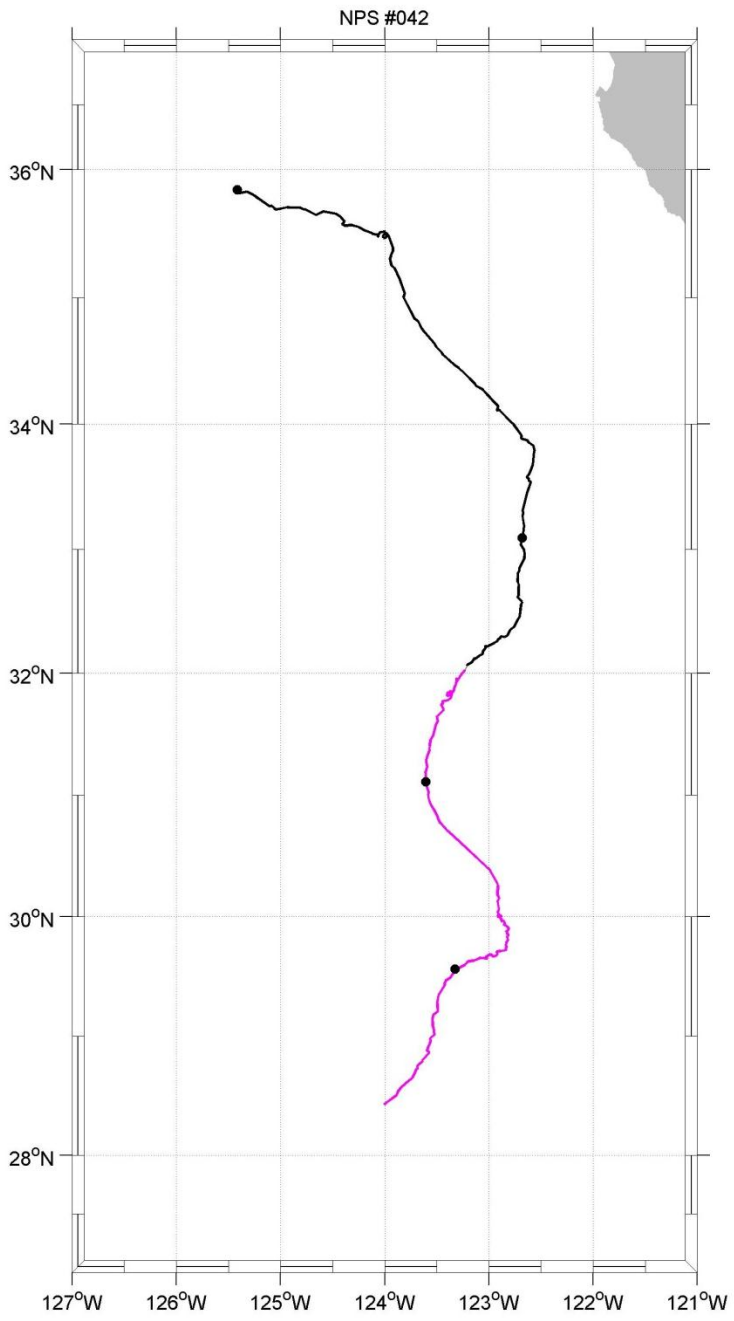

Figure A39. RAFOS float n042 obtained its first fix (35.84°N 125.41°W) May 12, 1997, and was tracked until June 30, 1997. The float generally drifted southward, initially moving southeastward to about 34°N, before thence moving south-southwestward. Dots along the trajectory are 15 days apart. Colors represent different seasons in the trajectory: spring(black) and summer (magenta).

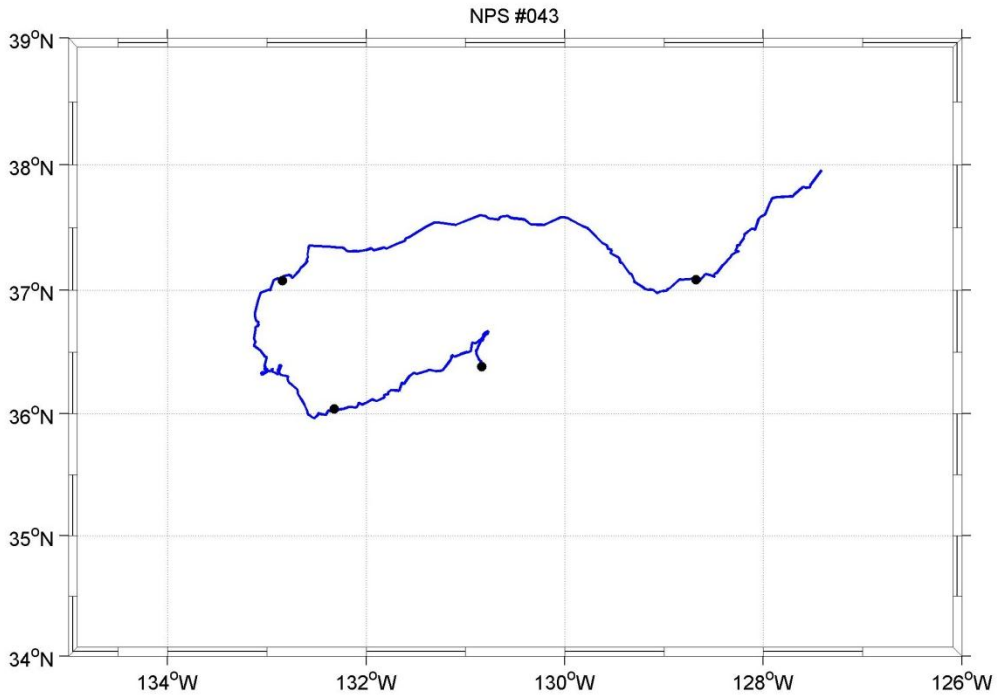

Figure A40. RAFOS float n043 obtained its first fix (35.84°N 125.41°W) December 13, 1997, and was tracked until January 30, 1998. The float briefly moved northward, completed a single, small anti-cyclonic loop, and then moved southwestward to 36°N. Next it turned northward to 37°N, before moving generally east-northeastward to about [38°N, 127.5°W]. Dots along the trajectory are 15 days apart. The blue trajectory denotes winter observations.

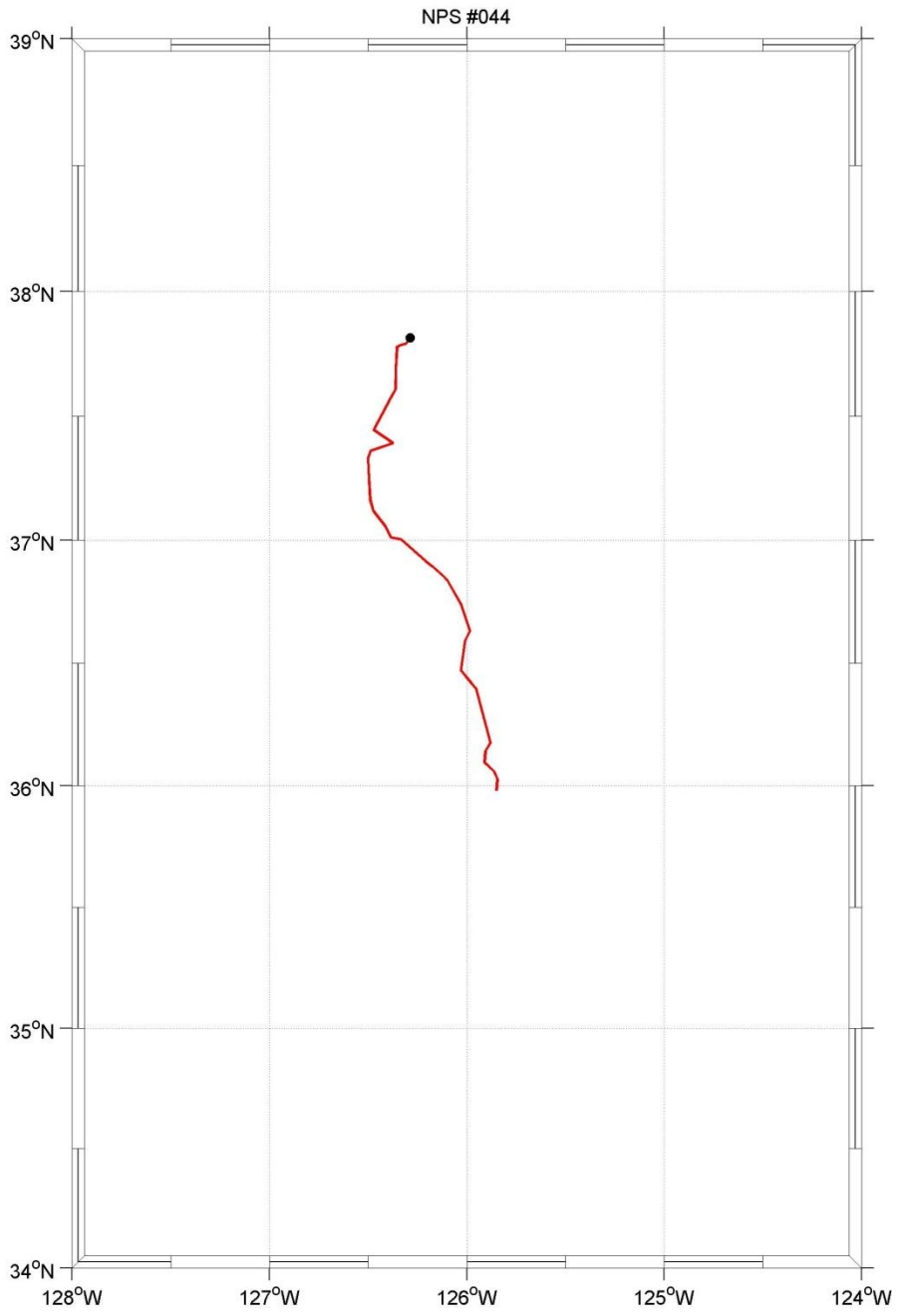

Figure A41. RAFOS float n044 obtained its first fix (37.81°N, 126.28°W) October 23, 1996, and was tracked only five days until October 27, 1996. Float n044's southerly trajectory was not used in this study. The red trajectory denotes fall observations.

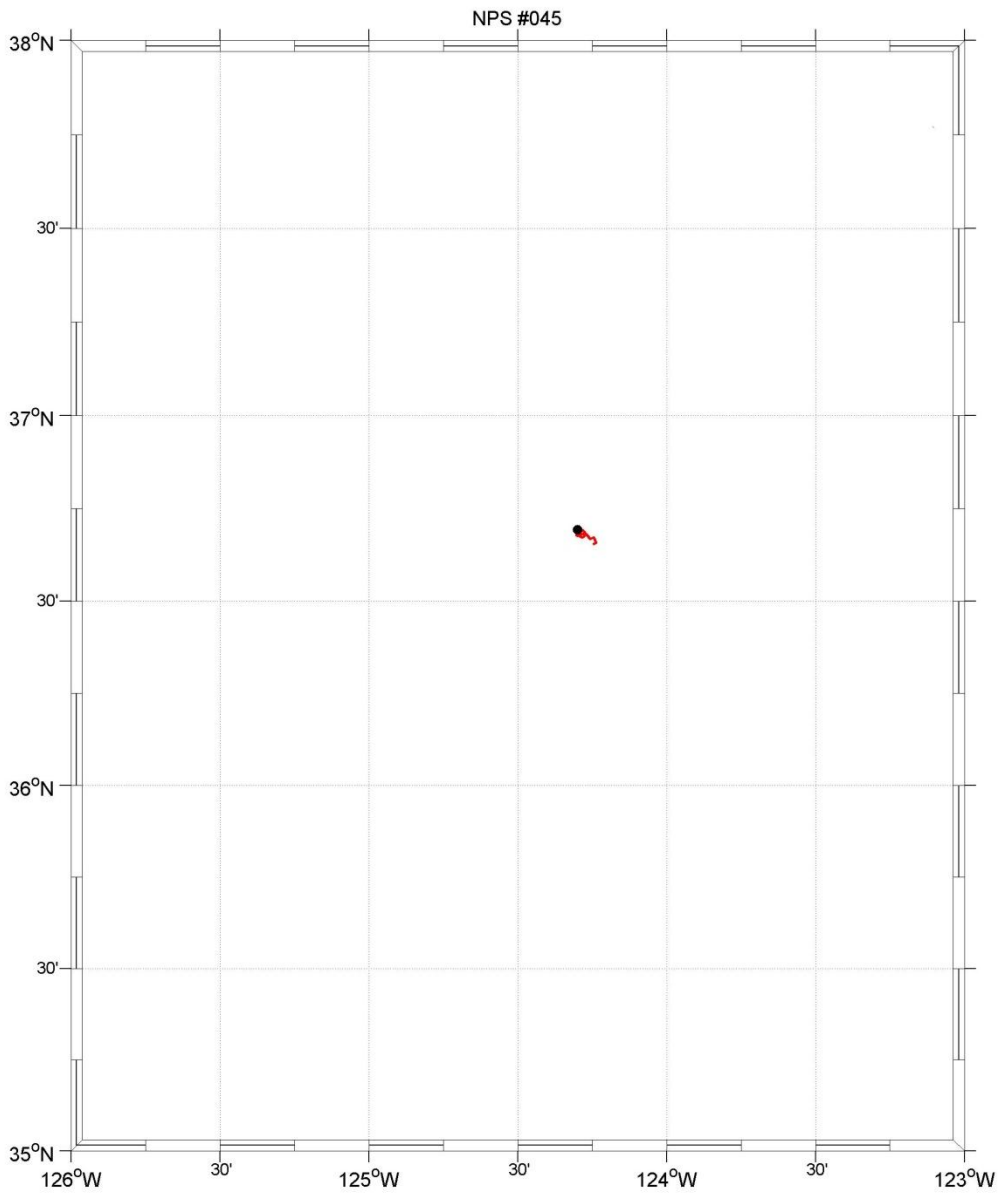

Figure A42. RAFOS float n045 obtained its first fix (36.69°N, 124.30°W) September 14, 1996, and was tracked only two days until September 15, 1996. Float n045's southwesterly trajectory was not used in this study. The red trajectory denotes fall observations.

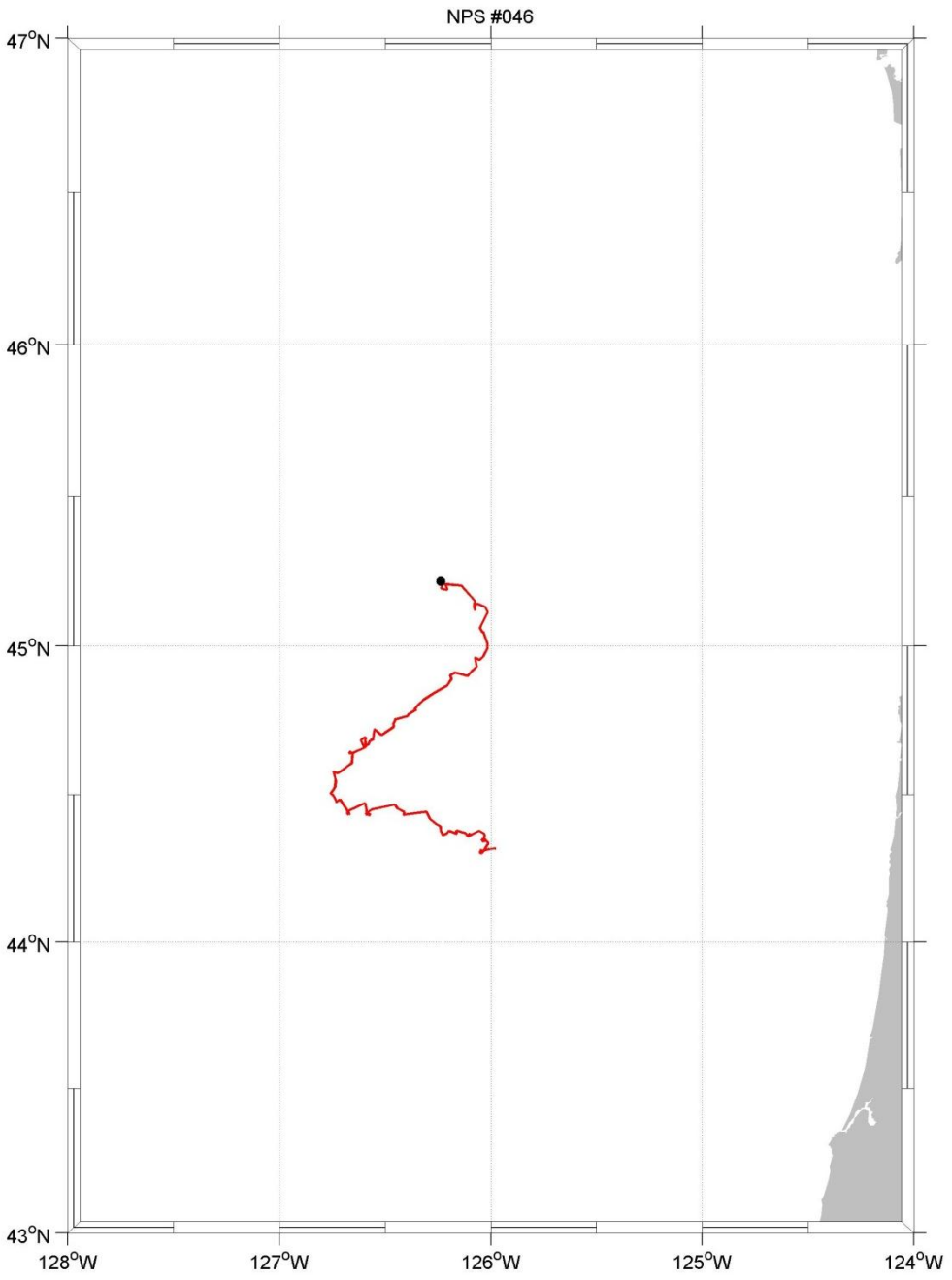

Figure A43. RAFOS float n046 obtained its first fix (45.21°N 126.24°W) September 16, 1997, and was tracked until September 30, 1997. The float followed a backwards "S" shape southward. There is also some indication of superimposed anticycloidal/epicycloidal motion superimposed on the underlying trajectory. Dots along the trajectory are 15 days apart. The red trajectory denotes fall observations.

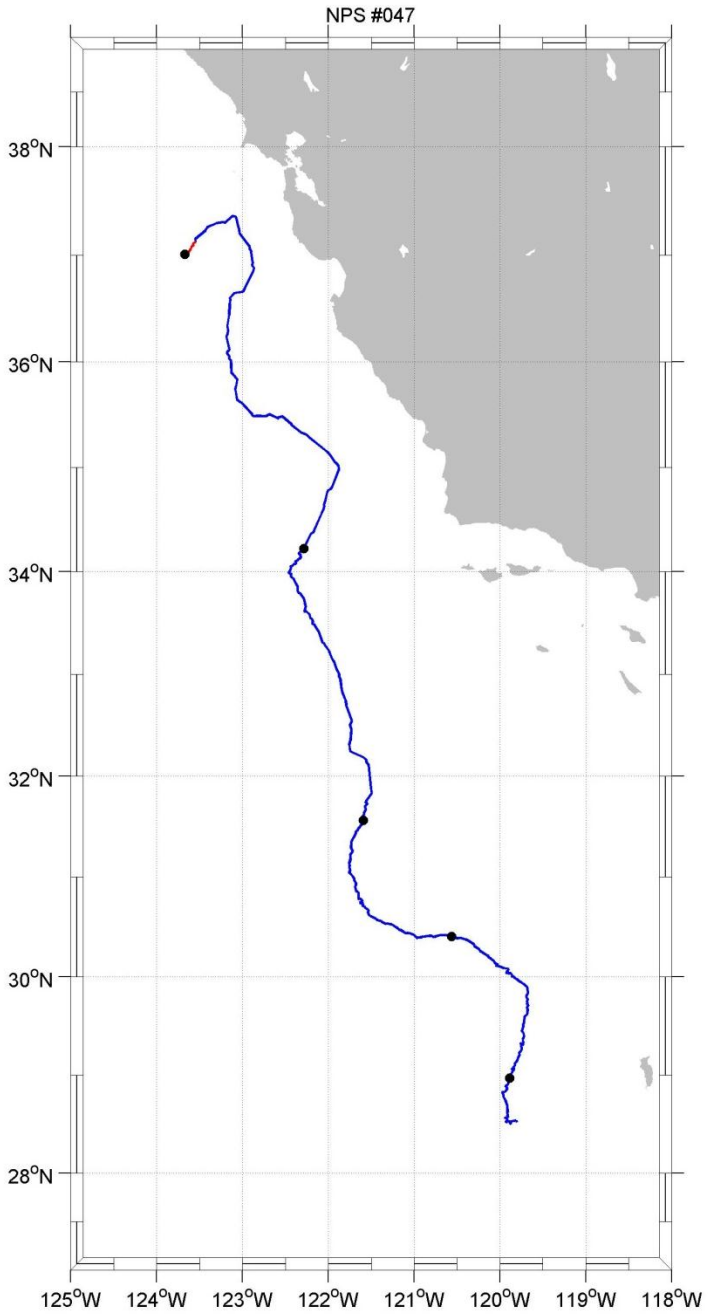

Figure A44. RAFOS float n047 obtained its first fix (37.01°N 123.67°W) November 30, 1998, and was tracked until January 31, 1999. After an initial northeastward track, the float generally moved south-southeastward. Dots along the trajectory are 15 days apart. Colors represent different seasons in the trajectory: fall (red) and winter (blue).

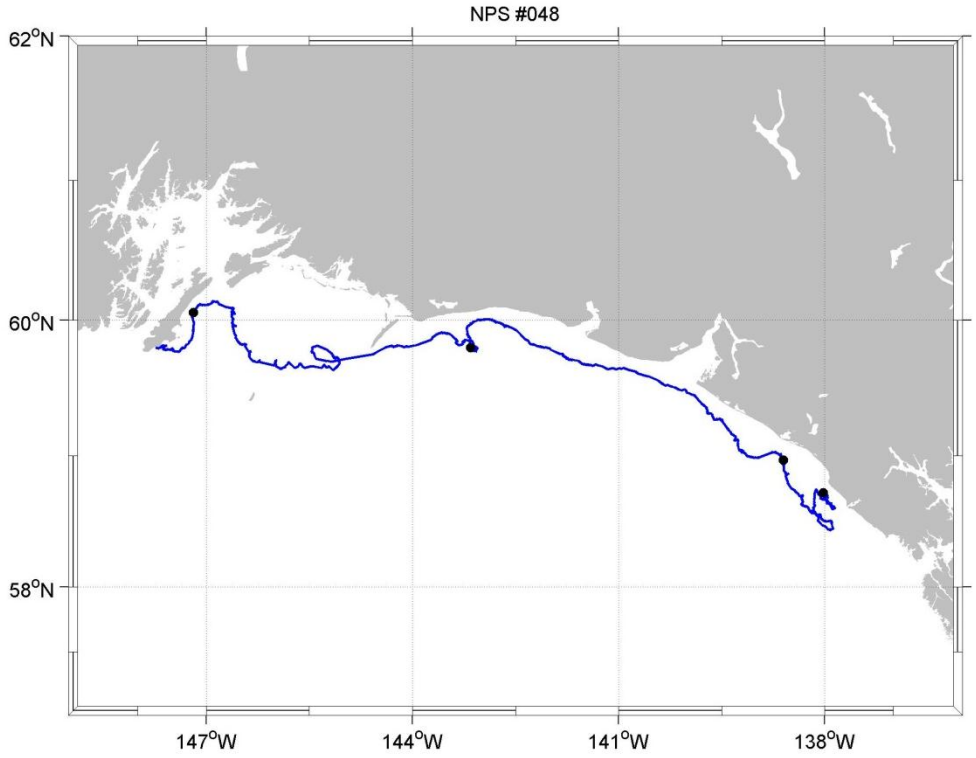

Figure A45. RAFOS float n048 obtained its first fix (58.72°N 138.03°W) January 10, 1998, and was tracked until February 24, 1998. After meandering near the coast at about [58.5°N, 138°W] for 15 days, the float moved slightly offshore and thence began tracking westward along the Alaskan coast to about 148°W. Dots along the trajectory are 15 days apart. The blue trajectory denotes winter observations.

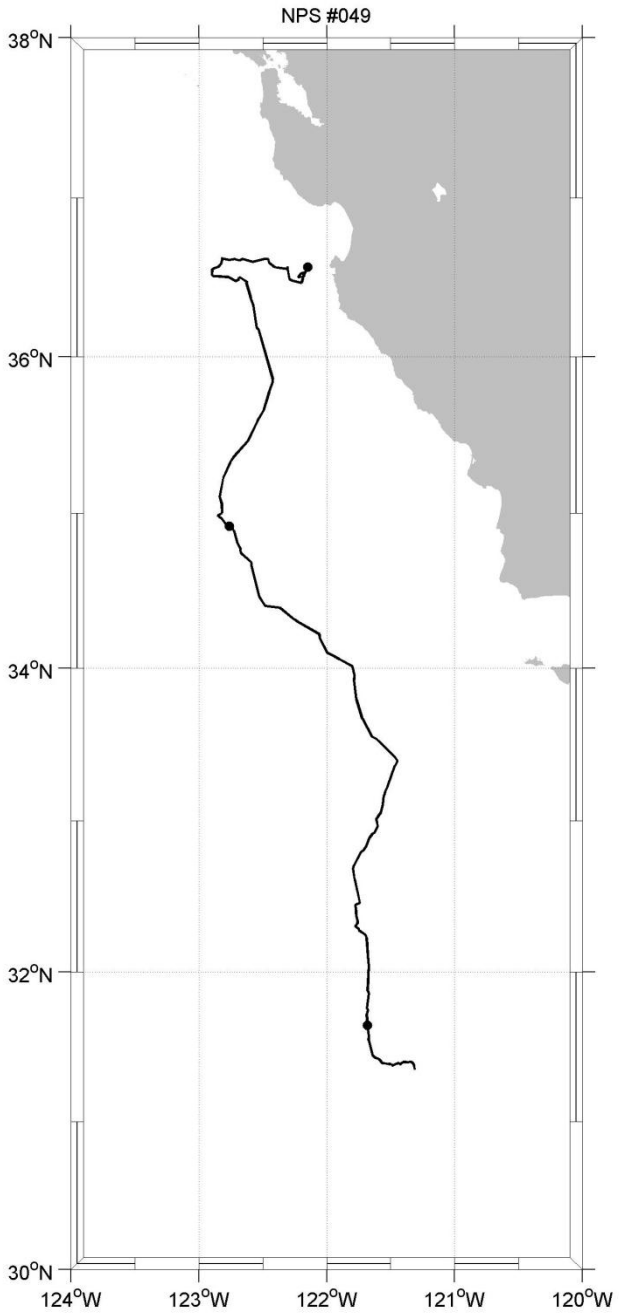

Figure A46. RAFOS float n049 obtained its first fix (36.57°N 122.15°W) March 23, 1997, and was tracked until April 25, 1997. After executing a small anticyclonic loop off Point Sur, the float moved westward offshore to nearly 123°W, where it turned to a south-southwesterly track. Dots along the trajectory are 15 days apart. The black trajectory denotes spring observations.

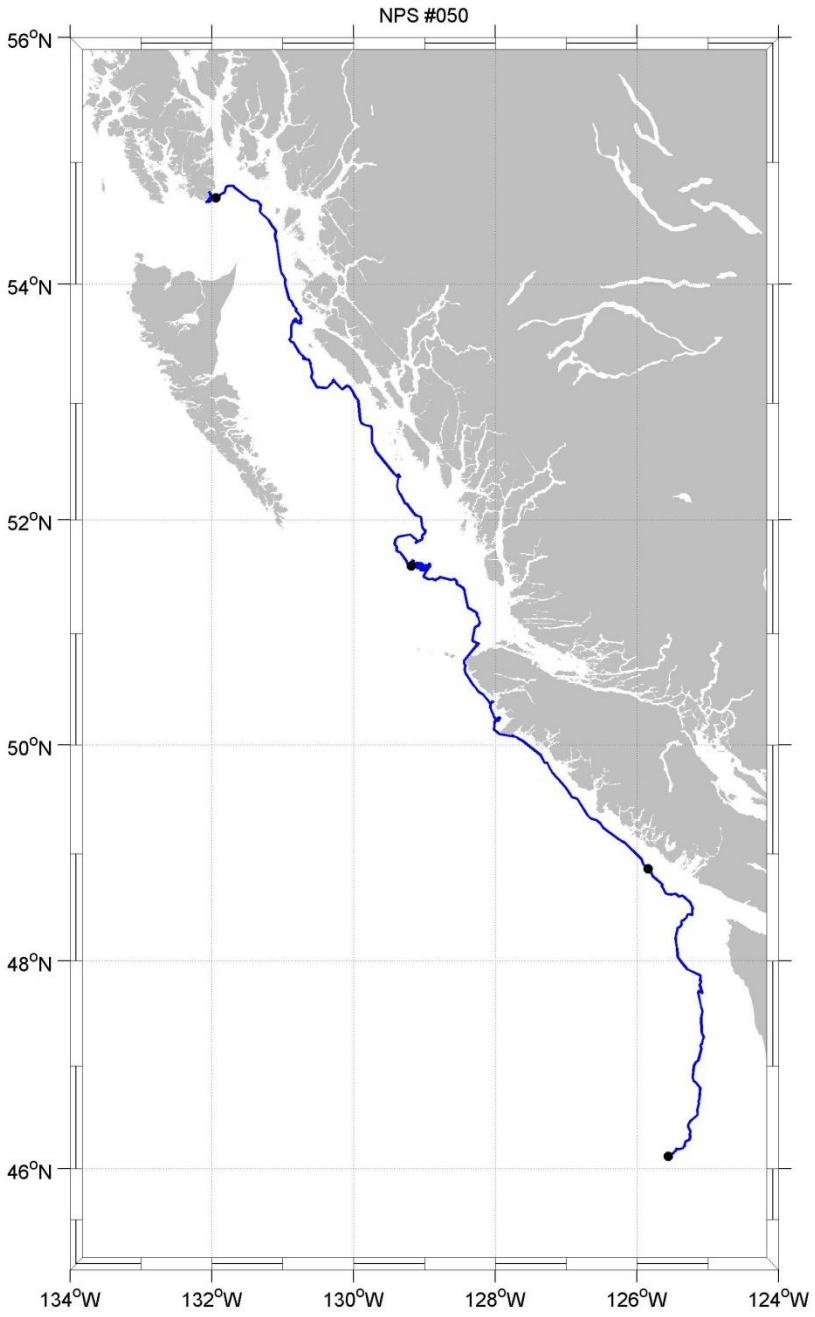

Figure A47. RAFOS float n050 obtained its first fix (46.12°N 125.56°W) January 9, 1998, and was tracked until February 24, 1998. The float initially headed northwards~~s~~ toward shore~~;~~, then turned northwestwards~~s~~, closely following the Vancouver Island shoreline. The float continued to follow the Canadian coast northwestward into the Queen Charlotte Islands, where it (presumably) ran aground. Dots along the trajectory are 15 days apart. The blue trajectory denotes winter observations.

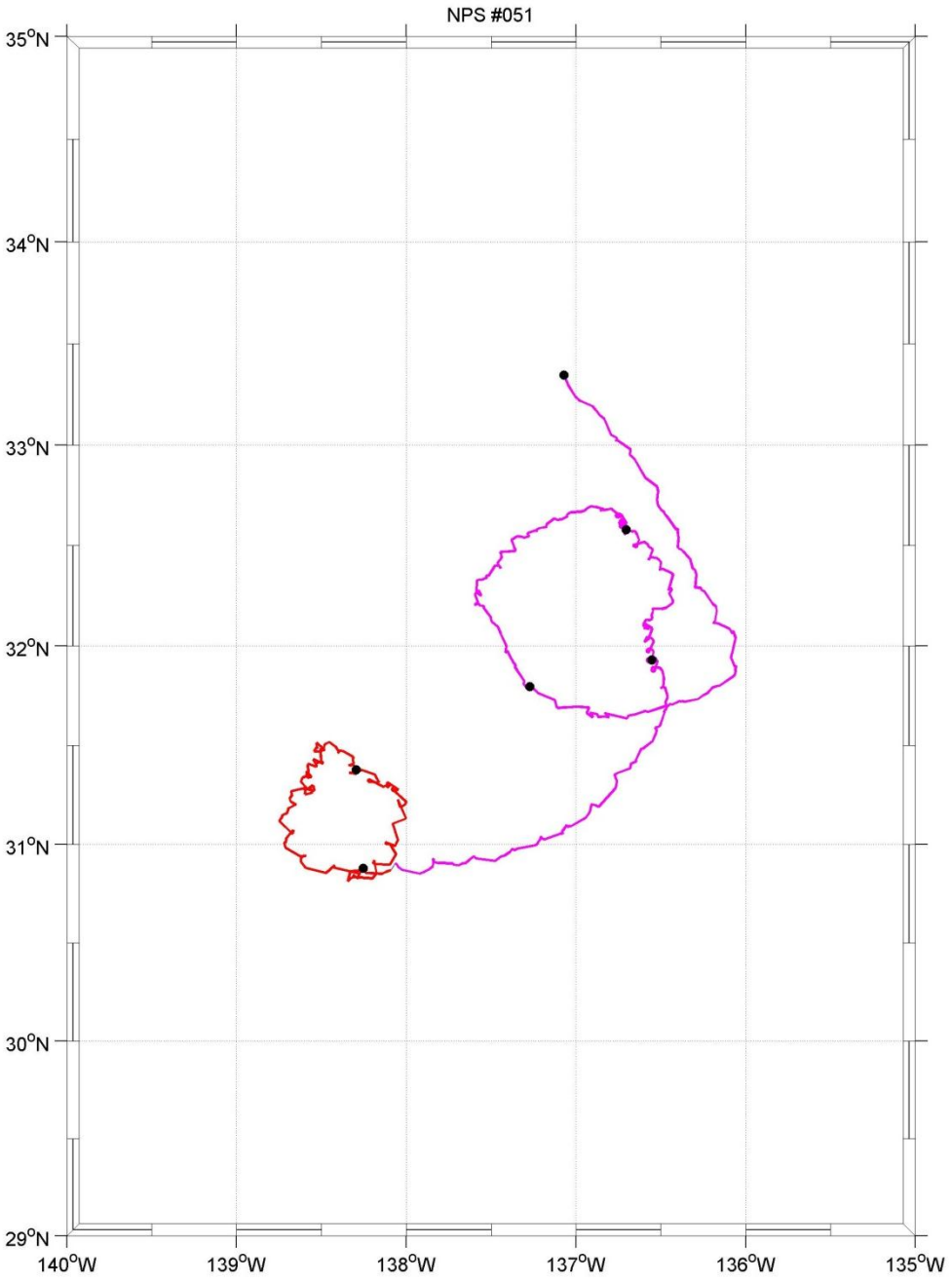

Figure A48. RAFOS float n051 obtained its first fix (33.35°N 137.07°W) July 8, 1998, and was tracked until September 26, 1998. The float made two complete anti-cyclonic rotations while moving in a generally southwesterly direction. Superimposed on much of that southwesterly trajectory appears to be a smaller anticyclonic eddy producing anticyclonic loops and epicycloids. Dots along the trajectory are 15 days apart. Colors represent different seasons in the trajectory: summer (magenta) and fall (red).

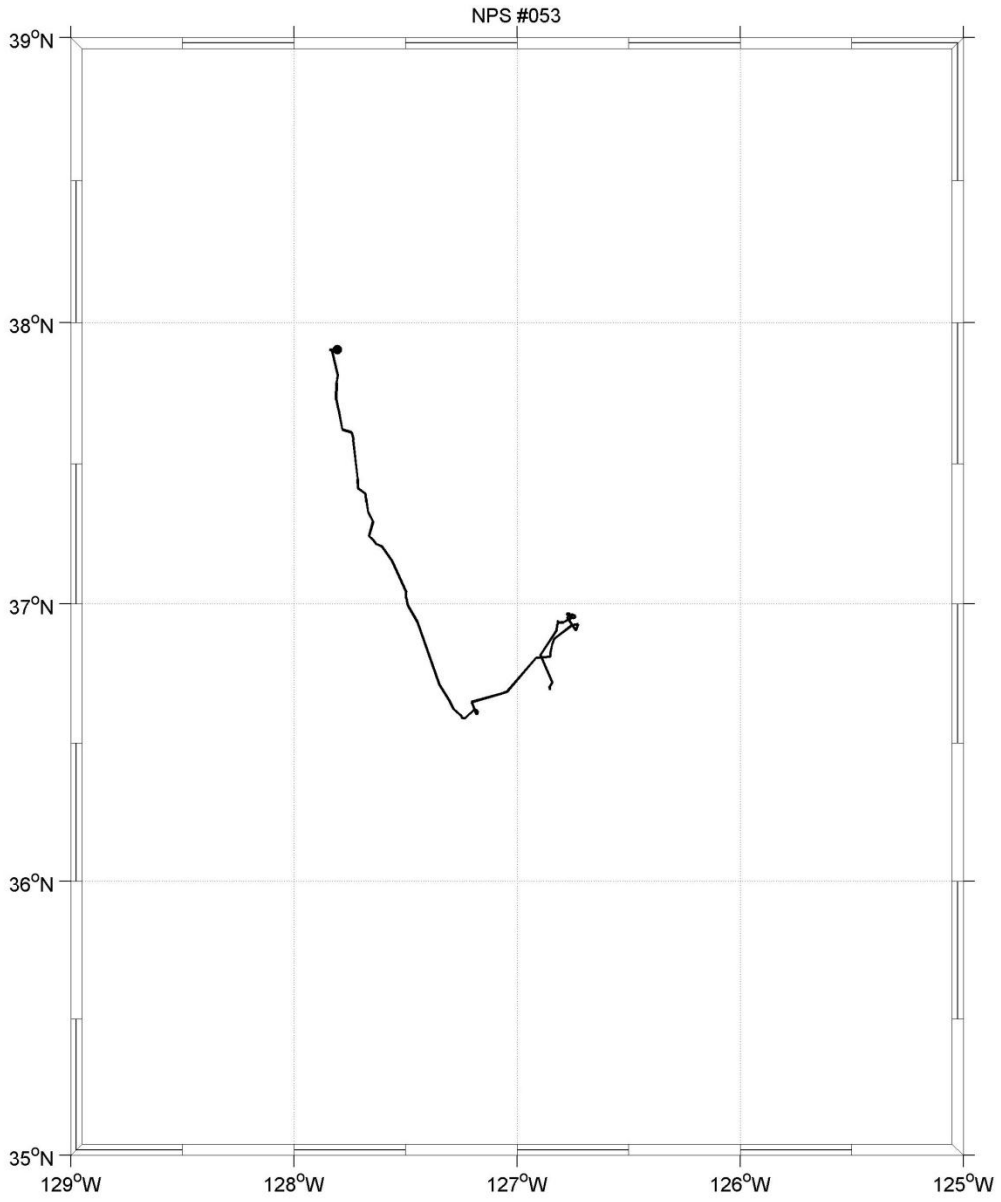

Figure A49. RAFOS float n053 obtained its first fix (37.90°N 127.81°W) April 22, 1998, and was tracked until May 6, 1998. The float headed south-southeast to about 36.5°N, then turned northeastwards to about [37°N, 126.75°W], before reversing course to about 127°WDots along the trajectory are 15 days apart. The black trajectory denotes spring observations.

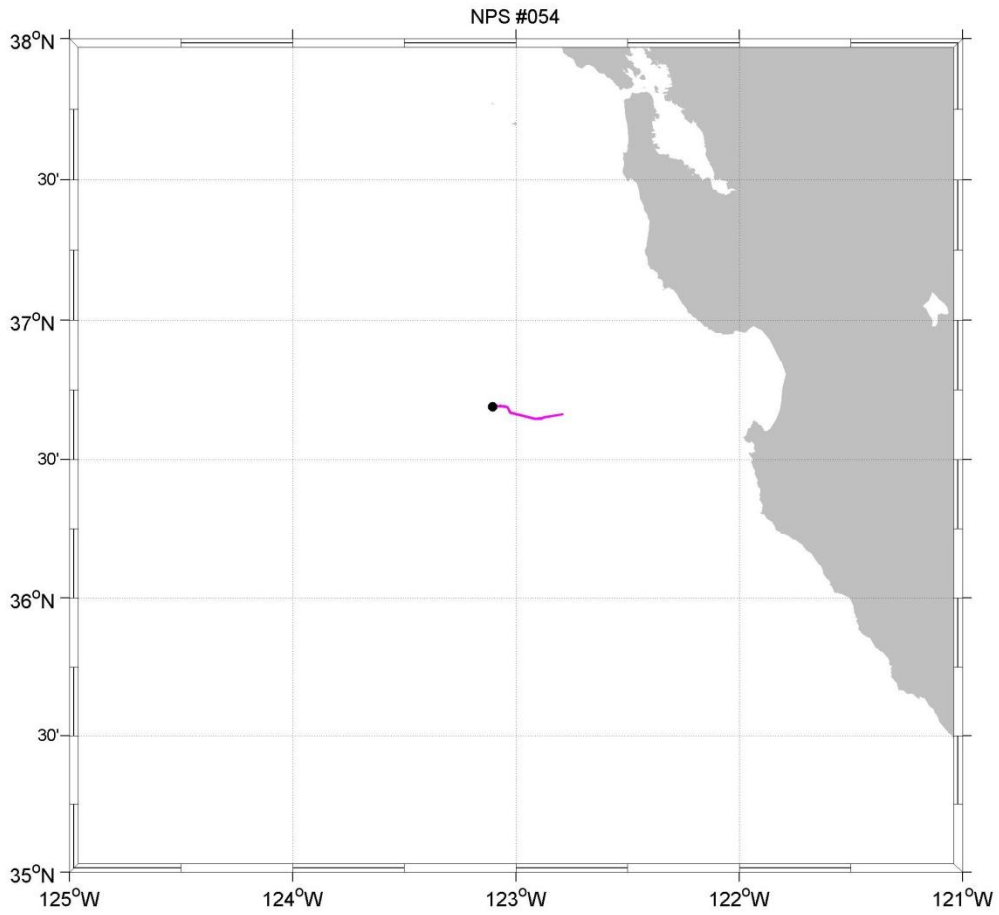

Figure A50. RAFOS float n054 obtained its first fix (36.69°N, 123.11°W) June 24, 1998, and was tracked only two days until June 25, 1998. Float n054's easterly trajectory was not used in this study. The magenta trajectory denotes summer observations.

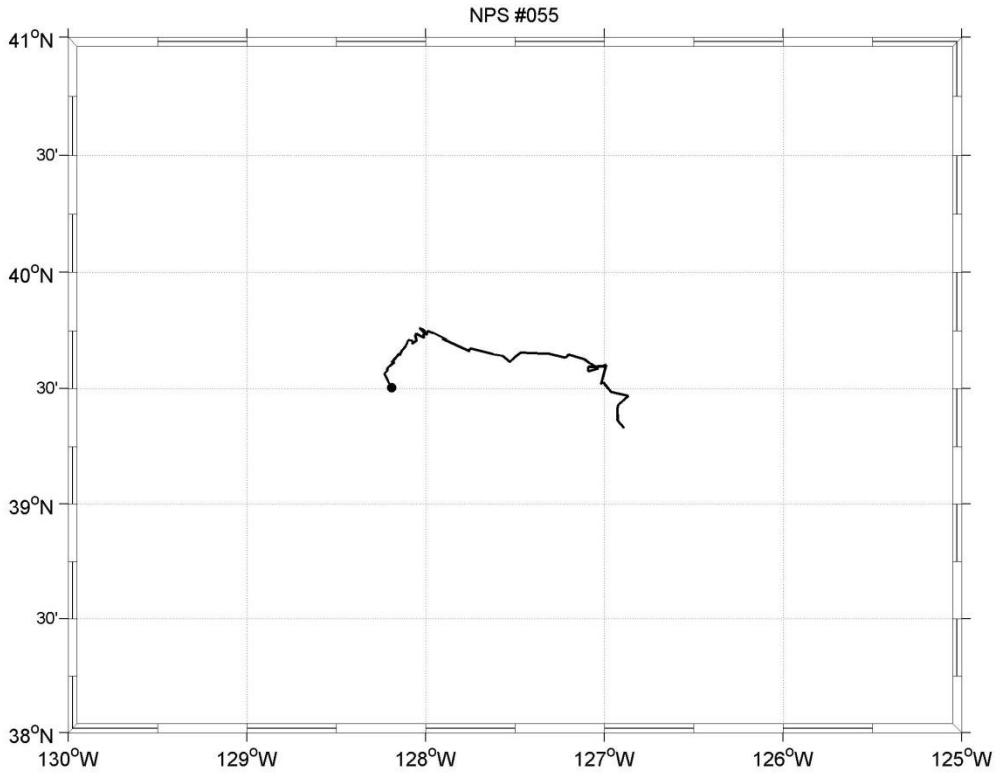

Figure A51. RAFOS float n055 obtained its first fix (39.50°N 128.19°W) April 23, 1998, and was tracked until May 4, 1998. The float generally headed eastward. Dots along the trajectory are 15 days apart. The black trajectory denotes spring observations.

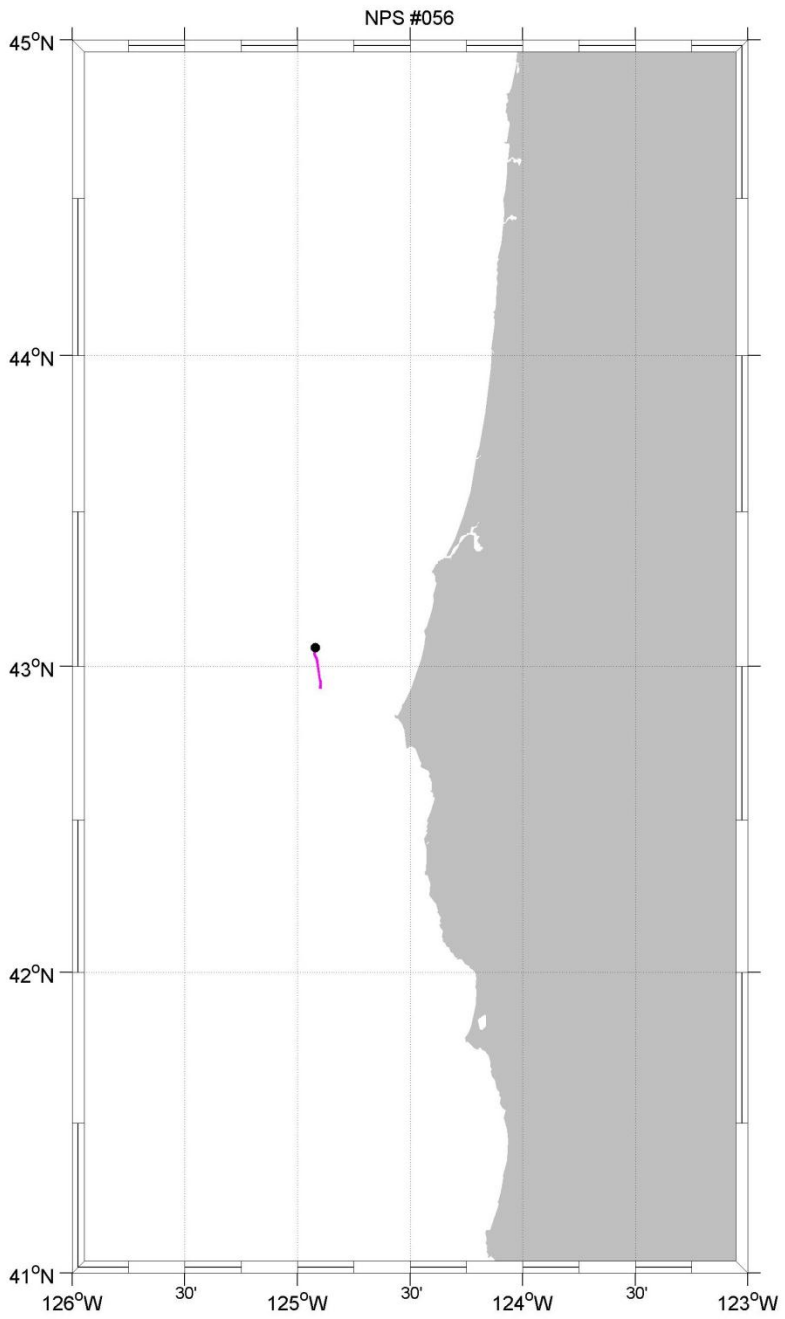

Figure A52. RAFOS float n056 obtained its first fix (43.06°N, 124.09°W) June 24, 1998, and was tracked only two days until June 25, 1998. Float n056's southerly trajectory was not used in this study. The magenta trajectory denotes summer observations

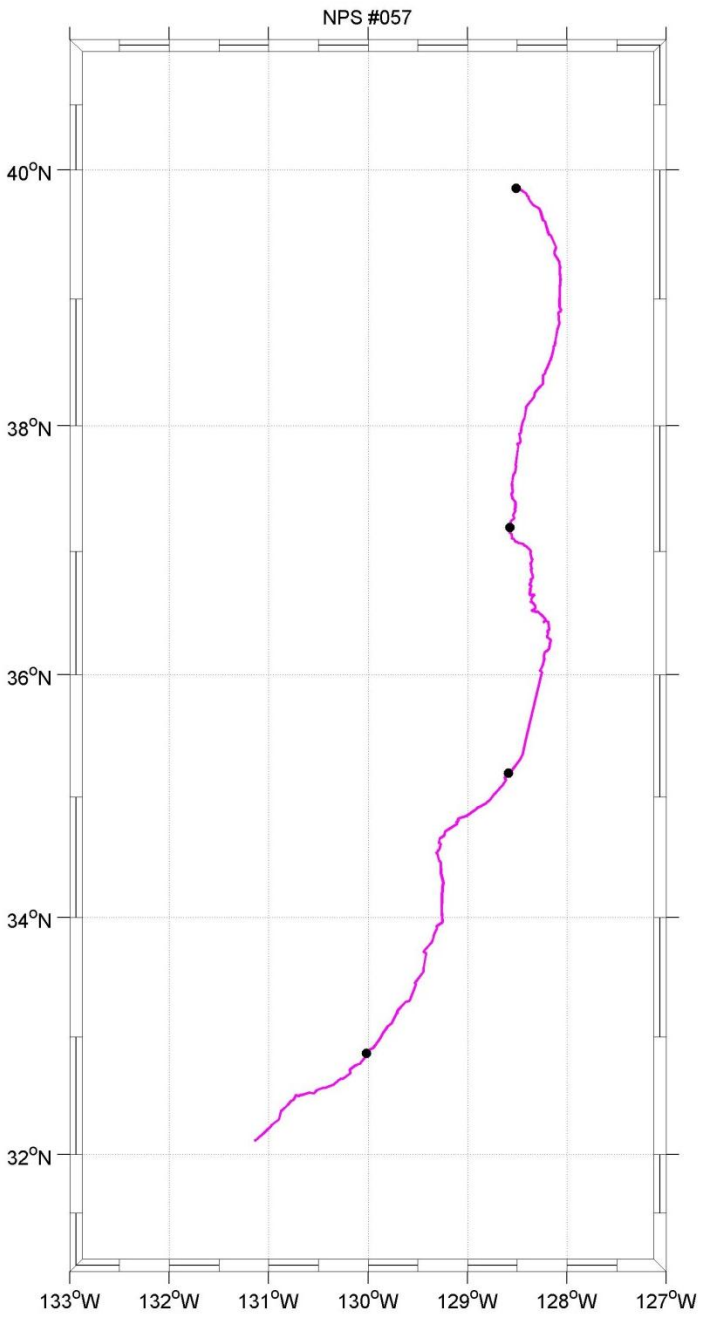

Figure A53. RAFOS float n057 obtained its first fix (39.86°N 128.51°W) June 24, 1998, and was tracked until September 13, 1998. The float drifted south-southwestward. Dots along the trajectory are 15 days apart. The magenta trajectory denotes summer observations.

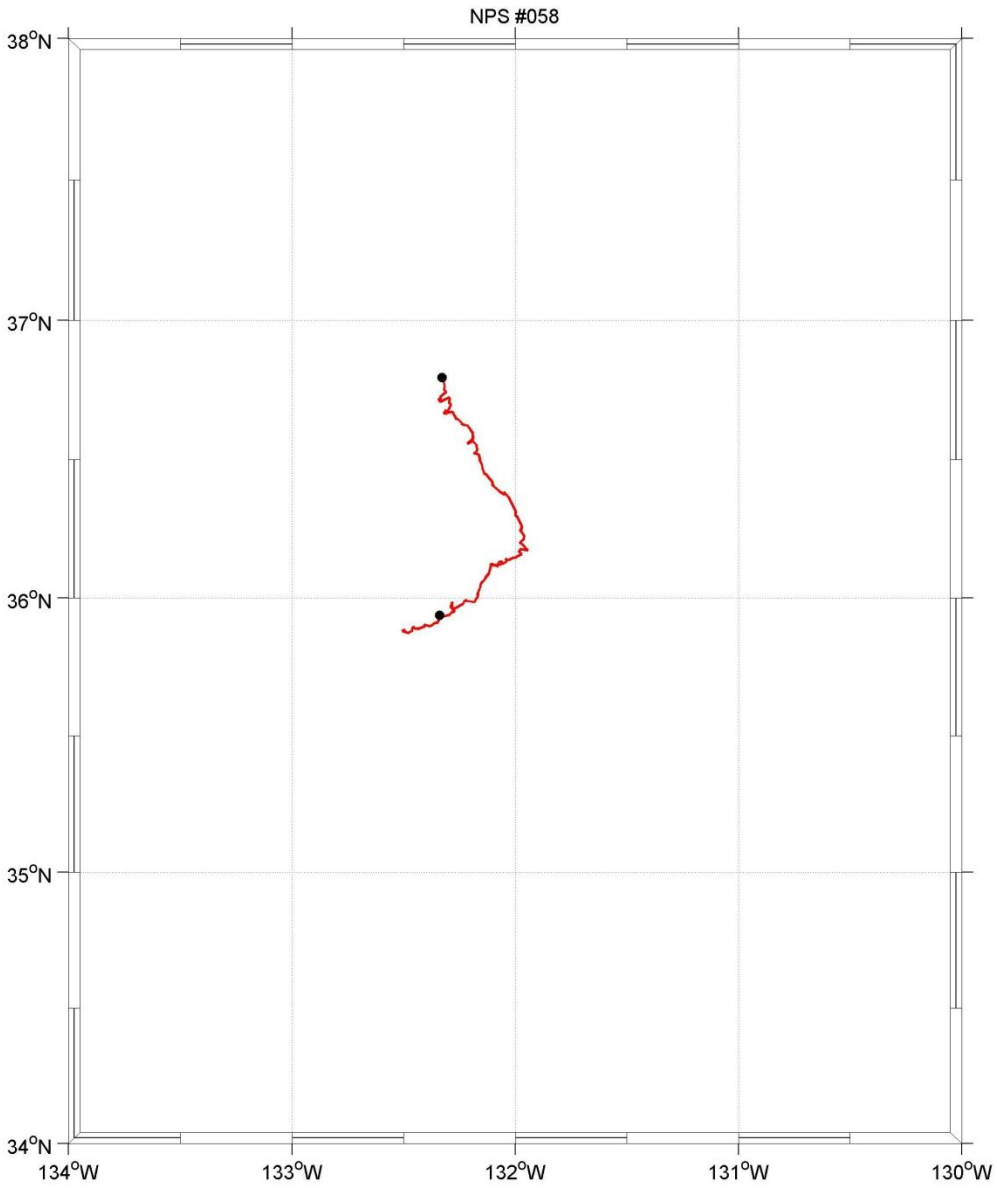

Figure A54. RAFOS float n058 obtained its first fix (36.80°N 132.33°W) September 14, 1998, and was tracked until September 30, 1998. The float initially drifted south-southeastward to about 36.25°N, and then turned southwestward to about 35.75°N. Dots along the trajectory are 15 days apart. The red trajectory denotes fall observations.

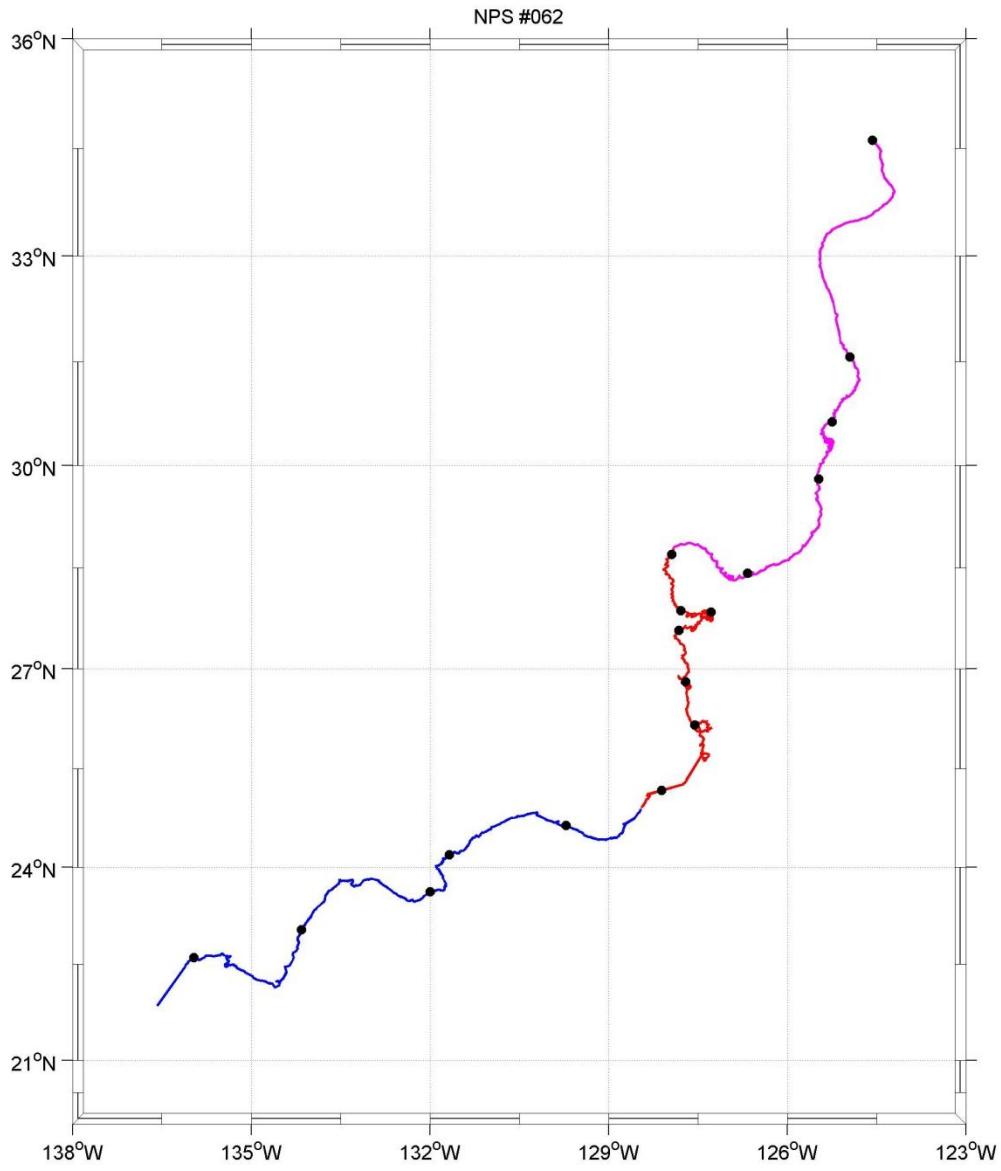

Figure A55. RAFOS float n062 obtained its first fix (34.61°N 124.57°W) June 25, 1999, and was tracked until February 7, 2000. Initially, the float drifted southward to about 28.5°N, where it briefly turned westward to about 127.5°W, before resuming its southward course to about 25.5°N. There it turned west-southwestward to about 136.5°W. Dots along the trajectory are 15 days apart. Colors represent different seasons in the trajectory: summer (magenta), fall (red), and winter (blue).

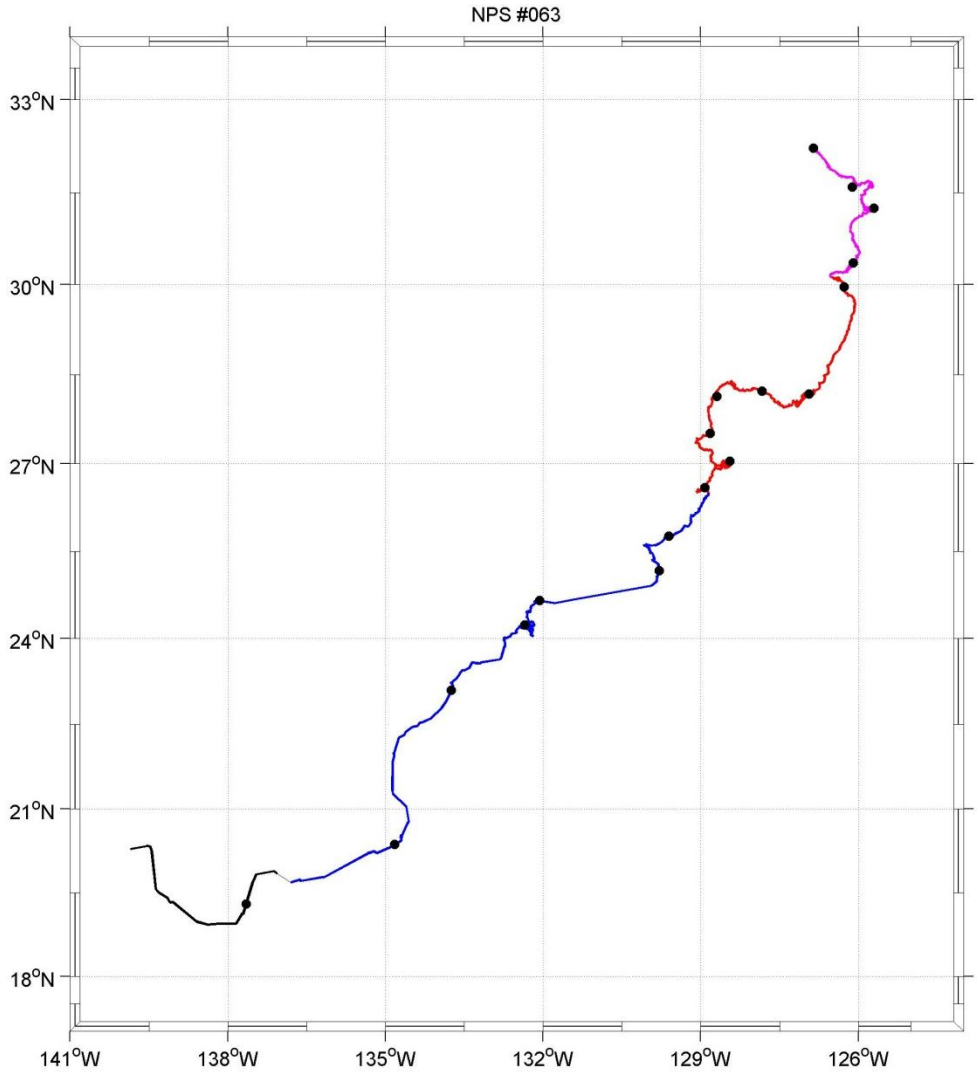

Figure A56. RAFOS float n063 obtained its first fix (32.22°N 126.86°W) July 12, 1999, and was tracked until March 19, 2000. The float headed generally southwestward until about 138°W, where it then turned northwestward near the end of its trajectory. Dots along the trajectory are 15 days apart. Colors represent different seasons in the trajectory: summer (magenta), fall (red), and spring (black).

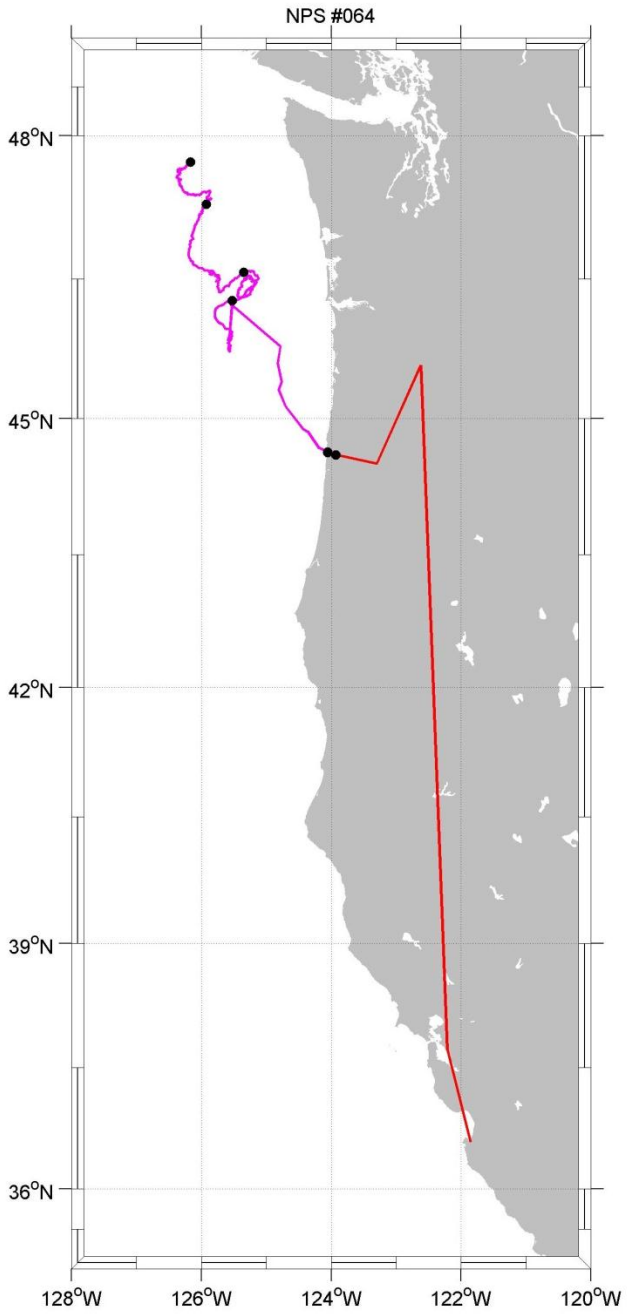

Figure A57. RAFOS float n064 obtained its first fix (47.73°N 126.16°W) June 25, 1999, and was tracked until September 22, 1999. The float generally drifted southward, except that it executed an anticyclonic loop at about 46.5°N. The float was recovered at about 45.75°N and eventually brought to ~~in~~ Newport, Oregon, from whence it was eventually brought back to the *N*aval *P*ostgraduate *S*chool (NPS). Dots along the trajectory are 15 days apart. Colors represent different seasons in the trajectory: surface drift/recovery in the summer (magenta) and return to NPS in the fall (red).

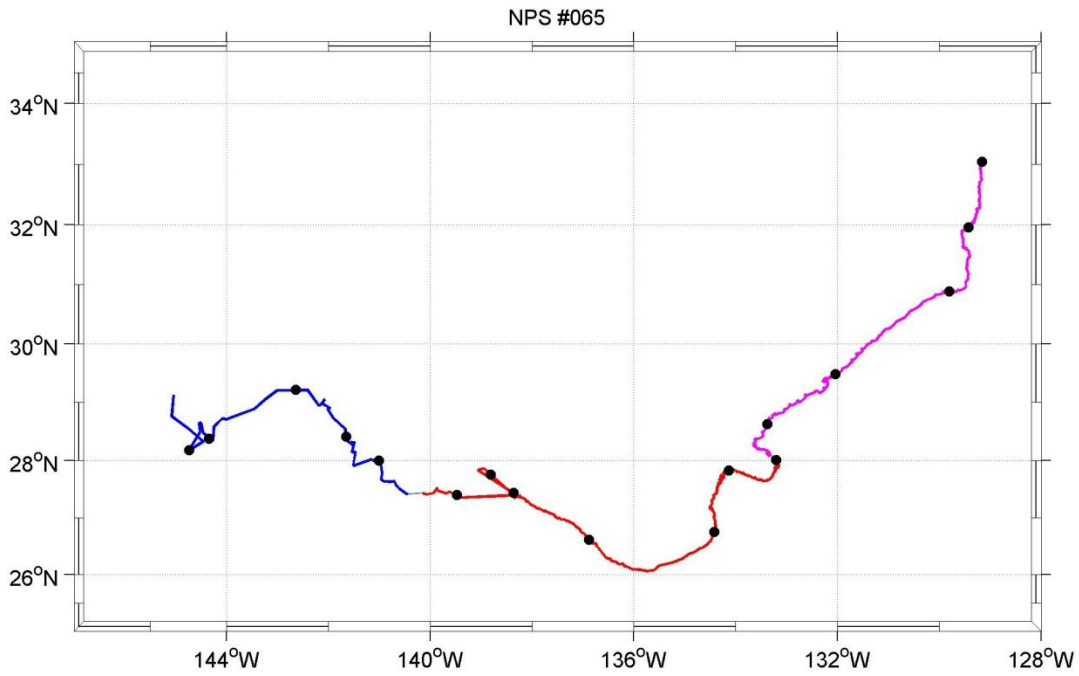

Figure A58. RAFOS float n065 obtained its first fix (33.05°N 129.16°W) June 24, 1999, and was tracked until February 14, 2000. The float drifted southwestward to about 135.5°W, then turned west-northwestward. Dots along the trajectory are 15 days apart. Colors represent different seasons in the trajectory: summer (magenta), fall (red), and winter (blue).

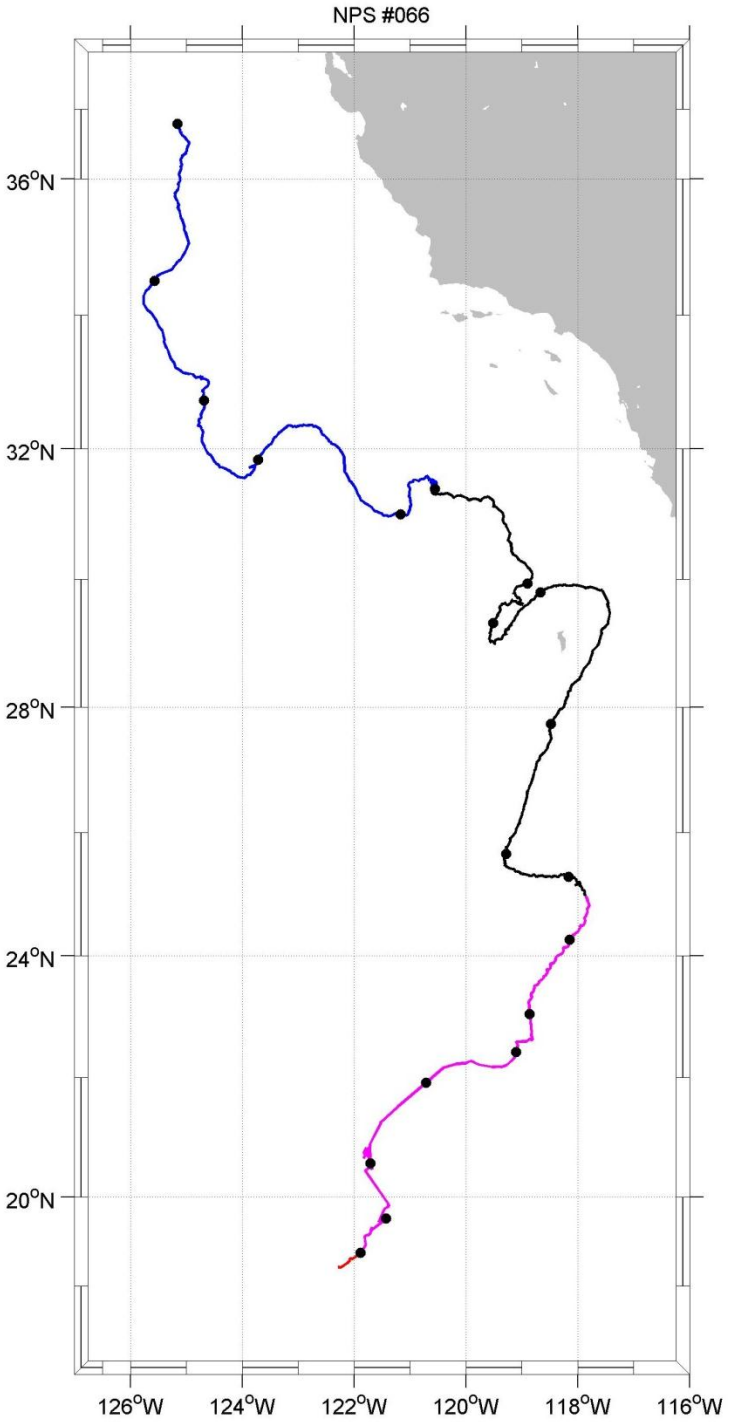

Figure A59. RAFOS float n066 obtained its first fix (36.79°N 125.16°W) December 23, 1999, and was tracked until September 5, 2000. The float travelled generally southward to about 32°N, thence southeastward to about 118°W, and finally southwestward to about 19°N. Dots along the trajectory are 15 days apart. Colors represent different seasons in the trajectory: winter (blue), spring (black), summer (magenta), and fall (red).

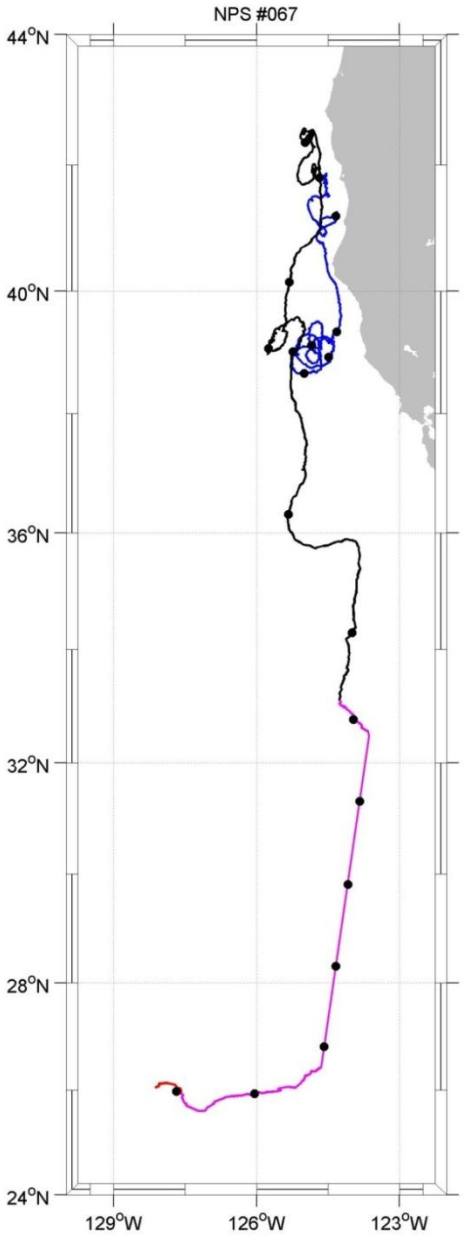

Figure A60. RAFOS float n067 obtained its first fix (39.13°N 124.85°W) December 23, 1999, and was tracked until September 10, 2000. After executing numerous anticyclonic loops off Point Arena, the float proceeded northward along the coast to about 42.25°N, where more anticyclonic loops were completed. The float then meandered back south to slightly farther offshore from Point Arena than initially and made a last anticyclonic loop before heading southward to about 32.25°N in June 2000. In August 2000 the float was re-acquired at about 26°N by the Argos satellites, which tracked it westward to about 128°W. Dots along the trajectory are 15 days apart. Colors represent different seasons in the trajectory: winter (blue), spring (black), and summer (magenta).

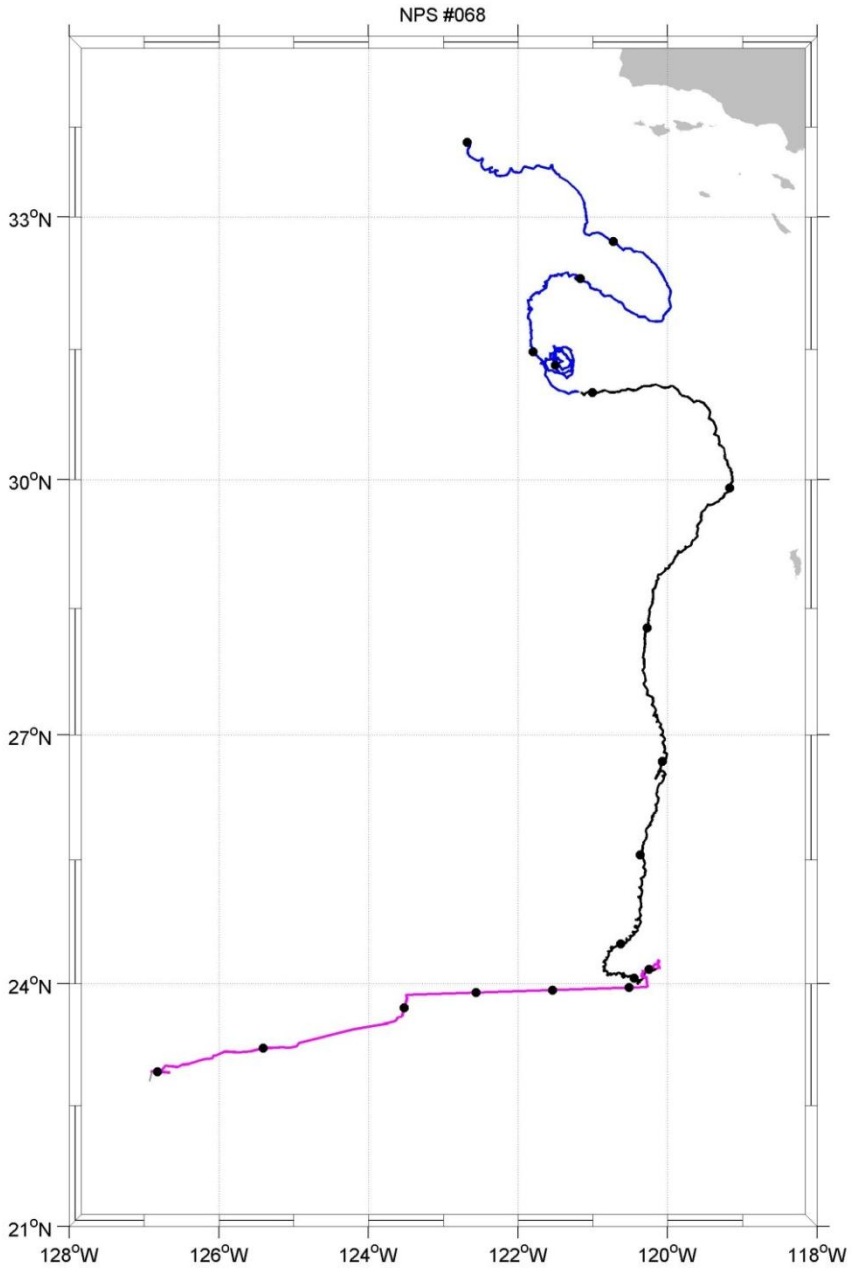

Figure A61. RAFOS float n068 obtained its first fix (33.83°N 122.69°W) December 23, 1999, and was tracked until September 1, 2000. The float generally headed southward to about 24°N in June 2000, except that it executed a number of cyclonic loops at about [31.4°N, 121.4°W]. The float was reacquired in August 2000 at about 123.5°W by the Argos satellites, which tracked it west-southwestward to about 127°W. Dots along the trajectory are 15 days apart. Colors represent different seasons in the trajectory: winter (blue) and spring (black).

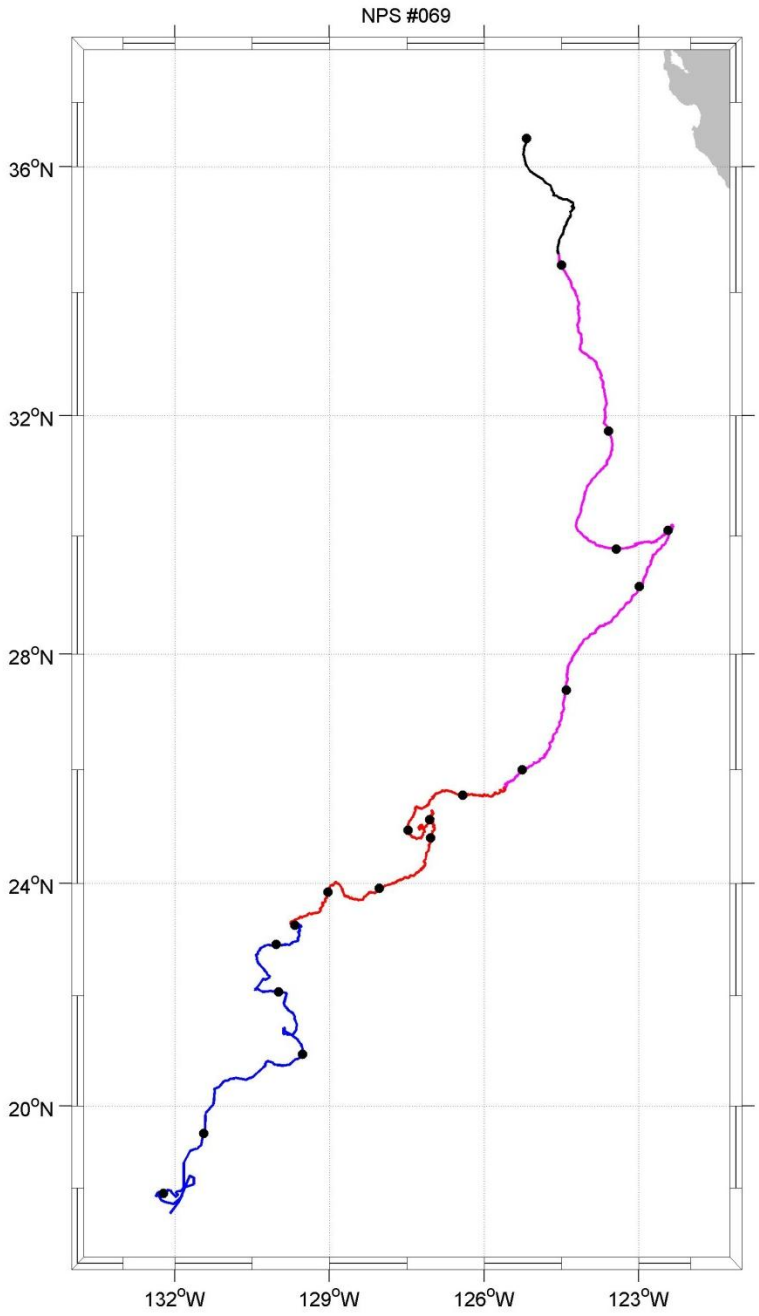

Figure A62. RAFOS float n069 obtained its first fix (36.44°N 125.18°W) May 18, 2000, and was tracked until February 22, 2001. From May to June 2000, the float generally headed southward to about 30°N, whence it then headed southwestward. Dots along the trajectory are 15 days apart. Colors represent different seasons in the trajectory: spring (black), summer (magenta), fall (red), and winter (blue).

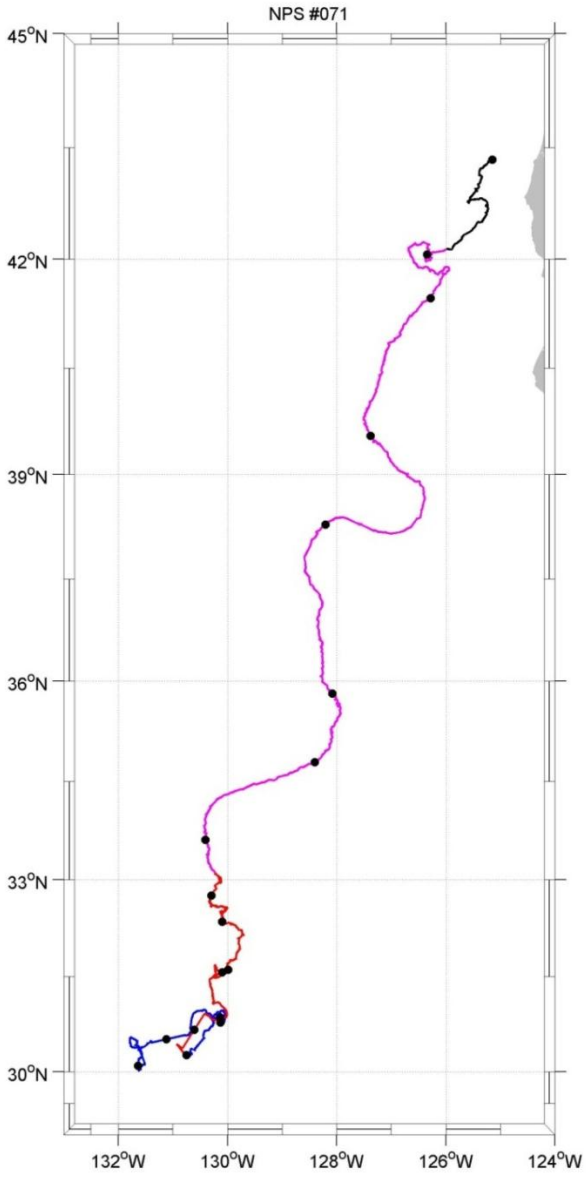

Figure A63. RAFOS float n071 obtained its first fix (43.34°N 125.15°W) May 18, 2000, and was tracked until January 19, 2001. The float generally travelled southwestwardDots along the trajectory are 15 days apart. Colors represent different seasons in the trajectory: spring (black), summer (magenta), fall (red), and winter (blue).

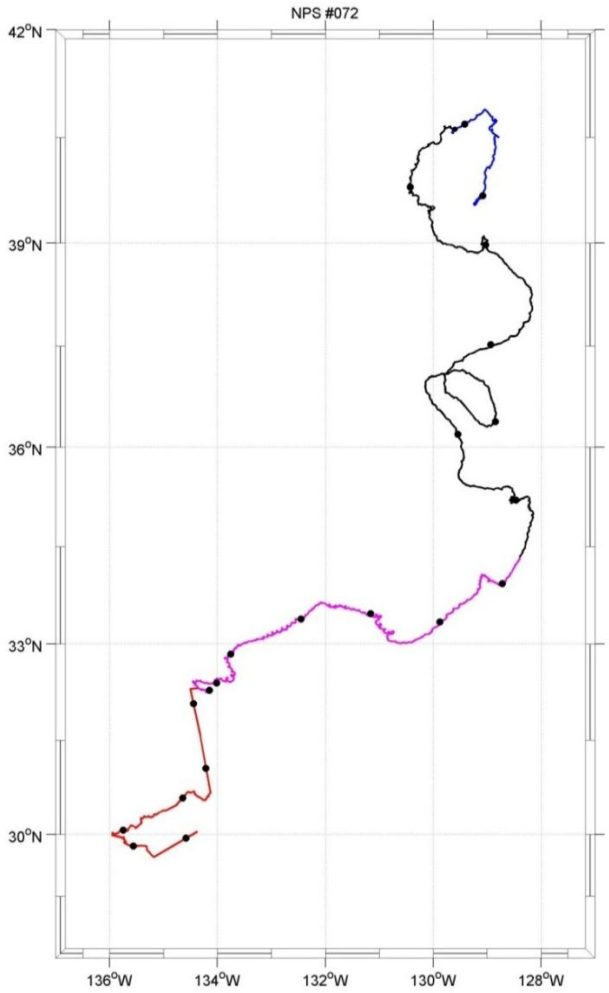

Figure A64. RAFOS float n072 obtained its first fix (39.68°N 129.08°W) February 12, 2001, and was tracked until November 22, 2001. The float generally drifted southward to about 35°N, whence it turned southwestward. The Argos satellites did not report any positions for the float essentially for the month of September 2001. Dots along the trajectory are 15 days apart. Colors represent different seasons in the trajectory: winter (blue), spring (black), summer (magenta), and fall (red).

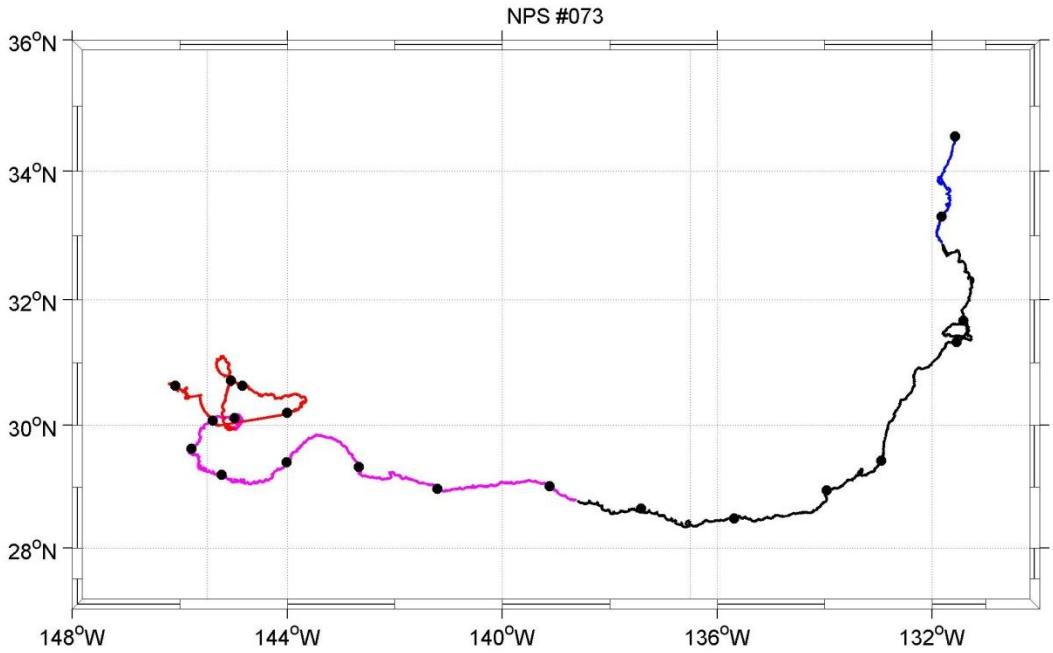

Figure A65. RAFOS float n073 obtained its first fix (34.54°N 131.57°W) February 12, 2001, and was tracked until November 9, 2001. The float drift was south-southwestward to about 29°N, whence the float then travelled west-northwestward. The float also executed an anticyclonic loop at about [31.5°N, 131.5°W]. Dots along the trajectory are 15 days apart. Colors represent different seasons in the trajectory: winter (blue), spring (black), summer (magenta), and fall (red).

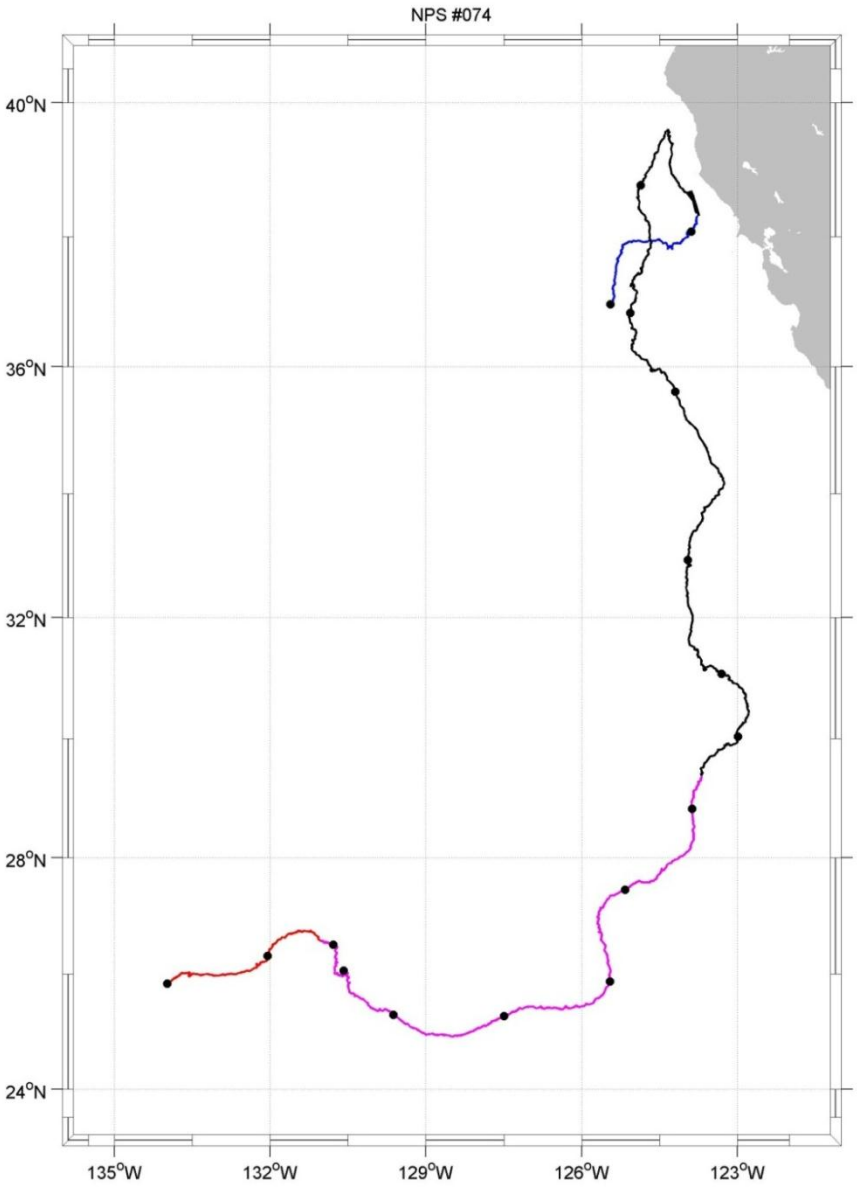

Figure A66. RAFOS float n074 obtained its first fix (36.97°N 125.45°W) February 12, 2001, and was tracked until September 25, 2001. The float initially moved northward toward, and then along, the coast to about 39.5°N, whence it next headed southward to about 30°N. The float then turned to a generally southwestern track. Dots along the trajectory are 15 days apart. Colors represent different seasons in the trajectory: winter (blue), spring (black), summer (magenta), and fall (red).

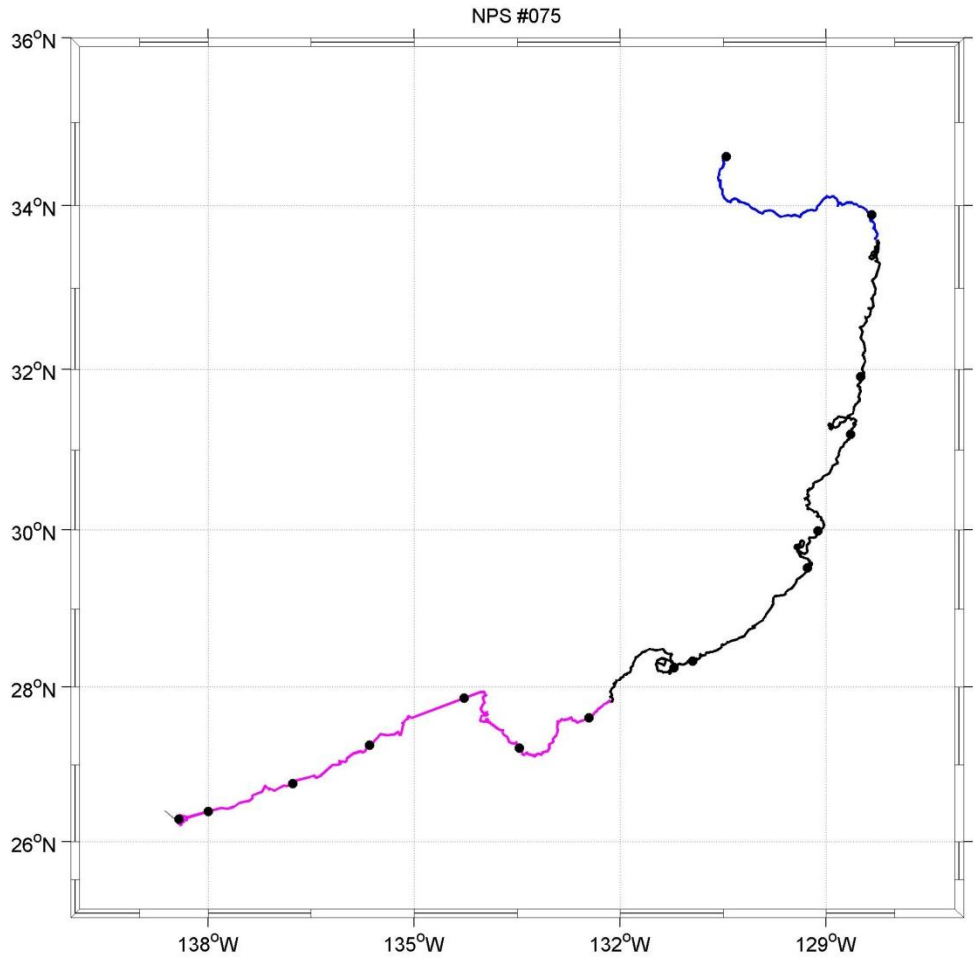

Figure A67. RAFOS float n075 obtained its first fix (34.59°N 130.47°W) February 12, 2001, and was tracked until September 2, 2001. The float initially moves eastward along about 34°N to about 128°W, thence southward to about 30°N, where it turned to a southwestward track. Along the trajectory are superimposed small anticyclonic/epicycloidal loops. The one exception is a set of cyclonic loops that the float traces at about [28.25°N, 131.35°W]. Dots along the trajectory are 15 days apart. Colors represent different seasons in the trajectory: winter (blue), spring (black), and summer (magenta).

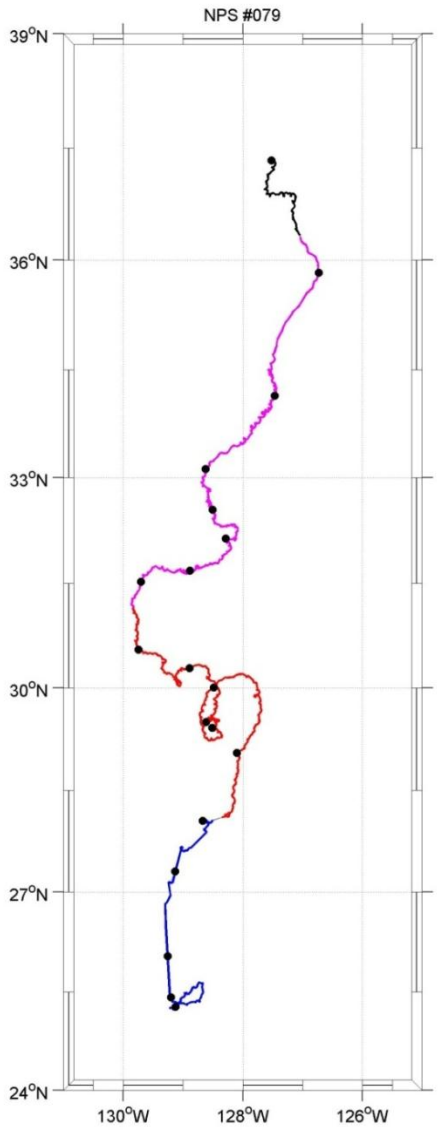

Figure A68. RAFOS float n079 obtained its first fix (37.34°N 127.52°W) May 22, 2002, and was tracked until January 29, 2003. Initially, the float traveled generally southward to about 34°N. At this point it appears that the float may have been caught by a rapidly south-southwestward translating anticyclonic eddy that superimposed small anticyclonic looping and epicycloidal motion on the overlying south-southwestward trajectory. At about [29.5°N, 128.5°W] the southward motion stalls briefly into a series of anticyclonic loops. Dots along the trajectory are 15 days apart. Colors represent different seasons in the trajectory: spring (black), summer (magenta), fall (red), and winter (blue).

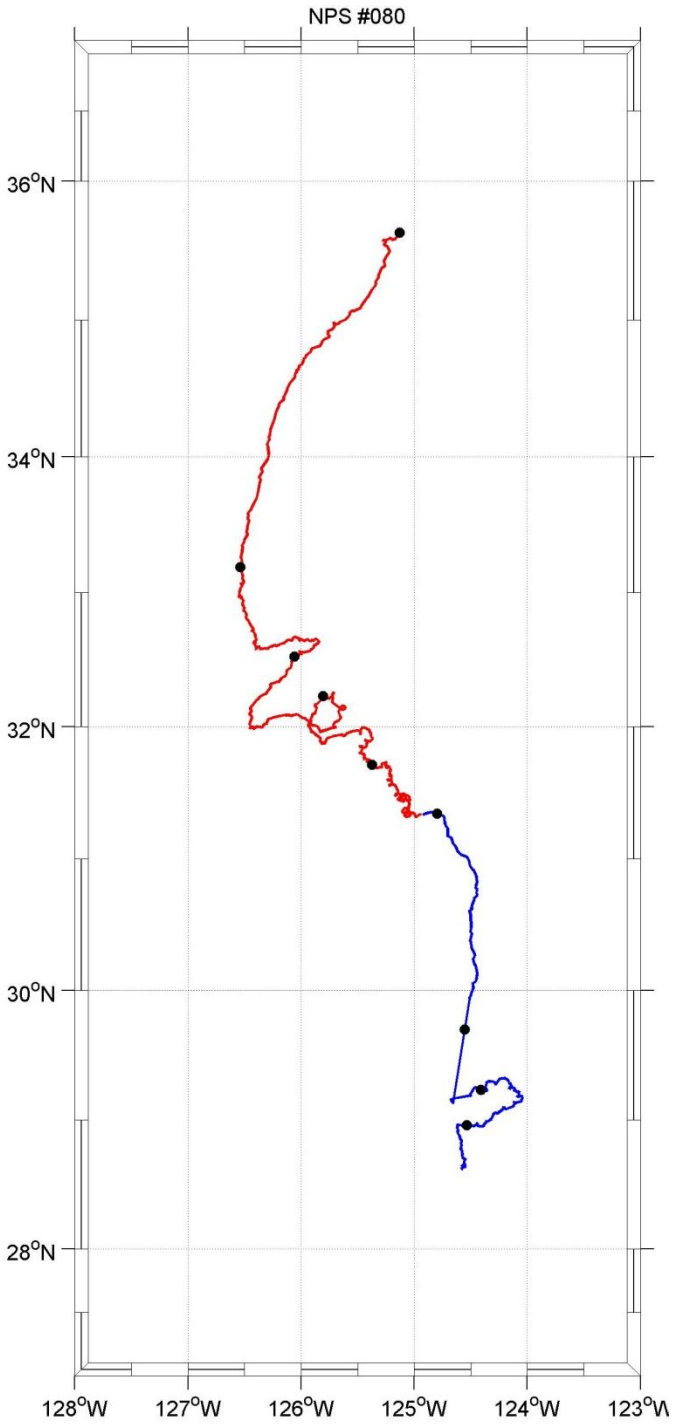

Figure A69. RAFOS float n080 obtained its first fix (35.63°N 125.13°W) September 23, 2001, and was tracked until April 2, 2002. The float's trajectory meandered southward, with some indication of anticyclonic looping/epicycloidal motion between about 32° and 31°N. Dots along the trajectory are 15 days apart. Colors represent different seasons in the trajectory: fall (red), winter (blue), and spring (black).

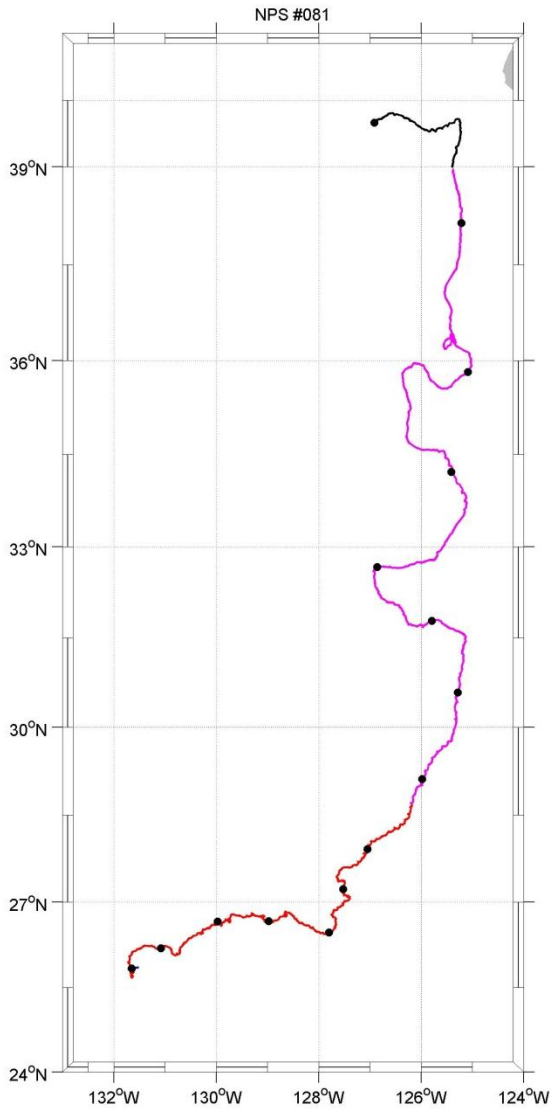

Figure A70. RAFOS float n081 obtained its first fix (39.67°N 126.91°W) May 22, 2002, and was tracked until January 25, 2003. After initially moving eastward for 9 days, the float travelled southward to about 27°N, where it turned to a more west-southwesterly course. Dots along the trajectory are 15 days apart. Colors represent different seasons in the trajectory: =spring (black), summer (magenta), and fall (red).

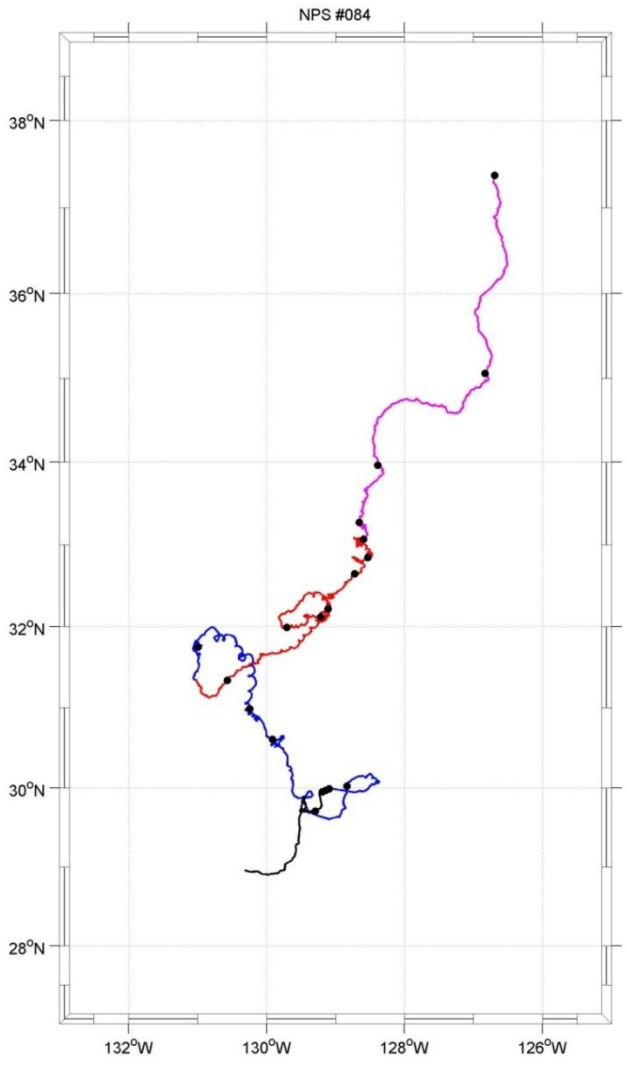

Figure A71. RAFOS float n084 obtained its first fix (37.37°N 126.60°W) July 9, 2002, and was tracked until March 30, 2003. In general, the float first moved southward to about 34.5°N, then southwestward to about [31°N, 131°W], then south-southeastward to about 29°N. At about 33°N, however, superimposed anticyclonic looping/epicycloidal motion appeared. Dots along the trajectory are 15 days apart. Colors represent different seasons in the trajectory: summer (magenta), fall (red), winter (blue), and spring (black).

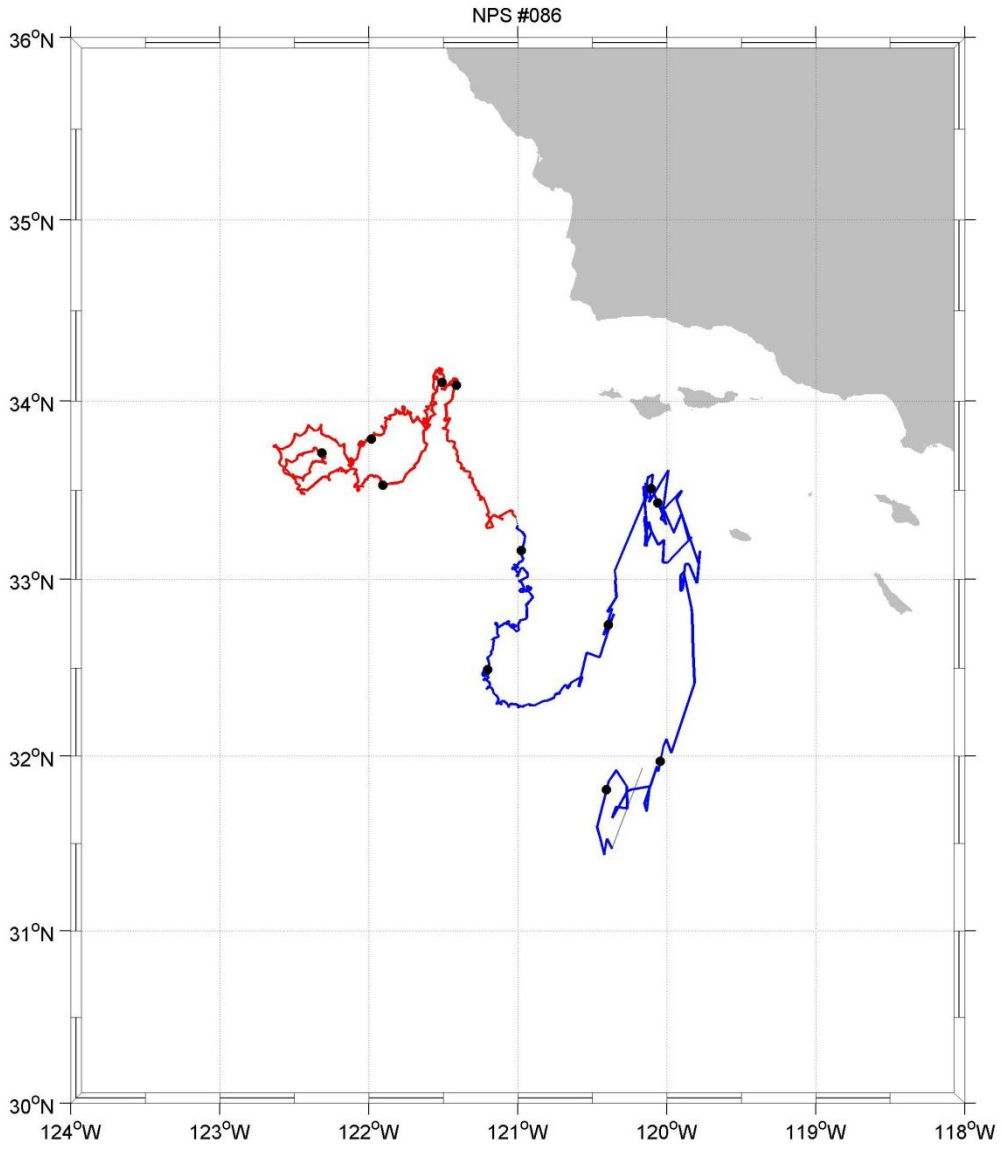

Figure A72. RAFOS float n086 obtained its first fix (34.10°N 121.51°W) September 23, 2004, and was tracked until March 4, 2005. The float initially moved west-southwestward to about 122.75°W, then retraced its path east-northeastward back to its surfacing location. It then drifted southward to about 32.25°N, thence northeastward to about [33.5°N, 120°W]. Finally, the float meandered southward to about 31.5°N. Additionally, there appears to be superimposed anticyclonic looping/epicycloidal motion through the end of 2004. Dots along the trajectory are 15 days apart. Colors represent different seasons in the trajectory: fall (red), winter (blue), and spring (black).

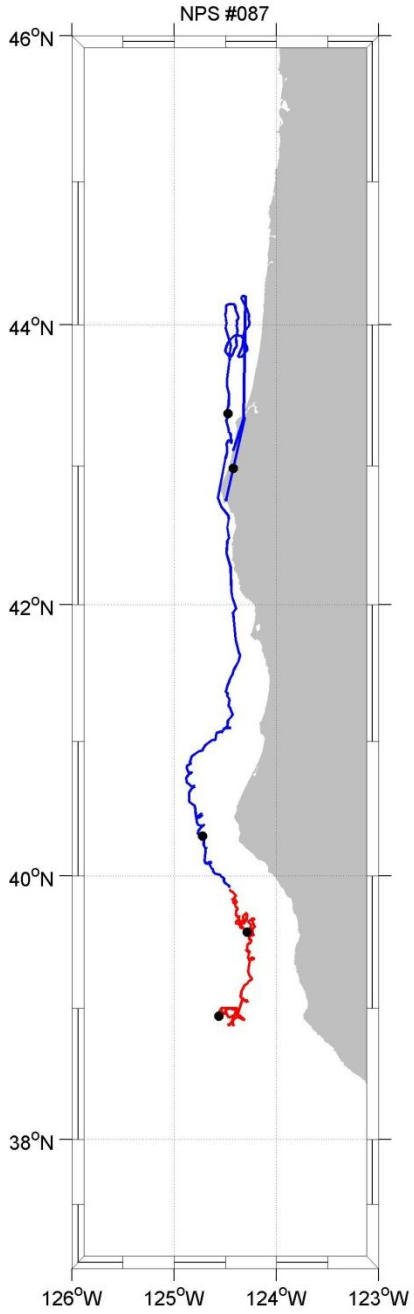

Figure A73. RAFOS float n087 obtained its first fix (38.95°N 124.56°W) November 6, 2002, and was tracked until January 13, 2003. The float drifted northward along the coast to about 44°N, where it was recovered by a fisherman, who brought it to Bandon, Oregon. Dots along the trajectory are 15 days apart. Colors represent different seasons in the trajectory: fall (red) and winter (blue). (The trajectory after recovery is included above.)

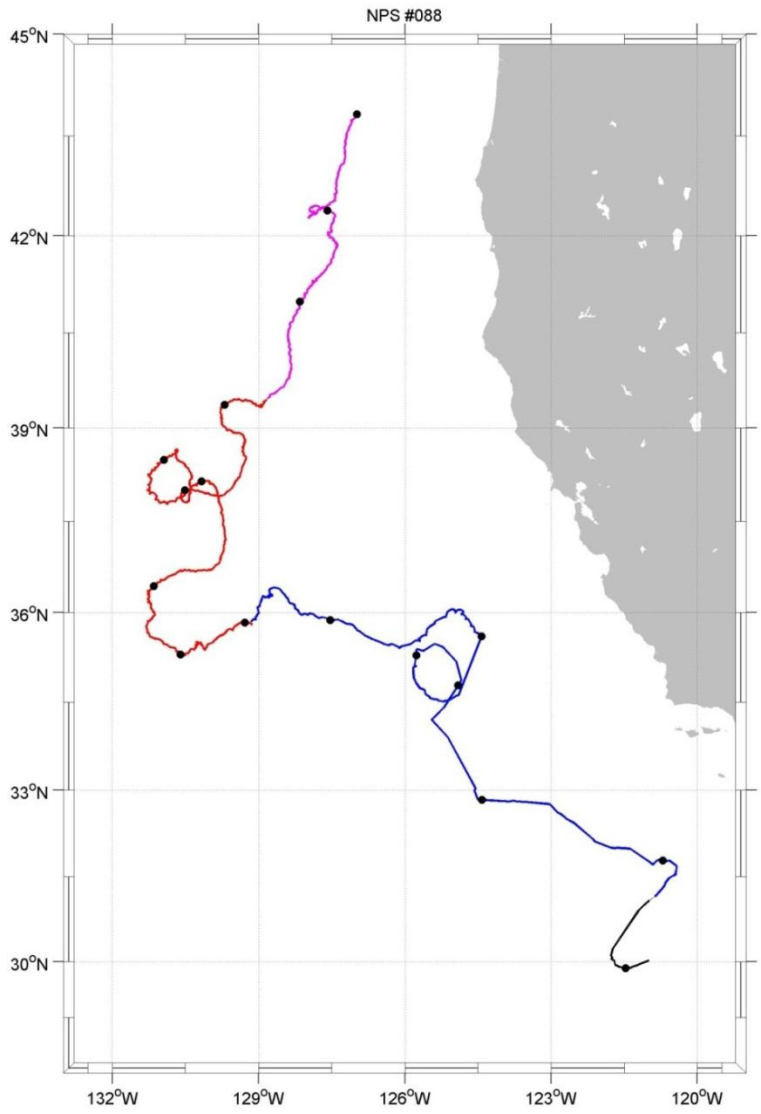

Figure A74. RAFOS float n088 obtained its first fix (43.83°N 126.99°W) July 28, 2003, and was tracked until March 9, 2004. The float headed south-southwestward to about 36°N, making one small cyclonic loop along the way (at about 38°N). It then headed eastward to about 125°W, where it made an anticyclonic loop before heading southeastward. Dots along the trajectory are 15 days apart. Colors represent different seasons in the trajectory: summer (magenta), fall (red), winter (blue), and spring (black).

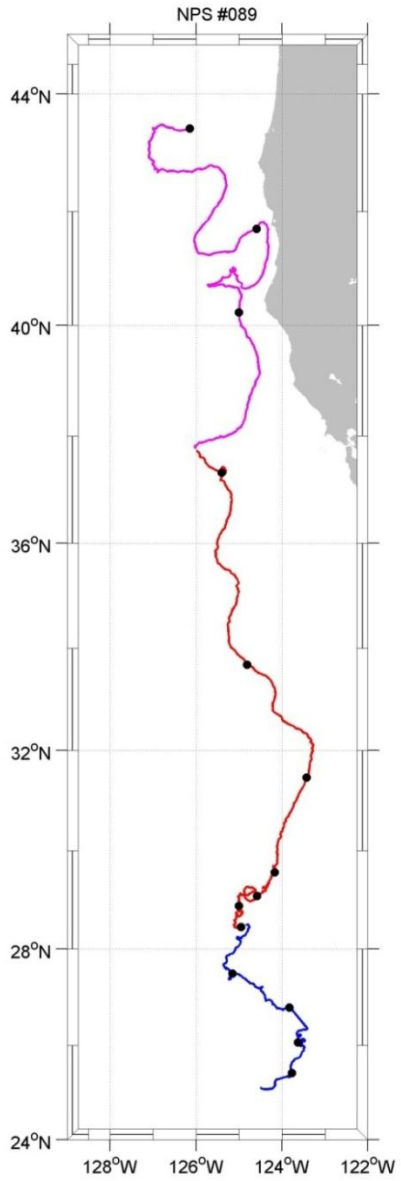

Figure A75. RAFOS float n089 obtained its first fix (43.42°N 126.19°W) July 28, 2003, and was tracked until February 2, 2004. In general, the float moved southward, with a single cyclonic loop at about 29°N. Dots along the trajectory are 15 days apart. Colors represent different seasons in the trajectory: summer (magenta), fall (red), and winter (blue).

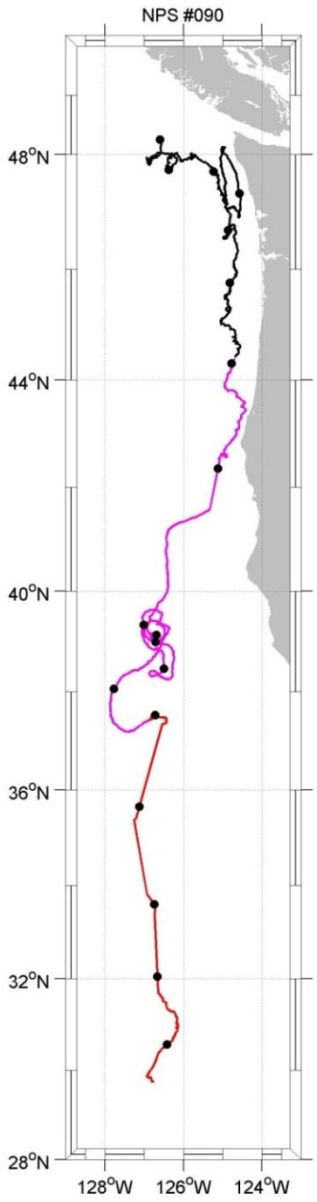

Figure A76. RAFOS float n090 obtained its first fix (48.83°N 126.60°W) March 9, 2004, and was tracked until November 11, 2004. The float initially moved eastward near the Washington coast, where it then moved along the coast first southward to mid_Washington, then northward to near Puget Sound. The float then moved southward to Cape Blanco, where it turned more south-southwestward to about 38°N. The float then meandered for about a month, mostly along a north/south axis, between about 38.25° and 39.75°N, before continuing southward to about 30°N. Dots along the trajectory are 15 days apart. Colors represent different seasons in the trajectory: spring (black), summer (magenta), and fall (red).

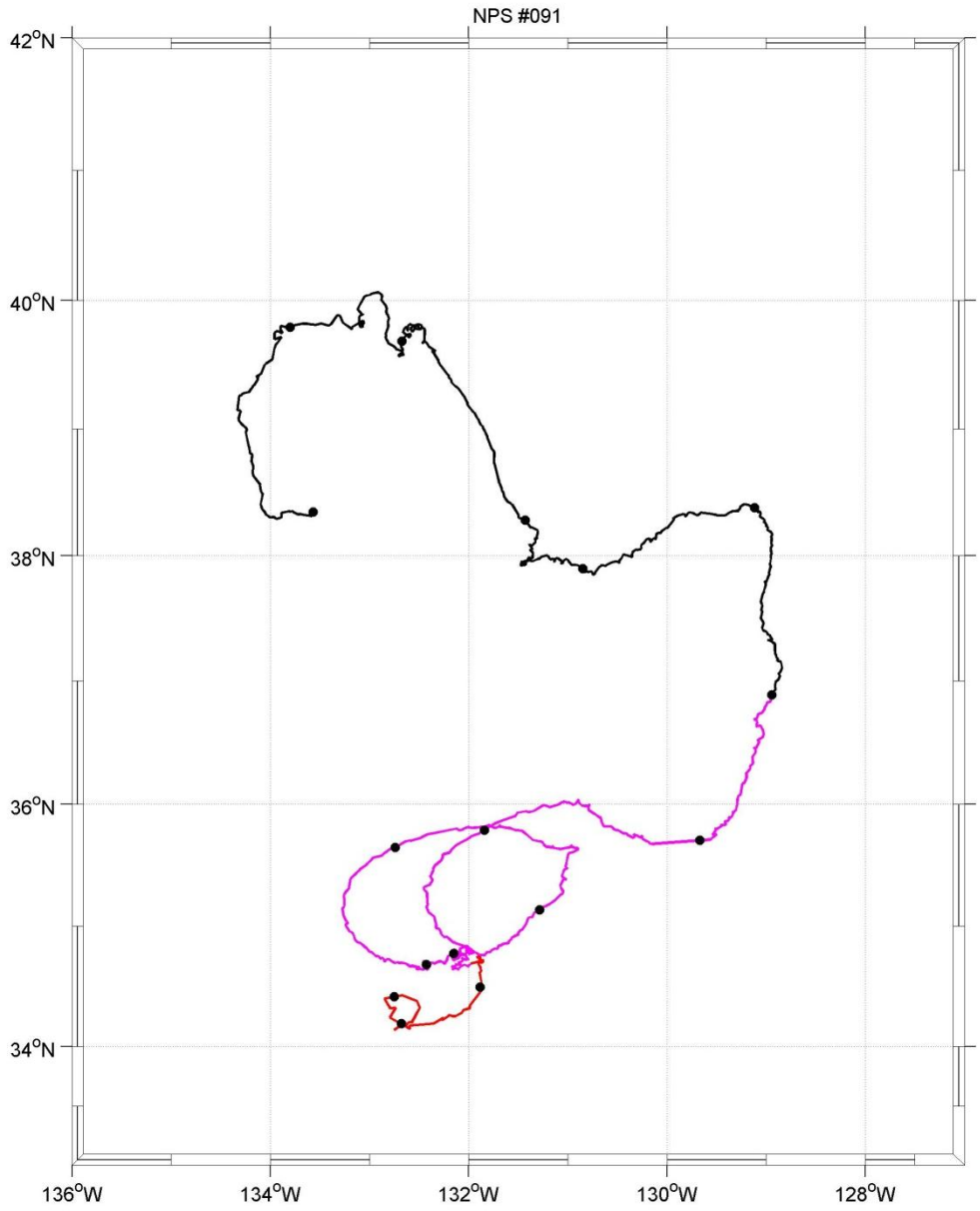

Figure A77. RAFOS float n091 obtained its first fix (38.35°N 133.57°W) March 9, 2004, and was tracked until October 13, 2004. The float effectively moved eastward to about 129°W, where it then moved southward to about 35.75°N. It then moved southwestward, executing first 1.5 larger cyclonic loops followed by a smaller anticyclonic loop. Dots along the trajectory are 15 days apart. Colors represent different seasons in the trajectory: spring (black), summer (magenta), and fall (red).

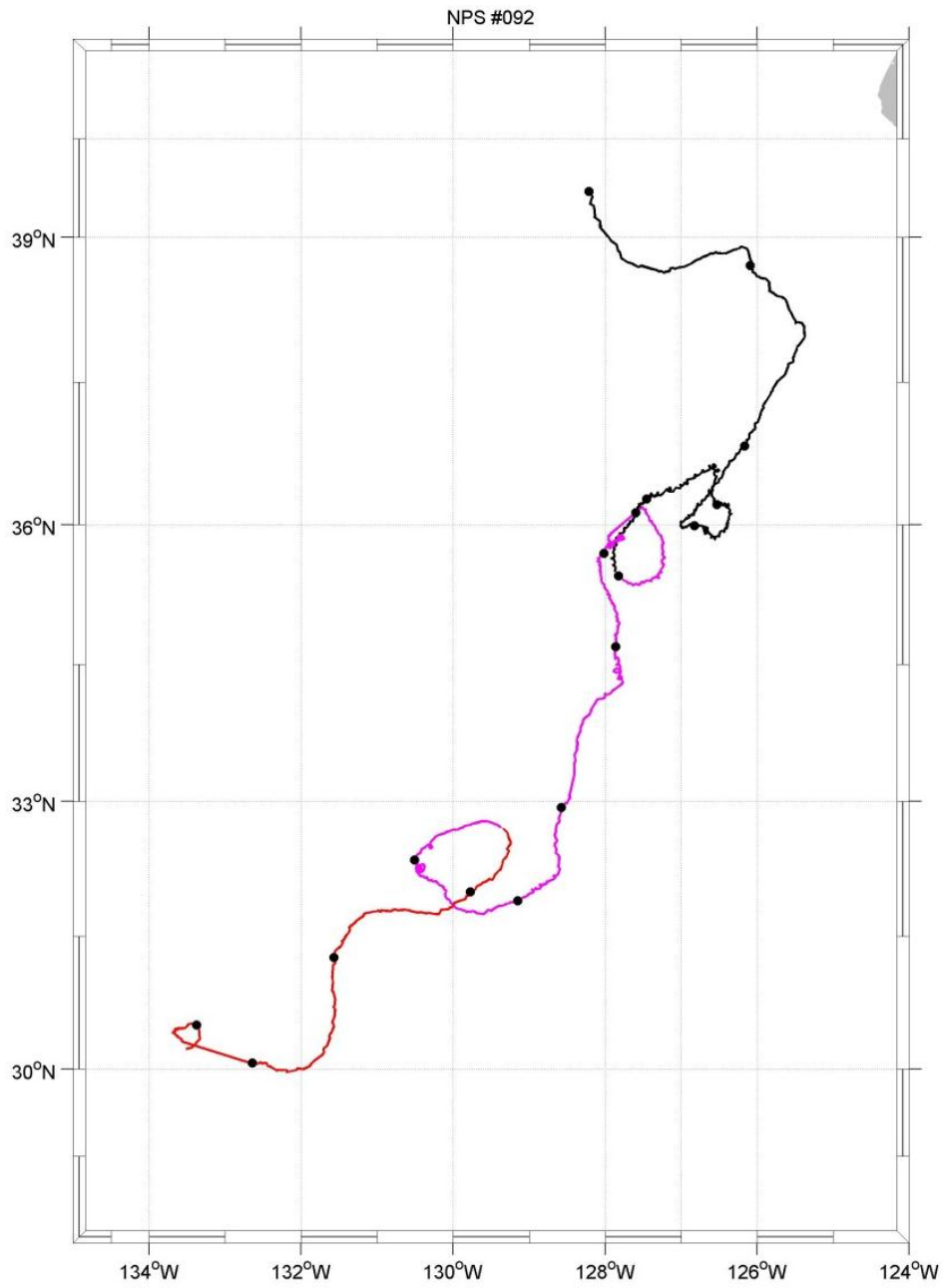

Figure A78. RAFOS float n092 obtained its first fix (39.47°N 128.21°W) March 9, 2004, and was tracked until October 22, 2004. Initially, the float drifted southeastward to about 38°N, thence southwestward to about 30°N, where it finally turned westward to about 134°W. Dots along the trajectory are 15 days apart. Colors represent different seasons in the trajectory: spring (black), summer (magenta), and fall (red).

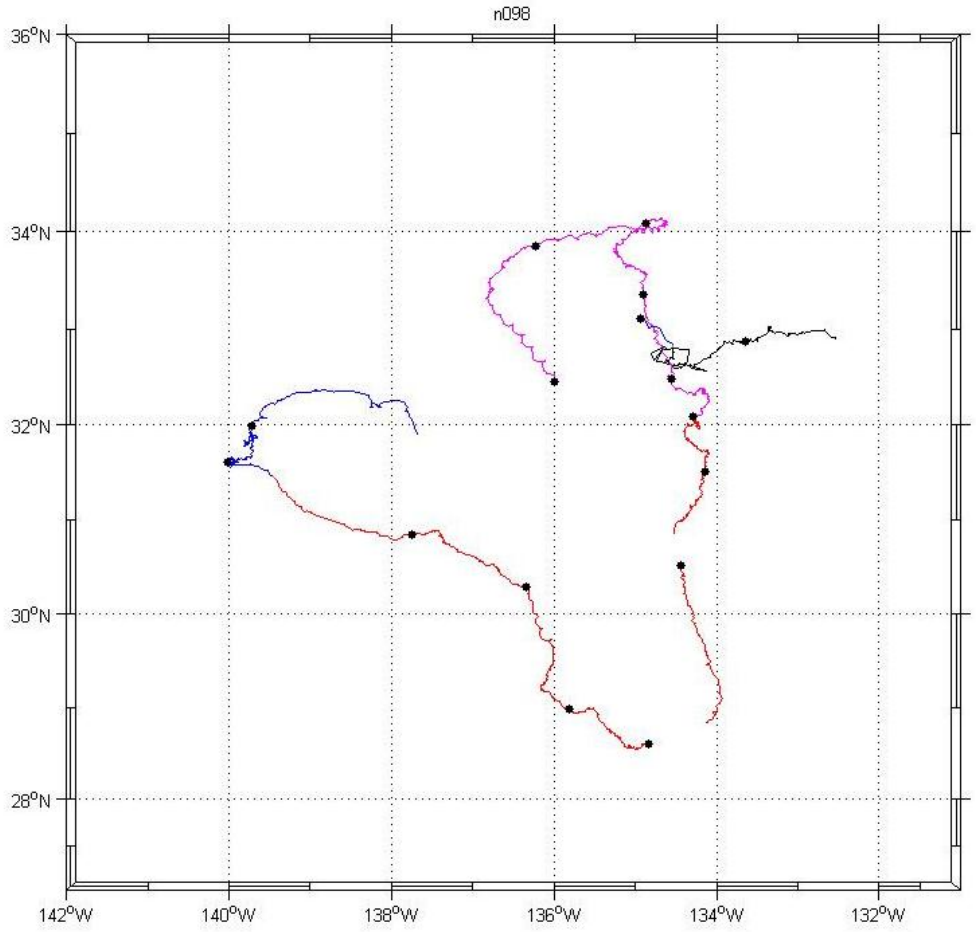

Figure A79. RAFOS float n098 surfaced June 23, 2006, at (32.46°N 135.00°W), and was tracked (with data gaps) until March 21, 2007. As stated, float n098 experienced data gaps in the trajectory. These gaps were removed and n098 was divided into four segments. Effectively, the first three segments (summer through winter) of the trajectory traced out a large anticyclonic loop contained within about 28.5^{o} and 34^{o}N in the south and north, respectively, and about 134^{o} and 140^{o}W in the east and west, respectively. The fourth segment of the trajectory, which resumed in the spring after a nearly two-month hiatus, took the float eastward from about 135^{o}W. Dots along the trajectory are 15 days apart. Colors represent different seasons in the trajectory: summer (magenta), fall (red), winter (blue), and spring (black).

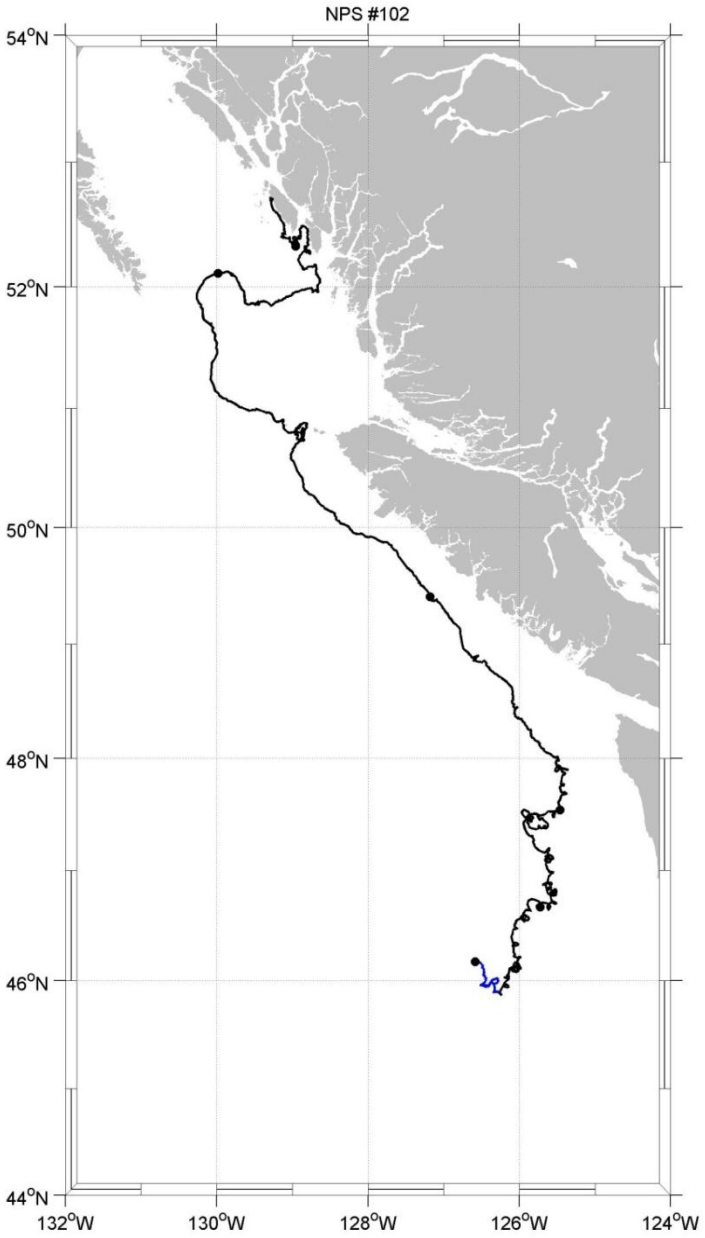

Figure A80. RAFOS float n102 obtained its first fix (46.17°N 126.58°W) February 23, 2006, and was tracked until May 8, 2006. Initially, the float moved northward (with considerable anticyclonic/epicycloidal motion) toward Vancouver. At about 40°N it turned northwestward (following the coast) to about 52°N, where it then headed eastward to near the Canadian mainland coast. From there it moved northwestward among the coastal islands until presumably running aground on one. Dots along the trajectory are 15 days apart. Colors represent different seasons in the trajectory: winter (blue) and spring (black).

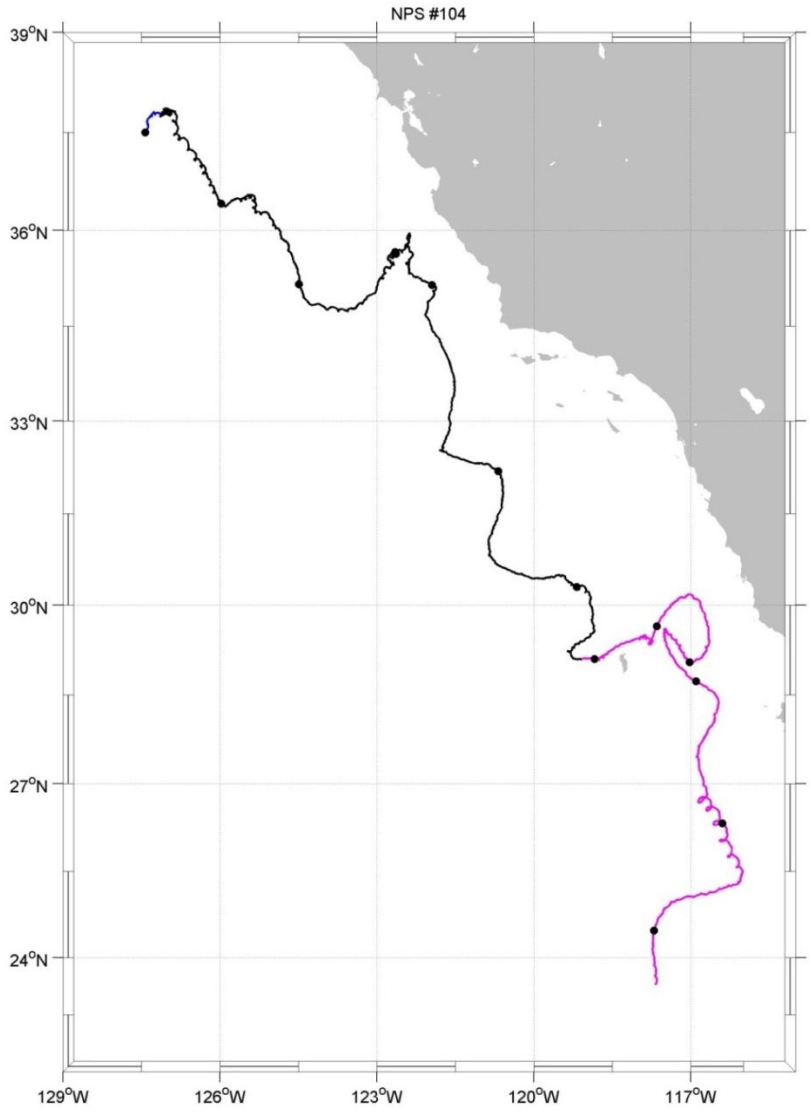

Figure A81. RAFOS float n104 obtained its first fix (37.49°N 127.430°W) February 25, 2006, and was tracked until August 18, 2006. Essentially, the float moved southeastward, with a brief east-northeastward excursion around 29°N. There is considerable anticyclonic/epicycloidal motion near the beginning and end of the trajectory. Dots along the trajectory are 15 days apart. Colors represent different seasons in the trajectory: winter (blue), spring (black), and summer (magenta).

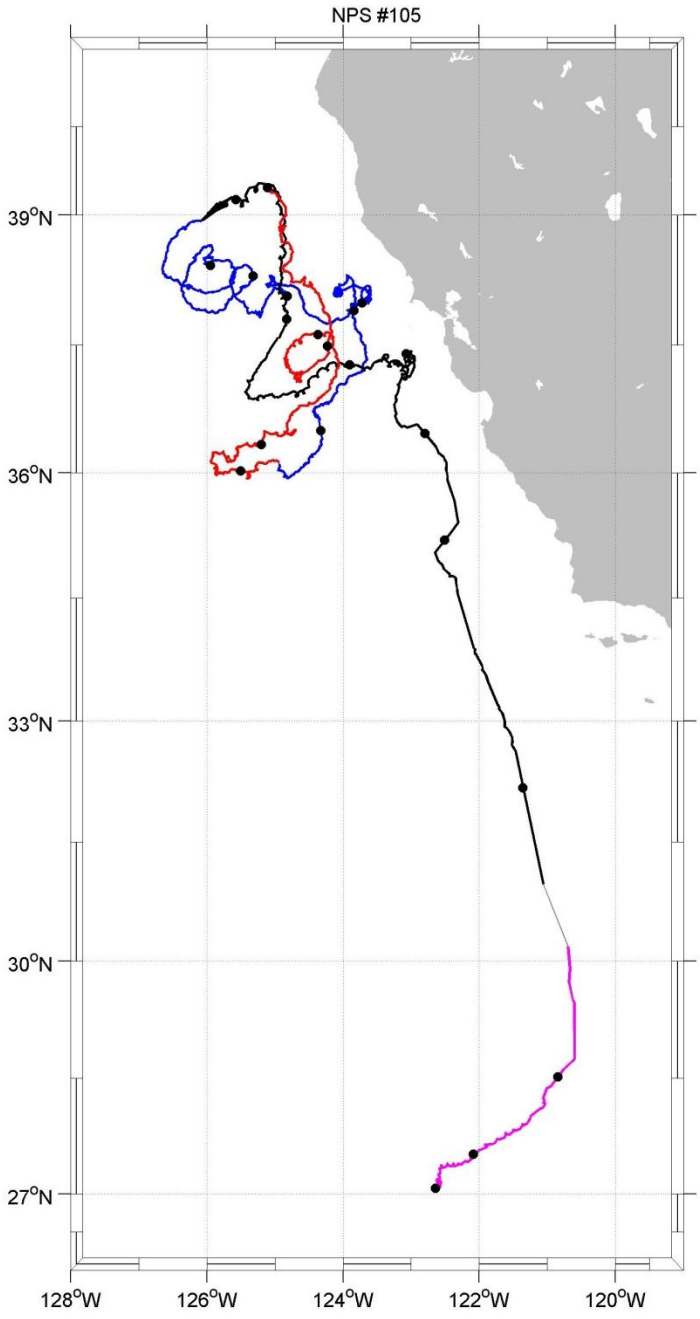

Figure A82. RAFOS float n105 obtained its first fix (39.31°N 125.11°W) September 30, 2005, and was tracked until July 7, 2006. Initially, the float moved southward (fall); thence northeastward toward, then west-northwestward away, from the California coast (winter); then southeastward to about 28.5°N (spring to early summer). Finally, the float moved southwestward to about 27°N. Dots along the trajectory are 15 days apart. Colors represent different seasons in the trajectory: fall (red), winter (blue), spring (black), and summer (magenta).

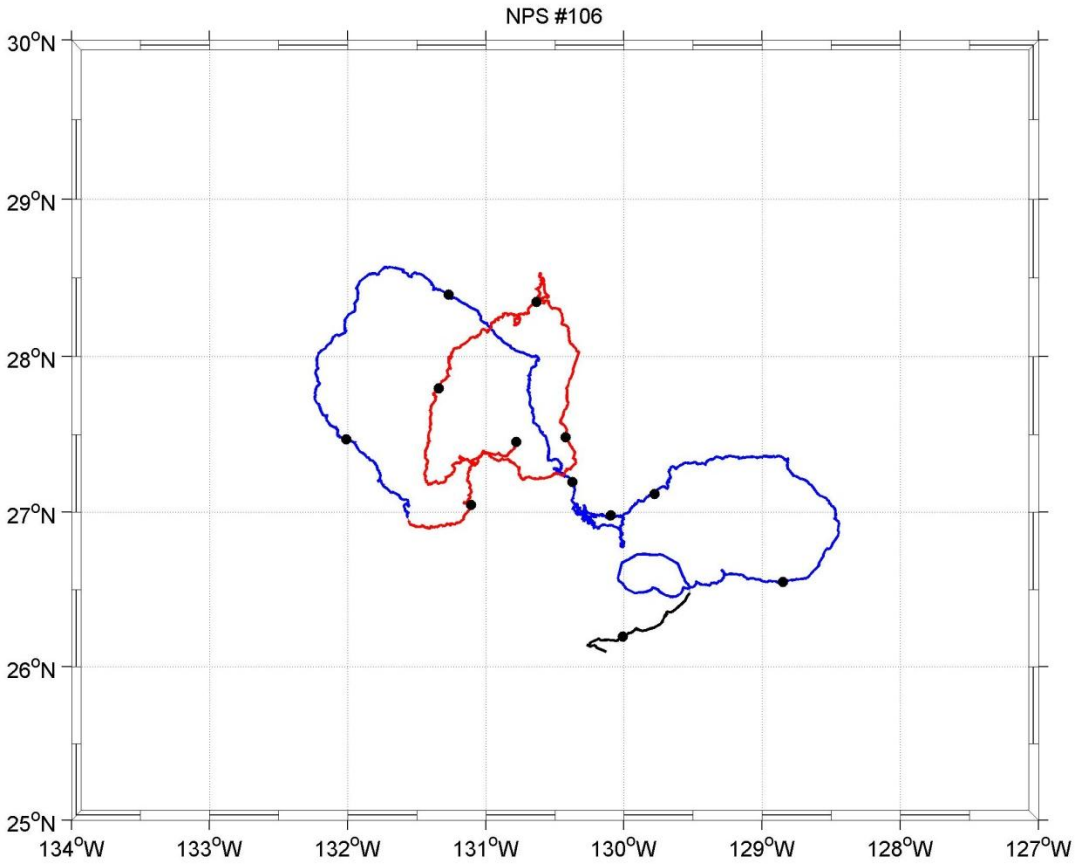

Figure A83. RAFOS float n106 obtained its first fix (27.45°N 130.78°W) September 30, 2005, and was tracked until April 24, 2006. Initially, the float traced out two anticyclonic loops contained approximately between 27° and 28.5°N and 130.25° and 132,5°W. It then drifted eastward to about 128.5°W, before then moving southwestward to about [26°N, 130.5°W]. Dots along the trajectory are 15 days apart. Colors represent different seasons in the trajectory: fall (red), winter (blue), and spring (black).

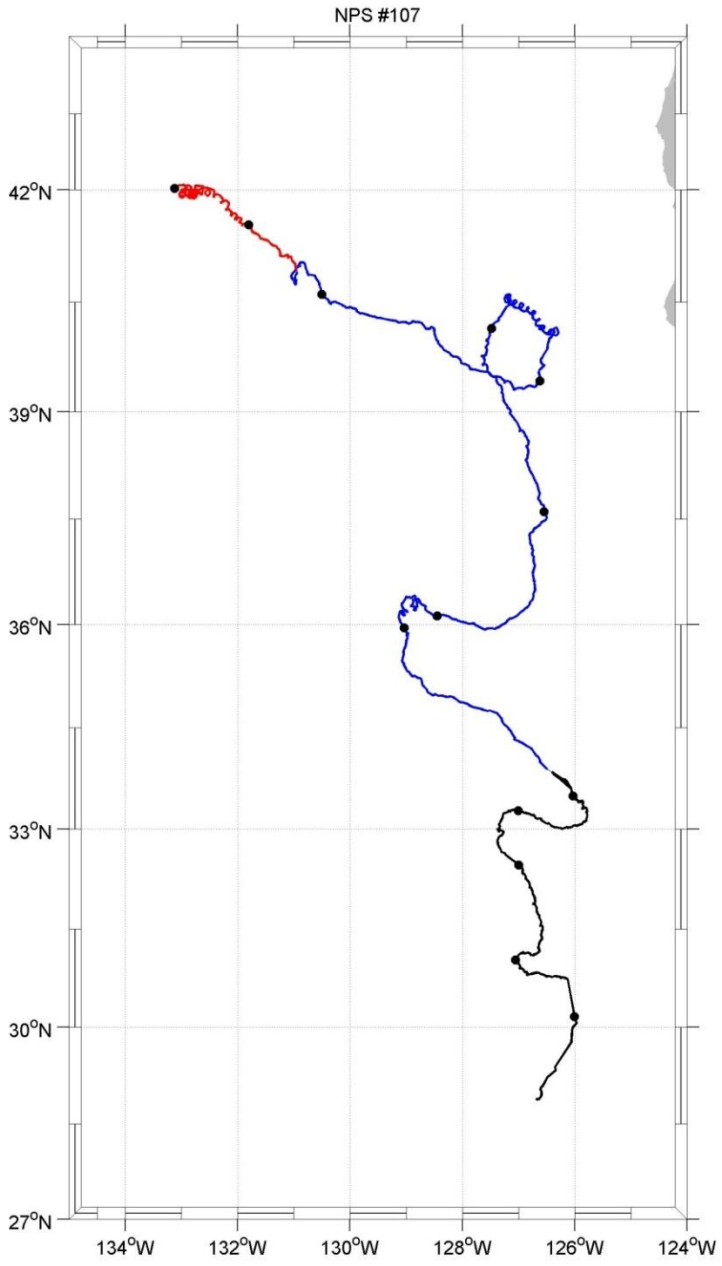

Figure A84. RAFOS float n107 obtained its first fix (42.02°N 133.12°W) November 12, 2006, and was tracked until May 11, 2007. For the first 45 days initially, the float traveled southeastward, with considerable anticyclonic/epicycloidal motion superimposed at the start of the underlying trajectory. At this point, the float made a larger cyclonic loop (with considerable anticyclonic/epicycloidal motion superimposed), then headed southward. At about 36°N there is some cyclonic/epicycloidal motion superimposed on the underlying trajectory. Dots along the trajectory are 15 days apart. Colors represent different seasons in the trajectory: fall (red), winter (blue), and spring (black).

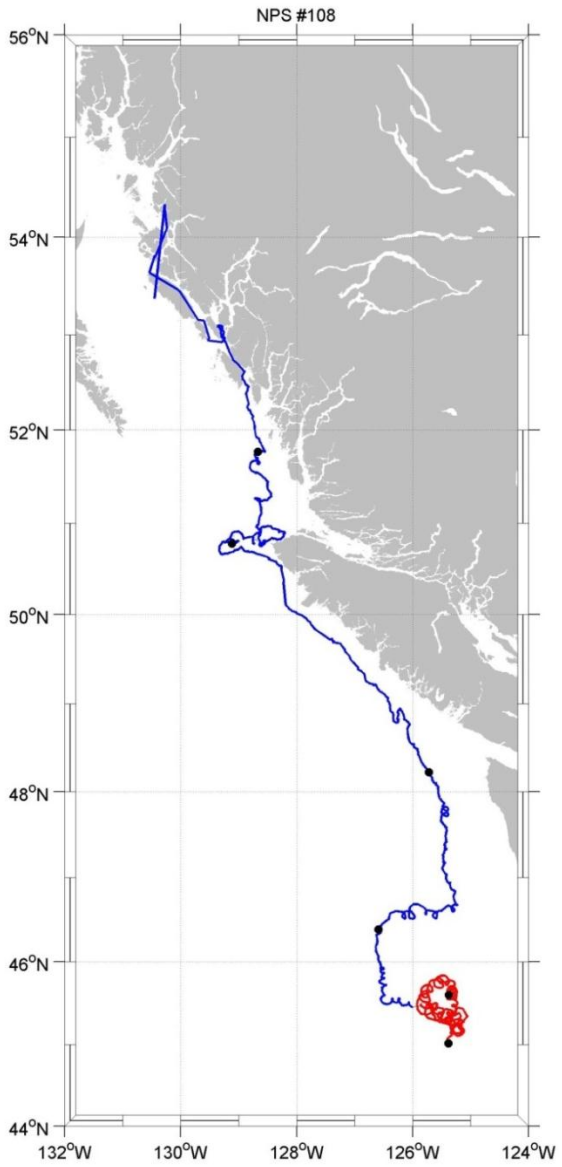

Figure A85. RAFOS float n108 obtained its first fix (45.01°N 125.39°W) November 12, 2006, and was tracked until January 27, 2007. Initially, the float was caught in an anticyclonic eddy centered about [45.5°N, 125.5°W]. Emerging from the eddy about a month later, the float then drifted northward (with considerable anticyclonic/epicycloidal motion superimposed) to the Vancouver coast, which it then followed northwestward. After meandering for a fortnight off the northern tip of Vancouver Island, the float then proceeded northward across Queen Charlotte Sound and into the Queen Charlotte Islands. It was among these islands that the Canadian Coast Guard found and recovered the float. Dots along the trajectory are 15 days apart. Colors represent different seasons in the trajectory: fall (red) and winter (blue).

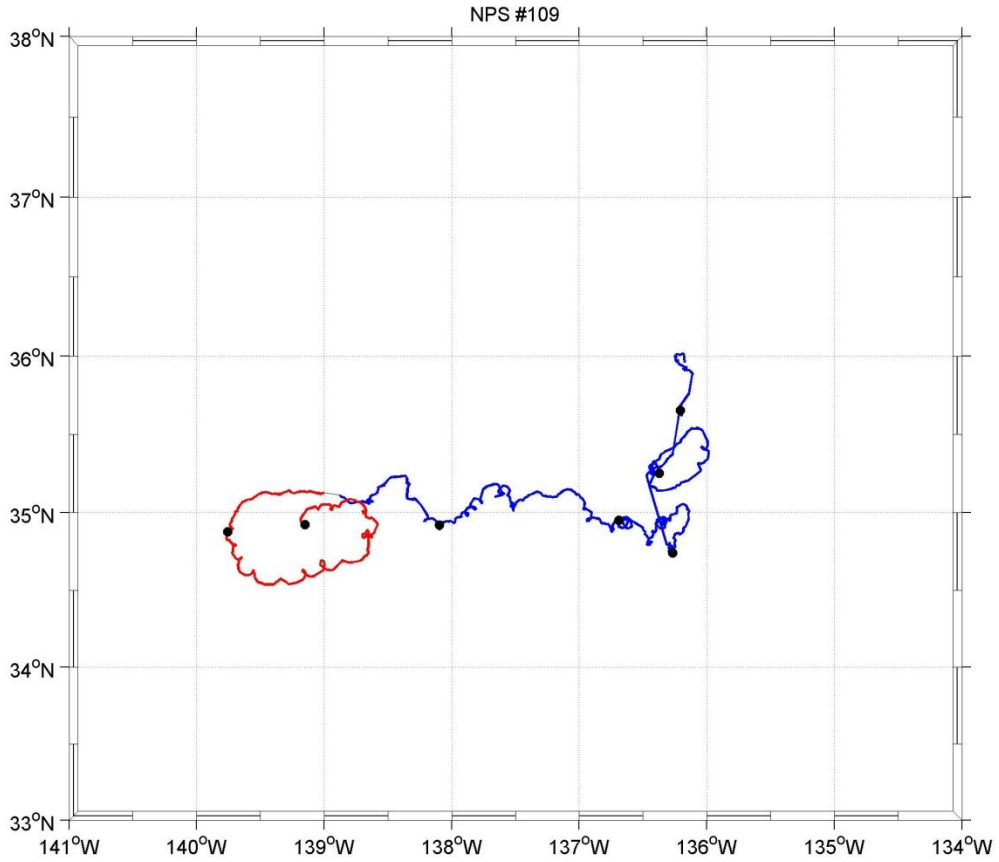

Figure A86. RAFOS float n109 obtained its first fix (34.92°N 139.15°W) November 12, 2006, and was tracked until February 7, 2007. Initially, the float executed an anticyclonic loop centered at approximately [34.75°N, 139.5°W]. There was considerable anticyclonic/epicycloidal motion superimposed on this loop. Next, the float moved eastward, again with considerable anticyclonic/epicycloidal motion superimposed, to about 136.5°W, thence northward to about 36°N. Dots along the trajectory are 15 days apart. Colors represent different seasons in the trajectory: fall (red) and winter (blue).

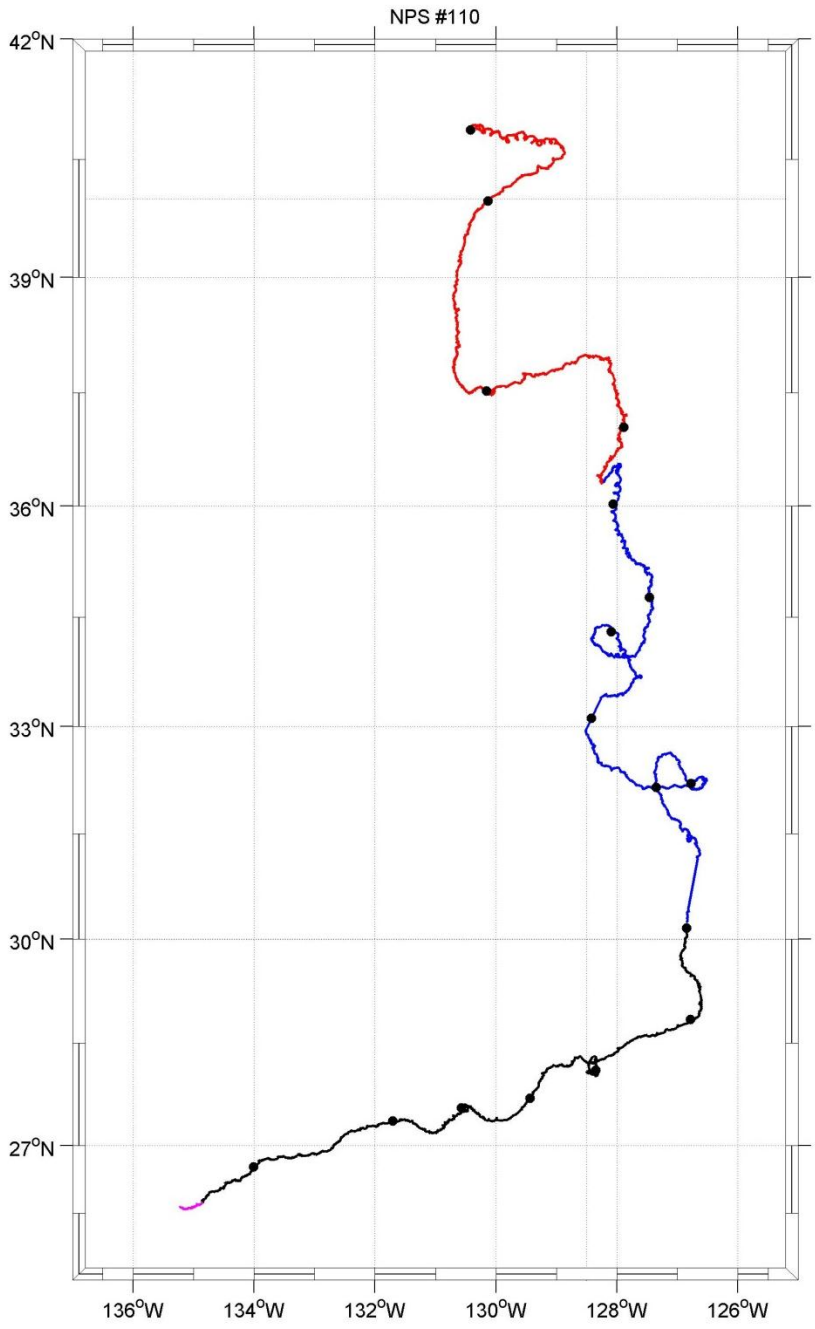

Figure A87. RAFOS float n110 obtained its first fix (40.87°N 130.42°W) October 15, 2007, and was tracked until June 4, 2008. The float effectively floated southward to about 29°N, where it then turned southwestward. There is scattered anticyclonic/epicycloidal motion superimposed throughout the underlying southward trajectory. Dots along the trajectory are 15 days apart. Colors represent different seasons in the trajectory: fall (red), winter (blue), spring (black), and summer (magenta).

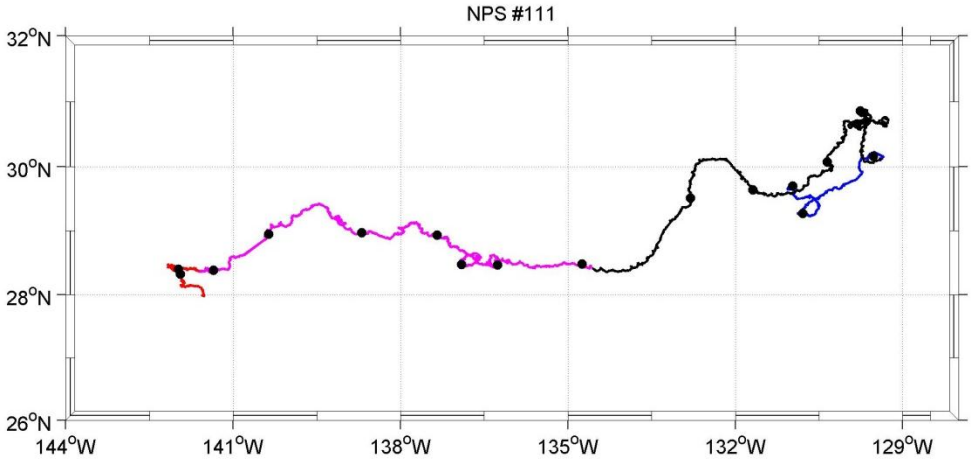

Figure A88. RAFOS float n111 obtained its first fix (29.70°N 130.98°W) January 28, 2008, and was tracked unitl September 30, 2008. Initially, the float moved eastward to about 130°W, before turning northward and then west-southwestward to about 142.5°W, before making a brief final trek southeastward. Dots along the trajectory are 15 days apart. Colors represent different seasons in the trajectory: winter (blue), spring (black), summer (magenta), and fall (red).

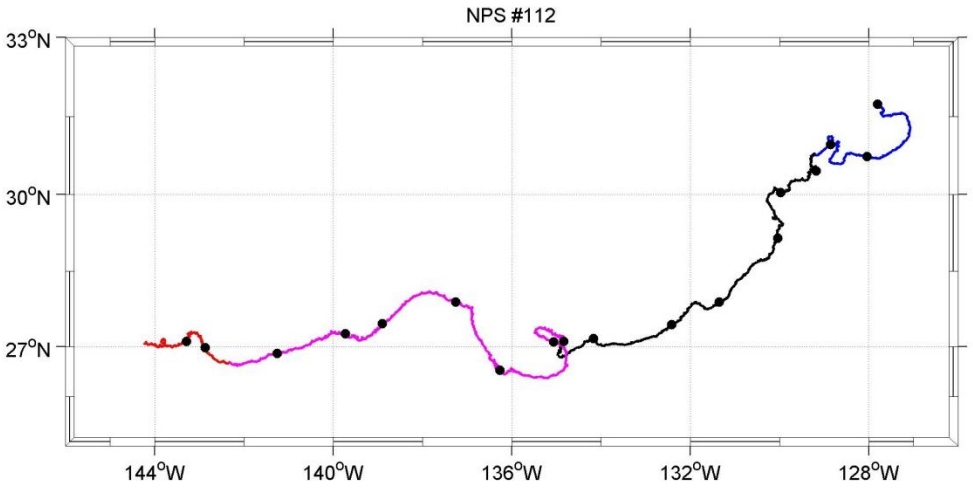

Figure A89. RAFOS float n112 obtained its first fix (31.73°N 127.81°W) January 28, 2008, and was tracked until October 5, 2008. The float moved southwestward to about 27°N, then continued westward to about 144°W. Dots along the trajectory are 15 days apart. Colors represent different seasons in the trajectory: winter (blue), spring (black), summer (magenta), and fall (red).

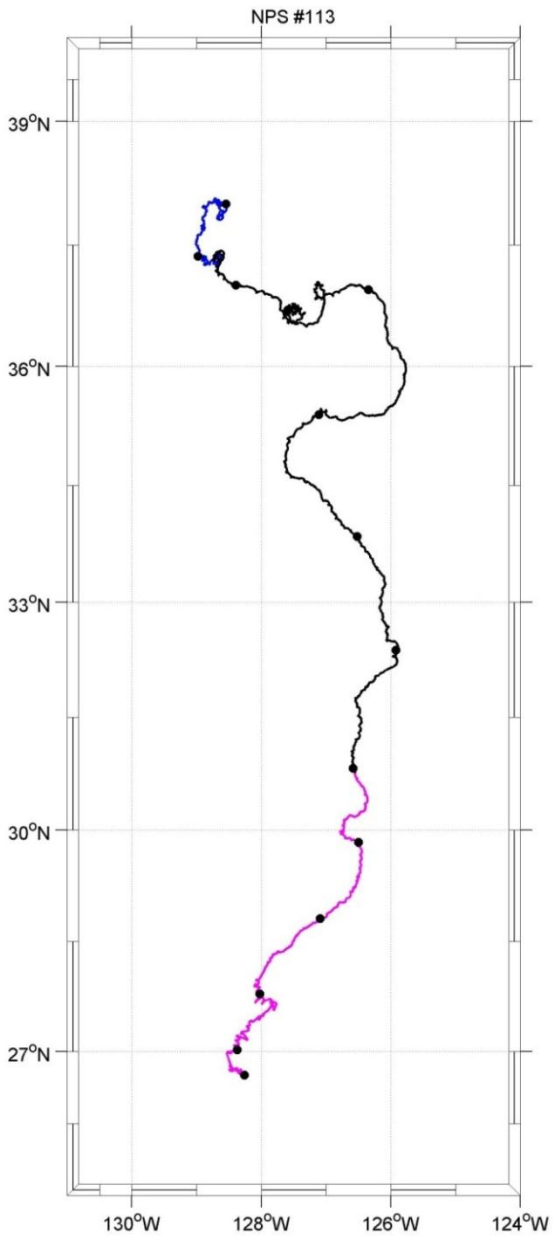

Figure A90. RAFOS float n113 obtained its first fix (38.00°N 128.55°W) February 8, 2010, and was tracked until August 12, 2010. Initially, the float moved southeastward to about 126°W. It then moved southward to about 32°N, where it then changed to a more south-southwestward course to about 26.5°N. There is some anticyclonic/epicycloidal motion superimposed along the underlying trajectory. Dots along the trajectory are 15 days apart. Colors represent different seasons in the trajectory: winter (blue), spring (black), and summer (magenta).

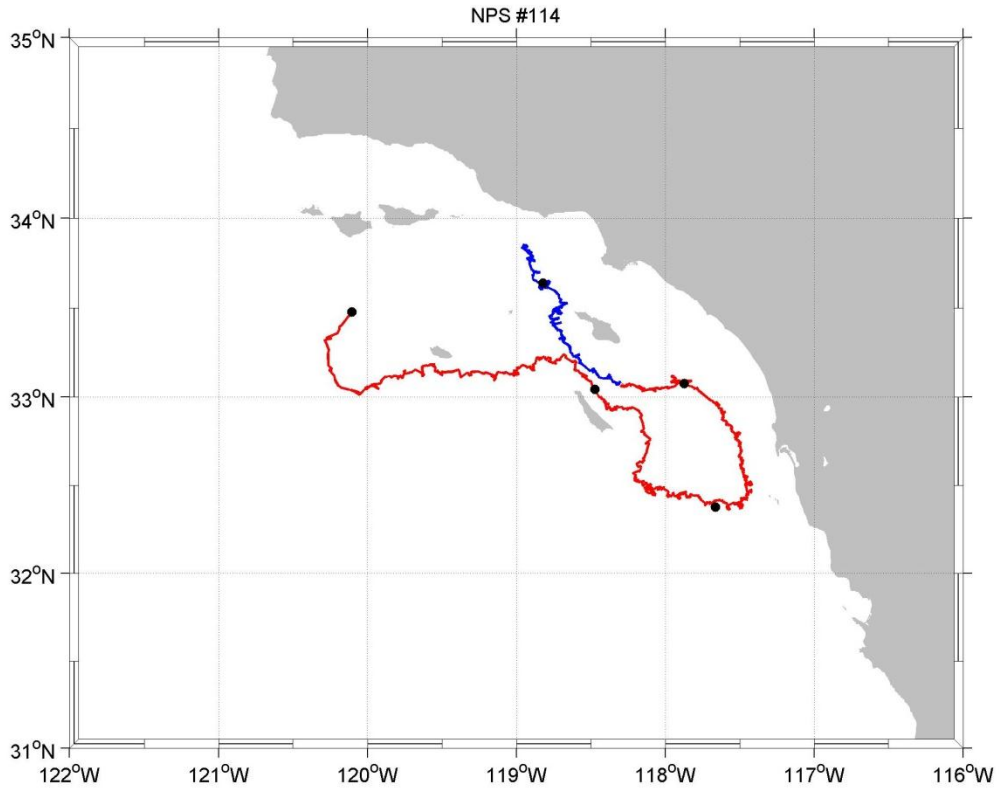

Figure A91. RAFOS float n114 obtained its first fix (33.48°N 120.10°W) October 16, 2006, and was tracked until December 16, 2006. Except for an initial southward track, the float first moved eastward to north of San Clemente Island, then headed southeastward past the eastern shore of San Clemente Island to 117.5°W, where it reversed course to drift northwestward past the western shore of Santa Catalina Island to about [33.75°N, 119°W]. There is some superimposed anticyclonic/epicycloidal motion throughout the underlying trajectory, particularly northwest of Santa Catalina Island. Dots along the trajectory are 15 days apart. Colors represent different seasons in the trajectory: fall (red) and winter (blue).

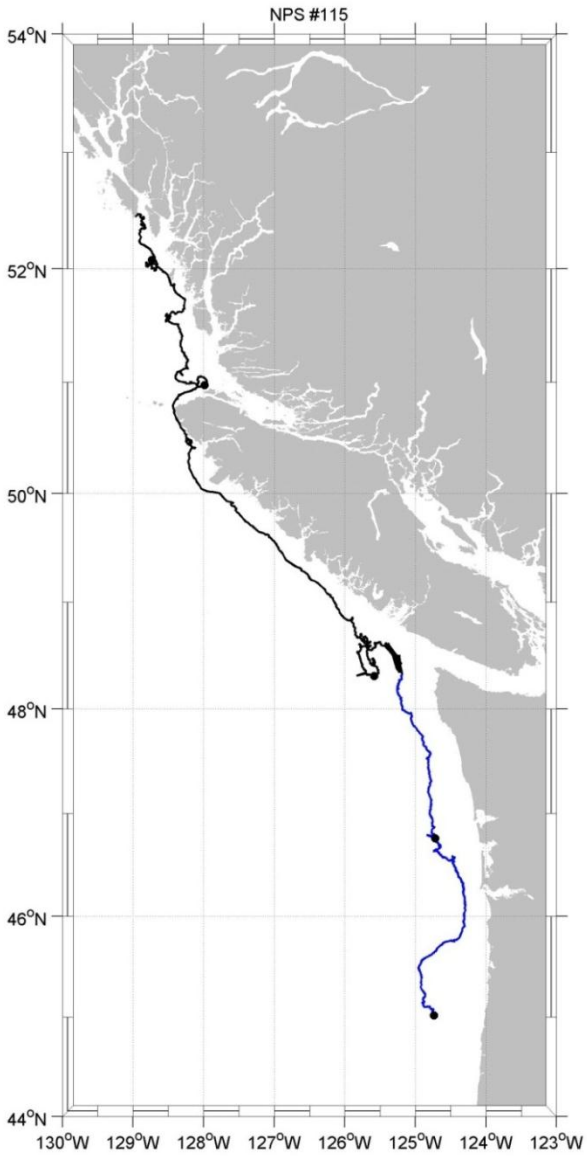

Figure A92. RAFOS float n115 obtained its first fix (45.02°N 124.74°W) February 8, 2010, and was tracked until April 10, 2010. The float followed the Washington, Vancouver, and Canadian coastlines north/northwestward, except for a small cyclonic loop at the mouth of Puget Sound, until the float (presumably) ran aground in the Queen Charlotte Islands. Dots along the trajectory are 15 days apart. Colors represent different seasons in the trajectory: winter (blue) and spring (black).

THIS PAGE INTENTIONALLY LEFT BLANK

APPENDIX B

Appendix B contains charts that compare the long-term drift of RAFOS floats to OSCURS, gNCOM, and HYCOM simulated model trajectories. The OSCURS model input parameters were set as follows: Wind Speed Current Coefficient (WCSC) equal to 1.0, Geostrophic Current Factor (GSF) equal to 1.0, and Wind Angle Deflection (WAD) equal to 0.0. The RAFOS trajectory is black, OSCURS is blue, gNCOM is red, and HYCOM is green. Black dots were placed every 15 days along the trajectory. Note that RAFOS float n098 suffered from data gaps of three, seven, and fifty-eight days.

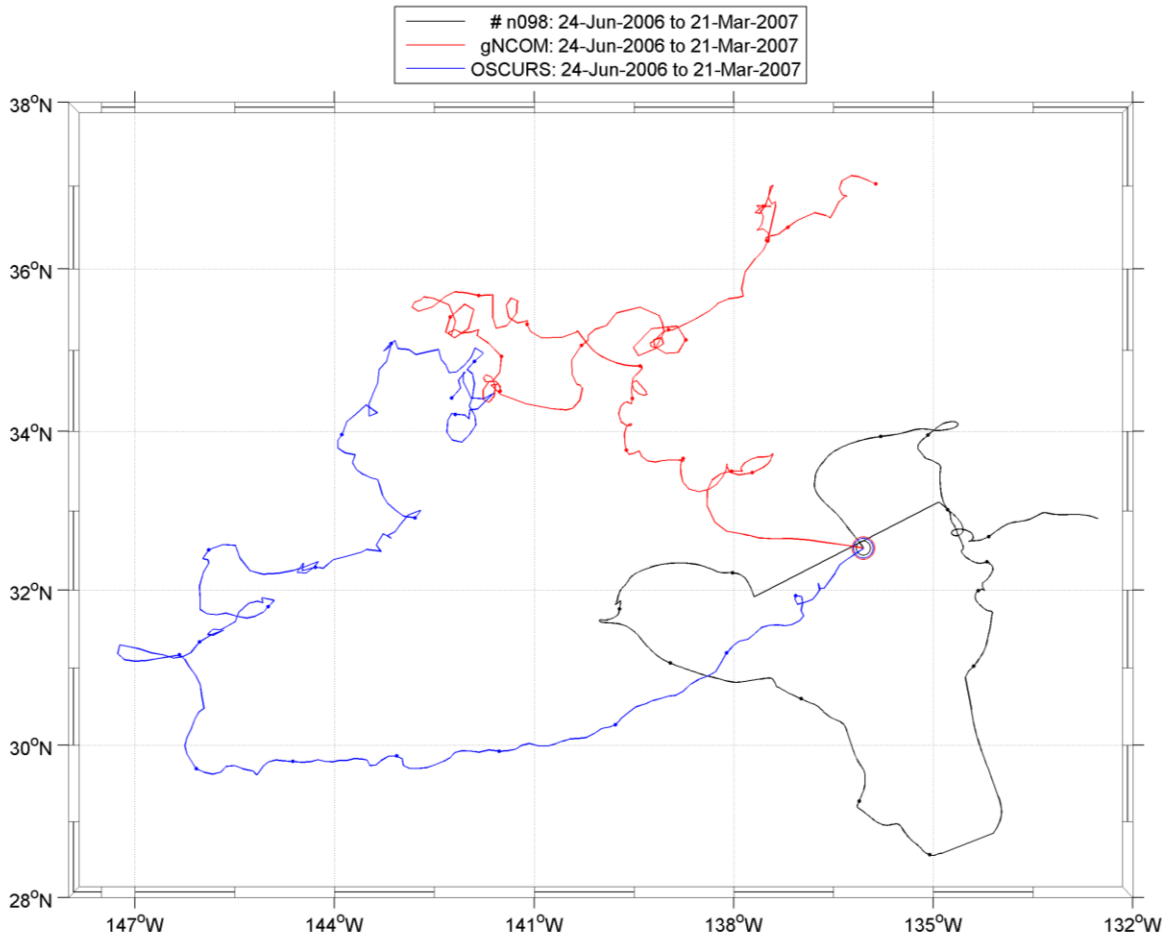

Figure B2. Numerical model and observed float drift t from RAFOS float n098 from 32.53°N 136.05°W on June 24, 2006 to March 21, 2007. RAFOS n098 is black, gNCOM is red, and OSCURS is blue. Dots along the trajectory are 15 days apart. The start position is circled.

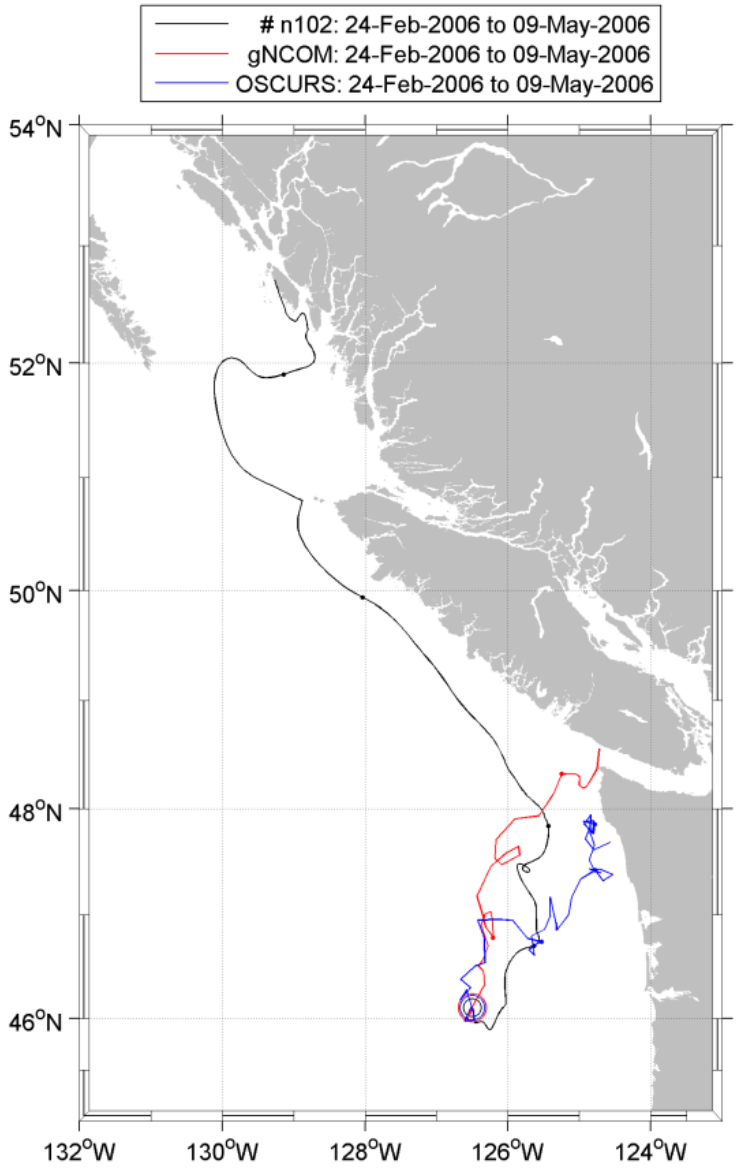

Figure B3. Numerical model and observed float drift from RAFOS float n102 from 46.14°N 126.58°W on February 24, 2006 to May 9, 2006. RAFOS n102 is black, gNCOM is red, and OSCURS is blue. Dots along the trajectory are 15 days apart. The start position is circled.

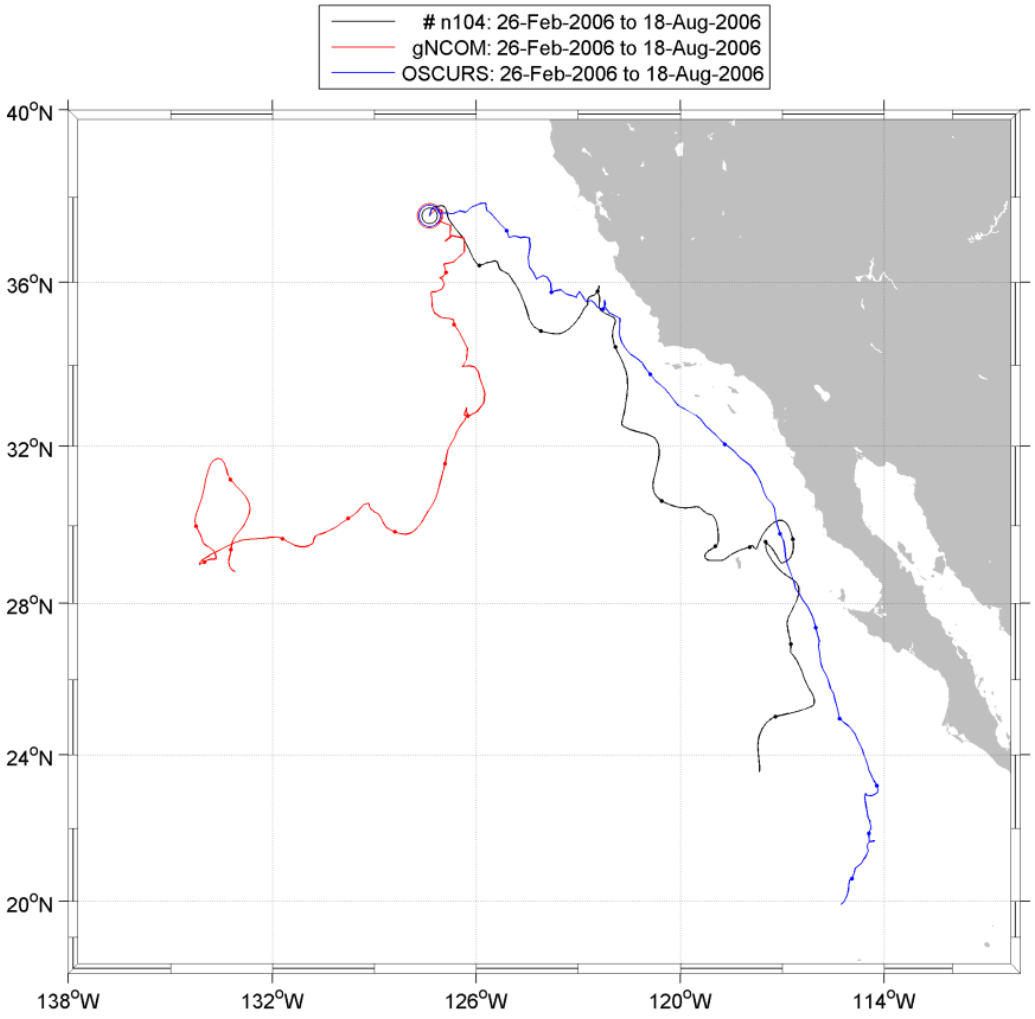

Figure B4. Numerical model and observed float drift from RAFOS float n104 from 37.49°N 127.43°W on February 26, 2006 to August 18, 2006. RAFOS n104 is black, gNCOM is red, and OSCURS is blue. Dots along the trajectory are 15 days apart. The start position is circled.

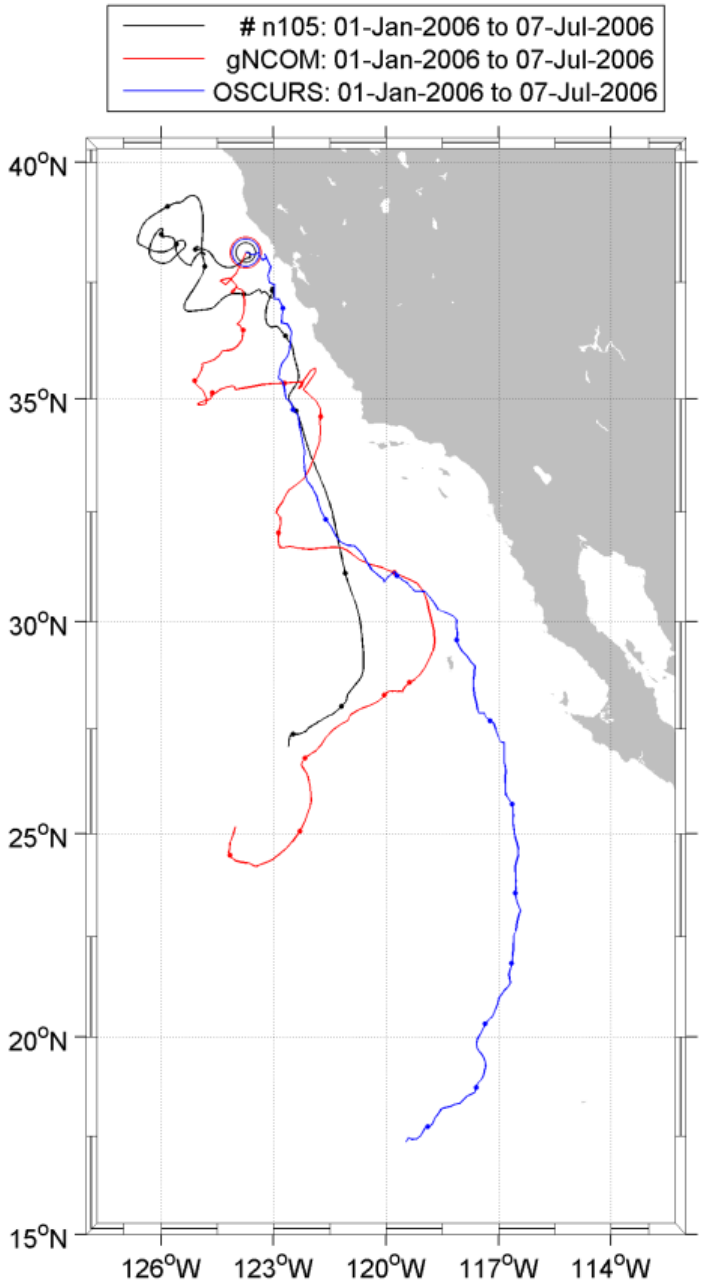

Figure B5. Numerical model and observed float drift from RAFOS float n105 from 39.31°N 125.11°W on September 30, 2005to July 7, 2006. Since gNCOM data was not available for 2005, January 1, 2006, was selected to initialize gNCOM and OSCURS simulated trajectories. RAFOS n105 is black, gNCOM is red, and OSCURS is blue. Dots along the trajectory are 15 days apart. The start position is circled.

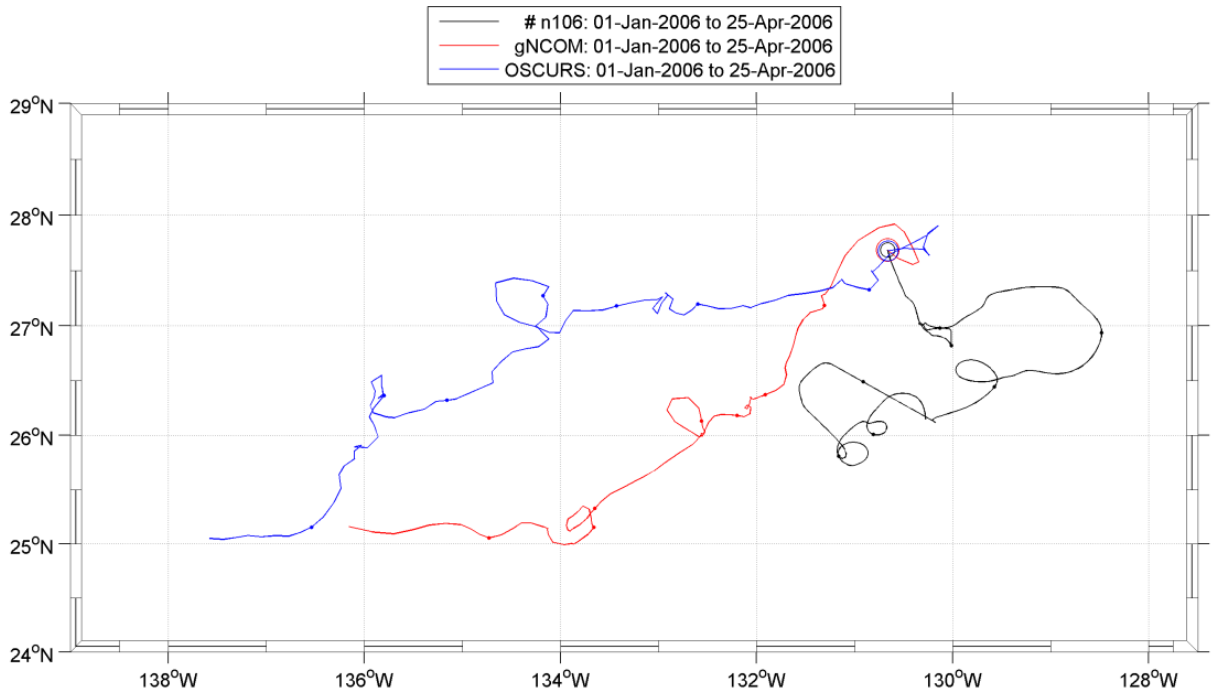

Figure B6. Numerical model and observed float drift from RAFOS float n106 from 27.45°N 130.78°W on September 30, 2005 to April 24, 2006. Since gNCOM data was not available for 2005, January 1, 2006, was selected to initialize gNCOM and OSCURS simulated trajectories. RAFOS n106 is black, gNCOM is red, and OSCURS is blue. Dots along the trajectory are 15 days apart. The start position is circled.

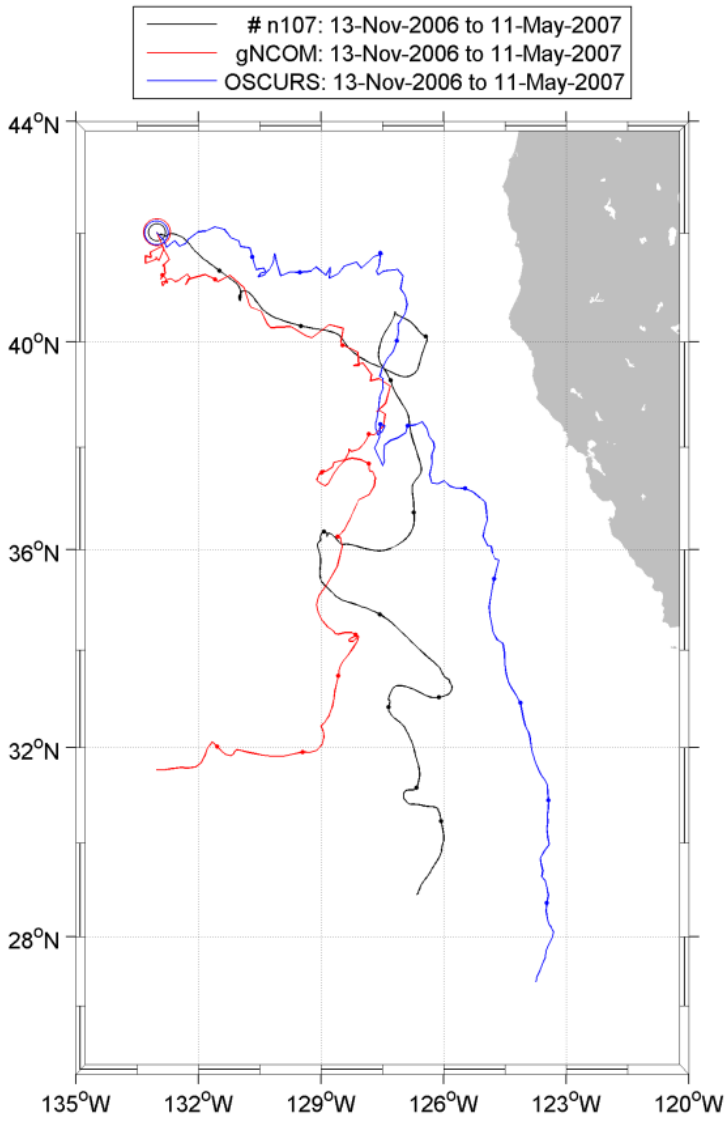

Figure B7. Numerical model and observed float drift from RAFOS float n107 from 42.02°N 133.12°W on November 13, 2006 to May 11, 2007. RAFOS n107 is black, gNCOM is red, and OSCURS is blue. Dots along the trajectory are 15 days apart. The start position is circled.

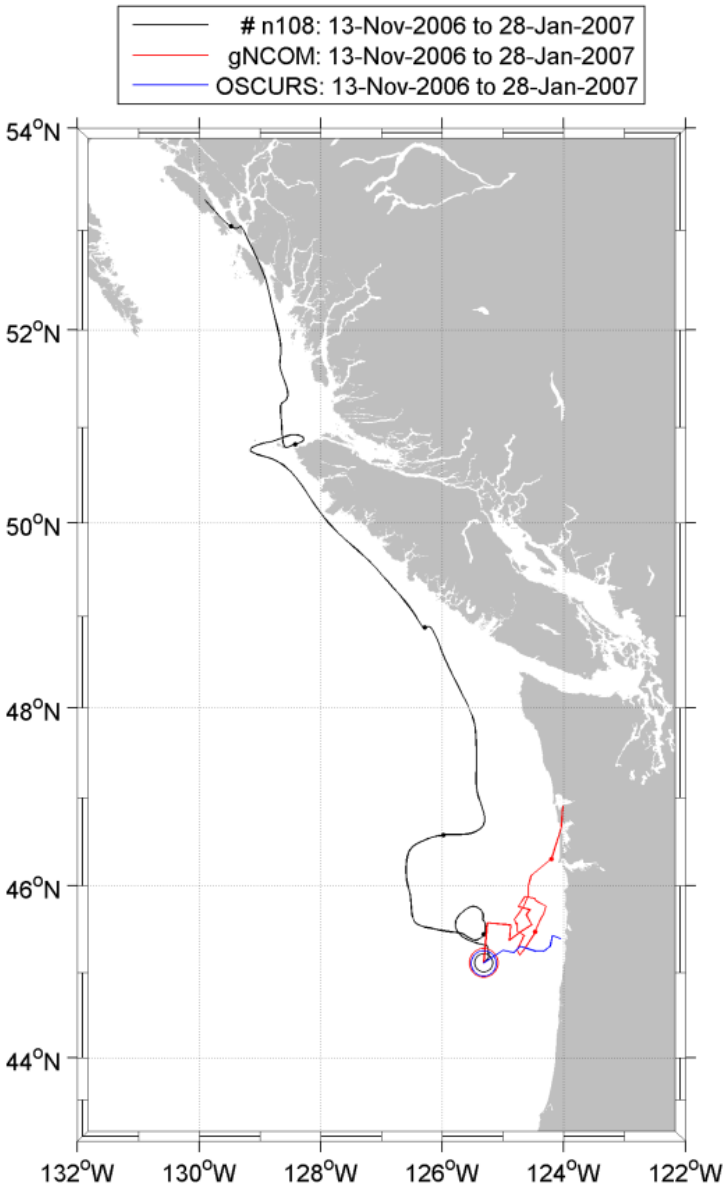

Figure B8. Numerical model and observed float drift from RAFOS float n108 from 45.02°N 125.38°W on November 13, 2006 to January 28, 2007. RAFOS n108 is black, gNCOM is red, and OSCURS is blue. Dots along the trajectory are 15 days apart. The start position is circled.

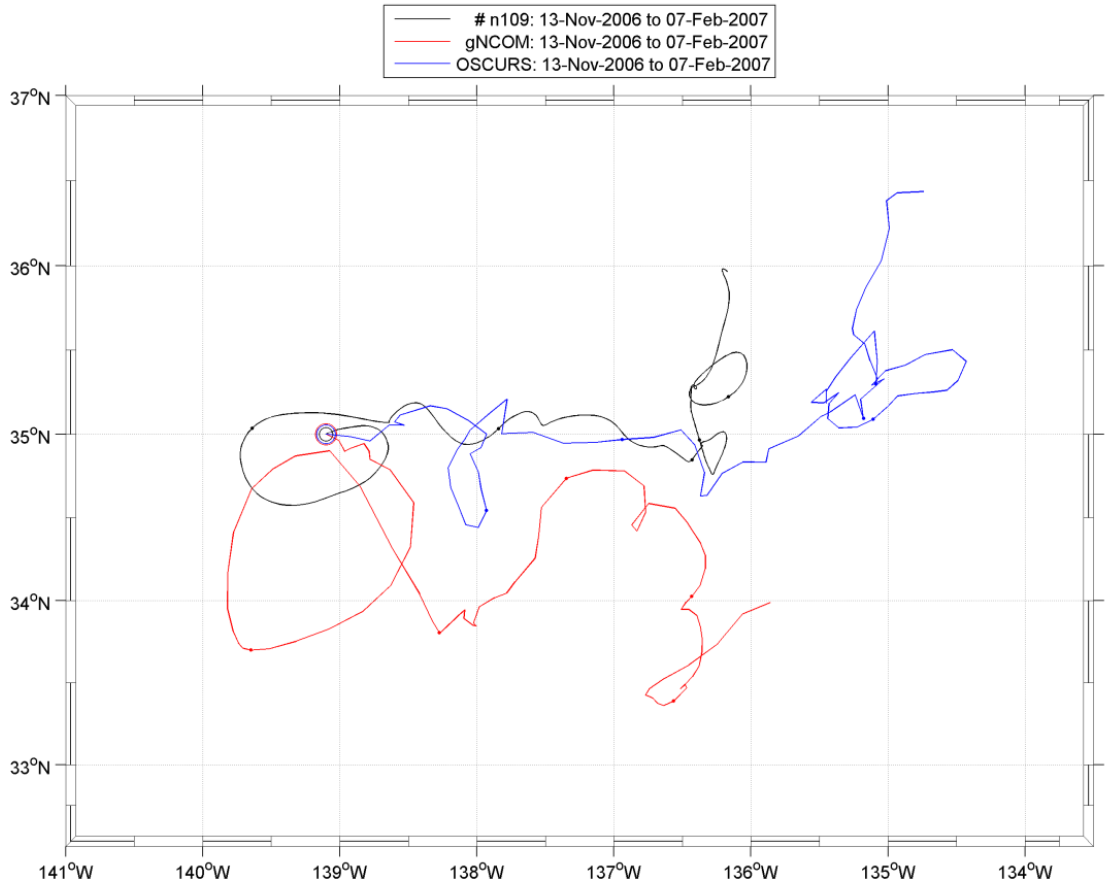

Figure B9. Numerical model and observed float drift from RAFOS float n109 from 34.92°N 139.15°W on November 13, 2006 to February 7, 2007. RAFOS n109 is black, gNCOM is red, and OSCURS is blue. Dots along the trajectory are 15 days apart. The start position is circled.

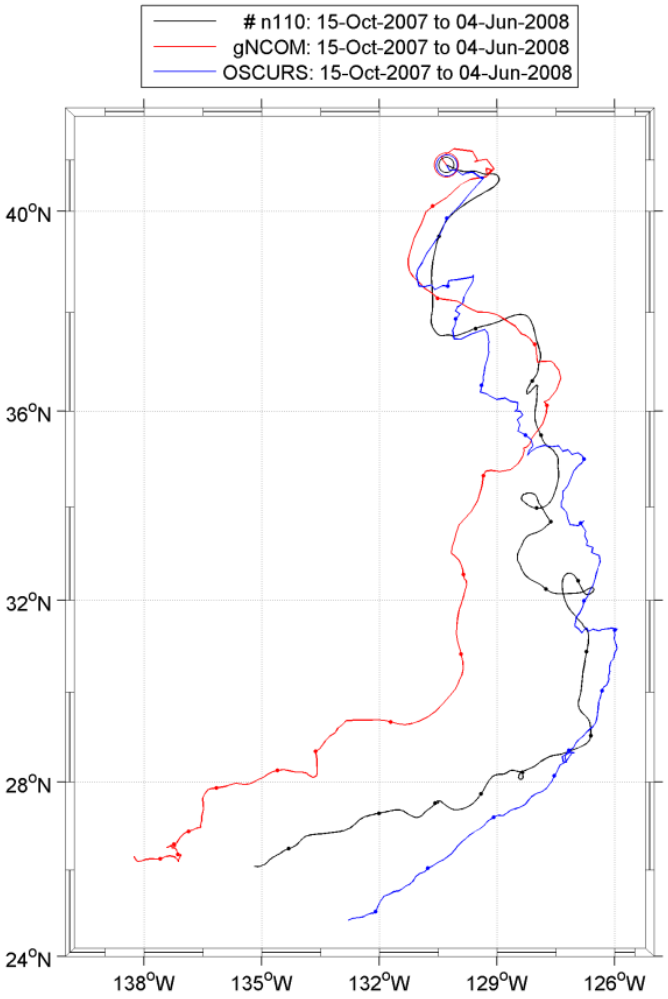

Figure B10. Numerical model and observed float drift from RAFOS float n110 from 40.87°N 130.42°W on October 15, 2007to June 4, 2008. RAFOS n110 is black, gNCOM is red, and OSCURS is blue. Dots along the trajectory are 15 days apart. The start position is circled.

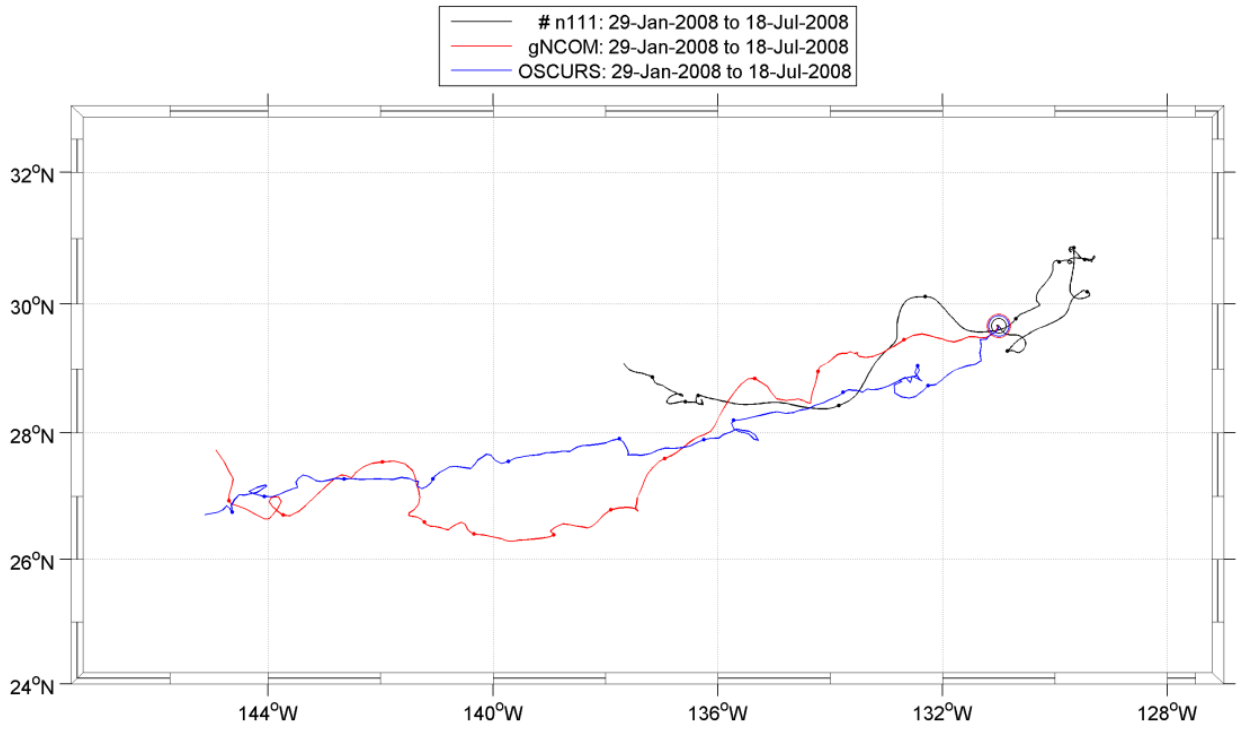

Figure B11. Numerical model and observed float drift from RAFOS float n111 from 29.70°N 130.97°W on January 29, 2008 to July 18, 2008. RAFOS n111 is black, gNCOM is red, and OSCURS is blue. Dots along the trajectory are 15 days apart. The start position is circled.

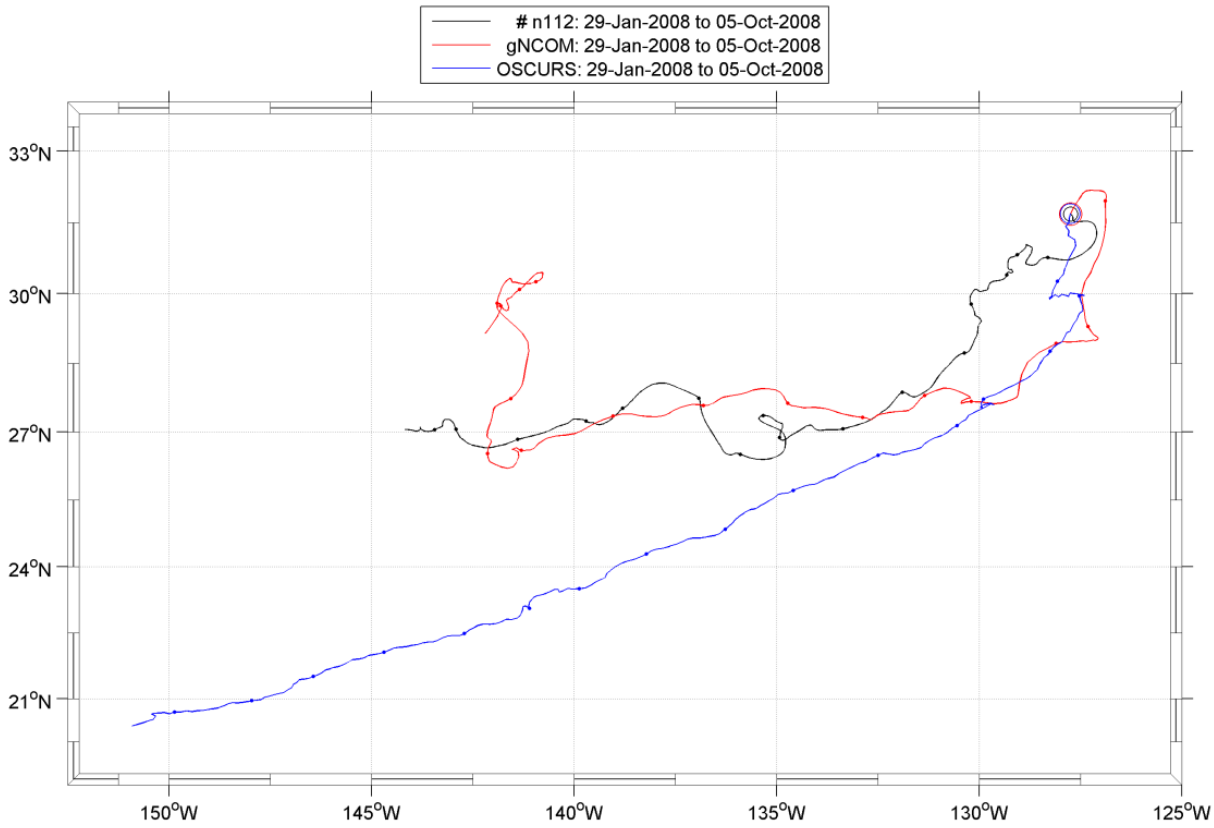

Figure B12. Numerical model and observed float drift from RAFOS float n112 from 31.73°N 127.81°W on January 29, 2008 to October 5, 2008. RAFOS n112 is black, gNCOM is red, and OSCURS is blue. Dots along the trajectory are 15 days apart. The start position is circled.

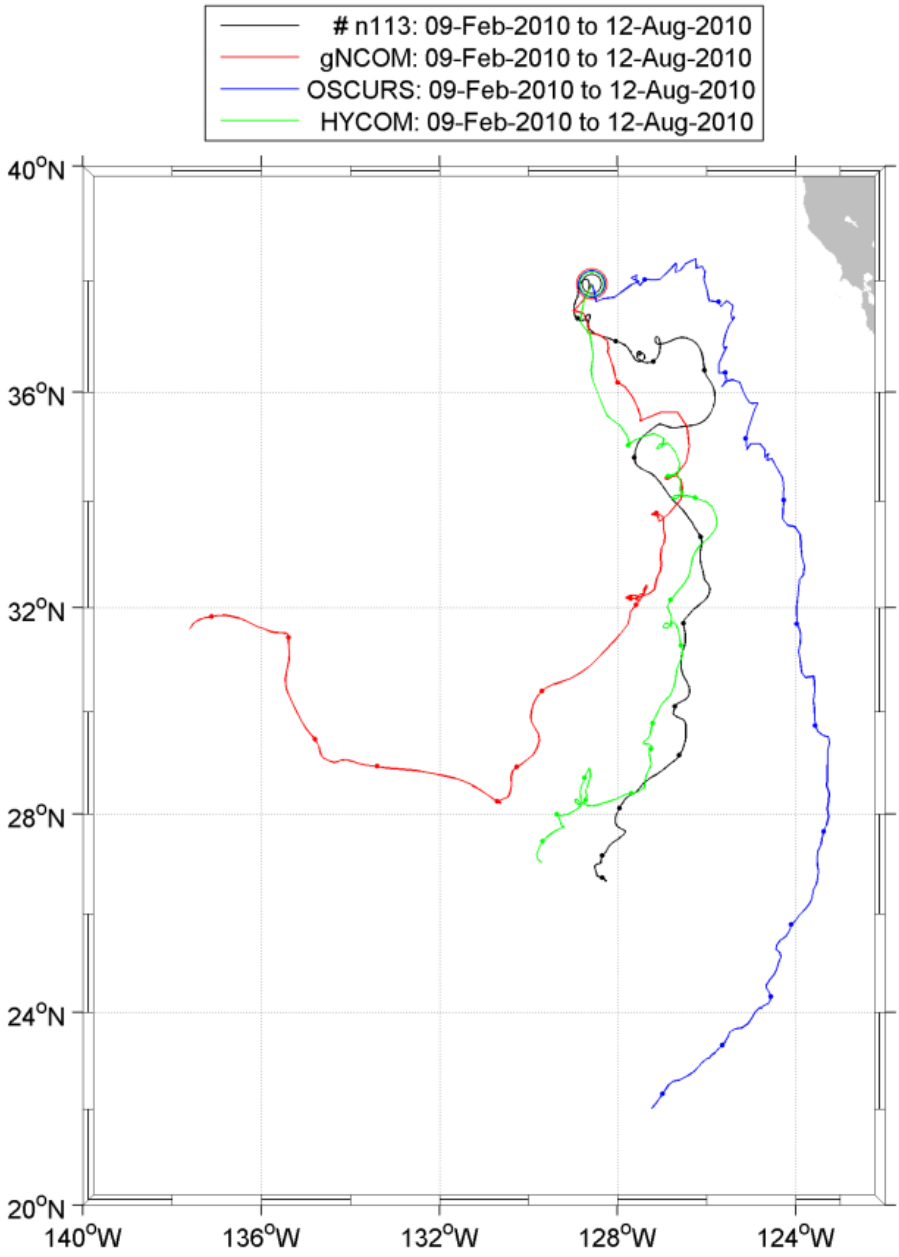

Figure B13. Numerical model and observed float drift from RAFOS float n113 from 38.00°N 128.54°W on February 9, 2010to August 12, 2010. RAFOS n113 is black, gNCOM is red, HYCOM is green and OSCURS is blue. Dots along the trajectory are 15 days apart. The start position is circled.

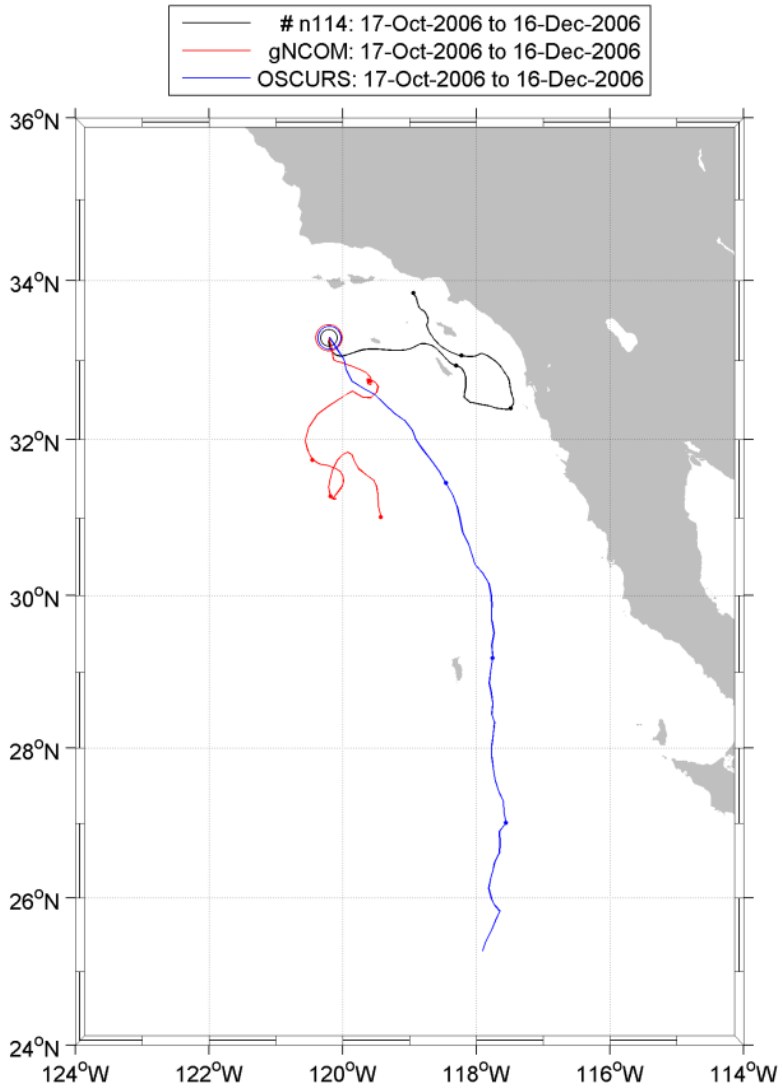

Figure B14. Numerical model and observed float drift from RAFOS float n114 from 33.47°N 120.10°W on October 17, 2006 to December 16, 2006. RAFOS n114 is black, gNCOM is red, and OSCURS is blue. Dots along the trajectory are 15 days apart. The start position is circled.

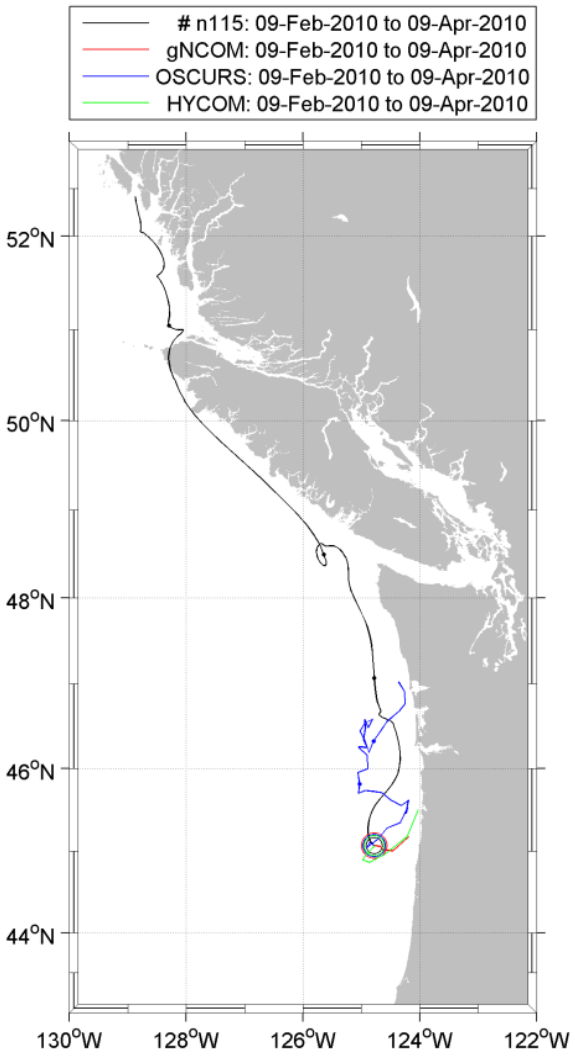

Figure B15. Numerical model and observed float drift from RAFOS float n115 from 45.01°N 124.74°W on February 9, 2010 to April 9, 2010. RAFOS n115 is black, gNCOM is red, HYCOM is green and OSCURS is blue. Dots along the trajectory are 15 days apart. The start position is circled.

THIS PAGE INTENTIONALLY LEFT BLANK

LIST OF REFERENCES

Argos, cited 2012: How does Argos Doppler-derived location work? [Available online at http://www.argos-system.org/web/en/78-faq.php#faq-265].

Atlas, R., R. N. Hoffman, J. Ardizzone, S. M. Leidner, J. C. Jusem, D. K. Smith, and D. Gombos, 2011: A cross-calibrated, multiplatform ocean surface wind velocity product for meteorological and oceanographic applications. Bull. Amer. Meteor. Soc., **92,** 157–174. doi: 10.1175/2010BAMS2946.1.

Barron, C. N., A. Birol Kara, P. J. Martin, R. C. Rhodes, and L. F. Smedstad, 2006: Formulation, implementation and examination of vertical coordinate choices in the Global Navy Coastal Ocean Model (NCOM). *Science Direct*, **11,** 347–375.

Barron, C.N., L. F. Smedstad, J.M. Dastugue, and O. M. Smedstad, 2007: Evaluation of Ocean Models Using Observed and Simulated Drifter Trajectories: Impact of Sea Surface Height on Synthetic Profiles for Data Assimilation. *J. Geophys. Res*., **112,** C07019, doi: 10.1029/2006JC003982.

Bleck, R., 2002: An Oceanic General Circulation Model Framed in Hybrid Isopycnic-Cartesian Coordinates. *Ocean Model.* **37,** 55–88.

Blumberg, A. F., and G. L. Mellow, 1987: A description of a Three Dimensional Coastal Ocean Circulation Model. Three-Dimensional Coastal Ocean Models. *Amer.Geophys. Union,* **45,** 55–88.

Bowditch, N., 2002: *The American Practical Navigator*. National Imagery and Mapping Agency, 879 pp.

Center for Ocean-Atmospheric Prediction Studies (COAPS), cited 2012: HYCOM + NCODA Global 1/12° Analysis (GLBa0.08/expt_90.8). [Available online at http://hycom.org/dataserver/glb-analysis/expt-90pt8].

Davis, R. E., 1985: Drifter Observation of Coastal Currents During CODE. The method and Descriptive View. *J. Geophys. Res*., **90,** 4741–4755.

Howell, E. A., S. J. Bograd, C. Morishige, M. P. Seki, and J. J. Polovina., 2012: On North pacific Circulation and associated Marine Debris Concentration. *Mar. Pollut. Bull.*, **65,** 2012.

Ingraham, J. W., and R. X. Miyahara, 1988: Ocean Surface Current Simulations in the North Pacific Ocean and Bearing Sea (OSCURS – Numerical Model). NOA Tech Memo. NMFS/NWC-130, 155 pp.

Ingraham, J. W. and R. K. Miyahara, 1989: Tuning of the OSCURS Numerical Model to Ocean Surface Current Measurements in the Gulf of Alaska. NOAA Tech. Memo. NMFS F/NWC – 168. 66 pp.

Ingraham, J. W., 1997: Getting to Know OSCURS, REFM's Ocean Surface Current Simulator. Alaska Fisheries Science Center Quarterly Report. 14 pp.

Lynn, Ronald J. and J. J. Simpson, 1987: The California Current System: The Seasonal Variability of its Physical Characteristics. *J. Geophys. Res*., **92,** 12947–12966.

Lumpkin, R., and Mayra Pazos, 2007. Measuring Surface Currents with Surface Velocity Program Drifters: the Instrument, its Data, and Some Recent Results. *Lagrangian Analysis and Prediction of Coastal and Ocean Dynamics*, Griffa, A. et al. (Eds), Cambridge University Press, 39–67.

Margolina, T., C.A. Collins, T.A. Rago, R.G. Paquette, and N. Garfield, 2006: Intermediate Level Lagrangian Subsurface Measurements in the Northeast Pacific: Isobaric RAFOS Float Data. *Geochem. Geophys. Geostyst.,* **7,** Q09002, doi:1029/2006GC001295.

Maximenko, N., J. Hafner, and P. Niiler, 2012: Pathways of Marine Debris Derived from Trajectories of Lagrangian Drifters. *Mar. Pollut. Bull.,* **65,** 51–62.

Metzger, E.J., H.E. Hurlburt, A.J. Wallcraft, O.M. Smedstad, J.A. Cummings, and E.P. Chassignet, 2009: Predicting "Ocean Weather" using the Hybrid Coordinate Ocean Model (HYCOM). *NRL Review*., 202–205.

Niiler, P. P. and J. J. Paduan. 1995: Wind-Driven Motions in the Northeast Pacific as Measured by Lagrangian Drifters. *J. Phys.Oceanogr*. **25,** 2819–2830.

NOAA. National Oceanic and Atmospheric Administration, cited 2012: The Global Drifter Program. [Available online at http://www.aoml.noaa.gov/phod/dac/gdp_objectives.php].

Potemra, J. T., 2012: Numerical Modeling with Application to Tracking Marine Debris. *Mar. Pollut. Bu.*, **65,** 42–50.

Poulain, P., R. Gerin, E. Mauri, and R. Pennel, 2009: Wind Effects on Drogued and Undrogued Drifters in the Eastern Mediterranean. *J. Atmos. Oceanic Tech.* **26,** 1144–1156.

Rossby, T., D. Dorson, and J. Fountain, 1986: The RAFOS System. *J. Atmos. Oceanic Tech.* **3,** 672–679.

Showstack, R. 2011: Oceanographer tracks marine debris from the Japan tsunami and other incidents, *Eos Trans. AGU*, 92(37), 306, doi:10.1029/2011EO370002.

Smedstad, L. F., C. N. Barron, T. L. Townsend, T. J. Campbell, P. J. Martin, P. G. Posey, and R. C. Rhodes, 2010: *User's Manual for the Global Ocean Forecast System (GOFS) Version 2.6*. Naval Research Laboratory, 27 pp.

Smith, Stuart D., 1988: Coefficients for Sea Surface Wind Stress, Heat Flux, and Wind Profiles as a Function of Wind Speed and Temperature. *J. Geophys. Res*., **93,** 15,467–15,472.

Stein, M. "Large sample properties of simulations using latin hypercube sampling." *Technometrics*. Vol. 29, No. 2, 1987, pp. 143–151. Correction, Vol. 32, p. 367.

Stein, M., 1987: Large Sample Properties of Simulations Using Latin Hypercube Sampling. *Technometrics,* **29,** 143–151. Correction, **32,** 367.

Sverdrup, H. U., M. W. Johnson, and R. H. Fleming, 1942: The Oceans Their Physics, Chemistry, and General Biology. New York Prentice-Hall, INC, 1087 pp.

Swenson, S. S. and P. P. Niiler. 1996: Statistical Analysis of the Surface Circulation of the California Current. *J. Geophys. Res.*, **101,** 22,631–22645.

Trenberth, K. E., W. G. Large, and J. G. Olson, 1989: The Effective Drag Coefficient for Evaluating Wind Stress Over the Oceans. *J. Climate* **2,** 1507–1516.

Trenberth, K. E., W. G. Large, William G., and Olson, Jerry G., 1990: The Mean Annual Cycle in Global Ocean Wind Stress. *J. Phys.Oceanogr.* **20,** 1742–1760.

Wackerly, D. D., W. Mendenhall, R. L. Scheaffer, 2007: *Mathematical Statistics with Applications.* Books/Cole Centage Learning, 912 pp.

Witting, R., 1909: Zur Kenntnie den vom Winde Erzeigtem Oberflachenstromes. *J. Phys.Oceanogr.***13,** 524–530

Woods Hole Oceanographic Institution, cited 2012: Ocean Instruments. [Available online at http://www.whoi.edu/instruments/viewInstrument.do?id=1061].

Xie J.P., and J. Zhu, 2010: Optimal ensemble interpolation schemes for assimilation of Argo profiles into HYCOM. *Ocean Model*. **33,** 283–298.

Yao, F., and W. E. Johns, 2010: A HYCOM modeling study of the Persian Gulf: 1. Model configurations and surface circulation, *J. Geophys. Res*., **115,** C11017, doi:10.1029/2009JC005781.

THIS PAGE INTENTIONALLY LEFT BLANK

INITIAL DISTRIBUTION LIST

1. Defense Technical Information Center
   Ft. Belvoir, Virginia

2. Dudley Knox Library
   Naval Postgraduate School
   Monterey, California

3. Curtis Ebbesmeyer
   Beachcombers Alert
   Seattle, Washington

4. Curtis Collins
   Naval Postgraduate School
   Monterey, California

5. Tetyana Margolina
   Naval Postgraduate School
   Monterey, California

6. Thomas Rago
   Naval Postgraduate School
   Monterey, California

7. Lucy Smedstad
   Naval Research Laboratory
   Stennis Space Center, Mississippi

8. Ole Smedstad
   Naval Research Laboratory
   Stennis Space Center, Mississippi

9. Patrick Hogan
   Naval Research Laboratory
   Stennis Space Center, Mississippi

10. Oleg Melnichenko
    University of Hawaii
    Honolulu, Hawaii

11. Nikolai Maximenko
    University of Hawaii
    Honolulu, Hawaii